Classical and Quantum Features of String Cosmology

Daniel H. Wesley

A Dissertation

Presented to the Faculty

of Princeton University

in Candidacy for the Degree

of Doctor of Philosophy

Recommended for Acceptance

by the Department of

Physics

June, 2006

© Copyright 2006 by Daniel H. Wesley.

All rights reserved.

for Marie

Abstract

We study classical and quantum features of cosmological models based on superstring theories. In the first part of this work, we consider the emergence of chaos during the collapse of the universe to a big crunch, which is a potential problem for recently proposed models in which cosmological history is cyclic. We describe two mechanisms by which chaos can be avoided. The first requires a matter component with an equation of state $w > 1$. The second mechanism, which we term "controlled chaos," requires the spacetime to satisfy a set of topological conditions, expressed in terms of its de Rham cohomology. We present techniques to systematically find solutions with controlled chaos and classify all solutions for the heterotic superstring theory. In the second part of this work, we turn to the problem of string pair production in time–dependent spacetimes. Through studying a specific background corresponding to two colliding gravitational waves, we show that the spectrum and production rate for string pairs differ significantly from point particle pairs. These results suggest unique signatures of string physics that may persist in cosmological spacetimes.

Acknowledgements

First and foremost, my parents Richard and Patricia deserve more thanks than I can give here. Their devotion to my intellectual and personal growth has been a great source of strength during the many twists and turns of my life. It is by no means an exaggeration to say that everything that I have accomplished has been made possible only through their constant, unflinching, and selfless encouragement and support.

My sister, Julia, deserves my gratitude for putting up with me through childhood and beyond, and for always being there when I needed her. I would also like to thank my daughter, Marie, for teaching me everything I know about birds (and quite a few additional topics), for being such a great hiking partner on our weekend trips to Washington's Crossing, and for just being a wonderful person in general.

In learning about physics, I have been very fortunate in having some excellent teachers. Two in particular stand out. I owe many thanks to my high school physics teacher, Robert Schwartz, for always having the time and energy to answer my questions, for making my high school education far more enriching than I had any right to expect, and for helping to get me started on the path that led to this thesis. My interest in the universe was sparked by another of my teachers, Paul Steinhardt. Paul introduced me to modern cosmology though a Junior Paper in 1999, and in a sense this thesis represents a few of the chapters that I am still adding to that report. I am grateful to him for sharing his scientific perspective, for his guidance in both the technical and non–technical aspects of life in science, and his help in getting me to

start thinking like a scientist.

Research at Princeton has been greatly enriched by my fellow–travelers. I owe a lot to the members of Paul's research group: Amol, Andrew, Annika, Däniël, Joel, Justin, Latham, Steve, and Mustapha. I'm happy to especially acknowledge Andrew, Jeff and Joel, who are both friends and collaborators, and many, many conversations (though, sadly, no papers) with Latham. I would like to thank Lyman Page and Suzanne Staggs for trusting me to work in their labs at various points during my time here, which has given me an appreciation and respect for the experimentalist's art. I am grateful to Laurel Lerner for always knowing what's going on, and for smoothing many a rough spot during my graduate school years.

Many people have played a part in making life in Princeton a lot more fun. I'm glad Nikhil put up with me on our many backpacking trips, especially on the Wonderland Trail. Ben is an old friend, was a great roommate, and remains a fellow fan of our years with Mr. Schwartz. Katie has brightened up my last year here; her virtuoso proofreading skills, and kindness in keeping me from starvation, have made the past few months almost survivable. It hasn't been hard to find climbing partners while in graduate school, and I'm happy to have spent some on the ropes with Ethan, Jeff, Micah, and Mike. I want to especially thank Toby in this respect, who talked me into my first pair of climbing shoes, has been tied into the other end more times than I could count, and has perfected "winging it" to the level of high art.

To everyone I may have forgotten – thanks!

Contents

Chapter 1

Introduction

When I behold this goodly frame, this world
Of heav'n and Earth consisting, and compute
Their magnitudes, this Earth a spot, a grain,
An atom, with the firmament compared
And all her numbered stars, that seem to roll
Spaces incomprehensible ...

Paradise Lost Book VIII, lines 15–20, [90]

Recent years have seen great advances in our understanding of models of quantum gravity, and in particular superstring theories. A natural application of any such model is to the physics of the very early universe. A theory of quantum gravity is clearly required to fully understand this epoch. In addition, it seems unlikely that Earth–bound experiments will be able to probe the quantum nature of gravity in the conceivable future. Thus, the early universe provides a convenient (and possibly the only) laboratory in which these theories may be tested.

We are thus led to ask an essential question: what are the unique features of a "stringy" cosmology? Do string models of the early universe make any characteristic predictions that might enable us to differentiate them from alternative models?

Does string theory provide any fundamentally new tools for constructing cosmological models, or does it merely enable us to embed old mechanisms in a new framework? In this work, we will touch on some aspects of these questions. Our discussion here may be divided into two parts. In the first, we focus on classical features of string cosmology. In the second, we investigate quantum features.

Part I: Chaos and the Classical Dynamics of String Models

One of the most striking predictions of Einstein's general relativity is that there will be an end to time. This has been appreciated in the context of some early (closed) cosmological models, where the universe expands from a big bang singularity, and re–collapses in a big crunch singularity. Misner, Thorne and Wheeler [92][1] put a fine point on this issue, calling the prediction of gravitational collapse and the resulting singularity "the greatest single crisis of physics to emerge from [Einstein's] equations." The inevitable breakdown of Einstein's equations is known to occur in more general settings, thanks to the work of Hawking and Penrose [64, 65]. Their theorems imply that the worldlines of observers will end, presumably in a singularity of some kind, at a finite time in the future. Furthermore, these same worldlines must have a beginning at some finite time in the past.

The construction of cosmological models touches upon another facet of this issue. Logically, either time extends without bound into the future or past, or it does not. In the conventional big bang model, time had a beginning at some finite time in the past, and current observations (along with a minimal set of assumptions) seem to indicate that the universe will continue to expand indefinitely. It may be possible, however, that cosmic history has a cyclic nature, with repeating phases of expansion and contraction. At issue here are the details of how the universe navigates the big crunch/big bang transition. In conventional Einstein gravity, the big crunch and big

[1] Box 18.1, page 437.

bang are singularities, and it is impossible to continue the equations through these events.

Recently, a model has been proposed in which the universe does possess a cyclic history [77, 78, 79, 80, 108, 109]. This "cyclic universe" is embedded in a particular superstring model, and appeals to features of string theory that might enable the universe to re–emerge after the big crunch event into a subsequent expanding phase. The big bang and big crunch are therefore not the beginning and end of cosmic time, but instead merely events in an eternally repeating sequence. Furthermore, a nearly scale invariant spectrum of density perturbations, required by observation, is generated during the collapsing phase. The spectrum of gravitational waves produced in this model is significantly different form that produced in the more conventional inflationary universe model [16], thus providing a distinctive observational signature.

A potential problem that any cyclic universe model must confront is the presence of chaos during the collapsing phase. It has been known since the 1940s that, in the context of Einstein gravity, a collapsing universe will undergo chaotic, anisotropic oscillations. In cyclic models, it is assumed that the universe is nearly homogeneous and isotropic during the collapsing phase, with a scale invariant perturbation spectrum. Chaotic oscillations arising during this epoch would destroy homogeneity and isotropy, producing a disordered, "turbulent" spacetime with structure down to arbitrarily small scales. In this situation, a big crunch/big bang transition is unlikely to be describable in a deterministic manner, and it is questionable whether a homogeneous and isotropic universe with the long range correlations required by observations could emerge [95]. Thus, avoiding chaos is an essential feature of cosmological models with a collapsing phase.

In the first part of this work, we explore the question of how cyclic models can avoid the emergence of chaos during gravitational collapse. Chapter 2 is devoted to

reviewing the relevant aspects of the literature regarding the emergence of chaos in collapsing spacetimes. We introduce the generalized Kasner solution as a description of the asymptotic dynamics of general relativity near a big crunch singularity. Using this solution enables chaos to be studied through a simple set of linear inequalities, known as the stability conditions. Within this approach, it is possible to see that chaos in vacuum Einstein gravity and superstring models is inevitable.

In Chapter 3 we introduce a new mechanism by which chaos can be avoided. We show that the inclusion of a matter component whose pressure exceeds its energy density (equivalently, its equation of state w satisfies $w > 1$) can allow the universe to contract smoothly and non–chaotically toward a big crunch. Intriguingly, cyclic models require a matter component with precisely these properties in order to generate a scale invariant spectrum of density fluctuations. This chapter summarizes published work [43], and includes an unpublished body of work on realizing the required matter component in a higher–dimensional framework.

We next describe a second mechanism by which chaos can be avoided that does not require the inclusion of additional matter components. This mechanism, which we term "controlled chaos," is introduced in Chapter 4. Working in the context of cosmological models with extra dimensions, such as those based on superstring theories, we show that the presence or absence of chaos is determined by topological features of the extra dimensions. For some topologies, chaos is present; for others, it is not. We give a set of selection rules that enable one to differentiate between these cases. These rules are based on the menu of matter fields and topological invariants of the extra dimensional space. We go on to study some simple solutions with controlled chaos. Most of this chapter represents published work [120].

In Chapter 5 we present a more systematic approach to the controlled chaos mechanism. This mechanism requires a delicate interplay between the topology of

the extra dimensional space and a choice of solution to Einstein's equation. Here, we present techniques that allow a systematic search for solutions with controlled chaos. These techniques are inspired by the remarkable connection between the dynamics of gravitational theories near a big crunch and the root lattices of hyperbolic Kac–Moody algebras [25, 28, 29], although they are flexible enough to apply to any model with gravity. We apply them to classify all solutions with controlled chaos for the heterotic superstring theory. This chapter represents recent work that has not yet been published.

Part II: Pair Production and Quantum Features of String Models

In the second part of this work, we turn to the quantum regime. We study the process of pair production, by which quanta of a field are produced in a time–dependent background. This process is quite important cosmologically: in all known models of the early universe, the primordial spectrum of density fluctuations is generated through a pair production process. If the pair production of strings possesses any unique features, then it is possible these could manifest themselves in these spectra, and provide a potential observational mechanism to probe string theory. In addition, strings in time–dependent backgrounds are currently poorly understood, so any information that can be gleaned about the theory in this regime is useful.

In Chapter 6, we study the pair production of point particles (as in field theory) and strings in a specific background. We seek differences between these two cases. We find that the spectrum of created strings, as well as the overall rate of string pair production, differs significantly from point particles. The background we use, corresponding to two colliding gravitational waves, is not of immediate cosmological relevance. However, these results do establish the fact that, at least in one case, there are differences between string and point particle pair production. One might hope

that these differences persist in backgrounds of cosmological interest, and potentially lead to observable signatures of string theory in the early universe. Thus, while these results are intriguing, much work remains to be done. This chapter is based on previously published work by the author [115].

Chapter 2

Chaos near a Big Crunch

...when strait behold the throne
Of Chaos, and his dark pavilion spread
Wide on the wasteful deep; with him enthroned
Sat sable-vested Night, eldest of things

Paradise Lost Book II, lines 959–962, [90]

In this chapter we review the instability of spacetimes undergoing gravitational contraction to a big crunch. Our goal is to understand cosmological spacetimes, and in this context we are accustomed to considering spaces that are both homogeneous and isotropic. It has been known for some time that these spaces cannot remain homogeneous and isotropic during collapse to a big crunch, but instead begin to oscillate anisotropically and chaotically. This phenomenon is often termed *BKL oscillations* or *Mixmaster* behavior. This occurs under fairly general conditions, including

- Vacuum Einstein gravity in spacetime dimension $D < 11$,
- Einstein gravity including typical matter and energy sources, such as radiation, dust or a cosmological constant,
- Low–energy limits of superstring and M–theory models.

This instability presents a problem for cosmological models in which the universe evolves through the big crunch into a subsequent expanding phase. Given this instability, it appears unlikely that a homogeneous and isotropic universe could arise from such a Mixmaster epoch.

It is the purpose of this review to introduce the methods employed to establish the presence of chaos near a big crunch. This subject has a long history, and the methods we discuss have been developed by a number of researchers [1, 8, 9, 10, 24, 25, 26, 27, 28, 29, 30, 33, 75, 84, 91]. In the chapters that follow, we will use these same methods to investigate cases in which it is possible to collapse smoothly to a big crunch.

2.1 Introduction

The presence of any kind of instability is entirely invisible when we confine our attention to the homogeneous and isotropic Friedmann–Robertson–Walker (FRW) spacetimes that form the basis of modern cosmological models. These spacetimes have the metric (See Appendix G for the our general relativity conventions)

$$\mathrm{d}s^2 = -\mathrm{d}t^2 + a(t)^2 \left[\frac{\mathrm{d}r^2}{1-kr^2} + r^2 \mathrm{d}\Omega^2 \right], \tag{2.1}$$

where $\mathrm{d}\Omega^2$ is the metric on a unit two–sphere $\mathbf{S}^2$, k a measure of the curvature of the spatial sections, and the *scale factor* $a(t)$ obeys the *Friedmann equation*

$$3\left(\frac{\dot{a}}{a}\right)^2 = \sum_i \rho_i(a) - \frac{3k}{a^2}. \tag{2.2}$$

Here, the ρ_i are the energy densities of the various matter sources in the model, which themselves depend on the scale factor a. Often the Friedmann equation is written in terms of the *Hubble parameter* H, defined by

$$H = \frac{\dot{a}}{a}. \tag{2.3}$$

From the Friedmann equation (2.2), it appears that a contracting universe collapses smoothly as $a \to 0$, and there is no sign of any instability.

To understand the behavior of the universe near a big crunch, it is necessary to study metrics more general than (2.1). One cannot see the emergence of anything other than isotropic and homogeneous contraction with (2.1) because the single degree of freedom $a(t)$ does not allow for the possibility of anything else. When we include more degrees of freedom, we will see that the homogeneous and isotropic solution is in fact unstable during a collapsing phase, and therefore (2.1) is no longer valid.

In this chapter we will motivate the remarkable fact that all of the essential features of cosmological dynamics near a big crunch can be studied through the *Kasner metric*

$$\mathrm{d}s^2 = -\mathrm{d}t^2 + \sum_{j=1}^{d} (t/t_0)^{2p_j} \mathrm{d}x_j^2, \tag{2.4}$$

where the constants p_j are known as the *Kasner exponents* [75]. We have chosen a reference time t_0 at which the spatial part of the metric is identical to that of flat space. For later convenience, this metric is written for $d+1$ spacetime dimensions. This metric is extremely useful, for as we shall show below, it captures the asymptotic behavior of cosmological solutions of general relativity in a particularly simple form.

The Kasner metric is an exact solution of the vacuum Einstein equations provided that the following *Kasner conditions* are satisfied

$$\sum_{j=1}^{d} p_j = 1, \tag{2.5a}$$

$$\sum_{j=1}^{d} p_j^2 = 1. \tag{2.5b}$$

In the d–dimensional space whose coordinates are the p_j, the first condition defines a plane called the *Kasner plane* and the second the *Kasner sphere*. We will denote the locus defined by (2.5) as the *Kasner circle*, although generically this locus will be the sphere $\mathbf{S}^{d-2}$.

Using the Kasner metric the conditions governing the stability or instability of the spacetime can be expressed very simply as a set of inequalities involving the Kasner exponents. There are three main types of stability conditions: the *gravitational stability conditions*, and the *electric* and *magnetic p–form stability conditions*. Therefore, using the Kasner metric as a model, the emergence or absence of chaos during gravitational collapse is reduced to an algebraic problem involving the Kasner exponents.

While the the Kasner metric (2.4) is the main focus of this chapter, we will have cause to introduce a number of other metrics that are useful for illustrating various aspects of physics near the big crunch. During the later chapters in this work we will switch back and forth between some of these points of view. In this chapter we will discuss results using

- A "minisuperspace" exact solution (Section 2.2)
- The "equation of state" w (Section 2.3)
- Power–counting in t (Section 2.4)
- The billiard representation (Section 2.6)

Along the way, we will introduce p–form matter components in Section 2.5 and discuss their influence on cosmological dynamics.

2.2 The Mixmaster Universe

The Mixmaster universe, first studied by Misner [91], and discussed in detail in Appendix A, provides an excellent prototype of the dynamics we wish to study. This universe is similar to a closed FRW universe, in that the spatial sections are all topologically three–spheres $\mathbf{S}^3$. Unlike the FRW case, the $\mathbf{S}^3$ is allowed to distort

anisotropically – that is, the lengths of the three independent great circles are dynamical. The spatial sections remain homogeneously curved, and thus the Mixmaster universe is the (diagonal) Bianchi–IX metric. (For information on the Bianchi classification, see [42, 103, 111]) The metric itself is

$$\mathrm{d}s^2 = -\mathrm{d}t^2 + a(t)^2 \sum_{j=1}^{3} \exp\left(2\beta_j\right) (\sigma^j)^2 \tag{2.6}$$

where a and the β_j are functions of time only. The one–forms σ^j are functions of the spatial coordinates only, and define the homogeneous metric on the spatial $\mathbf{S}^3$. In fact the closed FRW solution is included in the Mixmaster universe, being the isotropic case where all the β_j are identical. The three β_j are expressed in terms of two independent variables β_+ and β_- as follows

$$\beta_1 = -\frac{\beta_+}{\sqrt{2}} - \frac{\beta_-}{\sqrt{6}} \tag{2.7a}$$

$$\beta_2 = +\frac{\beta_+}{\sqrt{2}} - \frac{\beta_-}{\sqrt{6}} \tag{2.7b}$$

$$\beta_3 = \frac{2\beta_-}{\sqrt{6}} \tag{2.7c}$$

These two variable $\beta_\pm$ parameterize the possible homogeneity–preserving deformations of the $\mathbf{S}^3$, and the scale factor a parameterizes the change in its volume.

The Einstein equations for this metric yield an analogue of the Friedmann equation

$$3\left(\frac{\dot{a}}{a}\right)^2 = \frac{1}{2}\left(\dot{\beta}_+^2 + \dot{\beta}_-^2\right) + \frac{\tilde{U}(\beta_+, \beta_-)}{2a^2}, \tag{2.8}$$

where $\tilde{U}$ is a function of β_+ and β_-. Comparing this to the Friedmann equation (2.2) we recognize that the term involving $\tilde{U}$ is the analogue of the homogeneous curvature term, but that a new term related to the shape parameters $\beta_\pm$ has appeared on the right hand side. The equation above is supplemented by the equations of motion for the $\beta_\pm$, which are

$$\ddot{\beta}_\pm + 3\frac{\dot{a}}{a}\dot{\beta}_\pm + \frac{1}{2a^2}\frac{\partial \tilde{U}}{\partial \beta_\pm} = 0. \tag{2.9}$$

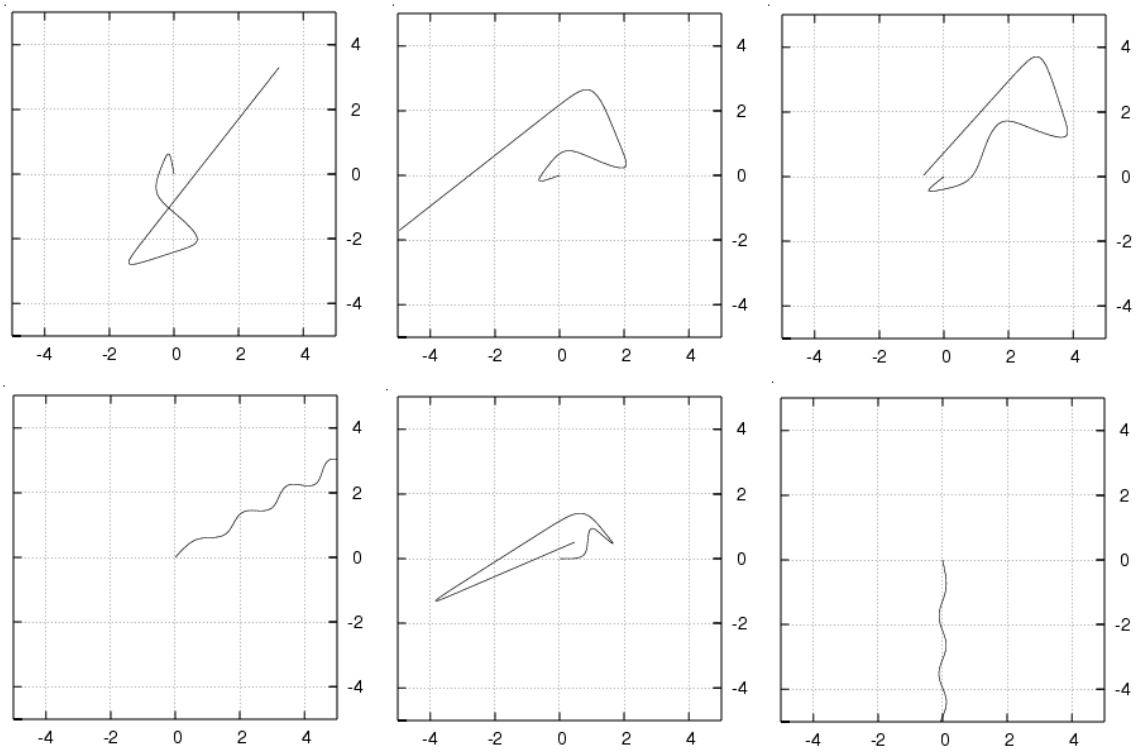

Figure 2.1: Trajectories of Mixmaster universes in the (β_+, β_-) plane. These plots represent a decrease in the scale factor a by $\sim 10^{-3}$.

Equations (2.8) and (2.9) provide a complete closed set of evolution equations for the Mixmaster universe. Some representative trajectories for these equations are given in Figure 2.1.

A vital consequence of (2.8) is that isotropic contraction is *not* possible. For isotropic contraction, we require that $\beta_\pm = \dot{\beta}_\pm = 0$. However, $\tilde{U} < 0$ for these values, and the effective Friedmann equation (2.8) implies that one may not simultaneously set $\dot{\beta}_\pm = 0$. The Mixmaster universe therefore inevitably evolves anisotropically. It illustrates that, when one includes new degrees of freedom beyond those of the FRW universe, the universe is rapidly driven away from the FRW solution.

The dynamics of the Mixmaster universe are quite complicated. As discussed in Appendix A, the potential $\tilde{U}$ is composed of a set of exponentially rising "walls." As

$a \to 0$, the point defined by the $\beta_\pm$ begins to move more and more rapidly, thanks to the gravitational blueshifting originating from the equation of motion (2.9). The point also begins bouncing off of the potential walls with ever–increasing frequency. It is possible to show that an infinite number of bounces occur before the big crunch is reached at $a = 0$. Thus in spacetime, the universe is expanding and contracting along different directions, with the rates of expansion and contraction changing ever more rapidly.

The Mixmaster universe is a useful example to have in mind since it is an exact solution to the Einstein equations which illustrates the instability of isotropic spacetimes near a big crunch. In the remainder of this chapter, we will both generalize the Mixmaster universe (by including non–homogeneous curvature) and simplify it, thus enabling us to distinguish between universes that undergo Mixmaster behavior and those that do not.

2.3 The Kasner Universe

In Section 2.2 we considered a universe without matter sources. Here we discuss the inclusion of matter sources and show that most types of matter *cannot* affect the dynamics near the big crunch. We will also show how the dynamics of the Mixmaster universe can be simplified and understood in terms of the Kasner metric, introduced in (2.4). Most of the calculations in this section will be carried out for a $(d + 1)$–dimensional spacetime, for later convenience. Our primary tool in this section will be the *equation of state*, denoted by w. We will see that w determines which quantities are relevant near a big crunch. Here, we focus on universes without spatial curvature, deferring the inclusion of curvature to Section 2.4.

We will focus on perfect fluid matter sources. These sources possess a stress–

energy tensor given by

$$T_\mu{}^\nu = (\rho + P)u_\mu u^\nu + P\delta_\mu{}^\nu \tag{2.10}$$

where ρ is the energy density, P the pressure, and u^μ the flow lines of the fluid. If the spacetime is homogeneous and isotropic, then we must have $u^\mu = (1, 0, \dots)$. The pressure and energy density are usefully parameterized by w, which is defined in terms of the pressure and energy density by

$$w = \frac{P}{\rho} = \frac{T_j{}^j}{-T_0{}^0}, \qquad \text{(no sum)} \tag{2.11}$$

Usually one considers equations of state that are constant, although w can vary with time.

The equation of state is useful for our purposes since it determines how the energy density scales with the volume of spatial slices. To include more general spacetimes, and in particular the anisotropic ones we focus on in the present work, we consider a general metric in synchronous gauge

$$\mathrm{d}s^2 = -\mathrm{d}t^2 + h^{(d)}_{ab}(t, \mathbf{x})\mathrm{d}x^a\mathrm{d}x^b \tag{2.12}$$

where $h^{(d)}_{ab}$ is the metric on the d–dimensional spatial slice. We will assume that the metric is compatible with the flow lines of the fluid, so that we can choose $u^\mu = (1, 0, \dots)$ while the metric is in synchronous form. Now define an *effective scale factor* a so that

$$a^{2d} = \det h^{(d)}(t, \mathbf{x}), \tag{2.13}$$

so that the volume of spatial slices varies with time as a^d. (Note that this coincides with the definition of a in the FRW universe). Further, it is useful to define an *effective Hubble parameter* H using (2.3) and the effective scale factor a. Then conservation of stress–energy for the perfect fluid implies that

$$\frac{d\ln(\rho)}{d\ln(a)} = -d\,(1 + w)\,, \tag{2.14}$$

which is valid if w varies with time. For constant equation of state w, one can integrate (2.14) and find that

$$\rho(a) = \frac{\rho_0}{a^X}, \qquad X = -d(1+w) \tag{2.15}$$

where ρ_0 is the energy density when $a = 1$. The simple relationship between w and the scaling of energy density with cosmic volume is quite useful for our discussion: we will frequently need to work in anisotropic spacetimes, and in the perfect fluid case the energy density of the sources depends only on the total volume of the spatial slices.

Next we consider a simple anisotropic metric which allows for differential expansion or contraction along different directions in spacetime. In Section 2.4 we will consider the addition of curvature in addition to anisotropy. A suitable choice is the Bianchi–I metric in $(d+1)$–dimensional spacetime

$$\mathrm{d}s^2 = -\mathrm{d}t^2 + a^2(t) \sum_{j=1}^{d} \exp\left(2\beta_j\right) \mathrm{d}x_j^2 \tag{2.16}$$

where the β_j are functions of time t. This is a generalization of the flat ($k = 0$) FRW metric (2.1). As in the Mixmaster universe we remove the degeneracy between a and the β_j through imposing the constraint

$$\sum_{j=1}^{d} \beta_j(t) = 0, \tag{2.17}$$

and therefore a satisfies the requirement of the effective scale factor (2.13). The Einstein equations arising from this metric are

$$\frac{d(d-1)}{2} \left(\frac{\dot{a}}{a}\right)^2 - \frac{1}{2} \sum_{j=1}^{d} \dot{\beta}_j^2 = \rho, \tag{2.18a}$$

$$\ddot{\beta}_j + d\frac{\dot{a}}{a}\dot{\beta}_j = 0 \tag{2.18b}$$

where we have included matter components with total energy density ρ. The second of these equations is similar to (2.9); the potential is absent since it arose from the

curvature of spatial slices in the Bianchi–IX metric, whereas the Bianchi–I metric considered here has flat spatial slices. Equation (2.18b) may be integrated to find

$$\dot{\beta}_j(t) = \frac{c_j}{a(t)^d} \tag{2.19}$$

for which the constraint on the β_j implies

$$\sum_{j=1}^{d} c_j = 0. \tag{2.20}$$

We next define the quantity $\rho_0^{(A)}$ via

$$\rho_0^{(A)} = \frac{1}{2}\sum_{j=1}^{d} c_j^2, \tag{2.21}$$

which measures the anisotropic nature of the contraction. When $\rho_0^{(A)} = 0$, the universe is perfectly isotropic. Note that $\rho_0^{(A)}$ is constant in time.

Using these results and definitions, the first of the Einstein equations may be rewritten as

$$\frac{d(d-1)}{2}\left(\frac{\dot{a}}{a}\right)^2 = \frac{\rho_0^{(A)}}{a^{2d}} + \sum_i \frac{\rho_0^{(i)}}{a^{d(1+w_i)}} \tag{2.22}$$

where we have assumed that the matter components all have constant equations of state w_i, and have energy densities $\rho_0^{(i)}$ at $a = 1$. Note that the resulting equation is precisely in the form of the Friedmann equation (2.2) but now with an additional term resulting from the anisotropic nature of the expansion. This new term enters in the same manner as a matter component with $w = 1$.

At this point we make a simple, yet crucial, observation: as $a \to 0$, the component with the largest value of w will dominate this Friedmann equation. Thanks to the presence of the anisotropy term in (2.22), all matter components are thus completely negligible near the big crunch, provided they all satisfy $w_i < 1$. This condition is satisfied for matter, radiation, homogeneous curvature, and the cosmological constant contributions to ρ, and therefore these sources are irrelevant near the big crunch. The

exceptions to this statement are quite important; the $w = 1$ exception possesses some important features which we will discuss below, and the $w > 1$ case will form the subject of the next chapter in this work.

Given that matter components with $w < 1$ become negligible near the big crunch, we can study the resulting asymptotic dynamics of this universe. This is where the Kasner metric will make its appearance. Dropping the source terms from (2.22) and using (2.19) one finds

$$a(t) \exp\left(\beta_j(t)\right) = (t/t_0)^{c_j+(1/d)} \tag{2.23}$$

which makes our original metric (2.16) precisely the same as the Kasner metric (2.4), under the identification

$$p_j = \frac{1}{d} + c_j \tag{2.24}$$

In this context, the first Kasner condition (2.5) results from the sum rule (2.20). The second is a consequence of the effective Friedmann equation (2.22) with matter sources neglected. These conditions are illustrated geometrically for $d = 3$ in Figure 2.2.

The arguments in this section have led us to two important conclusions. The first is that anisotropic (but flat) universes will tend to a Kasner universe near a big crunch. This occurs even in the presence of matter sources, provided they satisfy $w < 1$. The second relates to the behavior once the universe has entered the Kasner phase. As one can see from the Kasner conditions, isotropic contraction is impossible, there are no solutions to the Kasner conditions (2.5) with all of the exponents equal. Thus, we can conclude that, neglecting curvature, universes will tend to an anisotropic Kasner–like state near a big crunch.

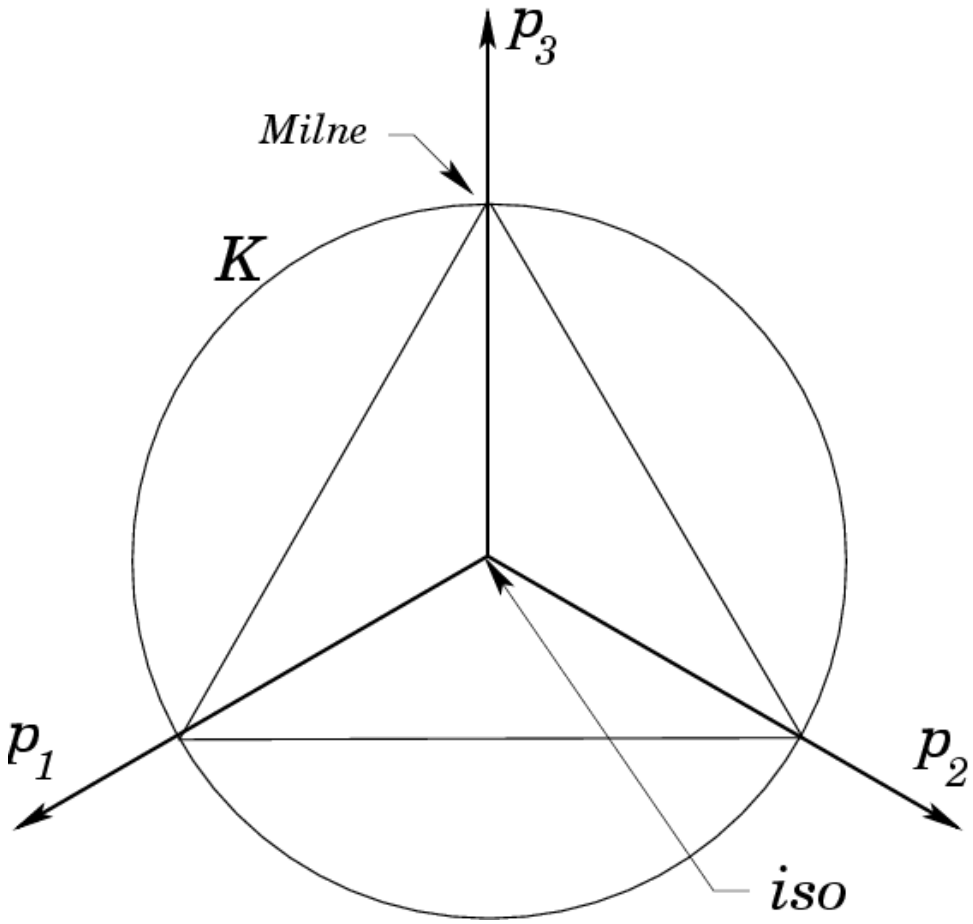

Figure 2.2: The $d = 3$ Kasner universe. We are looking at the origin in the $-(1, 1, 1)$ direction. The Kasner plane is illustrated by the triangle. The Kasner circle , where the Kasner conditions are satisfied, is shown by the circle labeled $\mathcal{K}$. Note that one Kasner exponent is always strictly negative, except where $\mathcal{K}$ intersects the axes at the points labeled "Milne." The isotropic solution, labeled "iso," is not among the solutions.

2.4 The Effects of Curvature

Having established the dynamics of universes without spatial curvature in Section 2.3, we now turn to the more general situation in which the spatial slices are curved. In this case, we will recover some of the features seen in the Mixmaster model. The effective Friedmann equation in anisotropic universes (2.22) features an effective energy density, scaling like $1/a^{2d}$, which depends on the anisotropy in the spacetime. This term dominated all of the other terms in the equation as $a \to 0$, since these terms scaled too slowly to dominate the anisotropy term. In the homogeneous and isotropic Friedmann universe, spatial curvature appears in the Friedmann equation in a term that scales like $1/a^2$. Thus by an identical argument it might seem as though curvature terms would grow too slowly to be relevant near the big crunch. In fact, the situation with curvature is rather more complicated, and in fact gives rise to significant effects not captured in the flat Kasner universe studied in Section 2.3. In this section we will explore these features, using as our tool the power law time dependence of various terms in the Einstein equations.

We begin by observing that the Kasner behavior is universal near a big crunch, as discussed in the Bianchi–I case in Section 2.3. To introduce curvature, we will use the *generalized Kasner metric*

$$\mathrm{d}s^2 = -\mathrm{d}t^2 + \sum_{j=1}^{d} (t/t_0)^{2p_j(\mathbf{x})} \left[\omega^j(\mathbf{x})\right]^2 \tag{2.25}$$

where

$$\omega^j(\mathbf{x}) = \omega(\mathbf{x})^j{}_k \mathrm{d}x^k. \tag{2.26}$$

are functions of the spatial coordinates $\mathbf{x}$, as are the Kasner exponents. This metric does not have a Bianchi type since we are not assuming homogeneous curvature of the spatial slices. With this metric, it is possible to study more general spacetimes in which equal time surfaces are inhomogeneously curved.

The generalized Kasner metric must satisfy the Einstein equations. Upon substitution of (2.25) into the Einstein equations, it is convenient to group the resulting terms into two types. The first type is terms involving only time derivatives of metric components. The second type includes all other terms; for example, those representing the intrinsic curvature of spatial slices, or gradients of the Kasner exponents. We will call this second type "spatial gradient terms." When the Einstein equations are decomposed in this way, one finds that the time derivative terms scale with cosmic time t as $1/t^2$. Thus we can represent each component of the Einstein equations schematically, at fixed spatial coordinate $\mathbf{x}$, as

$$\frac{A(\mathbf{x})}{t^2} + \sum_J \frac{B_J(\mathbf{x})}{t^{g_J(\mathbf{x})}} = 0 \tag{2.27}$$

where the index J runs over all spatial gradient terms, and the exponents $g_J(\mathbf{x})$ measures the scaling of each term with time. The coefficients $A(\mathbf{x})$ are different linear combinations of the Kasner conditions (2.5). If we neglect the spatial gradient terms $B(\mathbf{x})$ (as we did with the curvature–free Kasner metric in Section 2.3) then enforcing the Einstein equations (2.27) results in the familiar Kasner conditions (2.5).

When the spatial gradient terms are included, then the behavior of the metric (2.25) depends crucially on the values of the g_J relative to the threshold value of 2. We then have two cases:

- ***Case 1 (stable) with*** $g_J < 2$: In this case, the spatial gradient terms $B_J(\mathbf{x})$ scale more slowly than the time–derivative terms, and thus scale away to irrelevance as $t \to 0$. Because of this, the equations of motion at each spatial point $\mathbf{x}$ decouple from those of its neighbors – a phenomenon sometimes called *ultralocality*. To leading order in t, the Einstein equations are satisfied provided the Kasner conditions are. Therefore, each spatial point acts as an independent Kasner universe, although the specific Kasner exponents may vary from point

to point. In this sense, the generalized Kasner metric (2.25) is a kind of approximation, to leading order in t, of the behavior of generic solutions near the big crunch.

- ***Case 2 (unstable) with*** $g_J > 2$: When this is the case, then the pure time derivative terms $A(\mathbf{x})$ are no longer of leading order in t as $t \to 0$. Instead, the corresponding spatial gradient term grows rapidly enough to dominate the Einstein equations (2.27) as $t \to 0$. This means that the Kasner metric is no longer a leading–order approximate solution to the Einstein equations as $t \to 0$. If the spatial gradient terms $B(\mathbf{x})$ are initially subdominant, then the universe will be Kasner–like until they grow to dominate the Einstein equations. When this occurs, the Kasner behavior is modified.

To discover how the Kasner behavior is modified, it is instructive to return to the Mixmaster example, discussed in Section 2.2 and Appendix A. The Mixmaster universe shape parameters β_+ and β_- behave like the coordinates of a point mass moving in a triangular potential well. This potential well arose from the (homogeneous) curvature of the spatial slices. Near its minimum at $\beta_\pm = 0$, the potential well is nearly flat, and one can neglect its influence on the equations of motion for the $\beta_\pm$, (A.34) and (2.9). Thus one finds

$$\ddot{\beta}_\pm + 3\frac{\dot{a}}{a}\dot{\beta}_\pm = 0 \tag{2.28}$$

which is identical to the equations (2.18a) found for the β_j in Section 2.3. In fact, the $\beta_\pm$ are only different linear combinations of the β_j, and so in this regime the same solution goes through as found in the Bianchi–I case. Near the bottom of the potential well, or equivalently when it is nearly isotropic, the Mixmaster universe behaves like a Kasner universe. The straight–line trajectory of the (β_+, β_-) point in the Mixmaster example corresponds to a Kasner–like epoch of contraction. The exponents for the

corresponding Kasner universe are related to the velocity components of the point. This connection is made more explicit in Section 5.4.

The new features from curvature arise when the $\beta_\pm$ begin to climb one of the walls of the potential well. The point mass ceases to move in a straight line, but instead "bounces" off of the wall and returns to the neighborhood of the potential minimum. This corresponds to the end of one Kasner–like epoch, a rapid change in the Kasner exponents, and the beginning of a new Kasner–like epoch. We will term this phenomenon a *Kasner bounce*. In the context of our schematic Einstein equation (2.27), this corresponds to one of the spatial gradient terms dominating the Einstein equations, followed by a change in the g_J, possibly enabling other spatial gradient terms to dominate later on. For this reason, we will sometimes refer to the $B(\mathbf{x})$ terms in the Einstein equations, somewhat informally, as *dangerous terms*.

The generalized Kasner solution (2.25) enables one to express the conditions for a Kasner bounce (and resulting chaotic behavior) in a very simple manner. These conditions are known as the *gravitational stability conditions* (GSCs) [27, 33], take the form of a set of linear inequalities in the Kasner exponents, and are of essential importance for much of this work. Terms in the Einstein equations corresponding to spatial curvature all depend on the β_j through ratios of the scale factors $(t/t_0)^{2p_j}$ along different directions. (This can be seen explicitly for the Mixmaster example, and holds for the generalized Kasner metric as well). Thus returning to the schematic Einstein equations (2.27), one finds

$$J = \{ijk\}, \qquad g_J = 2(p_i + p_j - p_k) \tag{2.29}$$

where we have replaced our index J with a triple of (possibly duplicate) indices of Kasner exponents. As discussed above, the condition that these terms remain subdominant is that $g_J < 2$. This is equivalent to

$$p_i + p_j - p_k < 1, \qquad \text{for all } i, j, k. \tag{2.30}$$

These inequalities are the GSCs. When all the GSCs are satisfied, the universe follows smooth Kasner–like behavior to the big crunch; when they are violated, the spatial gradient terms $B(\mathbf{x})$ will dominate the universe, and it will undergo chaotic Mixmaster oscillations.

As we might expect from our experience with the Mixmaster example, it is impossible to satisfy the GSCs (2.30) and the Kasner conditions (2.5) simultaneously in the case $d = 3$. In this case, Einstein gravity in vacuum or with sources satisfying $w < 1$ will inevitably enter a Mixmaster phase. This conclusion also holds for all spatial dimensions up until $d = 10$, at which point it is now possible to satisfy both the Kasner and GSCs. Two simple solutions that *do* satisfy the Kasner conditions and GSCs when $d = 10$, and thus do not exhibit chaotic behavior, are

$$p_1 \dots p_3 = \frac{1 - \sqrt{21}}{10}, \qquad p_4 \dots p_{10} = \frac{7 + 3\sqrt{21}}{70} \tag{2.31}$$

which was first discussed by [33], and also

$$p_1 \dots p_4 = \frac{2 - 3\sqrt{6}}{20}, \qquad p_5 \dots p_{10} = \frac{1 + \sqrt{6}}{10} \tag{2.32}$$

These solutions are in fact representative points of open neighborhoods in the Kasner circle (which in this case is actually $\mathbf{S}^8$) for which these constraints are satisfied. In these neighborhoods, the contraction of the universe remains smooth and Kasner–like all the way to the big crunch. One can find similar solutions for spatial dimensions $d > 10$ as well: these open neighborhoods of the $d = 10$ Kasner circle can be trivially extended to higher dimensions by appending Kasner exponents $p_j = 0$ for $j > 10$. There has been some speculation that the vanishing of chaos in eleven spacetime dimensions is related to the fact that this is the maximal dimension for global supersymmetry. We will see below that this is just a coincidence, since the unique supergravity theory in $d = 10$ possesses additional matter fields which significantly change its chaotic properties.

Now that we have introduced the GSCs, we will also introduce some terminology that will enable us to describe the chaotic properties of a given theory. As described above, the Kasner conditions (2.5) for $(d+1)$–dimensional gravity define a sphere $\mathbf{S}^{d-2}$, which we have called the Kasner circle and will denote $\mathcal{K}$. Furthermore, there are open (but possibly empty) regions on the Kasner circle in which the GSCs are satisfied. Let us denote these regions by $\mathcal{S}$. Finally, there are points at which the GSCs are saturated, or in other words satisfied if all the "$>$" are replaced by "$\geq$." We will denote these points by $\overline{\mathcal{S}}$.

We will need to distinguish between models (currently, the only models are Einstein gravity in various dimensions, but later we will introduce matter content that comes along with its own stability conditions) and specific solutions to the Kasner conditions (points on the Kasner circle). First, we consider solutions:

- A solution $s \in \mathcal{K}$ is *non–chaotic* when $s \in \mathcal{S}$,
- A solution $s \in \mathcal{K}$ is *marginally chaotic* when $s \in \overline{\mathcal{S}}$ but $s \notin \mathcal{S}$.
- A solution $s \in \mathcal{K}$ is *chaotic* when $s \notin \mathcal{S}$.

An intuitive way to think about the marginally chaotic solutions is that they are somehow on the "boundary" of the set of non–chaotic solutions. However, since $\overline{\mathcal{S}}$ often contains isolated points it is not technically the boundary of $\mathcal{S}$. Note that the marginally chaotic solutions are considered a subset of the chaotic solutions. This is because arbitrarily small perturbations of a marginal solution puts it in the chaotic region. One important example of a marginal solution is the *Milne universe*, a solution of the Kasner conditions in any spacetime dimension with

$$p_1 = 1, \qquad p_2 = \cdots = p_d = 0, \tag{2.33}$$

which marginally satisfies the GSCs. This solution crops up frequently, and is relevant to the cyclic model that we will discuss in more detail in Section 3.1.2.

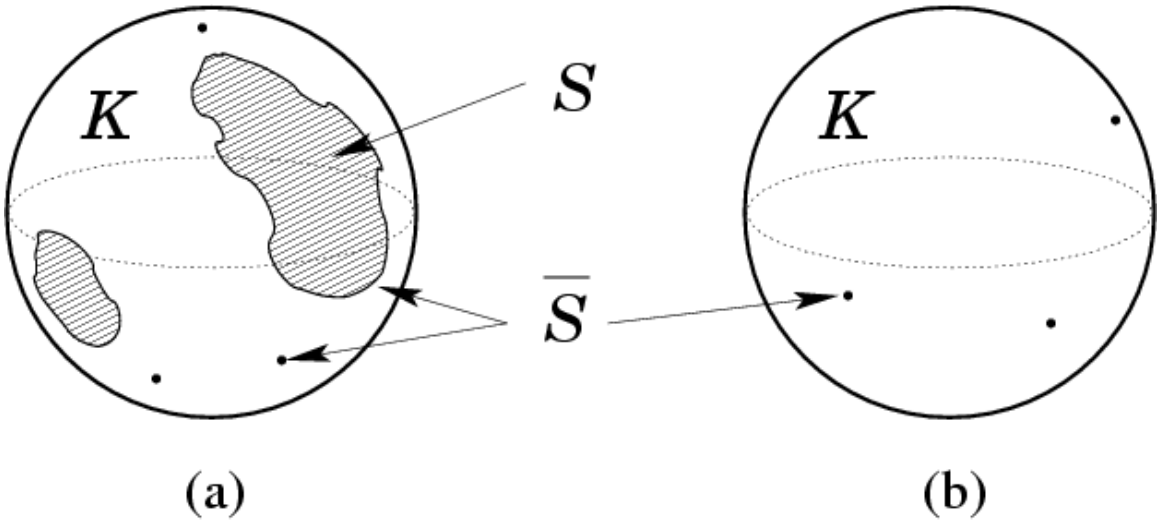

Figure 2.3: Various possibilities regarding the stability conditions on the Kasner circle $\mathcal{K}$. The stability conditions are satisfied in the region $\mathcal{S}$, (the shaded region) and saturated in $\overline{\mathcal{S}}$. (a) non–chaotic model. Note that $\overline{\mathcal{S}}$ includes not only the closure of $\mathcal{S}$ but also potentially isolated points. (b) a chaotic model, with possibly some points at which the stability conditions are marginally satisfied.

Moving on to models, we distinguish two types, depending on the nature of the solutions that they allow:

- A model is *chaotic* when $\mathcal{S}$ is empty,
- A model is *non–chaotic* when $\mathcal{S}$ is not empty.

These various possibilities are illustrated in Figure 2.3. Under this terminology, Einstein gravity in $d < 10$ is chaotic, since there are no solutions to the Kasner conditions and the GSCs. Furthermore, Einstein gravity in $d \geq 10$ is non–chaotic, since it possesses non–chaotic solutions, despite the fact that it possesses chaotic solutions as well.

2.5 p–forms and String Models

Up to now we have only discussed the properties of the Einstein equations in vacuum and with certain types of perfect fluid sources. Now we will consider an important class of matter components, the p–form fields. These are antisymmetric tensor fields with action

$$\mathcal{S}_{p-form} = -\frac{1}{(p+1)!}\int e^{\lambda\phi} F_{p+1}^2 \sqrt{-g}\; d^d x, \qquad F_{p+1} = \mathrm{d}A_p \tag{2.34}$$

where we have included an exponential coupling to a scalar field ϕ, with associated coupling constant λ. F_{p+1} is the field strength (by analogy to electromagnetism) and is a tensor with $p+1$ indices, while A_p is the potential, with p indices. In this work, we follow the convention that the "p" in p–form will refer to the number of indices on the gauge potential. String and supergravity models often contain p–form fields with precisely this type of exponential coupling to a scalar field, and so understanding the dynamics of these fields helps us better understand these models. As we will see below, the analysis of these matter sources result in p–form stability conditions and systems of inequalities quite similar to those found for the purely gravitational (or perfect fluid) case above.

2.5.1 $p = 0$: the free scalar

The presence of simple scalar field ϕ (which may also be considered a p–form with $p = 0$) significantly alters the behavior of the universe near a big crunch [9]. For the time being we will consider only the case where the scalar field is free – that is, is massless, has no potential, and has a canonical kinetic term. Assuming that this scalar field is homogeneous, the wave equation in the Kasner spacetime has the solution

$$\phi(t) = \phi_0 + p_\phi \ln(t/t_0) \tag{2.35}$$

with constants ϕ_0 and p_ϕ. For the homogeneous scalar field it is a simple matter to include the stress energy from ϕ into the Einstein equations. When this is done, the Kasner conditions (2.5) are modified to

$$\sum_{j=1}^{d} p_j = 1, \tag{2.36a}$$

$$\sum_{j=1}^{d} p_j^2 = 1 - p_\phi^2. \tag{2.36b}$$

The stability conditions remain unchanged after the addition of the scalar field.

The presence of the scalar field ϕ changes in the dynamics of the universe near the big crunch. For example, without the scalar field there are no isotropic solutions to the Kasner conditions. With the scalar field, such solutions are now possible. For example, the choice

$$p_\phi = \pm\sqrt{1 - \frac{1}{d}}, \qquad p_j = \frac{1}{d} \tag{2.37}$$

is an isotropic solution to the new Kasner conditions (2.36). In the presence of a free scalar, one can no longer conclude that the universe will be driven to anisotropy as the big crunch is approached. In addition, for the isotropic solution (and in a neighborhood thereof) the GSCs are satisfied. Therefore, it is no longer true that the universe inevitably enters a chaotic phase as it collapses. Instead, if enough of the energy density of the universe is in the form of the scalar field (or in other words, if $|p_\phi|$ is large enough) then chaos can be avoided. The maximum value of $|p_\phi|$ is given by the isotropic solution (2.37), and there exist solutions to the Kasner conditions (though not necessarily the GSCs) with $|p_\phi|$ varying from this value down to zero.

The essential difference between the behavior of the universe near the big crunch with and without the scalar field is that it is now possible to satisfy the gravitational stability conditions in any spacetime dimension, including the $d = 3$ case relevant for our universe. The scalar field can accomplish this for two reasons. For one, the energy density in a free scalar field scales like $1/t^2$, or $1/a^{2d}$. Equivalently, in the language

we have developed above, the free scalar field has $w = 1$. This is precisely the same dependence on cosmic volume as the leading–order terms in the Einstein equations. Therefore, while other matter sources grow too slowly near the crunch, the energy density in the scalar field is able to "keep pace" and thus influence the gravitational dynamics all the way to the crunch. This is reflected in the fact that the scalar field Kasner exponent p_ϕ appears in the Kasner conditions (2.36). Furthermore, the energy density associated with this field is isotropic, and therefore does not imprint or enhance any pre-existing anisotropy in the metric. Thus, the universe can remain isotropic all the way to the big crunch and chaos is avoided.

While it is possible when a scalar field present to avoid chaos near the big crunch, the presence of the scalar field alone is insufficient to guarantee stable contraction. For example, merely including a scalar field which is subdominant (for example, $|p_\phi| \ll 1$) it is still possible to satisfy the Kasner conditions (2.36) while violating the stability conditions. This state of affairs can be summarized by using the terminology introduced at the end of Section 2.4; Einstein gravity with a free scalar field is a non–chaotic model. The various possibilities with the free scalar field are represented in Figure 2.4.

2.5.2 $p > 0$: the re–emergence of chaos

While the addition of the scalar field can make it possible to avoid chaos near the big crunch, when more general p–form fields are also included then chaotic behavior can be restored [27, 33]. The equation of motion resulting from the p–form action (2.34) is

$$\left[\nabla \cdot (e^{\lambda\phi} F)\right]^{\mu_1\mu_2\cdots\mu_p} = 0. \tag{2.38}$$

This is supplemented by the Bianchi identity

$$[\mathrm{d}F]_{\mu_1\mu_2\cdots\mu_{p+2}} = 0, \tag{2.39}$$

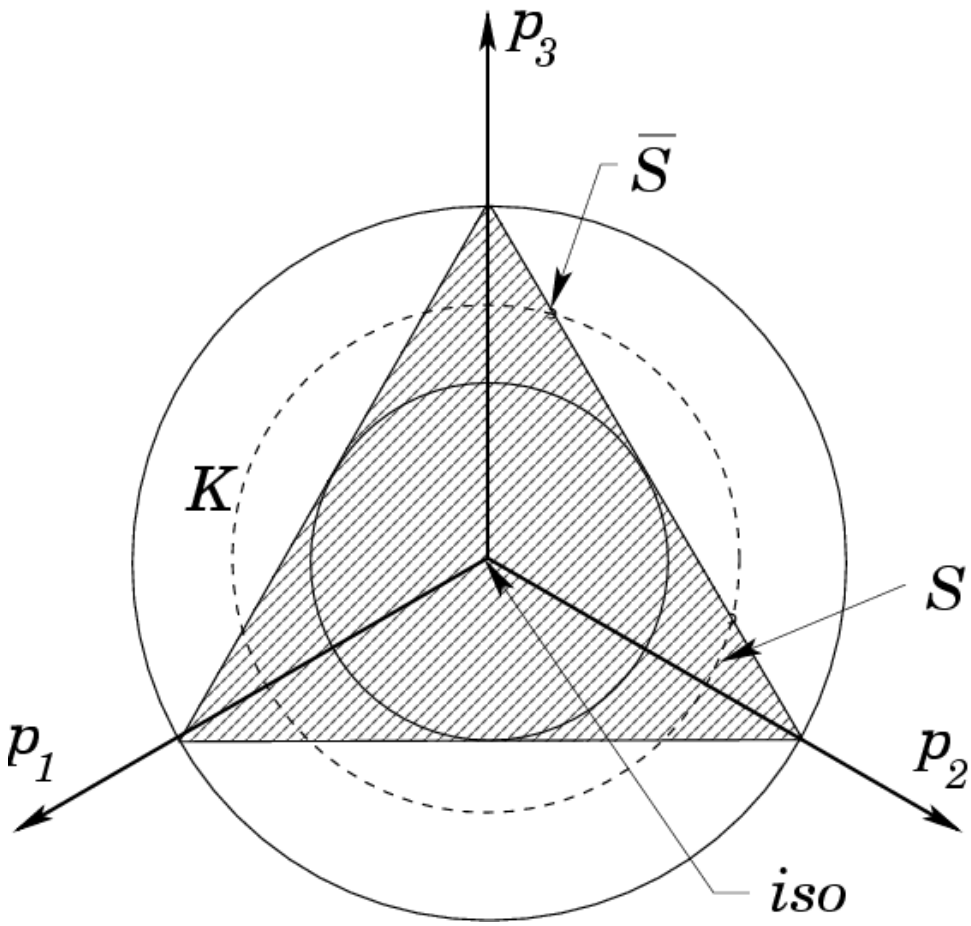

Figure 2.4: The $d = 3$ Kasner universe with a scalar field, *c.f.* Figure 2.2. We are looking at the origin in the $-(1, 1, 1)$ direction. The Kasner plane is shown by the triangle. Points in the shaded area satisfy the GSCs. . The radius of the Kasner sphere depends on p_ϕ which is suppressed in this plot. The Kasner circle $\mathcal{K}$ depends on the value of p_ϕ, and several examples are shown by the concentric circles.
(1): The outermost circle shows the Kasner circle $\mathcal{K}$ for the case $p_\phi = 0$.
(2): For $0 > p_\phi^2 > 1/2$, the Kasner circle $\mathcal{K}$ is illustrated by the middle (dashed) circle, and there are both chaotic and non–chaotic solutions. $\mathcal{S}$ denotes an arc along which the GSCs are satisfied, and $\overline{\mathcal{S}}$ are the points at which the GSCs are marginally satisfied, which all lie on the edge of the triangular shaded region.
(3): For $p_\phi^2 > 1/2$, $\mathcal{K}$ lies entirely within the shaded region, and thus all solutions are non–chaotic, illustrated by the innermost (solid) circle. The isotropic solution is also shown, labeled by "iso," for which p_ϕ^2 attains its maximum allowed value of $p_\phi^2 = 2/3$.

which is a consistency condition arising from the fact that $F = \mathrm{d}A$. Assuming the p–form field is homogeneous, these equations can be solved as follows, assuming a synchronous gauge metric as in (2.12). The equation of motion has the solution

$$F^{tj_1\cdots j_p}(t) = f^{j_1\cdots j_p}\frac{e^{-\lambda\phi}}{\sqrt{h}} \tag{2.40}$$

with $f^{j_1\cdots j_p}$ a constant and $\sqrt{h}$ the comoving volume element. These components of the p–form field (with exactly one time index) are referred to as the *electric* components, by analogy with electromagnetism. The Bianchi identity yields

$$F_{j_1\cdots j_{p+1}}(t) = b_{j_1\cdots j_{p+1}}, \tag{2.41}$$

where $b_{j_1\cdots j_{p+1}}$ is constant. Again by analogy with electromagnetism, these components of F (with all spatial indices) are referred to as the *magnetic* components of the p–form field.

Unlike the scalar field, if a p–form comes to dominate the energy density of the universe, it tends to drive it to anisotropic contraction and thus chaos. This arises from the fact that p–forms with $p > 0$ have anisotropic stress energy tensors; specifically

$$T_\mu{}^\nu = \frac{e^{\lambda\phi}}{(p+1)!}\left[F_{\mu\alpha_1\ldots\alpha_p}F^{\nu\alpha_1\ldots\alpha_p} - \frac{1}{2}\delta_\mu{}^\nu F^2\right] \tag{2.42}$$

Except for the scalar field ($p = 0$) these are always anisotropic. Therefore metrics that are isotropic cannot satisfy the Einstein equations in the presence of a source of this type.

The physics in the presence of p–forms turns out to be similar to the situation with curvature. As we will see in Section 2.6, p–forms lead to new potential walls, and the occurrence of Kasner bounces.. Therefore, in order to ensure smooth and Kasner–like contraction to a big crunch, we must ensure that p–form energy densities remain subdominant. Using the Kasner metric (2.4) and following a similar analysis

as in Section 2.3, this requirement is expressed as the inequalities

$$\sum_{j\in\langle p\rangle} p_j - \frac{\lambda p_\phi}{2} > 0, \tag{2.43a}$$

$$\sum_{j\in\langle p+1\rangle} p_j - \frac{\lambda p_\phi}{2} < 1. \tag{2.43b}$$

The notation $\langle n\rangle$ refers to a set of n indices with values from $1\ldots d$, necessarily all different. There is one stability condition for each such set. The first of these inequalities is known as the *electric stability condition* (ESCs), and the latter as the *magnetic stability condition* (MSCs).

A natural application of these results is to the menu of p–forms present in the low–energy effective actions of superstring theories and M–theory (eleven–dimensional supergravity). Each of the superstring theories includes a scalar field (the dilaton) and some include multiple scalars (such as Type IIB). As per our discussion above, the inclusion of this scalar enables one to satisfy the gravitational stability conditions. However, one must also take the other p–form fields into account, and when this is done it is impossible to simultaneously satisfy the electric and magnetic stability conditions (2.43) [26]. Therefore, all of the superstring models are inevitably chaotic near a big crunch. In the case of M–theory, there is no scalar field, but one might hope that since $d = 10$ pure gravity possesses stable solutions even in the absence of a scalar field, M–theory might enjoy similar properties. In fact, thanks to the presence of a three–form in M–theory, it is in fact impossible to satisfy the stability conditions in this case, and M–theory is inevitably chaotic as well.

2.6 Billiard Representation

The billiard representation provides yet another view on the dynamics of the universe near the big crunch [25, 28, 29]. It complements the approach using the Kasner

solution, in that the billiard representation allows us to study the dynamics of the Kasner bounces. We have already seen in Section 2.2 that the behavior of the Bianchi–IX model is given by the motion of a point in a potential. With the reparameterization we will describe below, the dynamics of the universe become even simpler. Near the big crunch, the potential reduces to a set of sharp walls, and so the point undergoes geodesic motion between specular reflections from the walls. For a detailed derivation of this viewpoint in the Mixmaster universe, see Appendix A, especially Section A.3. We will also rely heavily on this representation in Chapter 5.

We begin with the Mixmaster metric (2.6) and define new variables γ^j through

$$\gamma^j = \ln(a) + \beta_j \tag{2.44}$$

and the "supermetric" given by

$$G_{jk} = 2\begin{pmatrix} 0 & -1 & -1 \\ -1 & 0 & -1 \\ -1 & -1 & 0 \end{pmatrix} \tag{2.45}$$

which is seen to have a Lorentzian signature $(-++)$. We next define variables r, y^i through

$$r^2 = -G_{jk}\gamma^j\gamma^k, \qquad y^j = r^{-1}\gamma^j. \tag{2.46}$$

Note that as $a \to 0$, $r \to \infty$. Furthermore, since $G_{jk}y^jy^k = -1$, the y^j are constrained to lie on the future unit hyperboloid. Finally, we define a new time coordinate T related to proper time intervals $\mathrm{d}s$ through

$$\mathrm{d}s = r^2 \exp\left(\sum_j \gamma^j\right) \mathrm{d}T \tag{2.47}$$

With these definition, one finds that the dynamics of these variables is given by the variation of the following effective action

$$\mathcal{S}_{eff}[r, y^j] = \int \left(-\frac{1}{2}\left[\frac{d\ln r}{dT}\right]^2 + \frac{1}{2}G_{jk}\frac{dy^j}{dT}\frac{dy^k}{dT} - V_T(r, y^j)\right) dT \tag{2.48}$$

In the $r \to \infty$ limit, the potential V_T is given by

$$V_T(r, y^j) \sim \sum_A c_A \Theta\left(\left[w_A\right]_j y^j\right) \tag{2.49}$$

where $\Theta(x) = 0$ for $x < 0$, and $\Theta(x) = \infty$ for $x > 0$, and the $c_A > 0$. The potential describes a set of sharp walls, at positions given by the vectors w_A.

Taken together, the action (2.48) describes the geodesic motion of a billiard on a hyperboloid, undergoing specular reflections from a set of sharp walls defined by the w_A. Thanks to the ultralocal property of gravity near a big crunch, one can think about each spatial point as decoupling from its neighbors, and is described by its own independent billiard system. A remarkable property of the walls is that the vectors w_A are precisely the root lattice of the hyperbolic Kac–Moody algebra AE_3. It has been shown that the walls for vacuum Einstein gravity are described by the root lattice of AE_d for arbitrary dimension, which is hyperbolic for $d < 10$. Any p–forms that are present lead to additional walls, and it is known that the full set of walls for the low energy spectrum of string models are described by the root lattices of the hyperbolic algebras E_{10} and BE_{10}. It has been observed that a gravitational theory is chaotic precisely when the underlying Kac–Moody root lattice is hyperbolic [28]. Thus, in addition to providing a useful visualization of the dynamics we wish to study, th billiard representation hints at some deep properties of gravitational systems.

2.7 Summary

In this Chapter we have reviewed the fundamentals of dynamics near a big crunch singularity. The universe's dynamics are typically chaotic, and this behavior is robust through many spacetime dimensions and various types of matter content. Remarkably, much of the dynamics of this strongly gravitating, time–dependent system can be understood using the simple Kasner metric.

The most important results of this chapter are the various stability conditions, (2.30) and (2.43). These conditions enable us to determine the chaotic properties of a given model by searching for a solution to a set of inequalities. These stability conditions will be a crucial tool in the following chapters.

Chapter 3

Eliminating Chaos with $w > 1$

...then raise
From the conflagrant mass, purged and refined
New heav'ns, new earth, ages of endless date...

Paradise Lost Book XII, lines 548–549, [90]

Progress in string and M–theory models have led to the development of new possibilities for the cosmology of the early universe. Recently a model of the universe in which it undergoes an infinite series of cycles has been proposed [108]. This model, and indeed any cyclic model, must deal with the potential presence of chaos during its collapsing phase, for Mixmaster oscillations during the contracting phase can easily destroy the homogeneity and isotropy required for a viable cosmological model. In this chapter we will describe a mechanism by which chaos can be avoided. We will show that if the universe contains a matter component with equation of state $w > 1$, then it can contract smoothly and non–chaotically to the big crunch. It is especially relevant to the cyclic universe model since the additional elements required to avoid chaos are already present in the model!

We introduce the essential elements of the cyclic model in Section 3.1. We also

describe how its embedding in a M–theory framework enables it to avoid the problems that have plagued previous attempts at periodic cosmological models. Section 3.2 is the core result of this chapter. We use the tools developed in the previous chapter to show that a perfect fluid matter component with $w > 1$ can eliminate chaos during the collapsing phase. Intriguingly, such a component is already present in the cyclic model. We also describe how this new matter component can eliminate chaos due to p–form fields. Depending on the p–forms that are present, this may require a threshold value of w greater than unity, and we give expressions for the new threshold value. In Section 3.3 we go on to consider the problem of realizing the $w > 1$ component in the context of a higher dimensional theory. We consider the more general problem of realizing a matter component with given equation of state w in a general Kaluza–Klein (KK) compactification. Focusing on the case where the perfect fluid component is realized as the volume modulus of a KK compactification, we find that a four–dimensional solution with a given w can only be realized as the compactification of a discrete family of equivalent higher–dimensional geometries. We give the behavior of the higher–dimensional metric, the relationship between proper times in the higher and lower–dimensional frames, and the stress–energy required in the higher–dimensional theory. We conclude in Section 3.4.

In this chapter, Section 3.1 is a review of part of the literature. Section 3.2 represents published work by the author and collaborators [43]. The results in Section 3.3 are unpublished work by the author.

3.1 The Cyclic Universe

In this section we will give an introduction to the recently proposed cyclic universe model. We will begin with a brief review of some of the historical ideas surrounding cyclic universes in Section 3.1.1. This primarily useful as it shows that it is quite

difficult to accommodate models of this type in the context of conventional physics. We go on to describe a new idea for a cyclic universe in Section 3.1.2 which avoids some of the difficulties encountered in past attempts.

3.1.1 Some previous attempts

There are several logical possibilities for the overall history of the cosmos. A convenient enumeration is provided by Tolman [116]. The universe may:

- ***Type 1***: Evolve for some range of time (finite, semi–infinite, or infinite),
- ***Type 2***: Exist in a steady state,
- ***Type 3***: Undergo periodic or "cyclic" behavior.

The current consensus cosmological model is of the first type. Observations to date, along with minimal theoretical assumptions, indicate that cosmic history began roughly 13.7 billion years ago, and the universe will continue to evolve into the indefinite future. The strength of this consensus model is its experimentally verified predictions for the cosmic microwave background (CMB) [70, 106], the abundance of light elements produced in big bang nucleosynthesis (BBN), [107, 121] and the details of large–scale structure formation.

Models of the second type have been considered in the past. However, they appear to have insurmountable difficulties in explaining current observations. As one example, it is not possible to explain the CMB and its precisely thermal spectrum in the context of these models [96]. In addition, it is quite difficult to explain the light element abundances without BBN.

An early example of a model of the third type was considered by Tolman [116]. He begins by assuming a FRW universe whose scale factor oscillates periodically between a maximum value a_{max} and a minimum value a_{min}, both of which are nonzero.

Because this universe is supposed to be periodic, the total entropy cannot increase from cycle to cycle. Along with the second law of thermodynamics, this requires that the total entropy S (or the entropy in some finite comoving volume) is related to the scale factor a by

$$S(a) = \frac{S_0}{a^3} \tag{3.1}$$

with S_0 a constant. The evolution of the universe is therefore perfectly adiabatic.

Following Tolman we can quickly exclude this possibility, as it requires unrealistic matter sources. We assume that the universe is flat, as required by observation. Using the Friedmann equation (2.2) and the conservation equation we find

$$\dot{H} = -\frac{1}{2}(\rho + P) \tag{3.2}$$

where ρ and P denote the total energy density and pressure of all matter components. At a_{min}, we require $H = 0$, as well as $\dot{H} > 0$ in order to reverse the contraction. This implies the conditions

$$\rho_{min} = 0, \qquad P_{min} < 0 \tag{3.3}$$

which requires a very unusual form of matter [77]. The situation is not substantially improved by the addition of curvature [116], which at any rate is forbidden by experiment.

Tolman next considers another possibility whereby we allow $a_{min} = 0$. Since the Einstein equations break down at this minimum a, Tolman argues that there is no constraint on ρ and P at a_{min}. Tolman makes the further assumption that, while the Einstein equations break down, the universe should continue smoothly into a subsequent expanding phase. Nevertheless, even granting this assumption, there is a problem: we do not expect the adiabaticity assumption to hold all the way to $a = 0$. Adiabaticity can only hold if the rate Γ of reactions keeping the matter species in equilibrium satisfies $\Gamma \gg H$. As $a \to 0$, $H \to \infty$ and so at some point all reactions

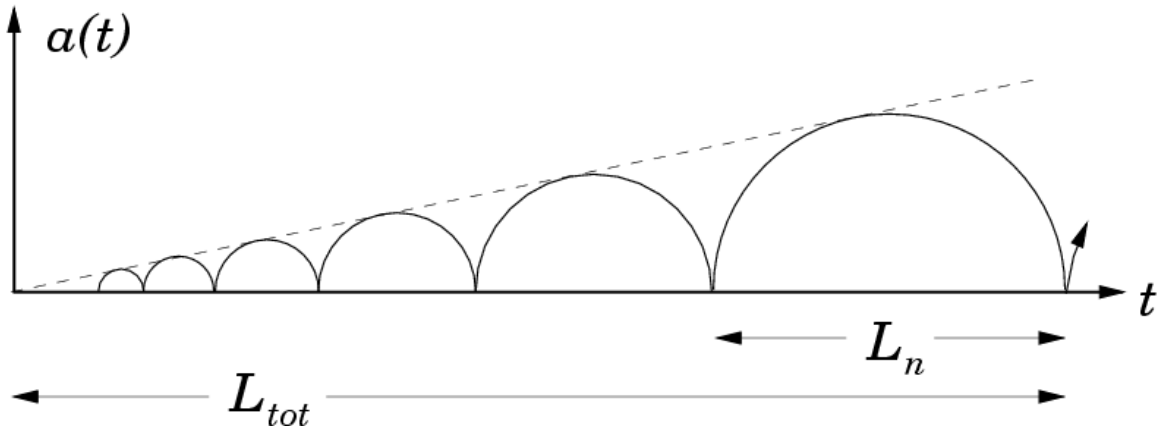

Figure 3.1: Tolman's "periodic" universe. Entropy increases with each big crunch/big bang would lead to the lifetime and maximum size of the universe increasing with each cycle. Thus, the total lifetime of the universe would be finite.

should fall out of thermal equilibrium [81]. Thus, thermodynamically irreversible processes will occur, and the entropy of the universe should increase with each pass through this big bang/big crunch transition [117].

This increase leads to a finite total lifetime of the universe. Let us suppose for simplicity that we have a radiation–dominated closed universe, and denote the total entropy during the n^{th} cycle by $S_0^{(n)}$. Suppose the entropy density increases by a factor $A^{3/2}$ during each cycle, (this exponent is chosen for later convenience) so that

$$S_0^{(n+1)} = A^{3/2} S_0^{(n)}, \qquad A > 1. \tag{3.4}$$

We expect that A will be a constant from cycle to cycle, since the physics will be identical each time. Now for our universe we have the Friedmann equation

$$3\left(\frac{\dot{a}}{a}\right)^2 = \frac{\rho_0^{(rad)}}{a^4} - \frac{3k}{a^2}, \qquad \rho_0^{(rad)} \sim \left[S_0^{(n)}\right]^{4/3} \tag{3.5}$$

This is is invariant under the transformation

$$S_0 \to A^{3/2} S_0, \qquad a \to Aa, \qquad t \to At \tag{3.6}$$

Therefore, if the universe has lifetime L_n for the n^{th} cycle, then its lifetime during the next cycle will be

$$L_{n+1} = AL_n \tag{3.7}$$

Now, thanks to this geometric progression, the total lifetime of the universe L_{tot} will be finite. Explicitly, if we are near the end of the n^{th} cycle, the total lifetime of the universe is

$$L_{tot} = L_n + L_{n-1} + \cdots = \frac{L_n}{1-A}. \tag{3.8}$$

The behavior of Tolman's solution is illustrated in Figure 3.1. Recalling the classification of cosmological histories on page 37, we see that in attempting to construct a cyclic model (type 3), we have failed to do anything other than create a baroque and problematic model with a finite lifetime (type 1). Perhaps the most serious of the problems we have introduced is that of passing through a big crunch singularity, and it is not at all clear how this is possible in the context of Einstein gravity.

3.1.2 The cyclic model

A way to construct a cyclic universe model that evades these problems is provided if we work within the context of string models. One example [77, 78, 79, 80, 108, 109] is framed in the context of heterotic M–theory [67, 68, 87]. This model postulates a compact extra dimension which is bounded on either end by infinite orbifold planes, as in Figure 3.2. There are six other compact dimensions, but these are not important for the construction of this model, and so we will neglect them. Matter fields (such as Standard Model particles) are confined to these planes.

In the five–dimensional description [78], the two orbifold planes are located at positions y_+, y_-. The five–dimensional bulk is warped, with metric

$$\mathrm{d}s^2 = W^2\left(-N^2\mathrm{d}t^2 + \mathrm{d}x_3^2\right) + \mathrm{d}y^2, \qquad W = \exp\left(y/L\right), \quad y_- \leq y \leq y_+, \tag{3.9}$$

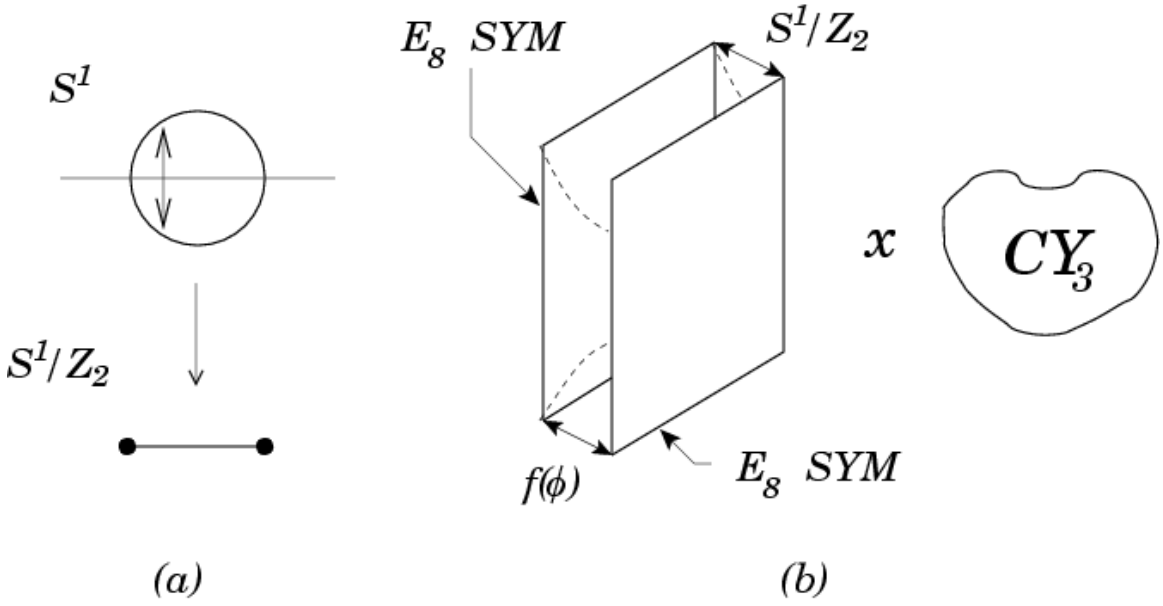

Figure 3.2: The structure of (a) the $\mathbf{S}^1/\mathbb{Z}_2$ orbifold and (b) the full eleven–dimensional spacetime in heterotic M–theory.

where the constant L is the curvature radius of the bulk space. The scale factors for the FRW geometry induced on each plane are given by

$$a_\pm = \exp\left(y_\pm/L\right). \tag{3.10}$$

It is convenient to change coordinates to

$$a_+ = a\cosh f, \qquad a_- = a\sinh f \tag{3.11}$$

where $a^2 = a_+^2 - a_-^2$. The separation between the branes is

$$L\ln\left(\frac{a_+}{a_-}\right) = L\ln\left(\coth f\right) \tag{3.12}$$

The field f is related to a canonically normalized scalar field ϕ that appears after KK compactification. With this parameterization, a is the Einstein frame scale factor in the four–dimensional theory after KK reduction. (We discuss the Einstein frame in more detail in Section 3.3). However, matter confined to the planes only couples to $a_\pm$. Thus gravity behaves slightly differently than normal Einstein gravity, thanks

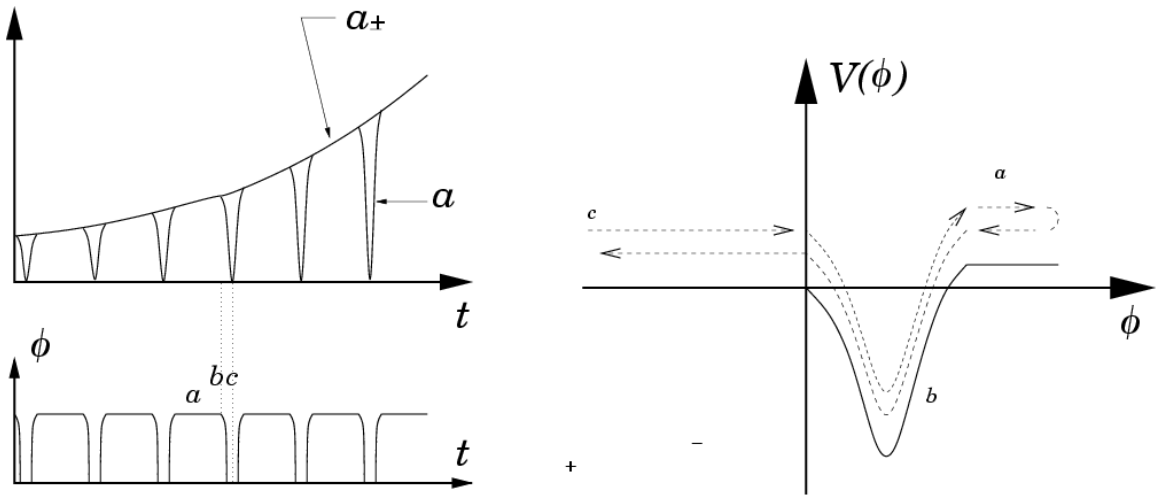

Figure 3.3: Evolution of the orbifold plane scale factor a_+, the four–dimensional Einstein frame scale factor a, and the scalar field ϕ during many cycles of the cyclic universe. The scale factors have an exponential envelope: *c.f.* Figure 3.1. The vertical scale is somewhat suppressed for clarity: many e–folds of expansion occur between cycles. Curently the field is nearly static (a), but then the universe undergoes a collapse (b) during which time the scale invariant perturbation spectrum is generated. The field ϕ travels to minus infinity and returns (corresponding to the orbifold planes colliding and rebounding) and returns to (a).

to the presence of the orbifold planes: the Einstein–Hilbert action is a function of a, while the FRW metrics corresponding to $a_\pm$ appear in the matter field Lagrangians.

We can describe a full cycle of the cyclic model by starting with the present day. This cycle is illustrated in Figure 3.3. During the present epoch, the distance between the two planes is approximately constant, and the scale factor a is undergoing exponential expansion, as current observations seem to indicate. The universe enters a contracting phase when the planes begin to move together. Quantum fluctuations on the planes are amplified during this contracting phase. The planes collide, and then return to their original fixed positions. The fluctuations established during the contracting phase grow and seed structure formation during the next cycle. BBN and the formation of the CMB goes through exactly as in the conventional cosmological model. Eventually, a cosmological constant comes to dominate the universe, and it

enters an accelerating phase similar to the present day, and the cycle can begin anew.

This model easily evades the problems of the Tolman universe. During the contracting phase, the Einstein frame scale factor $a \to 0$. However, the branes are moving together, and as their proper distance goes to zero, $f \to \infty$, and the orbifold plane scale factors $a_\pm$ are approximately constant. Even though a is the Einstein frame scale factor in the four–dimensional theory, the metric appearing in the matter field Lagrangian is that corresponding to $a_\pm$, and so as far as these fields are concerned there is no singularity since $a_\pm$ remains finite throughout this process (see the upper left panel of Figure 3.3). Furthermore, any entropy that is produced will be diluted away when the universe begins another epoch of exponential expansion. Viewed over many cycles, $a_\pm$ is a function which, for the most part, is well described by an exponential envelope function corresponding to eternal de Sitter expansion. Unlike the Tolman universe, the lifetime of each cycle L_n is therefore the same, and the age of the universe is infinite.

Another important feature of this model is the possibility of a smooth and non-singular big crunch/big bang transition. If all we had was the four–dimensional theory, the situation would be no better than in the Tolman universe. However, the four–dimensional effective theory is only a kind of projection of the higher dimensional theory. In this viewpoint, there are no curvature singularities: there is only an (time–dependent) orbifold singularity. String theory has made sense of orbifold singularities similar to, though not identical to, the one appearing when the branes come together. Much work has been done developing the precise matching prescription for fields across $t = 0$ [113, 114]. Nonetheless some controversy remains regarding whether it is possible to smoothly pass through this transition [77, 85, 86, 119].

In this model, a spectrum of nearly scale invariant density fluctuations is produced. It is more convenient to see this from the four dimensional perspective. Here, there is

a potential $V(\phi)$ for the scalar field ϕ. This has the higher dimensional interpretation of an attractive force between the orbifold planes. The condition for a nearly scale invariant spectrum of density fluctuations is that, while modes of cosmological interest are leaving the horizon, we have

$$\frac{1}{2}\dot{\phi}^2 \approx -V(\phi) \tag{3.13}$$

or $w \gg 1$ [17, 52]. The cyclic model differs from inflationary models in that it produces a very small spectrum of gravitational waves at observable scales [16, 79].

3.2 Chaos and a $w > 1$ Component

In the previous chapter (and especially in Section 2.3) we have discussed perfect fluids with $w \leq 1$. We found that fluids with $w < 1$ inevitably scale away to irrelevance as the universe contracts, and thus do not affect the emergence of chaos near the big crunch. Fluids with $w = 1$, such as a free scalar field, scale just rapidly enough to affect the emergence of chaos in certain cases. We will now explore the case where $w > 1$. The salient feature here is that it is now possible to eliminate chaos completely near the big crunch [43].

Fortunately most of the machinery that we require to discuss this result has already been developed in Chapter 2, and so we need only extend the results quoted there to the $w > 1$ case. In Section 3.2.1 we discuss the flat, anisotropic solution with a $w > 1$ component. In Sections 3.2.2 and 3.2.3 we discuss the stability of this solution to gravitational and p–form chaos. In these sections we show that all of the forms of chaos we have discussed can be eliminated by including a component with $w > w_{crit}$, where $w_{crit} > 1$ and depends on the theory under consideration.

3.2.1 The $w > 1$ Bianchi–I solution

The effects of a $w > 1$ component are most readily seen in the context of the flat Bianchi–I metric (2.16) first introduced in Section 2.3. For convenience, we will repeat some of the formulae from that section here. The metric (2.16) is

$$\mathrm{d}s^2 = -\mathrm{d}t^2 + a(t)^2 \sum_{j=1}^{d} \exp\left(2\beta_j\right) \mathrm{d}x_j^2 \tag{3.14}$$

and the corresponding effective Friedmann equation (2.22) resulting from this metric is

$$\frac{d(d-1)}{2}\left(\frac{\dot{a}}{a}\right)^2 = \frac{\rho_0^{(A)}}{a^{2d}} + \sum_i \frac{\rho_0^{(i)}}{a^{d(1+w_i)}}, \tag{3.15}$$

where $\rho_0^{(A)}$ is a constant measuring the anisotropy in the metric. Here we have only a single fluid with equation of state w sourcing the gravitational field, and thus we will suppress the summation over multiple fluids in the following. The equations for the β_j result in

$$\beta_j(a) = c_j \left(\frac{d(d-1)}{2}\right)^{1/2} \int_{a'=1}^{a} \left[\rho_0^{(A)} + \rho_0 (a')^{d(1-w)}\right]^{-1/2} \frac{da'}{a'} \tag{3.16}$$

where we have chosen the constants of integration so that $\beta_j = 0$ when $a = 1$. So far, everything has been completely general for any w greater or less than unity.

In Chapter 2 we considered matter components with $w < 1$, for which the matter term in (3.15) became irrelevant as $a \to 0$, and the effective Friedmann equation is dominated by the anisotropy term. When a $w > 1$ component is present, the opposite occurs; it is the anisotropy term that becomes negligible, and the Friedmann equation is dominated by the perfect fluid term instead. In this case, as $a \to 0$, we neglect the anisotropy term in (3.15) and (3.16) to find

$$a(t) = \left(\frac{t}{t_0}\right)^{2/[d(1+w)]}, \tag{3.17a}$$

$$\beta_j(t) = \frac{c_j}{w-1}\left[\frac{2}{\rho_0}\left(1 - \frac{1}{d}\right)\right]^{1/2}\left[\left(\frac{t}{t_0}\right)^{(w-1)/(w+1)} - 1\right] \tag{3.17b}$$

The integration constants in this solution are chosen so that $a = 1$ and $\beta_j = 0$ at a fixed reference time t_0.

This solution possesses the surprising feature that, unlike the $w < 1$ case, the universe becomes more isotropic as the big crunch is approached. The key is the exponent appearing in the expression for $\beta_j(t)$ in (3.17). When $w < 1$ this exponent is negative, and thus $\beta_j \to \infty$ near the big crunch. On the other hand, when $w > 1$, the exponent is positive, and thus β_j remain finite as $t \to 0$. Similar behavior may be seen in the general solution for $\beta_j(a)$ given in (3.16). The β_j will remain finite so long as the integral in (3.16) converges, which requires $w > 1$.

3.2.2 Gravitational Stability

Using our analysis of the $w < 1$ case as a template, we now show that the inclusion of a $w > 1$ component automatically ensures that the GSCs are satisfied. In our discussion of the free scalar field (see Section 2.5), we found that this field allowed an isotropic solution to the Kasner conditions (2.37), and this isotropic solution satisfied the GSCs. The fact that including a $w > 1$ component drives the universe to isotropy suggests that we might eliminate chaos through a similar mechanism.

In Section 2.4, we derived the GSCs by using the generalized Kasner metric (2.25), which is modeled on the Bianchi–I metric (2.16). The generalized metric is obtained by starting with the exact Bianchi–I solution and replacing

$$\mathrm{d}x^j \to \omega^j(\mathbf{x}) = \omega^j{}_k(\mathbf{x})\mathrm{d}x^k. \tag{3.18}$$

The GSCs arise as the conditions that the resulting metric is a leading–order approximation to the exact solution of the Einstein equations. As in the analysis given in Section 2.4, terms in the Einstein equations may be divided into those arising from

time derivatives and those involving spatial derivatives as

$$\frac{A(\mathbf{x})}{t^2} + \sum_J B_J(t, \mathbf{x}) = 0, \tag{3.19}$$

which should be compared to (2.27). The condition that the generalized Kasner metric is the leading–order approximation to the exact solution is that the B_J terms can be neglected as $t \to 0$, or equivalently that

$$t^2 B_J(t, \mathbf{x}) \to 0 \qquad \text{as} \qquad t \to 0. \tag{3.20}$$

If one computes the terms B_J, one finds they are all of the form

$$B_J(t, \mathbf{x}) = \frac{B_J(\mathbf{x})}{a(t)^2} \exp\left(2\beta_i - 2\beta_j - 2\beta_k\right) \tag{3.21}$$

where $J = \{ijk\}$ is a tuple of indices, not necessarily all distinct. Now using this result in our condition (3.20) we find

$$t^2 B_J(t, \mathbf{x}) \sim t^{2q} \qquad \text{where} \qquad q = 1 - \frac{2}{d(1+w)} > 0. \tag{3.22}$$

Because the exponent q is positive, then when $w > 1$ we are guaranteed that the B–terms will remain subdominant all the way to the big crunch. Therefore, chaos will be absent in these models.

3.2.3 p–form Stability

We have now demonstrated that in the case of pure Einstein gravity, a matter component with $w > 1$ can ensure that chaos is absent during a collapsing phase. In this section, we will consider the case where other forms of matter, specifically the p–form fields introduced in the last chapter, are present. We will show that a matter component with $w > 1$ can still ensure stable contraction. In the purely gravitational case, we found that w need only be larger than unity to eliminate chaos. In the p–form case, we will find a threshold equation of state, denoted $w_{crit}(p, \lambda)$, such that

chaos is eliminated for $w > w_{crit}(p, \lambda)$. If many p–forms are present, then chaos will be absent if w exceeds the largest w_{crit}. Showing this to be the case, and finding the critical w, is the purpose of this section.

Essentially, the presence of a $w > 1$ component can eliminate p–form chaos because it drives the universe to isotropy. Recall that p–forms in an anisotropic universe promote chaotic behavior for two essential reasons. First, the p–form stress energy tensor is anisotropic, and thus it tends to enhance anisotropy of the gravitational background if its energy density dominates. Secondly, the energy density of different p–form components grow at different rates, depending on precisely which spatial directions appear in the indices associated to each component. Therefore, anisotropy can enhance the growth of the energy density in some p–form components.

There are several possible cases we can consider. For example, we have the choice of whether:

- ***Case 1***: The p–forms are coupled to the $w > 1$ component only through the background spacetime. That is, we introduce a perfect fluid component ρ with $w > 1$ and study the dynamics of p–form fields on the resulting spacetime.

- ***Case 2***: The p–forms are directly coupled to the $w > 1$ component. This is the case if the $w > 1$ component is realized as a scalar field that couples to the p–forms.

The problem with the first case is that once the background is fixed, there is an additional free parameter. This parameter is the Kasner exponent associated to the scalar field exponentially coupled to the p–forms as in (2.34).

We will treat case 2, which has the greatest logical simplicity. We assume there is a single scalar field ϕ, which satisfies two conditions:

- ***Condition 1***: ϕ provides the $w > 1$ component,

- ***Condition 2***: ϕ is the only scalar field coupling to p–forms.

The first of these conditions gives the time dependence of the field ϕ. A scalar field ϕ with potential $V(\phi)$ is tightly constrained by the equations of motion for ϕ, and requirement that its total stress–energy tensor has a given fixed w. The general solution with these requirements is the *scaling solution*, given by

$$a(t) = (t/t_0)^{2/[d(1+w)]}, \tag{3.23a}$$

$$\phi(t) = \sigma_1 p_\phi \ln(t/t_0) + \phi_0, \tag{3.23b}$$

$$V(\phi) = V_0 \exp\left[A_\phi \sigma_1 (\phi - \phi_0)\right] \tag{3.23c}$$

where

$$p_\phi^2 = \frac{2}{1+w}\left(1 - \frac{1}{d}\right) = (d-1)t_0 H_0, \tag{3.24a}$$

$$V_0 = \frac{1-w}{1+w} \cdot \frac{p_\phi^2}{2t_0^2} = \frac{d(d-1)}{4} H_0^2 (1-w), \tag{3.24b}$$

$$A_\phi = -\frac{2}{p_\phi}, \tag{3.24c}$$

and we understand p_ϕ to be defined by the positive root. We have introduced the parameter $H_0 = H(t_0)$. The parameter $\sigma_1 = \pm 1$ determines whether ϕ is increasing or decreasing as we approach the big crunch; for $\sigma_1 = +1$, $\phi \to -\infty$ at the crunch. Otherwise, the space of solutions is parameterized by a reference time t_0, and a reference field value ϕ_0. We will take $\phi_0 = 0$ for simplicity in the following, since different values of ϕ_0 do not affect our results. Note that when $w = 1$ the potential vanishes and this solution reduces to that given in (2.37).

With these in hand we may now turn to the stress–energy tensor for a p–form that couples with coupling constant λ to the scalar field ϕ. Focusing on the 00 component of the stress–energy tensor for the p–form (2.42), and resolving it into electric and

magnetic components we obtain

$$\rho = \frac{e^{\lambda\phi}}{(p+1)!}\left[\frac{p+1}{2}F^{0j_1\cdots j_p}F^{0k_1\cdots k_p}g_{j_1k_1}\cdots g_{j_pk_p} + \frac{1}{2}F_{m_1\ldots m_{p+1}}F_{n_1\ldots n_{p+1}}g^{m_1n_1}\cdots g^{m_{p+1}n_{p+1}}\right] \quad (3.25)$$

It is possible to simplify this further, using the solutions to the equations of motion for the p–form field derived in the previous chapter, eqs. (2.40) and (2.41), along with the solutions for the scalar field and scale factor (3.23) and (3.24). Normally the presence of metric factors in the stress–energy tensor would require us to include the individual scale factors along the different spatial directions. However, in the $w > 1$ case, we know that the universe is driven to isotropy, and so we can take the metric to be that of an isotropic FRW universe.

As in some of the other arguments we have made, the substitution of the isotropic metric into the p–form stress–energy tensor is really more of a consistency check. If the p–forms come to dominate, we know that the universe is driven to anisotropy and the background metric will not be of the isotropic FRW type. So, we assume that the p–forms do not dominate, and consequently we can take the background spacetime to be FRW. Next we check that the p–forms do not come to dominate. If they do, then our starting assumption was inconsistent.

Now, assuming the universe is isotropic and writing everything in terms of a and w, we find that the electric energy density $\rho^{(E)}$ and magentic energy density $\rho^{(B)}$ scale as

$$\rho^{(E)} = \rho_0^{(E)}\,(t/t_0)^{p_E}\,, \qquad \rho^{(B)} = \rho_0^{(B)}\,(t/t_0)^{p_B} \quad (3.26)$$

where $\rho_0^{(E,B)}$ are the energy densities at t_0. The other components of the stress–energy are related to $\rho^{(E,B)}$ through constant factors of order unity, and thus scale identically.

p	λ_{min}	λ_{max}
0	$-\sqrt{8/3}$	0
1	$-\sqrt{2/3}$	$\sqrt{2/3}$
2	0	$\sqrt{8/3}$

Table 3.1: The stable range for the coupling λ between a p–form field and a scalar field. For couplings in the range $\lambda_{\min} < \lambda < \lambda_{max}$, a p–form field will not lead to chaos in an isotropic universe dominated by ϕ. The table assumes $\sigma_1 = +1$: for the opposite sign of σ_1, take $\lambda \to -\lambda$ in the table.

The exponents $p_{E,B}$ are given by

$$p_E = -\frac{4(d-p)}{d(1+w)} - \lambda\sigma_1 \left[\left(1-\frac{1}{d}\right)\frac{2}{1+w}\right]^{1/2}, \tag{3.27a}$$

$$p_B = -\frac{4(1+p)}{d(1+w)} + \lambda\sigma_1 \left[\left(1-\frac{1}{d}\right)\frac{2}{1+w}\right]^{1/2}, \tag{3.27b}$$

$$\tag{3.27c}$$

or, for the specific case $d = 3$, we have

$$p_E = -\frac{4(3-p)}{3(1+w)} - \lambda\sigma_1 \frac{2}{\sqrt{3(1+w)}}, \tag{3.28a}$$

$$p_B = -\frac{4(p+1)}{3(1+w)} + \lambda\sigma_1 \frac{2}{\sqrt{3(1+w)}} \tag{3.28b}$$

These equations obey the electric/magnetic duality for p–forms, which takes the Hodge dual of the field strength

$$F_{p+1} \to (*F_{p+1}) = \tilde{F}_{d-p} \tag{3.29}$$

and thus takes $p+1 \to d-p$. This duality also exchanges electric and magnetic components of the p–form field, and takes $\lambda \to -\lambda$.

Now that we have the dependence of the electric and magnetic energy densities we can find the conditions that ensure that they remain subdominant. Based on our discussion in Sections 2.4 and 2.5, this condition is that these energy densities scale

more slowly than $1/t^2$. Thus, the new p–form stability conditions are

$$p_E > -2 \quad \text{and} \quad p_B > -2 \quad \text{and } w > 1. \tag{3.30}$$

When these conditions are satisfied for all p–forms present in the theory, p–form chaos is guaranteed to be absent. There are several equivalent ways to view this result, as we will discuss below.

One way to view the result (3.30) is as a a constraint on the allowed values of λ when w is fixed. This case is relevant, for example, when the theory contains a free scalar field whose potential is neglected. (This condition is actually more general than it may at first appear, as we discuss in Section 4.2.1. For example, if the potential for the scalar field is positive–semi–definite, it becomes irrelevant near the big crunch and the scalar field behaves as a free field.) The free scalar is a matter component with $w = 1$, and in a universe with this background equation of state one finds the ranges summarized in Table 3.1. If these inequalities are satisfied for all of the p–forms present in the theory, then the contraction to the big crunch will be non–chaotic.

Another viewpoint on the result (3.30) is as a constraint on the lower bound on the possible values of w for which the contraction is assured to be stable. This perspective is more useful from model–building perspective; for example, in a theory whose p–form spectrum and couplings are fixed, it gives a constraint on the potentials used to generate a $w > 1$ phase. We will denote the minimum equation of state for a p–form with coupling λ by $w_{crit}(\lambda, p)$. Theories also have a w_{crit}, which is the maximum of the $w_{crit}(\lambda, p)$ for all of the p–forms in the theory. These do not have a simple algebraic expression, but are shown in Figure 3.4 for the case $d = 3$.

There are several extensions that we have not discussed here, but may be analyzed using the techniques employed in this work:

- Here we have assumed that a single scalar couples universally to all p–forms in the theory, and the same scalar is responsible for generating a $w > 1$ component

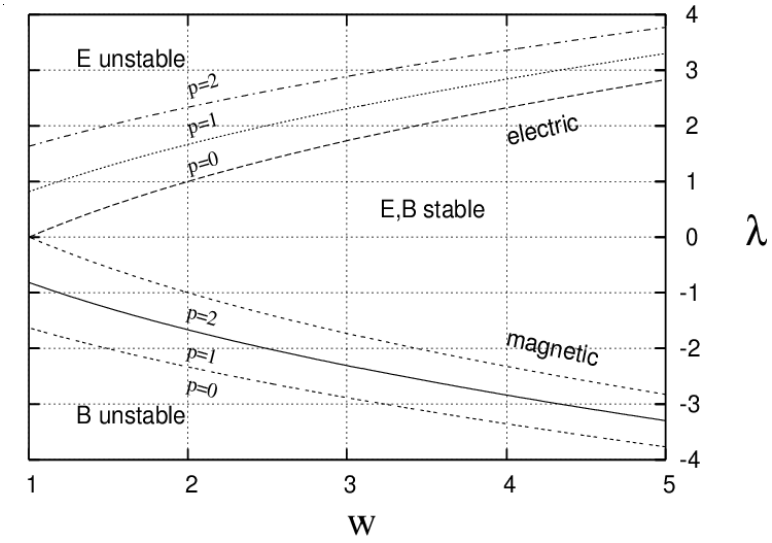

Figure 3.4: Stable ranges for λ for p–forms in $d = 3$. Magnetic components are unstable below the lower curves, electric ones above the upper curves. The figure assumes $\sigma_1 = +1$: for the opposite sign of σ_1, take $\lambda \to -\lambda$ in the figure.

through its potential. Another possibility is that the $w > 1$ component is uncoupled to the p–forms in the theory. Then, the constraint will include a combination of w, λ, and p_ϕ for the universally coupling scalar.

- In some models we might expect many scalars, with each p–form coupling to some linear combination of them. This is the generic situation after compactifying a theory with p–forms to a lower–dimensional effective theory. Again, the constraints will be more involved than in the case considered here.

We will not consider these extensions in the current work, since they can be studied using the same techniques employed herein. Furthermore, for applications to the cyclic universe model, the case studied here is sufficient.

3.2.4 Summary

In this section we have seen that the addition of a matter component with $w > 1$ can significantly affect the chaotic properties of a theory. For a theory without p–forms,

the shift in chaotic behavior occurs when w is larger than the threshold value of unity. For theories with p–forms, where the $w > 1$ component is realized by a scalar field ϕ with potential, the threshold value of w is a function of their couplings to ϕ which we have called $w_{crit}(\lambda, p)$.

The extension of these results to a time–dependent equation of state is known, and is discussed in [43]. This is especially relevant for realistic cosmological models, for which we are not guaranteed that w will be constant in time. One finds that if $w \to \tilde{w}$ as $a \to 0$, chaos is absent provided that $\tilde{w} > w_{crit}$, and thus the time dependence has little effect on the conclusions presented here.

The introduction of a $w > 1$ component, realized by a scalar field, presents a puzzle. It is known that the gravitational positive energy condition may be violated by scalar field systems with exponential potentials of certain types [14, 66]. These potentials are precisely those that give $w > 1$ scaling solutions. This may signify an instability in models with this kind of matter source, and may also make $w > 1$ components difficult to construct in supersymmetric models. Simple modifications of purely exponential potentials (e.g., by factors polynomial in ϕ) still lead to violations of the positive energy condition [43]. It is as yet unknown whether potentials can be constructed that yield $w > 1$ and simultaneously satisfy the positive energy condition.

3.3 The View from Upstairs

In this section we will discuss the situation where our four–dimensional theory is part of a model involving extra dimensions. We have in mind the cyclic model, where we have a $w > 1$ component that arises as the volume modulus of a single extra dimension. The requirement that the four–dimensional effective theory contains a component with fixed w has some interesting consequences for higher–dimensional theory. In this section we will focus on the case where the component is realized

as the volume modulus of a general Kaluza–Klein (KK) compactification, and show that this requirement allows one to bootstrap from the four–dimensional to higher dimensional descriptions. We find that a solution with a given w in four dimensions can only result from an discrete family of equivalent higher–dimensional geometries. Specifically, using the bootstrap, we will describe:

- The volume of the higher–dimensional space,
- The required stress–energy in the higher–dimensional space,
- The relation between the Einstein frame proper time in the lower and higher–dimensional spaces (this possesses some unusual features and big rip singularities in some cases)
- A relationship to a duality of cosmological perturbation theory propsed in [17].

Again, the case where the scalar ϕ is the volume modulus is far from the only possibility: however, it is the simplest possibility and enables us to derive many concrete results. In addition, this assumption is true in the cyclic model that forms the main application of these results.

The relation between lower and higher dimensional spacetimes can be quite complex. Specifically, different observers can view our four–dimensional spacetime as either expanding or contracting. Furthermore, observers can disagree about whether the big crunch occurs at a finite or infinite time in the future. Carefully navigating these subtleties will be one of the main goals of this section. In Section 3.3.1 we will give an overview of how KK reduction gives rise to these unusual features. In Section 3.3.2 we will derive the behavior of the metric in four and $(4 + n)$ dimensions, find the proper times until the big crunch/big bang, and give formulae for the higher–dimensional stress–energy required to realize a $w > 1$ component in four dimensions.

Most of our results are summarized in Table 3.5 and Figure 3.5 near the end of this Chapter.

3.3.1 Features of the Kaluza–Klein Reduction

KK reduction can have some surprising features in a cosmological (time–dependent) context. This comes about through the relationship of the effective four–dimensional Planck length to the "fundamental," higher dimensional Planck length. If the extra dimensional space is a n–dimensional compact space, denote by $L_{(4)}$ the effective four–dimensional Planck length, $L_{(4+n)}$ the $(4+n)$–dimensional Planck length, and V_n the volume of the extra dimensions. Then KK reduction yields the relation

$$L_{(4)}^2 = L_{(4+n)}^2 \left(\frac{L_{(4+n)}^n}{V_n} \right) \tag{3.31}$$

There are some important exceptions to this relation, particularly the "warped" Randall–Sundrum type compactifications [100, 101, 102], but in this work we will focus on classic KK models.

Suppose we follow the motion of two comoving test particles. The higher dimensional observer measures the distance between them using rulers calibrated in units of $L_{(4+n)}$, while the four–dimensional observer uses rulers calibrated by $L_{(4)}$. Let us suppose that the distance between the points is constant in units of $L_{(4+n)}$, so the universe appears static from this viewpoint. Using (3.31), we can readily see that if V_n is decreasing, then $L_{(4)}$ is increasing: thus the "grid" of the four–dimensional observer's ruler is expanding relative to the $(4+n)$–dimensional observer. Thus, the four–dimensional observer will see the distance between the particle decrease, and the universe will appear to be contracting. If V_n is increasing, then the four–dimensional observer sees an expanding universe. Either way, the changing compactification volume leads to observers disagreeing on whether the four–dimensional universe is expanding, contracting, or static!

The relation (3.31) comes about since there are really two metrics in play in KK reduction. Straightforwardly integrating out the higher dimensional degrees of freedom results in a four–dimensional action of Brans–Dicke [19] form

$$\mathcal{S}_{B-D} = \int \left[f(\phi) R(h) + L_m(\phi, \psi_j, h) + \cdots \right] \sqrt{-h}\, d^4x \tag{3.32}$$

where $f(\phi)$ is a function related to V_n. Typically, in KK reduction it is simply the volume of an extra–dimensional space. We will call the metric h appearing in this action, where the Ricci scalar has a prefactor, the *Jordan frame metric*. This metric is not uniquely determined, since we can do a ϕ–dependent conformal transformation

$$\tilde{h}_{\mu\nu} = \tilde{f}(\phi) h_{\mu\nu} \tag{3.33}$$

and thus define a new metric $\tilde{h}_{\mu\nu}$, the action for which also has a function multiplying the Ricci scalar, as well as some additional derivative terms in the "$\cdots$" part of (3.32).

There is however one distinguished metric we can use, the *Einstein frame* metric $g_{\mu\nu}$. This is defined by

$$g_{\mu\nu} = f(\phi) h_{\mu\nu} \tag{3.34}$$

The new action looks like

$$\mathcal{S}_{E-H} = \int \left[R(g) + L_m(\phi, \psi_j, g) + \cdots \right] \sqrt{-g}\, d^4x \tag{3.35}$$

where now the $\cdots$ include derivatives of $f(\phi)$ which we will neglect for now. This is the Einstein–Hilbert action for gravity coupled to other fields. The Einstein frame metric is uniquely determined, and furthermore yields a canonical theory of gravity. However, the metric appearing in the Lagrangian for matter fields L_m is a combination of the Einstein frame metric and ϕ.

There is always an ambiguity in defining the proper metric in the case of Brans–Dicke and similar theories. One can redefine the metric via a conformal transformation, and thus change the units of length (the effective Planck length) at will. In this

work we take the point of view that the proper conformal frame is always the one in which the action takes the Einstein–Hilbert form. This is the unique conformal frame in which the Planck length is constant for all observers, and removes the ambiguity in Brans–Dicke type theories. It has the consequence that observers in different dimensionalities may disagree on the Planck length and how it evolves with time. The relation between the Planck lengths for observers in various dimensionalities is summed up in the expression (3.31).

For the purposes of this section, it will be more convenient to work not with w, but with the related variable ϵ defined by

$$\epsilon = \frac{3(1+w)}{2} \tag{3.36}$$

where $w = P/\rho$ as before. In addition, we will use conformal time τ defined through the flat FRW metric

$$\mathrm{d}s^2 = a(\tau)^2 \left(-\mathrm{d}\tau^2 + \mathrm{d}x_3^2\right) \tag{3.37}$$

where τ_0 is a fixed reference time. The conformal time metric is more convenient since it has a a simpler behavior under KK reduction than the proper time. Finally, in this section we will specialize to the four–dimensional case where $d = 3$.

The next tool we will require is the scaling solution, already introduced using proper time and w in (3.23) and (3.24). If ϵ is constant, then the scaling solution in

ϵ range	w range	$a \to 0$ as	$a \to 0$ as	infinite future
$0 < \epsilon < 1$	$-1 < w < -1/3$	$t \to 0$	$\tau \to -\infty$	$\tau \to 0$
$1 < \epsilon < \infty$	$-1/3 < w < \infty$	$t \to 0$	$\tau \to 0$	$\tau \to \infty$

Table 3.2: The ranges of conformal time τ and physical time t differ in the $d = 3$ FRW universe. In both cases the range corresponds to the expanding FRW phase.

terms of conformal time and ϵ is summed up by

$$a(\tau) = (\tau/\tau_0)^{1/(\epsilon-1)}, \tag{3.38a}$$

$$a(\phi) = \exp\left(\sigma_1 \frac{\phi - \phi_0}{\sqrt{2\epsilon}}\right), \tag{3.38b}$$

$$\phi(a) = \sigma_1 \sqrt{2\epsilon} \ln(a) + \phi_0, \tag{3.38c}$$

$$\phi(\tau) = \sigma_1 \frac{2\epsilon}{\epsilon - 1} \ln(\tau/\tau_0) + \phi_0, \tag{3.38d}$$

$$V(a) = (3 - \epsilon) H_0^2 a^{-2\epsilon}, \tag{3.38e}$$

$$V(\phi) = (3 - \epsilon) H_0^2 \exp\left(-\sigma_1 \sqrt{2\epsilon}\,[\phi - \phi_0]\right) \tag{3.38f}$$

where $\phi_0 = \phi(a = 1)$, and H_0 is the proper time Hubble parameter when $a = 1$,

$$H_0 = \frac{1}{\epsilon t_0} = \frac{1}{(\epsilon - 1)\tau_0} \tag{3.39}$$

The parameter $\sigma_1 = \pm 1$ may be freely chosen. It reflects the choice of $\phi \to \infty$ or $\phi \to -\infty$ as $a \to 0$.

To relate the conformal time to the proper time, we have chosen conventions so that $a = 1$ when $t = t_0$ and also when $\tau = \tau_0$. Furthermore,

$$t = t_0 \, (\tau/\tau_0)^{\epsilon/(\epsilon-1)} \tag{3.40}$$

and

$$\tau_0 = \frac{\epsilon}{\epsilon - 1} t_0. \tag{3.41}$$

Therefore, while the big crunch/big bang at $a \to 0$ always occurs at $t = 0$, it may

occur at either $\tau = 0$ or $\tau = -\infty$, depending on the value of ϵ. The situation is summed up in Table 3.3.1.

3.3.2 Lifting w to Higher Dimensions

In this section, we describe in detail how the four– and $(4+n)$–dimensional spacetime geometries are related. We will find that it is possible to make general statements about the $(4+n)$–dimensional spacetime, when the four–dimensional model is undergoing a phase of inflationary or cyclic type.

Higher–Dimensional Metric

In this section, we will derive the expressions relating the metrics in higher and lower dimensions as a function of ϵ. We can use this information to draw some general conclusions regarding the behavior of the noncompact and compact spaces in the higher–dimensional theory.

The basic method for obtaining a four–dimensional effective theory from a $(4+n)$–dimensional one begins with assuming that the full spacetime is the product of a four–dimensional noncompact space Σ and a compact n–manifold $\mathcal{M}$, with metric

$$G_{MN}^{(4+n)}(x^\mu, y^m) = h_{\mu\nu}^{(4)}(x^\mu) \oplus f_{mn}^{(n)}(t, y^m), \tag{3.42}$$

with $G_{MN}^{(4+n)}$ the full metric, $h_{\mu\nu}^{(4)}$ the metric on Σ, and $f_{mn}^{(n)}$ the metric on $\mathcal{M}$. One then integrates the full action (including the Einstein–Hilbert term) over $\mathcal{M}$. This result universally includes Einstein gravity and a minimally coupled scalar field ϕ, whose expectation value gives the volume of $\mathcal{M}$. The field ϕ is the volume modulus of this compactification. Obtaining this result requires that we define the Einstein frame metric $g_{\mu\nu}$ by

$$g_{\mu\nu} = \exp\left(\sigma_2 \bar{c} \phi\right) h_{\mu\nu}, \tag{3.43}$$

and a the scalar field ϕ by

$$\exp\left(\sigma_2 \bar{c}\phi\right) = \frac{\mathrm{Vol}(\mathcal{M})}{L_{(4+n)}^n} = L_{(4+n)}^{-n} \int_{\mathcal{M}} \sqrt{f}\; d^n y. \tag{3.44}$$

The parameter $\sigma_2 = \pm 1$ is arbitrary: depending on the sign of σ_2, the limit $\phi \to +\infty$ corresponds to either $\mathcal{M}$ decompactifying, or going to zero volume. The constant $\bar{c}$, given by

$$\bar{c} = \sqrt{\frac{2n}{n+2}}, \tag{3.45}$$

is chosen so that ϕ has a canonically normalized kinetic term in the four–dimensional effective action. This action is

$$\mathcal{S} = \int R(g) - (\partial\phi)^2 - 2V(\phi) + \cdots \sqrt{-g}\; d^4x, \tag{3.46}$$

where we have introduced, by hand, a potential $V(\phi)$. The action (3.46) is "universal" in the sense that compactifications of higher–dimensional models with gravity always yield an action of this form. In general, there will also be other terms that depend explicitly on properties of $\mathcal{M}$ and on other matter fields that are present.

Now we can find the behavior of the compact space $\mathcal{M}$. As discussed above, we take the Einstein frame metric to be the conformal time FRW metric (3.37). To simplify our formulae, without loss of generality, we will set $\phi(a_0) = 0$ in the scaling solution (3.38). Now we can use (3.38) and (3.44) to find

$$\mathrm{Vol}(\mathcal{M}) = \exp\left(\sigma \bar{c}\sqrt{2\epsilon}\ln a\right) \tag{3.47}$$

Where we have defined

$$\sigma = \sigma_1\sigma_2. \tag{3.48}$$

Thus, when $\sigma = +1$, the compactification manifold $\mathcal{M}$ goes to zero volume as $a \to 0$. With $\sigma = -1$, the compactification manifold goes to infinite volume as $a \to 0$. Note that only the combination σ of our two arbitrary signs σ_1 and σ_2 is relevant.

σ	ϵ	A as $a \to 0$	V_n as $a \to 0$	model
$+1$	$\epsilon > \epsilon_n$	$A \to \infty$	$V_n \to 0$	cyclic
$+1$	$\epsilon = \epsilon_n$	$A \to$ const.	$V_n \to 0$	
$+1$	$\epsilon < \epsilon_n$	$A \to 0$	$V_n \to 0$	inflationary
-1	all ϵ	$A \to 0$	$V_n \to \infty$	all

Table 3.3: Four–dimensional scaling solutions, where the constant–w component is realized as the volume modulus of an extra–dimensional compact manifold. Behavior of the $(4+n)$ dimensional scale factor A, and the volume V_n of the extra–dimensional space, as the four–dimensional scale factor goes to zero.

Next we can turn to the behavior of the four–dimensional part of the $(4+n)$–dimensional Einstein frame metric. To preserve the FRW symmetry, the full higher–dimensional metric G_{MN} must be of the form

$$G_{MN}: \qquad ds^2 = A(\tau)^2 \left(-d\tau^2 + dx_3^2\right) + f_{mn} dy^m dy^n, \tag{3.49}$$

where $A(\tau)$ is the scale factor along the four noncompact spacetime dimensions, as seen by the observer in the $(4+n)$ dimensional spacetime. Focusing on the behavior of $A(\tau)$, and using (3.43) and (3.38), we find

$$A(\phi) = \exp\left[\left(1 - \sigma\sqrt{\frac{\epsilon}{\epsilon_n}}\right)\frac{\sigma_1\phi}{\sqrt{2\epsilon}},\right] \tag{3.50}$$

where we have introduced the quantity ϵ_n, defined as

$$\epsilon_n = \frac{2}{\bar{c}^2} = 1 + \frac{2}{n}, \tag{3.51}$$

corresponding to

$$w_n = -\frac{1}{3} + \frac{4}{3n} \tag{3.52}$$

This is an enormously useful parameter, whose significance will be clarified below.

Since (3.38) tells us that $\sigma_1\phi \to -\infty$ as $a \to 0$, for any ϵ, we can use (3.50) to reveal some general features of the relationship between A and a. Indeed, depending on ϵ, σ, and n, the behavior in $(4+n)$–dimensional frame can be very different from

the four–dimensional Einstein frame description, as summarized in Table 3.3. When $\sigma = -1$, then it follows that $A \to 0$ near the big crunch; thus, both a and A are either expanding or contracting. When $\sigma = +1$, then one finds a richer range of possibilities. These are determined completely by ϵ and the number of extra dimensions n. When $\epsilon < \epsilon_n$, then Σ is contracting to zero as $a \to 0$. When $\epsilon = \epsilon_n$, then the noncompact space Σ is *static* in the $(4 + n)$ dimensional Einstein frame. Finally, for $\epsilon > \epsilon_n$, Σ is actually expanding to infinite scale factor as $a \to 0$.

These results enable us to make general statements about the behavior of models in which ϕ seeds a scale–invariant spectrum of primordial fluctuations. Inflationary universes have $\epsilon \ll 1$, and thus $\epsilon < \epsilon_n$, while cyclic universes have $\epsilon \gg 1$, and thus $\epsilon > \epsilon_n$. Therefore, inflationary universes will always have A expanding from zero volume at the big bang, which cyclic universes can have A either expanding or contracting as the big crunch is approached, depending on the value of σ.

These general statements can change when ϵ varies with time, an essential feature of realistic cosmological models [52, 79]. As an example, in cyclic models $V(\phi)$ is often negligible near the big crunch, and thus $\epsilon \to 3$. Then, for the special value of $n = 1$, the higher–dimensional Einstein frame scale factor is static as the big crunch is approached. The statements in Table 3.3 should be taken as giving the behavior of the $(4 + n)$–dimensional spacetime during the epoch in which the scale–invariant primordial perturbation spectrum is being created. To understand how the spacetime is evolving near the big crunch and after the inflationary or cyclic epochs, one must have more information about the behavior of ϵ in these regimes.

Higher–Dimensional Proper Time

Unlike conformal time proper time transforms nontrivially under KK reduction. As our next step, we derive the full form of the higher–dimensional metric. We can

reparameterize a general time–dependent metric on the compact space by

$$f_{mn} = B(\tau)^2 \overline{f}_{mn}, \qquad \det \overline{f} = 1. \tag{3.53}$$

and therefore encode all of the evolution of the compact metric in the effective scale factor B. The scaling solution (3.38) enables us to immediately solve for A and B. One finds

$$A(\tau) = \left(\frac{\tau}{\tau_0}\right)^{\alpha}, \qquad B(\tau) = \left(\frac{\tau}{\tau_0}\right)^{\beta}, \tag{3.54}$$

with,

$$\alpha = \frac{1 - \sigma\sqrt{\epsilon/\epsilon_n}}{\epsilon - 1}, \tag{3.55a}$$

$$\beta = \frac{2\sigma}{n}\frac{\sqrt{\epsilon/\epsilon_n}}{\epsilon - 1}. \tag{3.55b}$$

We can now see the role played by the parameter ϵ_n. From the formula for A, we can see that when $\epsilon = \epsilon_n$, the scale factor for the noncompact space is static, when viewed from the extra dimensional perspective.

Since we know the conformal time scale factor in four and $(4 + n)$ dimensions, we can work out the relationships between the proper times in the two frames. If we denote these by $t^{(4)}$ and $t^{(4+n)}$, then we have

$$\frac{t^{(4+n)}}{t_0^{(4+n)}} = \left(\frac{t^{(4)}}{t_0^{(4)}}\right)^{E}, \quad E = 1 - \frac{\sigma}{\sqrt{\epsilon\epsilon_n}}, \tag{3.56a}$$

$$\frac{t_0^{(4+n)}}{t_0^{(4)}} = \left[1 - \frac{\sigma}{\sqrt{\epsilon\epsilon_n}}\right]^{-1} \tag{3.56b}$$

These lead to some unusual features, especially for models with accelerated expansion. Our comments are summed up in Table 3.4.

- ***Four–dimensional de Sitter***: First consider the pure de Sitter limit, where $\epsilon = 0$. Some of our formulae break down at this point because the proper

model	σ	ϵ	$\Delta t^{(4+n)}$ to $a = 0$	$\Delta t^{(4+n)}$ to $a = \infty$
de Sitter	$+1$	$\epsilon = 0$	∞	∞
inflationary	$+1$	$0 < \epsilon < 1/\epsilon_n$	∞	finite
	$+1$	$\epsilon > 1/\epsilon_n$	finite	∞
all	-1	$\epsilon > 0$	finite	∞

Table 3.4: Proper time in the higher dimensional Einstein frame. Note the unusual feature that observers for $0 < \epsilon < 1/\epsilon_n$ have an infinite proper time from the big bang, but a finite proper time to future infinity.

time four–dimensional scale factor is an exponential instead of a power law. Nonetheless, we have

$$a(\tau) = A(\tau) = \left(\frac{\tau}{\tau_0}\right)^{-1}, \qquad \tau_0 = -t_0, \qquad \frac{\tau}{\tau_0} = \exp\left(-\frac{t}{t_0}\right) \tag{3.57}$$

with $\tau \in (-\infty, 0)$ and $t \in (-\infty, +\infty)$. The proper time coordinates are identical in four and $(4+n)$ dimensions. The full metric in $(4+n)$ dimensions is

$$\mathrm{d}s^2 = \frac{1}{\tau^2}(-\mathrm{d}\tau^2 + \mathrm{d}x_3^2) + \mathrm{d}y_n^2, \qquad \text{(de Sitter)} \tag{3.58}$$

Thus the extra dimensions remain static during pure de Sitter expansion in the four–dimensional effective theory. One may understand why this is so by noting that in the $\epsilon \to 0$ limit, the scalar field ϕ is nearly static. Since it represents the volume of the compactification manifold, we see that it must be static as well.

- ***Four–dimensional inflationary***: Next let us consider an inflationary universe, with $\epsilon \ll 1$ but $\epsilon > 0$. When $\sigma = +1$, we can readily see from (3.56) that as $t^{(4)} \in (0, \infty)$ $t^{(4+n)} \in (-\infty, 0)$. Therefore, in the four–dimensional theory, the big crunch/big bang occurred at *finite* proper time in the past, while in the $(4+n)$–dimensional description it occurred at an *infinite* time to the past. The metric, to lowest order in ϵ, is

$$\mathrm{d}s^2 = \frac{1}{\tau^{2-2\gamma}}(-\mathrm{d}\tau^2 + \mathrm{d}x_3^2) + \tau^{-4\gamma/n}\mathrm{d}y_n^2, \quad \gamma = \sigma\sqrt{\frac{\epsilon}{\epsilon_n}} \qquad \text{(inflationary)} \tag{3.59}$$

In this case the noncompact directions are undergoing nearly de Sitter evolution, and the compact directions are either expanding or contracting depending on the sign of σ.

- ***Four–dimensional cyclic***: We have $\epsilon \gg 1$. The ranges of proper time in the lower and higher–dimensional theories are the same. In this limit, the $(4+n)$–dimension metric is,

$$\mathrm{d}s^2 = \tau^{-2\gamma}(-\mathrm{d}\tau^2 + \mathrm{d}x_3^2) + t^{(4/n)\gamma}\mathrm{d}y_n^2, \qquad \gamma = \frac{\sigma}{\sqrt{\epsilon\epsilon_n}}, \tag{3.60}$$

For $\sigma = +1$, this represents the noncompact directions expanding as the big bang/big crunch is approached, and contracting compact directions.

Higher–Dimensional Stress–Energy

We now wish to find the $(4+n)$–dimensional physics that leads to the scalar field with potential in four dimensions. Specifically, we will find the form of the stress–energy tensor $T_M{}^N$ in $(4+n)$ dimensions, corresponding to the scaling solution (3.38). The stress–energy is calculated assuming that the $(4+n)$–dimensional metric takes the form

$$f_{mn} = B(\tau)^2\delta_{mn} \tag{3.61}$$

corresponding to the homogeneous and isotropic contraction of flat extra dimensions. One may just as well carry out our analysis for cases in which $\mathcal{M}$ is not Ricci flat, and one finds terms proportional to the curvature of $\mathcal{M}$ added on to our results.

With the time evolution of the $(4+n)$–dimensional spacetime in hand, we may

now substitute in the $(4+n)$–dimensional Einstein equations, which read

$$G_0{}^0 = -\frac{1}{A^2}\left[3\left(\frac{A'}{A}\right)^2 + \frac{n(n-1)}{2}\left(\frac{B'}{B}\right)^2 + 3\frac{A'}{A}\frac{B'}{B}\right], \tag{3.62a}$$

$$G_3{}^3 = +\frac{1}{A^2}\left[-2\frac{A''}{A} - n\frac{B''}{B} + \left(\frac{A'}{A}\right)^2 + \frac{n(n-1)}{2}\left(\frac{B'}{B}\right)^2 + (2n-3)\frac{A'}{A}\frac{B'}{B}\right], \tag{3.62b}$$

$$G_n{}^n = +\frac{1}{A^2}\left[-3\frac{A''}{A} - (n-1)\frac{B''}{B} - \frac{(n-1)(n-2)}{2}\left(\frac{B'}{B}\right)^2 + (n-1)\frac{A'}{A}\frac{B'}{B}\right], \tag{3.62c}$$

where we have set $L_{(4+n)} = 1$. Using the Einstein equations, we find the stress energy tensor is diagonal, with components,

$$T_0{}^0 = [\tau(\epsilon-1)A]^{-2}(-3+\epsilon), \tag{3.63a}$$

$$T_3{}^3 = [\tau(\epsilon-1)A]^{-2}(-3+\epsilon), \tag{3.63b}$$

$$T_n{}^n = [\tau(\epsilon-1)A]^{-2}(-3+\epsilon)\left[2-\sigma\sqrt{\epsilon\epsilon_n}\right]. \tag{3.63c}$$

One can see that the stress–energy tensor vanishes for the unique value of $\epsilon = 3$, corresponding to a free massless scalar field in the four–dimensional theory. This is as we expect, since KK reduction of vacuum Einstein gravity on a Ricci–flat manifold $\mathcal{M}$ yields an effective action without potential for ϕ.

We now proceed to discuss in detail some cases of interest:

- ***Four–dimensional de Sitter and inflationary***: The stress–energy tensor corresponding to either the de Sitter or inflationary universe limits is, in the small ϵ limit

$$T_M{}^N = -\frac{3}{\tau^{2\gamma}}\begin{pmatrix} 1 & & \\ & 1_3 & \\ & & 2_n \end{pmatrix}, \tag{3.64}$$

ϵ	range τ	range $t^{(4+n)}$	A as $a \to 0$	B as $a \to 0$	notes
0	$(-\infty, 0)$	$(-\infty, +\infty)$	0	const.	1
$0 < \epsilon < 1/\epsilon_n$	$(-\infty, 0)$	$(-\infty, 0)$	0	0	1
$\epsilon = 1/\epsilon_n$	$(-\infty, 0)$	$(-\infty, \infty)$	0	0	2
$1/\epsilon_n < \epsilon < 1$	$(-\infty, 0)$	$(0, \infty)$	0	0	
$\epsilon = 1$	$(-\infty, \infty)$	$(0, \infty)$	0	0	
$1 < \epsilon < \epsilon_n$	$(0, \infty)$	$(0, \infty)$	0	0	
$\epsilon = \epsilon_n$	$(0, \infty)$	$(0, \infty)$	const.	0	
$\epsilon_n < \epsilon$	$(0, \infty)$	$(0, \infty)$	∞	0	

Table 3.5: A summary of some of our results. See also Tables 3.3.1, 3.3, and 3.4. We have assumed $\sigma = +1$ throughout, as well as taking $(0, \infty)$ as the range of $t^{(4)}$ (except in the de Sitter case). We can see that $1/\epsilon_n$ is the threshold for a sensible higher–dimensional stress energy (with no "big rip") and ϵ_n the threshold between expansion and contraction in the higher dimensional theory. Notes: (1) stress–energy has $-P > \rho$ along some directions, (2) stress–energy is that of a cosmological constant.

where subscripts denote the number of repetitions of a single factor. One can see that, despite the fact that the extra dimensions are static, there is a nonzero pressure along the compact directions.

- ***Four–dimensional cyclic***: For cyclic universes, The stress energy tensor is,

$$T_M{}^N = \frac{1}{\epsilon\tau^2} \begin{pmatrix} 1 & & \\ & 1_3 & \\ & & \left[-\sigma\sqrt{\epsilon\epsilon_n}\right]_n \end{pmatrix}, \tag{3.65}$$

  Unlike the inflationary case, σ appears throughout these formulae. Furthermore, in contrast to the inflationary case, the pressure along the compact directions can be either positive ($\sigma = +1$) or negative ($\sigma = -1$).

Relation to a Duality of Cosmological Perturbation Theory

Our results provide a geometric realization of a duality in cosmological perturbation theory, introduced in ref. [17]. The duality exchanges an expanding for contracting

universe, and switches $\epsilon \to 1/\epsilon$. The range of τ is $\tau \in \{-\infty, 0\}$ in both cases, to ensure that modes are exiting the horizon. Remarkably, these dual models produce density perturbations (though in different gauge–invariant variables) whose spectral indices are precisely equal, and are thus indistinguishable at late times by measurements of the scalar power spectrum.

We find this symmetry in our results as well. From (3.55), one can see that the expression for β is invariant under the combined operation,

$$\epsilon \to 1/\epsilon, \quad \sigma \to -\sigma. \tag{3.66}$$

Since the range of τ does not change, we see that the behavior of the extra dimensional volume is identical in both cases. Note that, as in [17], this duality holds for any ϵ. As in the four–dimensional case considered by these authors, the behavior of a (and, for us, A) is not invariant under this transformation, as may be seen from the expression for α in (3.55). However, the dual universes in the four–dimensional description share a common evolution of $\mathcal{M}$ with time in the $(4+n)$–dimensional view.

A curious feature of our realization of this duality is the sign flip for σ in (3.66). Its presence may be understood by considering the solution for ϕ,

$$\phi(\tau) = \frac{\sqrt{2\epsilon}}{\epsilon - 1} \ln(\tau). \tag{3.67}$$

This expression is not invariant under $\epsilon \to 1/\epsilon$, but instead acquires a minus sign. In a purely four–dimensional situation, this minus sign is irrelevant, as it is correlated to a minus sign in the expression for $V(\phi)$. In the intrinsically $(4+n)$–dimensional case discussed here, it has an important physical role coming from ϕ representing the volume of $\mathcal{M}$. To obtain the identical behavior for $\mathcal{M}$, we must therefore flip the sign of σ. This change does not affect the four–dimensional effective theory, and so the duality remains exact.

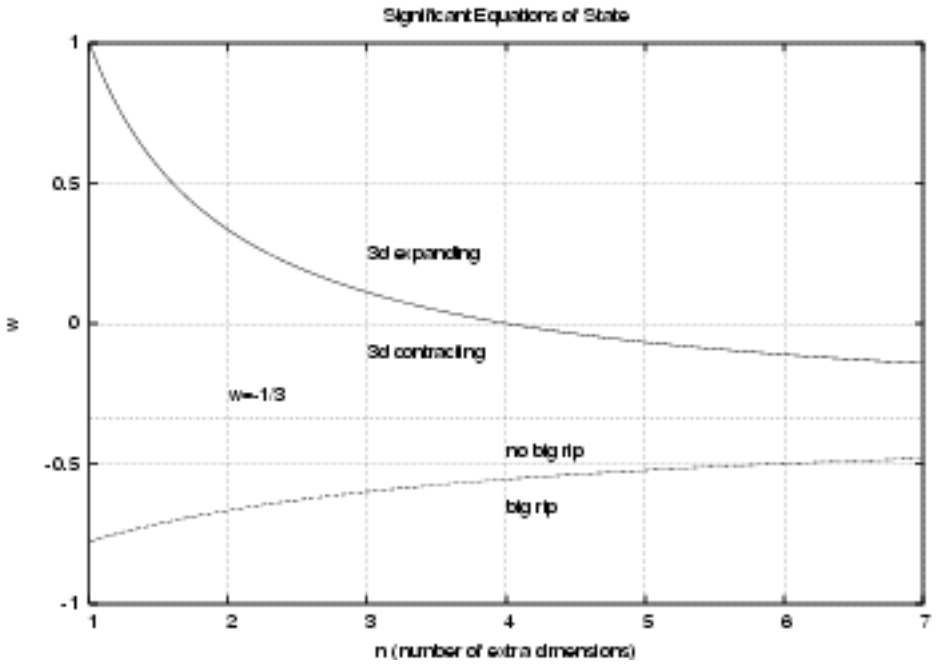

Figure 3.5: A plot of some special equations of state for $\sigma = 1$. Here, w is the four–dimensional equation of state. The notations above and below the lines refer to the $(4 + n)$–dimensional Einstein frame metric. The top line is defined by the w corresponding to ϵ_n, and the bottom by $1/\epsilon_n$. For large n, both w asymptote to $w = -1/3$.

3.4 Summary

In this Chapter we have described how introducing a matter component with and ultra–stiff equation of state can eliminate chaos from gravitational systems. Each theory with gravity defines a w_{crit}, and when $w > w_{crit}$, chaos is absent. For pure Einstein gravity in any dimension, w_{crit} is unity, while theories with p–forms may require a larger (but always finite) w_{crit}. This mechanism can eliminate chaos in any theory with p–form matter, and thus in particular can stabilize models based on the low–energy effective actions of string theories.

The primary application of this technique is to the recently proposed cyclic model, for which $w_{crit} = 1$. It is interesting that the model already requires a component

with $w > 1$ in order to generate a scale–invariant spectrum of density perturbations. Thus, the results of this chapter show that chaos is naturally absent in this model.

We have also considered the problem of realizing the $w > 1$ component in models with extra dimensions. Again, we are motivated by the cyclic model, for which the $w > 1$ component is realized through the volume modulus ϕ and its potential $V(\phi)$ in four dimensions. Remarkably, once the equation of state is fixed in the four–dimensional theory, it is possible to reconstruct the higher dimensional geometry up to a discrete family of equivalent geometries. Some features of these results are summarized in Table 3.5 and Figure 3.5. A better understanding of the higher dimensional realization of the $w > 1$ component may be useful for calculations of the perturbation spectrum in the cyclic model. Since we have derived results for arbitrary equation of state w, our results can also assist in constructing models of inflation or dark energy using higher–dimensional physics.

Chapter 4

Chaos and Compactification

As yet this world was not, and Chaos wild
Reigned where these heav'ns now roll, where earth now rests
Upon her center poised...

Paradise Lost Book V, lines 577–579, [90]

In previous chapters, we have discussed the emergence of chaos near a big crunch, and described a mechanism by which chaos can be eliminated. These results were fundamentally classical, and implicitly assume that Einstein's equations will be valid arbitrarily close to the big crunch. However, one expects classical general relativity to break down at a small but finite time before the big crunch is reached, perhaps of order a Planck time t_{PL} or string time t_S. After this point, quantum effects become significant and we can no longer trust the classical physics that predicts a chaotic approach to the big crunch. Provided the universe evolves smoothly and non–chaotically until t_{PL}, it is conceivable that quantum gravity effects allow the universe to pass smoothly through the big crunch and into a subsequent expanding phase.

Thus in this chapter we take the point of view that chaos need not be completely eliminated from the classical equations of motion all the way to $t = 0$, since these

equations break down before then. Instead, we need only ensure that chaos is suppressed or "controlled" until the universe enters the Planck regime. In this chapter we describe a mechanism by which this can be accomplished for theories with extra dimensions and p–form matter. Unlike other mechanisms which rely on local features of the theory (such as the matter content), this mechanism relies on global features of the spacetime topology. For some extra–dimensional topologies, chaos can be controlled until the universe enters the quantum regime. The selection rules governing this mechanism depend on simple topological invariants of the extra dimensions, namely the de Rham cohomology. A natural application of these results is to the low–energy effective actions of superstring models, and we give specific solutions below.

This chapter is organized as follows. We give a heuristic discussion of this mechanism, and its range of validity, in Section 4.1. In Section 4.2, we describe how the mass terms that arise from compactification modify the growth of the energy density in dangerous modes. We also introduce the relations between properties of the compactification manifold $\mathcal{M}$ and the mass spectrum of various fields in the four–dimensional action. Using these results, we go on to develop a set of *selection rules* in Section 4.3. These rules describe a subset of the stability conditions that, if satisfied, lead to absence of chaos. We next describe specific solutions with controlled chaos. In Section 4.4 we describe manifolds and choices of Kasner exponents that control chaos in vacuum Einstein gravity, and Einstein gravity with perfect fluid matter satisfying $w < 1$. In Section 4.5 we find simple examples of solutions for string models with $\mathcal{N} = 1$ supersymmetry. Section 4.6 summarizes a computer search of the Kasner sphere and some properties of the more general space of solutions it revealed. We conclude in Section 4.7.

This chapter is a summary of published work by the author [120], except for the

contents of Section 4.6 which are unpublished.

4.1 Introduction

The guiding principle behind controlled chaos is that, in a fully uncompactified model, one finds that chaos arises from dangerous modes that are nearly spatially homogeneous along all dimensions. The energy density in these modes scales rapidly enough to dominate the universe and cause chaos. For some choices of the compactification manifold $\mathcal{M}$, there are topological obstructions that forbid spatially homogeneous modes along the compact directions. In the four–dimensional effective theory, this is reflected in the appearance of large mass terms for the associated degrees of freedom. If it is possible to obstruct all of the dangerous modes, then chaos is controlled.

The key to the results in this chapter is that this control of the mass spectrum in four dimensions can allow us to change the dynamics of dangerous modes. Far from the big crunch, the four–dimensional metric is that of a nearly homogeneous and isotropic FRW universe, with small perturbations to the metric, matter and KK fields, and with the Hubble radius H^{-1} much larger than the compactification length scale R_c. Dangerous perturbations that formerly led to chaos acquire masses of order the inverse of the compactification length scale, $m \sim 1/R_c$. The presence of mass terms slows the growth of energy density in these fields, and prevents them from becoming cosmologically relevant so long as the Hubble parameter is larger than their mass. When the time until the big crunch becomes less than R_c, or equivalently $m < H$, the suppression ceases to operate, and the energy density in the dangerous modes can grow at their usual unsuppressed rate. However, since the energy density in these heavy modes has been greatly suppressed relative to light modes up to this point, they cannot dominate the energy density until the universe has contracted further by an exponential factor. Typically, the massive modes do not dominate before we enter

the quantum gravity regime at roughly t_{PL}, at which point the classical evolution equations cannot be trusted. In these circumstances, we say that chaos has been "controlled."

Controlling chaos through compactification is especially relevant for models based on string– or M–theory, in which the compactification of extra dimensions is an essential element. An excellent example is given by eleven–dimensional supergravity, whose bosonic sector contains a four–form field strength G_4 in addition to the metric. Without the four–form, pure eleven–dimensional gravity is not chaotic. With the G_4, the theory is chaotic. For some choices of the topology of the compactification manifold, it is possible to remove the light modes of the four–form field. For these topologies, the previously chaotic eleven–dimensional supergravity theory will behave like the non–chaotic eleven–dimensional pure gravity theory.

4.2 Dynamics and Origin of Massive Modes

In this section, we describe the details of the controlled chaos mechanism. The salient feature of controlled chaos is that dangerous modes are suppressed, relative to $1/t^2$, for an adjustable epoch of cosmic history. (See Section 2.4 for an introduction to this power–counting technique). In Section 4.2.1, we discuss how the growth of dangerous modes is suppressed by mass terms, and estimate the suppression factor. We give a simple argument based on a scalar field in an isotropic universe, leaving a discussion of the general p–form case to Appendix B. Sections 4.2.2 and 4.2.3 describe the mechanism by which compactification gives the required masses to p–form and metric degrees of freedom. In both cases, massless modes in the lower dimension can only exist when $\mathcal{M}$ admits p–form or vector fields with certain special properties. In Section 4.3, we will use these results to give the "selection rules" that express the correspondence between these special properties of $\mathcal{M}$ and the chaotic properties of

the compactified theory.

4.2.1 Massive and massless modes

The suppression of massive modes in a collapsing universe may be illustrated using the equation of state w, introduced in (2.10) and (2.11). It is defined as the ratio of the pressure to energy density for a perfect fluid

$$w = \frac{P}{\rho} = \frac{T_j^{\ j}}{-T_0^{\ 0}}, \qquad \text{(no sum)} \tag{4.1}$$

where we assume that we are in the comoving frame where the stress energy tensor is diagonal. As we are primarily interested in cosmological models, it is sufficient to consider the case where the universe is an isotropic, four dimensional FRW model after compactification. Conservation of stress energy implies that the energy density ρ of a perfect fluid with equation of state w depends on the scale factor a as

$$\rho = \rho_0 a^{-3(1+w)}, \tag{4.2}$$

where ρ_0 is the energy density when a is unity. (See (2.15) and preceding formulae for a discussion of this result in anisotropic universes).

In a contracting universe, the component with the largest w grows most rapidly, and eventually dominates the total energy density. A homogeneous, massive scalar field has a perfect fluid stress energy with equation of state

$$w = \frac{\dot{\phi}^2 - m^2\phi^2}{\dot{\phi}^2 + m^2\phi^2}. \tag{4.3}$$

From equations (4.2) and (4.3) it is readily seen that the energy density of a massive scalar field must scale more slowly than that of a massless one. A massless scalar field will always have $w = 1$, and thus its energy density ρ scales with a as $\rho \sim a^{-6}$. The energy density of a massive scalar will scale with an effective w between zero and unity, depending on the ratio m/H as follows:

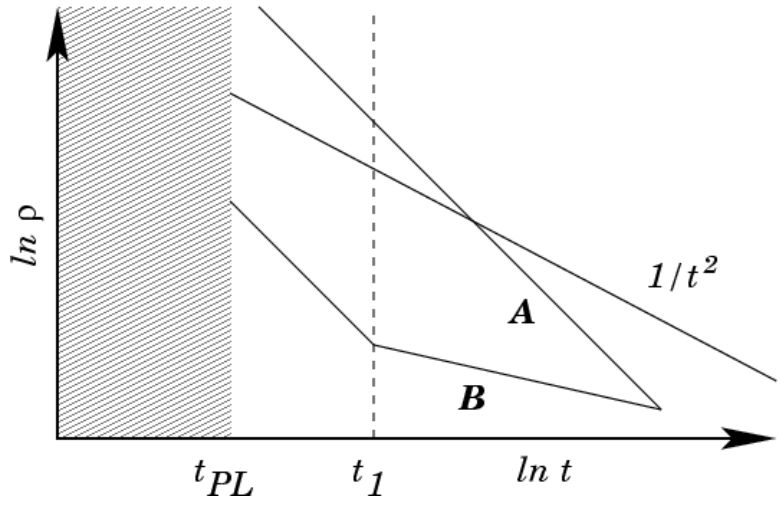

Figure 4.1: Scaling of the energy density in dangerous modes before and after compactification. Dangerous modes **A** scale faster than $1/t^2$ and eventually domiante the energy density of the universe. When they gain a mass **B**, they scale more slowly until $m = H$ at time t_1, and then resume their normal scaling behavior.

- $m/H \gg 1$ (far from the big crunch): The scalar field's dynamics is dominated by the mass term in its potential. Using $\langle\cdot\rangle$ to denote the time average, the virial theorem implies that $\langle\dot{\phi}^2\rangle = m^2\langle\phi^2\rangle$, and therefore $w = 0$ [118]. Thus the energy density in the massive field scales as $\rho \sim a^{-3}$, far more slowly than the massless field.

- $m/H \ll 1$ (near the crunch): the mass term has a negligible effect on the field's dynamics. In this limit, $\dot{\phi}^2 \gg m^2\phi^2$, and w approaches unity from below. In this regime, the energy density in massive and massless fields will scale identically with time.

This behavior is summarized in Figure 4.1. Although we have discussed only the scalar case above, the same $w = 0$ scaling when $m/H \gg 1$ obtains for general p–form fields, as discussed in Appendix B.

Estimated Suppression Factors

Using this equation of state argument, we can estimate the exponential suppression of the energy density in massive fields. It is important to emphasize that, while the energy density in massive modes is always growing, it grows more slowly than the $1/t^2$ scaling required for the field to be cosmologically relevant. Therefore, if we wish to estimate the importance of a given energy component, we should consider the ratio of the energy density in the component to $1/t^2$. This quantity, $t^2\rho(t)$, may be thought of as measuring the ratio of the energy density in a given component to the total density, for

$$t^2\rho(t) \sim \frac{\rho(t)}{H^2} \sim \frac{\rho(t)}{\rho_{tot}(t)}, \tag{4.4}$$

where we have used Planck units. Only when $t^2\rho(t)$ is increasing as $t \to 0$ can a given component grow to dominate the universe.

We begin by choosing a reference time t_0, at the beginning of the contracting phase. We consider a model where the four–dimensional effective theory begins to contract with a background equation of state $\overline{w}$, so that

$$a(t) = (t/t_0)^{2/[3(1+\overline{w})]}, \tag{4.5}$$

where we have normalized $a = 1$ when $t = t_0$. Combining this with (4.2), one finds that for massive modes

$$t^2\rho(t) = \left[t^2\rho(t)\right]_0 \cdot (t/t_0)^{2\overline{w}/[1+\overline{w}]}, \qquad (m/H > 1), \tag{4.6}$$

where $[t^2\rho(t)]_0$ denotes $t^2\rho(t)$ evaluated at t_0. This equation is valid up until $m/H \sim 1$, when the mass terms are becoming irrelevant. Denoting by t_1 the time at which $m = H$, one finds

$$\frac{t_1}{t_0} = R_c H_0, \tag{4.7}$$

where we have taken $m = 1/R_c$. We then have

$$\left[t^2\rho(t)\right]_1 = \left[t^2\rho(t)\right]_0 \cdot (R_c H_0)^{2\overline{w}/[1+\overline{w}]}, \qquad (m/H \sim 1). \tag{4.8}$$

This equation shows the suppression in the fractional energy density in massive modes during the period in which $m/H > 1$. The suppression is controlled by the ratio of the compactification length scale R_c to the Hubble horizon $L_H = 1/H_0$ at the beginning of the contracting phase.

As we approach the big crunch, we have $m/H < 1$, and the dangerous modes can grow as usual. We parameterize this growth by an exponent δ, so that

$$t^2\rho(t) = (t/t_1)^{-\delta}\left[t^2\rho(t)\right]_1, \qquad (m/H < 1). \tag{4.9}$$

when $\delta > 0$, a mode will grow and eventually dominate the energy density of the universe. One can see by comparing (4.9) to our discussion in Section 2.5 that δ is merely twice the amount by which a given mode violates the stability conditions. Typically, δ will be of order one. Now we define a time t_{eq}, at which the dangerous modes have grown sufficiently so that the fractional energy density in dangerous modes is equal to that at the beginning of the contracting phase, or

$$\left[t^2\rho(t)\right]_{eq} = \left[t^2\rho(t)\right]_0. \tag{4.10}$$

Using (4.8) and (4.9), we find

$$t_{eq} = t_0(R_cH_0)^{1+2\overline{w}/[\delta(1+\overline{w})]} \tag{4.11}$$

Finally, we define a time t_{dom}, at which the dangerous modes formally dominate the universe, corresponding to $t^2\rho(t) \sim 1$. Then one finds

$$t_{dom} = t_{eq}\left(\left[t^2\rho(t)\right]_0\right)^{1/\delta}. \tag{4.12}$$

Chaos is controlled provided that the dangerous modes do not dominate before a Planck time from the big crunch, corresponding to $t_{dom} < t_{PL}$.

Having established the formulae we will need for our estimate, we may now insert reasonable values for our variables. Let us assume the contraction phase begins when

$m \sim 1/R_c$	$[t^2\rho(t)]_1 \,/\, [t^2\rho(t)]_0$	t_{eq}/t_{PL}
$10^{-1}\ m_{PL}$	10^{-60}	10^{-29}
$10^{-16}\ m_{PL}$	10^{-45}	10^{-6}
$10^{-16}\ m_{PL}$	10^{-90}	10^{-29}

Table 4.1: Examples of the suppression of energy density in massive modes. The first two entries assume the background equation of state $\overline{w} = 1$, the last assumes $\overline{w} \gg 1$.

the Hubble parameter is of order the present value H_0 (as occurs in ekpyrotic and cyclic models). Then, $1/H_0 \sim 10^{61}\ L_{PL}$. As a first example, we assume that $\overline{w} = 1$ during the contraction as is characteristic of compactifications of Kasner universes. A typical value for δ that arises from working with the p–form spectrum of string models and gravity is $\delta = 2$, although the precise value of δ will of course depend on the specific model under consideration. If we take $R_c \sim 10 \cdot L_{PL}$, as an example, then we find the suppression factor (4.8) at $H \sim m$ to be

$$(R_c H_0)^{2\overline{w}/(1+\overline{w})} \sim 10^{-60}. \tag{4.13}$$

The dangerous modes grow to have the same fractional energy density as they had at the beginning of the contracting phase at the time

$$t_{eq} \sim 10^{-29}\ t_{PL}. \tag{4.14}$$

Thus, the dangerous modes cannot grow to be even as relevant as at the beginning of cosmic contraction, until the universe is well within the quantum regime. We would need to approach even closer to the big crunch for these modes to dominate the universe, but at this point we no longer expect our classical equations to be valid.

As another example, we consider a case with large compact dimensions, where m is of order the weak scale, $10^{-16}\ M_{PL}$, which corresponds to taking $R_c \sim 10^{16}\ L_{PL}$. Now we find that the suppression when the Hubble radius equals the compactification

scale is

$$(R_c H_0)^{2\overline{w}/(1+\overline{w})} \sim 10^{-45}, \tag{4.15}$$

and

$$t_{eq} = 10^{-6}\, t_{PL}. \tag{4.16}$$

Again, we will be well within the quantum gravity regime before the dangerous modes can potentially dominate.

If $\overline{w} \gg 1$ during the contraction phase, as occurs in ekpyrotic and cyclic models, the dangerous modes are suppressed by a much greater factor than above. For example, let us reconsider the last example with $R_c \sim 10^{16}\, L_{PL}$, and take $\overline{w} \sim \mathcal{O}(10)$. We have the suppression factor at $H \sim m$ given by

$$(R_c H_0)^{2\overline{w}/(1+\overline{w})} \sim 10^{-90}, \tag{4.17}$$

and the time at which the dangerous mode can grow to its original fractional energy density is

$$t_{eq} = 10^{-29}\, t_{PL}. \tag{4.18}$$

The suppression is thus exponentially more powerful in the $\overline{w} \gg 1$ universe.

Time–Dependent Mass

As a final relevant issue, note that we have taken the mass m of the dangerous modes to be constant in time. Generally we expect that the mass m of a given field will be time dependent. This occurs since the field's mass is determined by the compactification manifold $\mathcal{M}$, and $\mathcal{M}$ will be evolving with time during cosmic contraction. Let us say that the mass $m(t)$ evolves as

$$m(t) = m_0 \left(\frac{t}{t_0}\right)^b \tag{4.19}$$

during the contracting phase, where for simplicity we take $\overline{w} = 1$. Then, because the energy density will go like $\rho \sim m/a^3$, we find that

$$t^2\rho = \left[t^2\rho\right]_0 \left(\frac{t}{t_0}\right)^{1+b} \tag{4.20}$$

However, the time t_1 at which $m/H \sim 1$ is now

$$t_1^{1+b} = \frac{t_0^b}{m_0}, \tag{4.21}$$

and therefore the suppression when $m/H \sim 1$ is

$$\frac{[t^2\rho]_1}{[t^2\rho]_0} = (H_0/m_0) \sim (H_0 R_{c,0}), \tag{4.22}$$

where $R_{c,0}$ is the characteristic length of $\mathcal{M}$ when $t = t_0$. This is precisely the factor found in the case where m is constant in time (4.8). The difference is that the time t_1, at which $m/H \sim 1$, shifts. This shift compensates for the different growth rate of ρ, with the net result that the suppression factor remains the same.

From the equations above, it is clear that there is a potential problem if $b < -1$, which would lead to $t^2\rho$ increasing during the contracting phase. However, our assumption that the universe is of Kasner type excludes this possibility. Field masses m are related to the compactification length scale R_c by $m \sim 1/R_c$. In a Kasner universe, we expect that $R_c \sim t^p$, with p a Kasner exponent, or average of several Kasner exponents. However, the Kasner conditions (2.5) or (2.36) imply that $p \leq 1$, and thus m must vary more slowly than $1/t$. This implies that $b \geq -1$, and so the suppression operates as before.

4.2.2 The p–form spectrum

Having established that the massless modes are the only relevant modes near the big crunch, we now describe how these massless modes are determined in terms of

the compactification manifold $\mathcal{M}$. The story is familiar from the study of higher–dimensional models of particle physics [40, 54, 98] although we discuss some special features of the time dependent situation which must be taken into account. A useful feature of the p–form mass spectrum is that the existence of massless modes is determined entirely by the topology of $\mathcal{M}$, and not by its metric. This simplifies the task of finding manifolds $\mathcal{M}$ that lead to controlled chaos, since we need only specify their topological properties.

Time independent compactification

First, we will review the situation for the time independent case. For clarity, we will neglect here the exponential coupling to the dilaton field, which amounts to an overall multiplication by $e^{\lambda\phi}$ of the Lagrangian density. The coupling is fully accounted for in the analysis given in Appendix B. We begin with the action for a p–form gauge potential A_p (2.34) generalized to $4+n$ dimensions

$$\mathcal{S} = -\frac{1}{(p+1)!}\int \mathrm{d}A_p \cdot \mathrm{d}A_p \sqrt{-G}\, d^{4+n}x, \tag{4.23}$$

where A_p can depend on all coordinates, and has indices along both Σ and $\mathcal{M}$

$$A_p = \left[A_p(x^\mu, x^m)\right]_{\alpha_1\alpha_2\ldots\alpha_r a_1 a_2\ldots a_{p-r}}. \tag{4.24}$$

The conventional compactification analysis begins with an expansion of the p–form A_p as

$$A_p = \sum_{r+s=p}\sum_i \alpha_r^{(i)} \wedge \beta_s^{(i)} \tag{4.25}$$

using a basis of s–forms $\beta_s^{(i)}$, with indices and coordinate dependence only along $\mathcal{M}$

$$\beta_s^{(i)} = \left[\beta_s^{(i)}(x^m)\right]_{a_1 a_2\ldots a_s}. \tag{4.26}$$

The abstract index i labels the s–form under consideration, and when $\mathcal{M}$ is compact it takes discrete values, infinite in number. The "coefficients" in this expansion are

r–forms $\alpha_r^{(i)}$, that depend on the noncompact coordinates on Σ, and have indices along Σ only

$$\alpha_r^{(i)} = \left[\alpha_r^{(i)}(x^\mu)\right]_{\alpha_1\alpha_2\ldots\alpha_r}. \tag{4.27}$$

It is convenient to choose the gauge $\mathrm{d}^\dagger\beta_s^{(i)} = 0$, and select the $\beta_s^{(i)}$ to be eigenfunctions of the Hodge–de Rham Laplacian $\Delta = \mathrm{d}\mathrm{d}^\dagger + \mathrm{d}^\dagger\mathrm{d}$ on $\mathcal{M}$, with eigenvalues $\lambda_s^{(i)}$

$$\Delta\beta_s^{(i)} = \lambda_s^{(i)}\beta_s^{(i)}. \tag{4.28}$$

The $\beta_s^{(i)}$ are normalized so that

$$\int_{\mathcal{M}} \beta_s^{(i)} \cdot \beta_s^{(j)} \sqrt{-f}\; d^n x = \delta_{ij}. \tag{4.29}$$

Substituting the expansion (4.25) into the original action (4.23) results in

$$\mathcal{S} = -\sum_{i,s} \frac{1}{(r+1)!} \int \left(\mathrm{d}\alpha_r^{(i)} \cdot \mathrm{d}\alpha_r^{(i)} + \lambda_s^{(i)}\alpha_r^{(i)} \cdot \alpha_r^{(i)}\right) \sqrt{-h}\; d^4x, \tag{4.30}$$

where we have rescaled the $\alpha_r^{(i)}$ by a constant in order to canonically normalize the kinetic terms. This demonstrates that a single p–form in $4+n$ dimensions yields many r–forms $\alpha_r^{(i)}$ after compactification, whose masses $m_r^{(i)}$ are related to the eigenvalues $\lambda_s^{(i)}$ by $\left(m_r^{(i)}\right)^2 = \lambda_s^{(i)}$. These are the *Kaluza–Klein modes* or *KK modes*. The operator Δ has a positive semi–definite spectrum on manifolds which, like $\mathcal{M}$, have a Euclidean metric. Therefore the effective masses are all real.

The $(p-s)$–forms with zero effective mass are determined entirely by the topology of $\mathcal{M}$, and not by its metric structure. As discussed above, massless $(p-s)$–forms arise from s–forms β_s satisfying $\Delta\beta_s^{(i)} = 0$, conventionally termed *harmonic forms* or *zero modes*. Hodge's decomposition theorem [41, 94] states that the number of harmonic s–forms is equal to the dimension of $\mathcal{H}^s(\mathcal{M})$, the s^{th} de Rham cohomology class of $\mathcal{M}$. The dimension $\dim\mathcal{H}^s(\mathcal{M})$ is also known as the s^{th} *Betti number* of $\mathcal{M}$, conventionally denoted $b_s(\mathcal{M})$. This is a topological invariant, which does not change

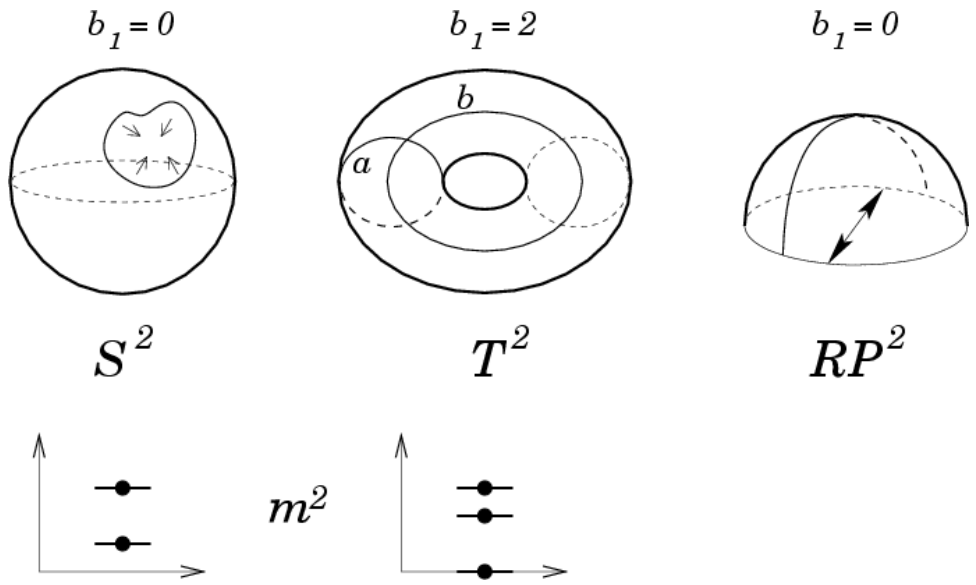

Figure 4.2: Simple examples of cohomology in two dimensions, discussed in the text. Some representative submanifolds, and the four–dimensional mass spectra for a p–form with a single index along these spaces are shown.

under smooth deformations of $\mathcal{M}$ and its associated metric structure. The Poincaré duality theorem [88, 89] gives a simple geometric interpretation of these cohomology classes. Roughly speaking, for orientable $\mathcal{M}$, the quantity $\dim \mathcal{H}^s(\mathcal{M})$ counts the number of s–dimensional submanifolds that can "wrap" $\mathcal{M}$, and cannot be smoothly contracted to zero. In this counting, two submanifolds are considered equivalent if one can be smoothly deformed into the other. Thus, for every inequivalent noncontractible submanifold of $\mathcal{M}$ with dimension s, a p–form gives rise to a massless $(p-s)$–form field after compactification.

Some examples of this construction are given in Figure 4.2. In the figure we focus on $b_1 = \dim \mathcal{H}^1(X)$ for each space, and give the mass spectra for p–forms with one index along the relevant manifold. The sphere $\mathbf{S}^2$ has $b_1 = 0$, since any loop (one–dimensional submanifold) can be smootly contracted to zero. The torus $\mathbf{T}^2$ has $b_1 = 2$ since there are two independent submanifolds, labeled by a and b. The real projective space $\mathbf{RP}^2$ (or Klein bottle) is obtained by taking the disk and identifying antipodal

points. It is not orientable and is therefore unsuitable for KK compactification, since one cannot integrate fields over $\mathbf{RP}^2$. It has $b_1 = 0$, despite the fact that there is a one–dimensional submanifold. This submanifold is not detected by cohomology since the submanifold has the unusual property that if it wraps $\mathbf{RP}^2$ twice it can then be contracted to zero. This example illustrates a property known as torsion which is occasionally found in manifolds that are suitable for compactification, such as some Calabi–Yau spaces. The nontrivial submanifold on $\mathbf{RP}^2$ is detected by the fundamental group topological invariant $\pi_1\mathbf{RP}^2 = \mathbb{Z}_2$, but this is not relevant to p–form compactification.

Time dependent compactification

The case where the compactification manifold $\mathcal{M}$ changes with time introduces new features, but in the end does not substantially modify the conclusions reached above. The main difference is that it is no longer possible to assume that the eigenbasis of forms $\beta_s^{(i)}$ defined by (4.28) depends only on the compact coordinates x^m. In particular, the forms will depend on time. This introduces additional cross terms which must be taken into account. Below, we will neglect the variation of $\mathcal{M}$ along directions x^M other than time. We denote by $\mathrm{d}|_{\mathcal{M}}$ the exterior derivative tangent to the manifold $\mathcal{M}$. Thus

$$\mathrm{d}\beta_s^{(j)} = \mathrm{d}|_{\mathcal{M}}\beta_s^{(i)} + \mathrm{d}t \wedge \dot{\beta}_s^{(i)}. \tag{4.31}$$

We may now use our freedom to choose the basis modes $\beta_s^{(i)}$, and define the modes $\beta_s^{(i)}(t)$ with $\lambda_s^{(i)}(t) > 0$ to be the instantaneous eigenforms of the Hodge–de Rham operator, restricted to act on $\mathcal{M}$ only

$$\Delta|_{\mathcal{M}}\beta_s^{(i)}(t) = \lambda_s^{(i)}(t)\beta_s^{(i)}(t). \tag{4.32}$$

We find it convenient to relax the requirement that the zero modes $\beta_s^{(i)}(t)$ with $\lambda_s^{(i)} = 0$ be eigenforms of the Hodge–de Rham Laplacian. Instead, we will merely require that

they be representatives of the de Rham cohomology of $\mathcal{M}$. Inspection of the reduced action shows that this condition is sufficient to guarantee that the zero modes still result in massless form fields. Furthermore, we adopt the normalization convention

$$\int_{\mathcal{M}} \beta_s^{(i)} \cdot \beta_s^{(j)} \sqrt{-f}\; d^n x = \delta_{ij} \int \sqrt{-f}\; d^n x. \tag{4.33}$$

This differs from the usual normalization convention (4.29) by only a multiplicative constant in the static case. It has the advantage of not introducing any spurious time dependence of the $\beta_s^{(i)}$ from the changing volume of $\mathcal{M}$. Maintaining this normalization condition requires

$$\int_{\mathcal{M}} \dot{\beta}_s^{(i)} \cdot \beta_s^{(j)} \sqrt{-f}\; d^n x = 0. \tag{4.34}$$

With these conventions and definitions, we find that the p–form action (4.23) splits into two parts, $\mathcal{S}_1$ and $\mathcal{S}_2$, with

$$\mathcal{S}_1 = -\sum_{s,i} \frac{1}{(r+1)!} \int \mathrm{d}\alpha_r^{(i)} \cdot \mathrm{d}\alpha_r^{(i)} + \lambda_s^{(i)}(t) \alpha_r^{(i)} \cdot \alpha_r^{(i)} \sqrt{-G}\; d^{4+n} x \tag{4.35}$$

and

$$\mathcal{S}_2 = -\sum_{s,i} \frac{2}{(r+1)!} \int (\alpha_r^{(i)} \wedge \dot{\beta}_s^{(i)}) \cdot (\dot{\alpha}(i)_r \wedge \beta_s^{(i)}) + (\alpha_r^{(i)} \cdot \alpha_r^{(i)})(\dot{\beta}_s^{(i)} \cdot \dot{\beta}_s^{(i)}) \sqrt{-G}\; d^{4+n} x, \tag{4.36}$$

where terms that are identically zero due to mismatched indices are not included. Again, we have rescaled the $\alpha_r^{(i)}$ to obtain canonically normalized kinetic terms. The terms in S_2 threaten to substantially modify the action in the time dependent case. However, these terms vanish or are negligible. The first term is zero due to our normalization convention (4.33) and its consequence (4.34). The second term is a contribution to the effective mass of $\alpha_r^{(i)}$. For the $\lambda_s^{(i)} = 0$ modes, the representatives $\beta_s^{(i)}$ of the de Rham cohomology are time–independent, and so the $\dot{\beta}^2$ terms vanish. When $\lambda_s^{(i)} > 0$, the additional contribution to the effective mass will be positive, but since these modes are already massive it will not change the qualitative features of

their behavior. Thus, time dependent compactifications do not substantially modify the p–form spectrum; massless modes are still given by the de Rham cohomology of $\mathcal{M}$.

4.2.3 The gravitational spectrum

A key property of KK reduction is that degrees of freedom in the full metric G_{MN} appear in lower dimensions as metric, vector, and scalar degrees of freedom. As in the p–form compactification discussed above, the masses of these fields depend on the properties of the compactification manifold $\mathcal{M}$. In contrast to the p–form case, the masses are not determined by the cohomology of $\mathcal{M}$, but by the existence of Killing fields on $\mathcal{M}$. The properties of KK reduction, along with our discussion of chaos in Chapter 2, provide some useful simplifications. Since some of the metric degrees of freedom in the higher dimensional theory appear as zero– and one–forms, chaos arising from these degrees of freedom can be suppressed if they acquire a mass, just as in the conventional p–form case.

As an explicit example of the reduction process, and of how chaos in higher and lower dimensions are related, we consider below the simple case with a single extra dimension [9]. The KK reduction begins with a reparameterization [3, 40, 97] of the metric

$$G_{MN} = \begin{pmatrix} e^{-\bar{c}\phi} g_{\mu\nu} + e^{2\bar{c}\phi} A_\mu A_\nu & e^{2\bar{c}\phi} A_\nu \\ e^{2\bar{c}\phi} A_\mu & e^{2\bar{c}\phi} \end{pmatrix}, \tag{4.37}$$

where we assume that A_μ and ϕ are independent of the fifth dimension. We substitute this metric into the Einstein–Hilbert action and integrate over the fifth dimension. The coefficient $\bar{c}$, defined in (3.45), assumes the value $\sqrt{2/3}$ so that the scalar field ϕ has a canonically normalized kinetic term in the resulting action

$$\mathcal{S} = \int R(g) - (\partial\phi)^2 - \frac{1}{4} e^{\sqrt{6}\phi} F_{\mu\nu} F^{\mu\nu} \sqrt{-g}\, d^4x, \tag{4.38}$$

with $F_{\mu\nu} = \partial_\mu A_\nu - \partial_\nu A_\mu$. This describes Einstein gravity coupled to a scalar field ϕ, and a vector field with ϕ–dependent coupling. It can be seen that all of the five–dimensional metric degrees of freedom in (4.37) are reproduced in this four–dimensional action, in the guise of a *KK vector* A_μ, and a *KK scalar* ϕ. Furthermore, the vector term in the action possesses an exponential coupling to ϕ, of the type introduced in (2.34).

Our starting point, the five dimensional pure gravity theory, is chaotic since the GSCs cannot be satisfied for any choice of the Kasner exponents. After reduction, chaos also inevitably arises since the gravitational and one–form stability conditions cannot be satisfied simultaneously. (This is because the value of the KK vector coupling, $\lambda = \sqrt{6}$, is outside the stable range shown in Table 3.1) Thus violations of the gravitational stability conditions in five dimensions can appear as violations of the p–form stability conditions in four dimensions.

In this example, chaotic properties are left unchanged after dimensional reduction. As we will discuss in more detail below, the preservation of chaos is not a generic feature of KK reduction in dimensions greater than one. The mass spectrum for KK vectors in the the general case of $n > 1$ extra dimensions is derived in Appendix C. There, we show that these masses are zero only when $\mathcal{M}$ possesses Killing vectors. (This calculation parallels standard treatments of KK reduction [40], but in these treatments the fact that $\mathcal{M}$ may not possess isometries is often not emphasized.) Each Killing field on $\mathcal{M}$ gives rise to a massless vector in the four–dimensional effective theory; thus by analogy with the p–form case we may term these gravitational *zero modes*. Since the only compact one–dimensional manifold is $\mathbf{S}^1$, and since any one–dimensional manifold possesses a Killing vector, the $n = 1$ case discussed here is in a sense degenerate.

4.3 Selection Rules for the Stability Conditions

With the tools developed in the previous sections, we are now prepared to discuss conditions on $\mathcal{M}$ that result in controlled chaos. We will show that stability conditions for the metric and p–form fields, introduced in Chapter 2, are modified by compactification. Not all of the stability conditions remain relevant, and only a subset need be satisfied to ensure that chaos is controlled. This subset is defined by the *selection rules* that are the focus of this section. The selection rules that determine when a stability condition remains relevant are given for matter fields in Section 4.3.1, and for gravitational modes in 4.3.2. The selection rules, in turn, are determined by the de Rham cohomology (in the p–form case) and existence of Killing vectors (in gravitational case) of the compactification manifold $\mathcal{M}$. Here, we focus on discussing the origin of the selection rules. Once established, we will use them to find compactifications that control chaos in Sections 4.4, 4.5 and 4.6.

4.3.1 The p–form selection rules

As discussed in Section 2.5, each component of a p–form field results in an ESC or MSC, given in (2.43), which expresses whether the energy density in that component scales rapidly enough to dominate the energy density of the universe and cause chaos. This analysis assumes that all dimensiona are noncompact. If the component gains a mass by compactification, then we have shown in Section 4.2.1 that it always scales too slowly to be cosmologically relevant, and therefore we should ignore the corresponding stability condition. Thus we should ignore all electric and magnetic stability conditions involving indices that do not correspond to massless p–form modes. This results in the *p–form selection rule*, which is

The p–form Selection Rule: When $\dim \mathcal{H}^s(\mathcal{M}) = 0$ for some s, then

of the p–form stability conditions,

$$\sum_{j\in\langle p\rangle} p_j - \frac{\lambda p_\phi}{2} > 0 \qquad \text{(electric)}, \tag{4.39a}$$

$$\sum_{j\in\langle p+1\rangle} p_j - \frac{\lambda p_\phi}{2} < 1 \qquad \text{(magnetic)}, \tag{4.39b}$$

ignore those with exactly s Kasner exponents along the compact space $\mathcal{M}$. *Retain* only those stability conditions with s exponents along $\mathcal{M}$ and $\dim \mathcal{H}^s(\mathcal{M}) \neq 0$. If the reduced subset of stability conditions are satisfied, then chaos is absent.

In the following, we will use the results of previous sections to prove this rule, and give some simple examples of its use.

This rule arises from considering the p–form modes that give rise to massless fields after compactification. From Section 4.2.2, we know that a p–form A_p gives rise to a massless r–form α_r if and only if A_p is of the form

$$A_p = \alpha_r \wedge \beta_s \tag{4.40}$$

where $\beta_s \in \mathcal{H}^s(\mathcal{M})$, and $r + s = p$. Since $\mathrm{d}\beta_s = 0$, this gauge potential results in the field strength

$$F_{p+1} = (\mathrm{d}\alpha)_{r+1} \wedge \beta_s. \tag{4.41}$$

When the energy density of this field is calculated, one finds a stability condition involving exactly s Kasner exponents along $\mathcal{M}$, and the remainder along Σ. Since only stability conditions of this type correspond to massless modes, they are the only ones that should be retained.

The case (4.41) deals only with field strengths having at least one index along the noncompact space Σ. In fact, the same selection rule applies when all indices of the field strength are along $\mathcal{M}$. In this case, the field strength must satisfy the Bianchi identity and the Gauss law

$$\mathrm{d}F_{p+1} = 0, \qquad \mathrm{d}^\dagger F_{p+1} = 0. \tag{4.42}$$

Field strengths of this type are commonly termed *nonzero modes* [54]. These degrees of freedom correspond to fluxes that can be "turned on" while satisfying the p–form equations of motion, and have attracted much interest recently in the string theory community due to their applications in superstring phenomenlogy and so–called *flux compactifications* [15, 39, 74]. The conditions (4.42) imply that F_{p+1} is harmonic, and by Hodge's theorem the number of such forms is given by $\dim \mathcal{H}^{p+1}(\mathcal{M})$. When $\dim \mathcal{H}^{p+1}(\mathcal{M})$ vanishes, we cannot have a p–form field strength with all indices along $\mathcal{M}$, and we should therefore delete the corresponding stability condition, with $(p+1)$ Kasner exponents along $\mathcal{M}$. Thus this case falls under the p–form selection rule as well.

The selection rule may be illustrated by comparing compactification on a sphere $\mathbf{S}^n$ and a torus $\mathbf{T}^n$. These manifolds encompass the best and worst case scenarios for controlling chaos through compactification. The sphere has the minimum number of massless modes for any orientable compact manifold, while the torus has massless modes for every dimension and involving every combination of indices on $\mathcal{M}$. Therefore compactification on $\mathbf{T}^n$ and $\mathbf{S}^n$ will have very different influences on chaotic behavior.

Compactification on $\mathbf{T}^n$ does not modify any of the p–form stability conditions. The cohomology classes of the torus are

$$\dim \mathcal{H}^r(\mathbf{T}^n) = \frac{n!}{r!(n-r)!}, \qquad 0 \leq r \leq n. \tag{4.43}$$

If we realize the torus as $\mathbf{R}^n/\mathbb{Z}^n$, with coordinates $\theta_1, \ldots \theta_n$, then we may choose the following set of generators for the r^{th} de Rham class,

$$\omega_r = \mathrm{d}\theta_{j_1} \wedge \mathrm{d}\theta_{j_2} \wedge \cdots \wedge \mathrm{d}\theta_{j_r}, \tag{4.44}$$

where $\{j_r\}$ are any set of distinct indices on $\mathbf{T}^n$. Therefore, massless modes exist for p–form fields with any combination of indices along the $\mathbf{T}^n$. Any p–form stability

condition that appears in the noncompactified theory will remain in the compactified theory.

By contrast, compactification on a sphere $\mathbf{S}^n$, with $n > 1$, deletes many of the stability conditions. The sphere has only two nonzero cohomology groups, each of unit dimension

$$\dim \mathcal{H}^r(\mathbf{S}^n) = \begin{cases} 1, & \text{for} \quad r = 0 \quad \text{and} \quad r = n \\ 0, & \text{otherwise.} \end{cases} \tag{4.45}$$

The class $\mathcal{H}^0(\mathbf{S}^n)$ is generated by the constant scalar function on $\mathbf{S}^n$, while the class $\mathcal{H}^n(\mathbf{S}^n)$ is generated by the volume form,

$$\omega_n = \sqrt{g}\, \mathrm{d}\theta_1 \wedge \mathrm{d}\theta_2 \wedge \cdots \wedge \mathrm{d}\theta_n, \tag{4.46}$$

where g_{mn} is the metric, $g = \det g_{mn}$, and θ_j the coordinates on the sphere. Massless modes therefore contain either no indices along the $\mathbf{S}^n$, or all indices at once. This implies that the only surviving stability conditions are those with either no internal Kasner exponents, or all internal Kasner exponents together. In the case where $n > p$, none of the internal Kasner exponents appear at all, and only those stability conditions involving Kasner exponents on Σ survive.

Our statement of the selection rule is the strongest possible in the generic case, and fortunately also the most conservative in terms of deleting the minimum number of stability conditions. Manifolds with a specific relationship between the frames ω^j appearing in the generalized Kasner metric (2.25) and the cohomology representatives of $\mathcal{M}$ may require that we delete additional p–form stability conditions. For example, consider the case in which $\mathcal{M}$ factors as $\mathcal{M} = \mathcal{M}_1 \times \mathcal{M}_2$, both topologically and metrically. A straightforward application of the selection rules results in retaining all stability conditions with s indices along $\mathcal{M}$ whenever $\dim \mathcal{H}^s(\mathcal{M}) \neq 0$. These stability conditions correspond to p–form modes with s_1 indices along $\mathcal{M}_1$ and s_2

indices along $\mathcal{M}_2$, with $s_1 + s_2 = s$. However, in general a massless mode will not exist for every choice of s_1 and s_2, and therefore we may be able to delete additional stability conditions. We should only retain the even smaller subset of stability conditions with s_1 Kasner indices along $\mathcal{M}_1$ and s_2 indices along $\mathcal{M}_2$ when $\dim \mathcal{H}^{s_1}(\mathcal{M}_1) \neq 0$ and $\dim \mathcal{H}^{s_2}(\mathcal{M}_2) \neq 0$. Generally, however, we do not expect any special relationship between the ω^j and the cohomology classes. In this example, we have imposed the condition by hand that the ω^j point only along exactly one of $\mathcal{M}_1$ or $\mathcal{M}_2$. Examples such as this one must be considered on a case–by–case basis, and lie beyond the scope of our selection rule.

4.3.2 The gravitational selection rules

The selection rules for the gravitational stability conditions arise in a manner similar to those for the p–form modes. We identify the degree of freedom corresponding to each of the gravitaional stability conditions (2.30), and then ignore the stability condition if the degree of freedom gains a mass through compactification. Unlike the p–form case, in general one must also check that the masses gained in this way satisfy $m^2 \geq 0$. In this work, we make the assumption that all of the masses of KK vectors are real.

With the assumption that KK vectors have real masses, we arrive at the *gravitational selection rule*, which is

> **The Gravitational Selection Rule:** When $\mathcal{M}$ possesses no Killing vectors, *retain* only the subset of gravitational stability conditions
>
> $$p_i + p_j - p_k < 1, \qquad \text{all triples} \quad i, j, k, \tag{4.47}$$
>
> with all three Kasner exponents along Σ, or all three along $\mathcal{M}$, and *ignore* stability conditions with a mixture of exponents along both Σ and $\mathcal{M}$.

In proceeding, we are guided by the KK reduced Jordan frame action (C.8). There

are three cases we need to consider: all indices along Σ, all indices along $\mathcal{M}$, and a mixture of indices:

- ***Case 1***: Three indices along Σ. These GSCs should be retained, as the corresponding modes do not gain a mass from compactification. These represent the metric degrees of freedom in the lower dimensional theory.

- ***Case 2***: Three indices along $\mathcal{M}$. Physically, these correspond to metric degrees of freedom of the compact space $\mathcal{M}$. These appear as scalar fields in the lower dimensional theory, but can result in a subtle form of chaos. Violations of these stability conditions appears as a chaotic system of interacting scalars in the lower dimensional theory. Thus, to ensure that all degrees of freedom are evolving smoothly to the big crunch, we should retain these stability conditions.

- ***Case 3***: Mixed. The "mixed" stability conditions are those with Kasner exponents along both Σ and $\mathcal{M}$. These appear as the kinetic and mass terms for the KK vectors in (C.8). When the compact space $\mathcal{M}$ possesses no Killing vectors, then all of these vector fields acquire a mass and become cosmologically irrelevant. Thus, we can delete the stability conditions in this case.

When $\mathcal{M}$ possesses even one Killing vector, then in general none of the mixed stability conditions can be discarded. This is because a single Killing field will generally involve all indices along $\mathcal{M}$, and also results in a vector field with arbitrary indices on Σ. As in the p–form case, there can be special cases where additional stability conditions may be deleted. However, as we are more interested in the generic case we will not discuss examples here.

4.4 Examples: Pure Gravity models

The previous sections have established that compactification allows us to ignore a number of the gravitational and p–form stability conditions. At this point, it is natural to ask if there are examples where enough stability conditions are deleted to control chaos. We will show in this and succeeding sections that this is indeed the case. In this section, we will focus on the case of models with Einstein gravity alone. This should be understood to be either vacuum Einstein gravity, or Einstein gravity with arbitrary perfect fluid sources satisfying $w < 1$. These matter sources become irrelevant during a contracting phase, as described in Section 2.3.

4.4.1 $n = 1$ and the $\mathbf{S}^1/\mathbb{Z}_2$ orbifold

The simplest case, with $n = 1$ extra dimensions (discussed in Section 4.2.3) is also a somewhat exceptional one. This is because there is exactly one compact one dimensional manifold, the circle $\mathbf{S}^1$. Regardless of the metric on the $\mathbf{S}^1$, it will always possess a Killing vector, and so no gravitational stability conditions can be deleted. Furthermore, $\mathcal{H}^1(\mathbf{S}^1)$ is nonzero, and so no p–form stability conditions are deleted. Therefore, all chaotic models remain chaotic when compactified on $\mathbf{S}^1$.

To eliminate chaos when $n = 1$, we must consider a more general class of spaces than manifolds. For Einstein gravity without matter, a simple example that eliminates chaos when $n = 1$ is given by the orbifold $\mathbf{S}^1/\mathbb{Z}_2$, previously discussed in Ref. [43]. If we take a coordinate θ on $\mathbf{S}^1$, ranging from $[-\pi, \pi]$, then the orbifold results from identifying the $\mathbf{S}^1$ under the reflection $\theta \to -\theta$. This takes $G_{\mu\theta} \to -G_{\mu\theta}$, and thus the Killing field is projected out, giving mass to all the KK vectors. The resulting action for massless fields in four dimensions is then

$$\mathcal{S} = \int R(g) - (\partial\phi)^2 \sqrt{-g}\, d^4x, \tag{4.48}$$

in comparison with the classic KK result (4.38). Being only Einstein gravity with a scalar field, this theory is not chaotic. We will discuss compactification on this particular orbifold in more detail when we discuss string and M–theory solutions with controlled chaos.

4.4.2 $n > 1$ and Einstein manifolds

When we have $n > 1$ extra dimensions, then chaos can be eliminated by compactifying on a manifold without continuous isometries, and therefore without Killing vectors. This deletes the mixed gravitational stability conditions, as discussed in Section 4.3.2. The remaining stability conditions can always be satisfied: for example, we can take all of the Kasner exponents to be equal to each other, and all of the compact Kasner exponents equal to each other. This is of course subject to the assumption, discussed at the end of Section 4.3.2, that the mass matrix for the KK vectors has no negative eigenvalues.

While we have seen that the masses of the KK vectors are determined by isometric properties of $\mathcal{M}$, there is a useful class of manifolds for which these properties are themselves determined by the topology, specifically by the de Rham cohomology. In this case, the gravitational and p–form selection rules are determined entirely by the cohomology of $\mathcal{M}$. These are the *Einstein manifolds*, which are Riemannian manifolds equipped with a metric g_{MN} satisfying

$$R_{MN}(g) = \lambda g_{MN}, \tag{4.49}$$

with λ arbitrary. When $\mathcal{M}$ is Einstein, the number of Killing vectors is given by $\dim \mathcal{H}^1(\mathcal{M})$ [12]. One example of a solution with controlled chaos is then obtained by taking $\mathcal{M}$ to be an isotropically evolving Einstein manifold with $\dim \mathcal{H}^1(\mathcal{M}) = 0$.

There are many examples of Einstein manifolds with this property. One class of

examples are the complex projective spaces $\mathbb{C}\mathrm{P}^n$ [88] with de Rham cohomology

$$\dim \mathcal{H}^s\left(\mathbb{C}\mathrm{P}^{n_C}\right) = \begin{cases} 1 & \text{if } s \text{ even}, \\ 0 & \text{if } s \text{ odd}, \end{cases} \tag{4.50}$$

where n_C is the complex dimension, and $n = 2n_C$. These are Einstein manifolds if equipped with the Fubini–Study metric [41]. Other important examples are the Calabi–Yau spaces, [54, 98] with

$$\dim \mathcal{H}^s\left(\mathcal{M}_{CY}\right) = \begin{cases} 1, & s = 0, 6, \\ 0, & s = 1, 5, \\ h^{1,1} & s = 2, 4, \\ 2(1 + h^{2,1}) & s = 3. \end{cases} \tag{4.51}$$

These manifolds have Ricci–flat metrics, and so are Einstein manifolds. The parameter $h^{1,1}$ counts the number of *Kähler moduli*, and must be nonzero. The parameter $h^{2,1}$ counts the number of *complex structure moduli*. In principle, $h^{2,1}$ can vanish in some cases, for example the Eguchi–Hanson space EH_3, though it is generically nonzero.

4.5 Examples: Doubly Isotropic String models

In the previous section we gave examples of pure gravity models for which chaos can be controlled. These examples had no p–form matter and so did not involve the p–form selection rules. Now, we will describe examples that include p–form fields. We will focus on the low–energy bosonic sectors of string models. We will discuss several solutions with controlled chaos in string models with $\mathcal{N} = 1$ supersymmetry in ten dimensions, and will show how these solutions are interrelated by string duality relationships.

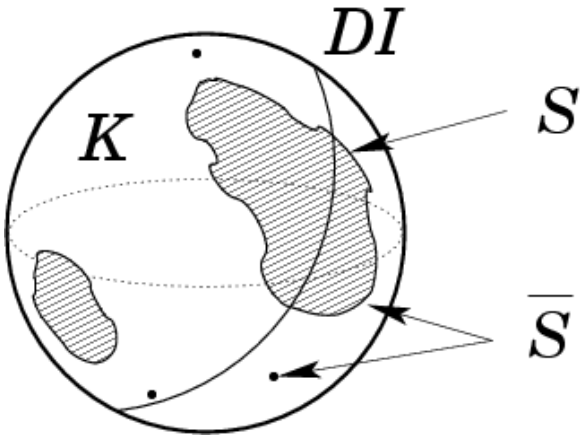

Figure 4.3: Doubly–isotropic solutions and the Kasner circle. The doubly isotropic solutions **DI** take a "slice" of the Kasner circle, which may intersect with the non–chaotic regions $\mathcal{S}$ of the circle. There may also be other non–chaotic regions that are not doubly isotropic. See also Figure 2.3.

For simplicity, we focus on regions on the Kasner sphere near what we will term *doubly isotropic* solutions. These are schematically illustrated in Figure 4.3. Doubly–isotropic solutions are choice of Kasner exponents such that a Kasner exponents take the value p_a, and b take the value p_b, with $a + b = D - 1$. These are the simplest solutions we can consider, since they correspond to both the compact and non–compact parts of spacetime evolving isotropically. In the absence of a dilaton, the Kasner conditions (2.5) result in a quadratic equation for p_a and p_b, and therefore two solutions for each choice of a and b. When a dilaton is present, then there are two one–parameter families of p_a and p_b, which depend on the value of the dilaton "Kasner exponent" p_ϕ. These solutions are given in (D.10) and (D.11). Only models that are isotropic in three noncompact directions are of interest cosmologically, and so we fix $a = 3$. The KK reduction of such models results in an isotropic universe with $p_1 \dots p_3 = 1/3$, corresponding to a FRW universe dominated by a component with equation of state $w = 1$.

It is important to emphasize that the specific examples that we will discuss are

only *representative points* of an open region on the Kasner circle for which chaos is controlled, chosen so that the Kasner exponents assume a particularly simple, symmetric form. For a given compactification, the selection rules define a reduced set of stability conditions, which in turn define an open region of the Kasner circle for which all stability conditions are satisfied. When this open region is non–empty, then chaos is controlled. Thus, there will be choices of the Kasner exponents with controlled chaos in open neighborhoods of all of the solutions discussed herein.

For string models with $\mathcal{N} = 1$ supersymmetry in ten dimensions (Type I and heterotic), the simple class of doubly isotropic solutions is sufficient to give examples of solutions with controlled chaos. As we will discuss in more detail below, some of our solutions are related to others through standard string duality relationships. Interestingly, we find that theories with $\mathcal{N} = 2$ supersymmetry (Type II) do not admit compactifications that lead to controlled chaos with doubly isotropic solutions. Unfortunately, we have found no examples where the compactification manifold could be a Calabi–Yau, thanks to the fact that the only vanishing cohomology class for Calabi–Yau spaces is $\mathcal{H}^1(\mathcal{M}) = 0$.

In the following, we will always give the Kasner exponents in the Einstein conformal frame, defined in Section 3.3.1. Conventionally, the bosonic sector of string theory actions is presented in the *string frame* form, in which the Ricci scalar appears in the action multiplied by a factor involving the string theory dilaton Φ. The formulae giving the relation between the metric and couplings in the Einstein and string frames are given in Appendix D and the relevant p–form couplings are given in Table D.1. In particular, note that we will refer to the dilaton field ϕ which is

$$\phi = \Phi/\sqrt{2}. \tag{4.52}$$

This is useful for us in that ϕ has a canonical kinetic term in the ten–dimensional Einstein frame.

A theme common to our examples is the compatibility of our results concerning controlled chaos and the duality relationships connecting various string theories. In Section 4.5.1 we first examine the $E_8 \times E_8$ heterotic theory in detail. Through a combination of string duality relationships and compactifications we will be able to discuss its limits in eleven, ten, five and four dimensions. In particular, the S–duality relating the $E_8 \times E_8$ heterotic string and M–theory [67, 68] is made apparent by relating the ten dimensional heterotic solution with controlled chaos and the compactification of eleven dimensional M–theory on $\mathbf{S}^1/\mathbb{Z}_2$. We will then discuss all compactifications of doubly isotropic solutions with controlled chaos for string theories with $\mathcal{N} = 1$ supersymmetry in ten dimensions. We give four representative solutions, two each for the heterotic and Type I theories. We show that these four solutions organize into two pairs of solutions, related by the S–duality connecting the heterotic SO(32) and Type I strings [98, 99].

It is important to keep in mind some features of the space of string solutions with controlled chaos. Each compactification we discuss, defined by the vanishing de Rham cohomology classes, defines an open region on the Kasner circle where chaos is controlled. Our restriction to doubly isotropic models, in turn, takes a one dimensional "slice" out of this open region. In our examples, we give a representative point from the "slice" where the Kasner exponents assume a convenient and symmetric form. Thus we have found the compactifications that admit doubly isotropic solutions, but the choices of Kasner exponents are not unique.

4.5.1 The heterotic string and M–theory

Here we focus on the $E_8 \times E_8$ heterotic theory, in the neighborhood of a specific choice of Kasner exponents. Using string duality relationships and compactification, we will discuss the various guises of this solution in eleven, ten, five and four dimensions

theory	spacetime	dim	$p_1 \dots p_3$	$p_4 \dots p_9$	p_{10}	p_ϕ
M–theory	$\Sigma \times \mathcal{M} \times \mathbf{S}^1/\mathbb{Z}_2$	11	-0.1206	0.0662	0.9644	
het $E_8 \times E_8$	$\Sigma \times \mathcal{M}$	10	0	1/6		$\sqrt{5/6}$
"braneworld"	$\Sigma \times \mathbf{S}^1/\mathbb{Z}_2$	5	0.0105		0.9686	0.2486
FRW	Σ	4	1/3			$\sqrt{2/3}$

Table 4.2: The solution discussed in the text for the $E_8 \times E_8$ heterotic string in various dimensions. The Kasner exponent p_ϕ is a combination of the dilaton and volume modulus for the compactified dimensions. Chaos is controlled provided that $\mathcal{H}^3(\mathcal{M}) = 0$.

[67, 68, 87], summarized in Table 4.2. We will make extensive use of the formulae relating compactified Kasner universes in various dimensions given in Appendix D. While the specific solution we discuss also controls chaos for the SO(32) heterotic theory in ten dimensions, string dualities for this theory do not enable us to discuss the five dimensional and M–theory limits. To begin, we consider the heterotic theory in Einstein frame, where it contains the metric G_{MN}, dilaton ϕ, one–form A_1 and two–form B_2. The dilaton couples to the one– and two–forms via exponential couplings of the type (2.34), with $\lambda_1 = -1/\sqrt{2}$, and $\lambda_2 = -\sqrt{2}$.

Without compactification, one finds violations of the ESCs and MSCs for the choice of Kasner exponents

$$p_1 \dots p_3 = 0, \quad p_4 \dots p_9 = 1/6, \quad p_\phi = \sqrt{5/6} \qquad \text{(10D)}. \tag{4.53}$$

We assume that $p_1 \dots p_3$ lie along the noncompact spacetime Σ, and $p_4 \dots p_9$ lie along the compact manifold $\mathcal{M}$. In this solution, the magnetic stability conditions are violated for the magnetic component of $H_3 = \mathrm{d}B_2$ with all three indices along $\mathcal{M}$. None of the GSCs are violated.

Applying the selection rules introduced in Section 4.3.1, we find that chaos is controlled by compactifying on a six–manifold $\mathcal{M}$ with $\mathcal{H}^3(\mathcal{M}) = 0$, such as $\mathbf{S}^6$ or $\mathbb{C}\mathrm{P}^3$. The choice of $\mathbb{C}\mathrm{P}^3$ has the advantage that it has $\mathcal{H}^1\left(\mathbb{C}\mathrm{P}^3\right) = 0$, and is an

Einstein manifold if given the Fubini–Study metric. From the discussion in Section 4.4 we know that such manifolds have special properties with respect to gravitational chaos, and so this manifold may be a useful starting point for models that differ from the doubly isotropic ones. Unfortunately, a Calabi–Yau space will always have $\dim \mathcal{H}^3(\mathcal{M}) > 0$, and is thus unsuitable for rendering this solution non chaotic.

The four dimensional limit of the solution (4.53) possesses a simple form. This is obtained by compactifying on the six–manifold $\mathcal{M}$, resulting in

$$p_1 \ldots p_3 = 1/3, \qquad (4D). \tag{4.54}$$

This describes a collapsing, flat FRW universe dominated by a perfect fluid with $w = 1$. The $w = 1$ component is a combination of the dilaton and the volume modulus arising from the KK reduction of the heterotic theory on the six–manifold $\mathcal{M}$.

String duality relationships imply that the (strongly coupled) $E_8 \times E_8$ heterotic theory is obtained by compactifying M–theory on the orbifold $\mathbf{S}^1/\mathbb{Z}_2$ [67, 68, 87]. Phenomenology implies that the orbifold $\mathbf{S}^1/\mathbb{Z}_2$ is somewhat larger than the compactification six manifold $\mathcal{M}$. Thus, depending on the scale of interest, the strongly coupled heterotic theory can appear four, five, or eleven dimensional. The five and eleven dimensional limits of the solution (4.53) are not as simple as the ten and four dimensional views, but are nonetheless instructive.

This duality relationship implies that the heterotic string in ten dimensions can be described by eleven dimensional M–theory on $\Sigma \times \mathcal{M} \times \mathbf{S}^1/\mathbb{Z}_2$. The eleven dimensional lifting of (4.53) to M–theory yields Kasner exponents whose precise expression is not very illuminating, but whose approximate numerical values are

$$p_1 \ldots p_3 = -0.1206, \quad p_4 \ldots p_9 = 0.0662, \quad p_{10} = 0.96442 \qquad (11D). \tag{4.55}$$

This describes a rapidly shrinking orbifold, a slowly contracting six–manifold $\mathcal{M}$, and a slowly expanding noncompact space.

To see that the compactification of M–theory on $\Sigma \times \mathcal{M} \times \mathbf{S}^1/\mathbb{Z}_2$ leads to controlled chaos requires us to consider some subtle features of the theory. The bosonic sector of M–theory includes only the graviton and a four form field strength $F_4 = \mathrm{d}A_3$. Our selection rules are only strictly applicable to the case where the compactification space is a manifold, an assumption which fails to include orbifolds such as $\mathbf{S}^1/\mathbb{Z}_2$. The approach most convenient here follows usual techniques [67, 68, 87] for determining the spectrum after compactification. Specifically, we compactify M–theory on $\mathbf{S}^1$, and then impose the identification $\theta \to -\theta$. The presence of the Chern–Simons term $A_3 \wedge F_4 \wedge F_4$ in the M– theory Lagrangian requires that $F_4 \to -F_4$ under parity transformations, of which the identification $\theta \to -\theta$ is an example. Thus, the massless components of F_4 on $\Sigma \times \mathcal{M} \times \mathbf{S}^1/\mathbb{Z}_2$ are those with exactly one index along the $\mathbf{S}^1/\mathbb{Z}_2$.

Before compactification, the eleven–dimensional solution given above violates the p–form stability conditions for three components of the four form field. The first and second are electric, with the first having three indices along Σ, and the second having two along Σ and one along $\mathcal{M}$. The third is magnetic, with one index along $\mathbf{S}^1/\mathbb{Z}_2$ and three along $\mathcal{M}$. The magnetic component is rendered massive by the condition $\mathcal{H}^3(\mathcal{M}) = 0$, and so we can neglect this stability condition. The two electric components are rendered massive since they do not have exactly one index along the $\mathbf{S}^1/\mathbb{Z}_2$, and their stability conditions can be neglected as well. Thus, chaos is controlled in the M–theory limit.

The five dimensional guise of our solution, obtained by KK reducing the eleven dimensional form on the six– manifold $\mathcal{M}$, describes a "braneworld" with structure $\Sigma \times \mathbf{S}^1/\mathbb{Z}_2$. This yields the solution,

$$p_1 \ldots p_3 = 0.01048, \quad p_{10} = 0.9686, \quad p_\psi = 0.24804. \qquad \text{(5D)} \qquad (4.56)$$

The scalar field ψ is the volume modulus of the six–manifold $\mathcal{M}$. This solution describes a nearly static Σ and a rapidly contracting orbifold. This solution bears a

sol'n	$p_1 \dots p_3$	$p_4 \dots p_9$	p_ϕ	theories	zero betti
A	0	1/6	$+\sqrt{5/6}$	heterotic	b_3
B	0	1/6	$-\sqrt{5/6}$	Type I	b_3
C	1/3	0	$+\sqrt{2/3}$	Type I	b_1, b_2
D	1/3	0	$-\sqrt{2/3}$	heterotic	b_1, b_2

Table 4.3: Representative string theory solutions with controlled chaos and isotropic behavior along the noncompact and compact directions. Each compactification leads to open regions of the Kasner circle with controlled chaos, and we have given a representative point for each open region here. The string theories which exhibit controlled chaos for each solution are shown, as well as the Betti numbers $b_j = \dim \mathcal{H}^j(\mathcal{M})$ of $\mathcal{M}$ that are required to vanish.

suggestive similarity to the set–up studied in the ekpyrotic/cyclic scenario. In these models, near the big crunch, the five–dimensional spacetime approaches the Milne solution

$$p_1 \dots p_9 = 0, \quad p_{10} = 1. \tag{4.57}$$

This solution is in fact on the boundary of the open region of the Kasner sphere for which our example solution (4.53) exhibits controlled chaos. This is predicated on the assumptions that $w = 1$ in the four–dimensional theory all the way to the big crunch, and that compactification is the only mechanism for controlling chaos. In the ekpyrotic/cyclic scenarios, there is a long $w \gg 1$ phase during the contraction, in which the energy density in p–form modes is exponentially suppressed [43]. This suppression further reduces the time t_{dom} at which dangerous modes can formally dominate the universe. Therefore, in the full model, the onset of chaos will be delayed far beyond what our estimates, based only on the compactification mechanism, would suggest.

4.5.2 The heterotic and Type I strings

Having focused in detail on a single compactification of a single string theory, we now focus on finding all compactifications with controlled chaos and doubly isotropic Kasner exponents. There are four doubly isotropic examples with controlled chaos, with representative choices of the Kasner exponents summarized in Table 4.3. The $E_8 \times E_8$ and SO(32) heterotic theories exhibit the same chaotic behavior, since their p–form spectrum and couplings to the dilaton are identical; these theories differ only in the gauge groups for their non–abelian gauge multiplets. One may also include the ten–dimensional (noncritical) bosonic string, which contains only the Neveu–Schwarz fields of the heterotic string and no gauge fields. One finds that chaos is controlled in the ten dimensional bosonic string in the same solutions (**A** and **D**) as in the heterotic string.

In the absence of any compactification, these examples are all chaotic. None of them suffer from gravitational chaos, and in all cases the chaotic behavior arises from the p–form fields alone. Upon compactification to four dimensions, these models all result in a FRW universe dominated by a free scalar field with $w = 1$.

The examples given in Table 4.3 include not only models that go to weak coupling at the crunch, (**A** and **C**) but also models where the dilaton runs to strong coupling (**B** and **D**). The fact that the solutions include both those where the string theory goes to strong and weak coupling is interesting from a model building perspective. The dilaton is never static in the solutions discussed here, a feature also found in some cosmological models based on string theory. In the ekpyrotic/cyclic models, for example, the string coupling goes to zero at the big crunch. In pre big–bang models, on the other hand, the dilaton goes to strong coupling at the crunch [48]. Thus the controlled chaos mechanism may be relevant to both scenarios.

The heterotic SO(32) and Type I theories are related by an S–duality transforma-

tion [98, 99], and this symmetry is respected by our examples here. Under this duality, the string frame actions of the heterotic SO(32) and Type I theories are related by

$$G^{(I)}_{MN} = e^{-\Phi_h} G^{(het)} \tag{4.58a}$$

$$\Phi^{(I)} = -\Phi^{(het)} \tag{4.58b}$$

with the p–form fields remaining unchanged. Carefully working through the resulting transformation of the Einstein frame Kasner exponents, one finds that the spatial Kasner exponents are unchanged, while $p^{(I)}_\phi = -p^{(het)}_\phi$. Therefore, S–duality exchanges the pairs of solutions $\mathbf{A} \leftrightarrow \mathbf{B}$ and $\mathbf{C} \leftrightarrow \mathbf{D}$. More information on string dualities and Kasner exponents may be found in Appendix D and in [83].

The properties of string theories regarding controlled chaos appear correlated to their supersymmetry properties in ten dimensions. The $\mathcal{N} = 1$ theories, (heterotic, Type I, and M–theory on $\mathbf{S}^1/\mathbb{Z}_2$) possess simple compactifications that control chaos. The Type IIA/B theories and uncompactified M–theory, with $\mathcal{N} = 2$ supersymmetry, have no doubly isotropic solutions with controlled chaos.

It is natural to expect that the $\mathcal{N} = 1$ and $\mathcal{N} = 2$ string theories will have different characteristics with respect to controlled chaos. There is a useful formulation of the dynamics of gravity near a big crunch, discussed briefly in Section 2.6 and in great detail in Chapter 5. In this formulation, the dynamics of metric and p–form fields is recast as the motion of a billiard ball in a hyperbolic space, undergoing reflections from a set of walls. The walls correspond to p–form kinetic terms and curvature terms in the Einstein equations. The positions and orientations of these walls are identical for all of the $\mathcal{N} = 1$ theories, and different from the common set of walls shared by the $\mathcal{N} = 2$ theories [28]. Our suppression of the energy density in massive p–form and gravitational modes amounts to "pushing back" these walls. Thus, it is not surprising that we should find that $\mathcal{N} = 1$ and $\mathcal{N} = 2$ models have different characteristics with respect to controlling chaos.

4.6 Examples: A Computer Search

Here we describe a more thorough search for solutions of the stability conditions as truncated by the selection rules. This search was carried out using a computer program that searches the Kasner sphere for solutions with controlled chaos. During this search, solutions with controlled chaos for the $\mathcal{N} = 2$ theories were found. We also find additional solutions for the $\mathcal{N} = 1$ theories. No solutions with $\dim \mathcal{H}^1(\mathcal{M})$ were discovered. In Chapter 5 we describe a systematic method for finding solutions with controlled chaos, and the computer search we discuss below provides a useful check against the results we will present in that chapter.

The program makes use of a explicit parameterization of the Kasner sphere for the Einstein–scalar system. For a spacetime with a free scalar field, recall that there are $d+1$ Kasner exponents, where we have grouped the metric exponents p_j and the scalar field exponent p_ϕ together. Furthermore, we are searching for solutions that are isotropic in three spatial dimensions, and so three of the spatial exponents should be identical. Denote by p_3 the value of the Kasner exponents along the noncompact directions, and $p_1, \ldots p_6$ the exponents along the compact directions. Because of the Kasner conditions (2.36), the exponents must satisfy

$$A = \sum_{j=1}^{6} p_j, \qquad B = \sum_{j=1}^{6} p_j^2, \tag{4.59}$$

where

$$A = 1 - 3p_3, \qquad B = 1 - 3p_3^2 - p_\phi^2 \tag{4.60}$$

The Kasner circle associated with each choice (p_3, p_ϕ) is an $\mathbf{S}^4$ of radius ρ, with

$$\rho^2 = B - \frac{A^2}{6} \tag{4.61}$$

When $\rho^2 > 0$, there is a nontrivial space of solutions. When $\rho^2 = 0$, there is a single solution, corresponding to the doubly isotropic solutions discussed above. When

$\rho^2 < 0$, there are no solutions to the Kasner conditions. Not every value of (p_3, p_ϕ) admits solutions to the Kasner conditions.

This sphere of solutions is not centered on the origin. It is both displaced and rotated. First define a vector $\vec{x}$ in $\mathbf{R}^6$ as a function of the four angles $\theta_1, \ldots \theta_4$ on the Kasner circle by

$$x_1 = 0, \tag{4.62a}$$

$$x_2 = \cos\theta_1, \tag{4.62b}$$

$$x_3 = \sin\theta_1 \cos\theta_2, \tag{4.62c}$$

$$x_4 = \sin\theta_1 \sin\theta_2 \cos\theta_3, \tag{4.62d}$$

$$x_5 = \sin\theta_1 \sin\theta_2 \sin\theta_3 \cos\theta_4, \tag{4.62e}$$

$$x_6 = \sin\theta_1 \sin\theta_2 \sin\theta_3 \sin\theta_4 \tag{4.62f}$$

This is just the standard embedding of $\mathbf{S}^4$ in $\mathbf{R}^5$, with x_1 a spectator dimension. Next we define a rotation matrix by

$$\mathbf{R} = \begin{pmatrix} \vec{c}_1 & \vec{c}_2 & \vec{c}_3 & \vec{c}_4 & \vec{c}_5 & \vec{c}_6 \end{pmatrix} \tag{4.63}$$

with

$$\vec{c}_1 = \begin{pmatrix} 1 & -1 & 0 & 0 & 0 & 0 \end{pmatrix} / \sqrt{2}, \tag{4.64a}$$

$$\vec{c}_2 = \begin{pmatrix} 1 & 1 & -2 & 0 & 0 & 0 \end{pmatrix} / \sqrt{6}, \tag{4.64b}$$

$$\vec{c}_3 = \begin{pmatrix} 1 & 1 & 1 & -3 & 0 & 0 \end{pmatrix} / \sqrt{12}, \tag{4.64c}$$

$$\vec{c}_4 = \begin{pmatrix} 1 & 1 & 1 & 1 & -4 & 0 \end{pmatrix} / \sqrt{20}, \tag{4.64d}$$

$$\vec{c}_5 = \begin{pmatrix} 1 & 1 & 1 & 1 & 1 & -5 \end{pmatrix} / \sqrt{30}, \tag{4.64e}$$

$$\vec{c}_6 = \begin{pmatrix} 1 & 1 & 1 & 1 & 1 & 1 \end{pmatrix} / \sqrt{6}, \tag{4.64f}$$

The column vectors $\vec{c}_1, \ldots \vec{c}_5$ are thus an orthonormal basis for vectors in $\mathbf{R}^6$ with

vanishing "trace." Now form the product

$$\vec{y} = \mathbf{R}\vec{x} = \sum_{j=1}^{5} x_j \vec{c}_j \tag{4.65}$$

This rotates the circle away from the 23456 plane. Note that thanks to the properties of the $\vec{c}_j$, we have

$$\sum_j y_j = 0, \qquad \sum_j y_j^2 = 1. \tag{4.66}$$

Finally, define the Kasner exponents by

$$p_j = \rho y_j + \frac{A}{d} \tag{4.67}$$

It is readily seen that these satisfy the Kasner conditions. This procedure therefore parameterizes the full Kasner circle in terms of the four angles $\theta_1 \cdots \theta_4$. This procedure is easily generalized to any number of dimensions.

With this parameterization in hand, the problem of finding solutions with controlled chaos amounts to traversing all values of the four angles $\theta_1, \cdots \theta_4$ and the two variables p_3 and p_ϕ. Then one checks that the stability conditions are satisfied for a given set of nonzero cohomology classes. In practice, a gridding of the sphere turns out to be impractical – the grid must be extremely fine to capture any solutions with controlled chaos: for example, a 10^2 grid points per dimension yields 10^{12} required chaos checks, and each chaos check is computationally expensive. Instead, the program uses a weighting function and crawls over the Kasner circle, attempting to minimize the amount by which the stability conditions are violated. Within the program, it is also possible to specify the symmetry of the solution, and both marginal and non–chaotic solutions can be displayed.

A summary of the results of this computer search is given in Table 4.4. We have used a notation in which exponents give the number of times an exponent is repeated: for example,

$$a^2 b^4 \to (a, a, b, b, b, b) \tag{4.68}$$

theory	zero Betti	sol'n	p_ϕ	p_3	p_j	type
het	b_1	1	$+2\sqrt{2}/5$	1/5	$-3/5, (1/5)^5$	marginal
"	b_1, b_2	2=**D**	$-\sqrt{2/3}$	1/3	0^6	non–chaotic
"	b_3	3=**A**	$+\sqrt{5/6}$	0	$(1/6)^6$	non–chaotic
IIA	b_1, b_2	1	0	0	$-2/3, (1/3)^5$	marginal
"	b_1, b_2	2	$-2\sqrt{2}/5$	1/5	$-3/5, (1/5)^5$	marginal
"	b_1, b_2, b_3	3				non–chaotic
IIB	b_1, b_2	1	0	0	$-2/3, (1/3)^5$	marginal
"	b_2, b_3	2	0	1/5	$(-1/5)^4, (3/5)^2$	marginal
"	b_2, b_3	3	0	1/3	$(-1/3)^3, (1/3)^3$	marginal
"	b_1, b_2, b_3	4				non–chaotic

Table 4.4: Some representative solutions with controlled chaos in string models with $\mathcal{N} = 1$ and $\mathcal{N} = 2$ in ten dimensions. Of the $\mathcal{N} = 1$ models, only the heterotic is shown. Milne solutions are left out of this table. See text for solution notation.

It is clear from the table that non–chaotic solutions exist in the $\mathcal{N} = 2$ theories, although the only ones found thus far are those that require all possible cohomology classes to vanish, probably too stringent a requirement for interesting compactifications. As in Table 4.3, some of these solutions are connected by string dualities. The formulae governing these transformations are given in Section D.3. For example, denote by "Milne" the solution with

$$\text{Milne} \ : \ p_\phi = 0, \ p_3 = 0, \ 0^5, 1. \tag{4.69}$$

Then, for example

$$\text{IIA}_2 = \mathbf{T}_6 \cdot \text{Milne} \tag{4.70}$$

and

$$\text{het}_1 = \mathbf{S} \cdot \mathbf{T}_6 \cdot \text{Milne} \tag{4.71}$$

where $\mathbf{S}$ denotes S–duality and $\mathbf{T}_n$ denotes T–duality along x^n, respectively. The presence of T–duality symmetries is especially surprising, since they map a small (compactified) dimension into a large one.

Overall, there are two main conclusions we can draw from in Table 4.4. The first is that solutions with controlled chaos exist for string models with $\mathcal{N} = 2$ supersymmetry. This was not entirely clear from the analysis of doubly isotropic solutions in Section 4.5. Focusing on the heterotic string, we can also conclude that it appears that either $b_3 = 0$, or $b_1 = b_2 = 0$ in order for solutions with controlled chaos to exist. This fact will provide a useful check for the results we discuss in the next chapter.

4.7 Conclusions

The results presented here build on the many years of previous research in the behavior of general relativity near a big crunch. Previous research has primarily focused on "local" properties of theories with gravity, such as the dimensionality of spacetime, or the types and interactions of matter fields, and has revealed how these influence the emergence of chaos. Here we have investigated "global" features, in particular the topology of spacetime. We have found that these features can lead to a suppression of chaos in many models of interest. The control of chaos can be expressed simply in terms of selection rules for the gravitational and p–form stability conditions. These in turn can be used to find compactifications of chaotic theories in which chaos is suppressed right up to the quantum gravity regime.

Our results bear an intriguing connection to some cosmological models that are founded on current ideas in string and M–theory. Among the simple examples of string theory solutions with controlled chaos, we find those that resemble both the ekpyrotic/cyclic [78, 108] and pre–big bang [48] scenarios. For future models, this work suggests a method to control chaotic behavior near a big crunch that does not require postulating additional interactions and matter fields, or depending on higher order corrections to the Einstein equations. While this work sheds no light on the behavior of these models in the quantum gravity regime or through the big

crunch/big bang transition, it provides a natural mechanism that ensures that the universe evolves smoothly so long as classical physics may be trusted.

Recent work suggests that maintaining this smooth contraction during the classical regime may be sufficient to allow a nonsingular quantum evolution through a big crunch/big bang transition. One approach to this problem begins from the fact that, in string and M–theory, the degrees of freedom during the quantum regime are very different from those of the classical regime studied here. The fundamental degrees of freedom are extended objects, such as strings and branes. As one approaches the scale set by their tension, classical general relativity breaks down, and these extended objects become the relevant degrees of freedom. In particular, it is the evolution of these strings and branes that one should study near the big crunch. Working within the context of the ekpyrotic/cyclic scenario, it was found in [119] that if the universe is sufficiently smooth and homogeneous at the beginning of the quantum regime, the fundamental excitations (M2 branes) evolve smoothly through the big crunch with negligible backreaction. This suggests that a sufficiently smooth "in" state can evolve through the big crunch to a smooth "out" state, precisely what one requires for cosmology. This result complements the present work. The mechanism described herein can be viewed as providing the required conditions for smooth classical evolution before the Einstein equations break down, preparing the universe for nonsingular quantum evolution through the big crunch.

Our results have further implications for high energy theory and phenomenology. String models and M–theory require compactification in order to produce the correct number of observed noncompact dimensions. Obtaining the correct low energy physics, such as $\mathcal{N} = 1$ supersymmetry in four dimensions or the correct number of lepton generations, puts constraints on the compactification manifold $\mathcal{M}$, many of which are topological in nature. Even with these constraints, there still seems to be a

large number of possible choices for $\mathcal{M}$. Controlling chaos through compactification in cosmological models with a collapsing phase places additional constraints on $\mathcal{M}$. Thus in the context of these cosmological models one obtains additional viewpoints on string phenomenology

These results also inspire more speculative scenarios. When the universe enters a chaotic regime, the Kasner exponents will undergo an infinite number of "jumps" to different points on the Kasner sphere as the big crunch is approached. We also might expect that the topology of $\mathcal{M}$ is changing at the same time. For example, there are situations in string theory where the topology of $\mathcal{M}$ can change dynamically, such as the conifold [23, 55, 110] or flop [4] transitions. If the combination of Kasner exponents and topology lead to controlled chaos, then the universe will subsequently contract smoothly to the big crunch. In this way, the universe will have dynamically selected not only some properties of $\mathcal{M}$, but also a "preferred" cosmological solution near the big crunch. Analysis of such a scenario would require a much deeper understanding of cosmology in the quantum gravity regime than is currently available, clearly an important topic for further research.

Chapter 5

Enumeration of Solutions

He took the golden compasses, prepared
In God's eternal store, to circumscribe
This universe, and all created things:
One foot he centered, and the other turned
Round through the vast profundity obscure
And said, "Thus far extend, thus far thy bounds,
This be thy just circumference, O world."

Paradise Lost Book VII, lines 225–231, [90]

In the previous chapter, we introduced a mechanism to control chaos thruogh compactification. Each compactification, described by its vanishing Betti numbers, defines a set of linear inequalities in the Kasner exponents. For a typical string model there are $\sim 10^2$ of these conditions. If these inequalities are simultaneously satisfied, then chaos is controlled by the compactification. The problem of finding solutions to controlled chaos thus amounts to determining whether a system of inequalities possesses a solution. We have presented some solutions with special symmetry properties in the previous chapter, but no systematic techniques for finding solutions other than hit–or–miss.

In this chapter, we describe techniques that allow one to systematically find solu-

tions with controlled chaos. For a given model and compactification, these techniques make it straightforward to

- determine the existence of solutions with controlled chaos,
- explicitly parameterize the set of solutions,
- find all solutions with desired isotropy properties.

These techniques owe much to the billiard picture of gravitational dynamics near a big crunch, as developed by a number of researchers. In this picture, the evolution of a gravitational system is mapped into the motion of a point in an auxiliary spacetime. The point undergoes motion under the influence of conservative forces, which as the big crunch is approached take the form of a set of sharp "walls." This picture has led to fascinating connections between the gravitational dynamics of certain string models, and the root lattices of certain Kac–Moody algebras. We will depend heavily on this representation in this chapter.

This chapter is organized as follows. Section 5.1 is largely a review of the billiard representation. We introduce this representation, and describe the metric structure of the auxiliary spacetime for pure gravity and string models. We also introduce the concept of *relevant walls*, which enable the full set of stability inequalities to be reduced to a much smaller and more manageable set. The discussion in this section is based primarily on [25, 27, 28, 29]. In Section 5.2 we describe the conditions necessary for chaos to be avoided in the billiard picture. We embed the $w \geq 1$ mechanism, described in Chapter 3, in the billiard picture. We also give an interpretation of the controlled chaos mechanism, and describe the technique by which solutions can be found. In Section 5.3 we analyze all compactifications of the heterotic string theory. We discriminate those that possess solutions with controlled chaos, and those that do not. In Section 5.4 we complete the connection with previous work by giving the

mapping between the billiard picture and the Kasner exponent picture. Here we give formulae relating the trajectory of the point in the billiard representation to a specific Kasner exponent. We then apply these formulae in worked examples.

The work in this section represents unpublished work by the author.

5.1 Introduction: Cosmology as Billiards

Up to now, we have primarily considered the gravitational and p–form stability conditions as a set of inequalities that may (or may not) be satisfied for choices of the Kasner exponents satisfying the Kasner conditions. In the following we will change perspective somewhat. We show in Appendix A that the dynamics of the universe can be described in terms of the motion of a point mass, under the influence of conservative forces, in an auxiliary Lorentzian spacetime. These forces arise from potentials taking the form of exponential walls, and collisions with these walls correspond to the Kasner bounces characteristic of chaotic behavior. Here we will develop this point of view more systematically, setting the stage for our analysis later in the chapter.

A basic idea in the billiard picture is that we are viewing the time evolution of the universe in terms of the time evolution of the spatial d–metric. The configuration space of this dynamical system is thus the "space of metrics," which sometimes goes by the name *superspace* [92]. (There is no connection to supersymmetry implied) Points in superspace are d–metrics of physical space. In addition, there is often a natural metric structure on superspace, and we can thus define a *supermetric* giving the "distance" between two infinitesmally close metrics. In this chapter, we will take all metrics to be of the generalized Kasner type (2.25). These metrics are parameterized by the d functions of time γ^j. We can think of the generalized Kasner metrics as a d–dimensional slice of superspace, with coordinates γ^j on the slice. In the following, by considering the action for generalized Kasner universes, we will find the associated

canonical supermetric on the space of scale factors. These supermetrics will be crucial to the analysis of these theories with respect to controlled chaos.

This section is largely a review of results from the literature. We especially make use of [25, 29] and the descriptions therein for constructing the billiard system corresponding to a given gravitational theory. In these references, the generalized Kasner metric is parameterized in terms of a vector β^μ, which is related to our vector γ^μ (to be defined below) by $\beta^\mu = -\gamma^\mu$. We have chosen to keep the γ^μ parameterization for consistency with the rest of this work. Also, our naming conventions for the wall forms (also to be defined below) differ from those in the literature.

5.1.1 Vacuum Gravity

We first consider the case of pure Einstein gravity, which also covers the case of matter sources satisfying $w < 1$. After computing the Ricci scalar for this metric (described for the $d = 3$ case in Appendix A) and integrating by parts, one arrives at the effective action

$$\mathcal{S} = \int N^{-1} e^{\sum_j \gamma^j} \left(\sum_j \left[\dot{\gamma}^j\right]^2 - \sum_{j,k} \dot{\gamma}^j \dot{\gamma}^k \right) - N e^{\sum_j \gamma^j} U(\gamma)\, dt \tag{5.1}$$

The potential $U_{grav}(\gamma)$ is a sum of terms of the form

$$\exp\left(2\left[\gamma^i - \gamma^j - \gamma^k\right]\right), \tag{5.2}$$

and describes the influence of spatial curvature and inhomogeneity of the universe. The natural choice for the lapse function N is

$$N = e^{\sum_j \gamma^j}, \tag{5.3}$$

which makes the action that of a point moving under the influence of conservative forces. The corresponding potential is denoted by $V(\gamma)$ and is given by

$$V(\gamma) = e^{2\sum_j \gamma^j} U_{grav}(\gamma) \tag{5.4}$$

This point moves in an auxiliary Lorentzian spacetime, whose corresponding supermetric is given by

$$(1/2)G_{ij}u^i v^j = \sum_j u^j v^j - \sum_{jk} u^j v^k \tag{5.5}$$

with inverse

$$G^{ij}u_i v_j = \frac{d}{d-1}\sum_j u_j v_j - \frac{2}{d-1}\sum_{jk} u_j v_k \tag{5.6}$$

with

$$G^{ij} = \begin{cases} \frac{d-2}{d-1} & \text{for } i = j, \\ -\frac{1}{d-1} & \text{for } i \neq j \end{cases} \tag{5.7}$$

For example, in $d = 3$ we have

$$G_{ij} = \begin{pmatrix} 0 & -1 & -1 \\ -1 & 0 & -1 \\ -1 & -1 & 0 \end{pmatrix} \qquad G^{ij} = \frac{1}{2}\begin{pmatrix} 1 & -1 & -1 \\ -1 & 1 & -1 \\ -1 & -1 & 1 \end{pmatrix} \tag{5.8}$$

The "timelike" direction in this metric is that corresponding to the collective coordinate $\gamma^1 + \gamma^2 + \cdots$, which one can see is simply the volume of spatial slices in the physical spacetime.

It has been pointed out that in the limit that the volume goes to zero, there is a choice of time coordinate so that the potential $V(\gamma)$ is a sum of sharp wall potentials. We describe this in Appendix A for the Mixmaster universe example. With this choice of time, the point undergoes geodesic motion in regions far from the walls and reflects specularly when it encounters a wall. The point is therefore confined to the region defined by

$$e^{2\sum_j \gamma^j} U(\gamma) \sim 0 \implies 2\gamma^i + \sum_m \gamma^m < 0, \qquad \text{where } m \neq i, j, k \tag{5.9}$$

This is the analogue of the gravitational stability conditions introduced earlier; when it is satisfied, the geodesic motion of the point corresponds to smooth Kasner–like

contraction. It can be re–expressed by introducing a 1–form, called the *wall form*, corresponding to this stability condition. Thus,

$$w_{ijk|m}\gamma^m < 0, \qquad w_{ijk,m} = \begin{cases} 2 & \text{for } m = i, \\ 1 & \text{for } m \neq i, j, k, \\ 0 & \text{for } m = j, k \end{cases} \tag{5.10}$$

where the wall form is indexed by the subscripts before the "|," and its components indexed by the subscript afterwards. These wall forms describe the *gravitational walls* arising from spatial curvature.

It is also convenient to introduce additional walls to simplify the problem. Note that everything is symmetric under the interchange $\gamma^i \leftrightarrow \gamma^j$ for any i, j, and so our configuration space is somewhat redundant. We can fix this redundancy by imposing the requirement that

$$\gamma^1 > \gamma^2 > \cdots > \gamma^d \tag{5.11}$$

through the introduction of the inequalities

$$\gamma^j - \gamma^{j-1} < 0, \qquad j = 2 \ldots d \tag{5.12}$$

which correspond to *symmetry walls*

$$w_{j|m} = \begin{cases} 1 & \text{for } m = j, \\ -1 & \text{for } m = j - 1, \\ 0 & \text{otherwise.} \end{cases} \tag{5.13}$$

These walls restrict the point to move in a wedge of the full configuration space.

The symmetry walls are somewhat different than the gravitational walls. Hitting a gravitational wall corresponds to a Kasner bounce, as introduced in Chapter 2. On the other hand, hitting a symmetry wall corresponds to a reshuffling of the labels on

the γ^j as one grows to be larger than another. In addition, one should perhaps think about the "$<$" as being "$\leq$" in order to not exclude solutions with some degree of isotropy. These subtleties will not be vitally important to us, but it is good to keep the differences between the symmetry walls and the gravitational walls in mind.

Not all of the walls we have introduced are independent; some are "hidden" behind other walls. Algebraically, we say a wall is "hidden" behind others if the corresponding inequality is a linear combination of other inequalities with positive coefficients. A wall is a *relevant wall* it it is not hidden. All of the inequalities are consequences of the relevant ones, or equivalently all of the wall forms are linear combinations of the relevant wall forms with positive coefficients. In the case of pure gravity, the relevant walls are

$$\gamma^j - \gamma^{j-1} < 0 \quad j = 2 \ldots d, \qquad 2\gamma^1 + \gamma^2 + \cdots + \gamma^{d-2} \tag{5.14}$$

which correspond to the d wall forms $w_{1,d-1,d|m}$ and $w_{j|m}$ for $j = 2 \ldots d$.

5.1.2 String Actions

For applications to string models, we must carry through a similar analysis for the corresponding gravitational action. It differs in that the Ricci scalar couples non-trivially to the dilaton Φ through

$$\mathcal{S}_{str} = \int e^{-2\Phi} \left(R[G] + 4(\partial\Phi)^2 \right) + \cdots \sqrt{-G}\, d^{10}x \tag{5.15}$$

Following a calculation similar to the case for vacuum Einstein gravity, we insert the Ricci scalar for the generalized Kasner metric and integrate by parts. In this case it turns out to be more convenient to rescale the dilaton field and define

$$\gamma^0 = 2\Phi - \sum_j \gamma^j. \tag{5.16}$$

Unlike the dilaton, the new parameter γ^0 is invariant under T–duality transformations (see Section D.3.1). In the literature, it is sometime referred to as the *shifted dilaton*.

These steps result in the effective action

$$\mathcal{S} = \int N^{-1} e^{-\gamma^0} \left(- \left[\dot{\gamma}^0 \right]^2 + \sum_j \left[\dot{\gamma}^j \right]^2 \right) - N e^{-\gamma^0} U_{grav}(\gamma) \, dt \tag{5.17}$$

Clearly the natural choice for the lapse function is

$$N = e^{-\gamma^0}. \tag{5.18}$$

As in the case of pure Einstein gravity, we have the action for a point moving in a Lorentzian auxiliary spacetime, with supermetric

$$G_{00} = -1, \qquad G_{jk} = \delta_{jk} \tag{5.19}$$

and so the parameter γ^0 plays the role of "time" for the point. Because of this correspondence, we will use Greek indices to refer to components of the tuple $\gamma^\mu = (\gamma^0, \gamma^j)$. It should be clear when the index is referring to the physical spacetime or the auxiliary spacetime.

The contributions to the potential $V(\gamma)$ coming from the metric are all of the form

$$\exp\left(2\left[-\gamma^0 + \gamma^i - \gamma^j - \gamma^k\right]\right) \tag{5.20}$$

and thus give rise to gravitational walls

$$w_{ijk|m} = \begin{cases} -1 & \text{for } m = 0, i \\ 1 & \text{for } m = j, k \\ 0 & \text{otherwise} \end{cases} \tag{5.21}$$

which should be compared to the walls in the pure gravity case.

To fully analyze string models it is necessary to include p–form fields. If in the string frame metric the p–form field is coupled to the dilaton Φ through

$$\mathcal{S} = -\frac{1}{(p+1)!} \int e^{\lambda \Phi} F_{p+1}^2 \sqrt{-G} \, d^{10}x, \qquad F_{p+1} = \mathrm{d}A_p \tag{5.22}$$

then after using the solutions to the p–form equations of motion, one finds that the electric components give rise to the inequalities

$$\gamma^{j_1} + \gamma^{j_2} + \cdots + \gamma^{j_p} - \frac{1}{2}\left(\frac{\lambda}{2} + 1\right)\left(\gamma^0 + \sum_j \gamma^j\right) < 0 \tag{5.23}$$

and the magnetic modes yield

$$-\gamma^{j_1} - \gamma^{j_2} + \cdots - \gamma^{j_{p+1}} + \frac{1}{2}\left(\frac{\lambda}{2} - 1\right)\gamma^0 + \frac{1}{2}\left(\frac{\lambda}{2} + 1\right)\sum_j \gamma^j < 0 \tag{5.24}$$

These inequalities in the γ^μ are analogues of the electric and magnetic stability conditions used previously in this work. These give rise to the *p–form walls* and wall forms in the same manner as the other stability conditions. As in the pure gravity case, we also include a set of symmetry walls.

5.1.3 Relevant walls and Kac–Moody Root Lattices

Above we have found the full set of wall forms for pure gravity and string models. As mentioned, some of the walls are "hidden" behind others. By focusing on the set of relevant walls we find a remarkable connection with the root lattices of hyperbolic Kac–Moody algebras. Excellent references for the algebraic structure and representation of Kac–Moody algebras are [51, 73], and for background material on Dynkin diagrams and Cartan matrices one can turn to [49, 72]. Henceforth, when discussing string models we will focus on the heterotic string theory, although it is possible to extend this analysis to the full set of string models in a straightforward way.

First consider the pure gravity case. A wall is irrelevant if it is a linear combination of other wall forms with positive coefficients: this corresponds to its inequality being implied by the satisfaction of other inequalities. The relevant walls for pure gravity in $d+1$ spacetime dimensions are

$$w_1 = w_{1,d-1,d}, \qquad w_j \text{ for } j = 2 \ldots d \tag{5.25}$$

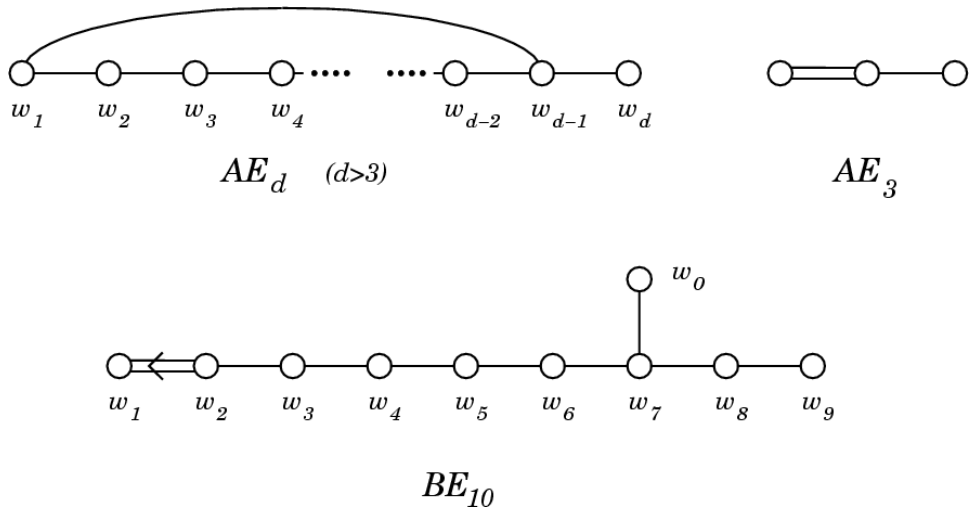

Figure 5.1: Dynkin diagrams for the relevant walls in two theories. For pure gravity in $d+1$ spacetime dimensions, one obtains the Dynkin diagram of AE_d. For the uncompactified heterotic string, one obtains the diagram for BE_{10}.

for a total of d walls. All of these walls have squared norm of 2 in the supermetric (5.6). Now, we can calculate the Cartan matrix A_{AB} for this set of vectors, where

$$A_{AB} = 2\frac{w_A \cdot w_B}{w_A \cdot w_A} \tag{5.26}$$

and A, B index the wall forms, running from $1 \ldots d$. The resulting Cartan matrix for $d > 3$ is given by

$$A_{AB} = \begin{cases} 2 & \text{for } A = B, \\ -1 & \text{for } |A-B| = 1 \text{ and } A, B \in 2 \ldots 9 \\ -1 & \text{for } (A,B) = (1,2) \text{ or } (A,B) = (1, d-1) \\ 0 & \text{otherwise} \end{cases} \tag{5.27}$$

This is the Cartan matrix for the Kac–Moody algebra AE_d, whose Dynkin diagram is shown in Figure 5.1. For $d = 3$, one obtains the Dynkin diagram of AE_3, also shown in the figure. Thus, there is a natural identification between the simple roots of a hyperbolic Kac–Moody algebra and the relevant gravitational walls.

Now let us turn to a string model, in particular the heterotic string. We have the metric and dilaton, as well as p–forms with $p = 1, 2$ and the same coupling $\lambda = -2$ to the dilaton in string frame. There are many wall forms here, but they are all consequences (sums with positive coefficients) of the smaller subset of relevant walls given by

$$-\gamma^0 - \gamma^7 - \gamma^8 - \gamma^9 < 0 \qquad w_0 \qquad \text{magnetic } H_3 \tag{5.28a}$$

$$\gamma^1 < 0 \qquad w_1 \qquad \text{electric } F_2 \tag{5.28b}$$

$$\gamma^j - \gamma^{j-1} < 0 \qquad w_j \qquad \text{symmetry, with } \; j = 2 \ldots 9 \tag{5.28c}$$

Now using the supermetric corresponding to string actions (5.19), we find the Cartan matrix

$$A_{AB} = \begin{cases} 2 & \text{for } A = B \neq 1 \\ 1 & \text{for } A = B = 1 \\ -1 & \text{for } |A - B| = 1 \text{ and } A, B \in 2 \ldots 9, \\ -1 & \text{for } (A, B) = (7, 0) \text{ or } (0, 7) \\ -1 & \text{for } (A, B) = (2, 1), \\ -2 & \text{for } (A, B) = (1, 2) \end{cases} \tag{5.29}$$

This is the Cartan matrix for the Kac–Moody algebra BE_{10}, illustrated in Figure 5.1.

This correspondence enables one to compactly prove some facts about the chaotic properties of these theories. Away from the walls, the actions tell us that the point described by the γ^μ moves along null lines. Thus, it is possible to project its motion onto the hyperboloid defined by

$$G_{\mu\nu} y^\mu y^\nu = -1 \tag{5.30}$$

Through the definitions

$$\rho^2 = -G_{\mu\nu} \gamma^\mu \gamma^\nu, y^\mu = \rho^{-1} \gamma^\mu \tag{5.31}$$

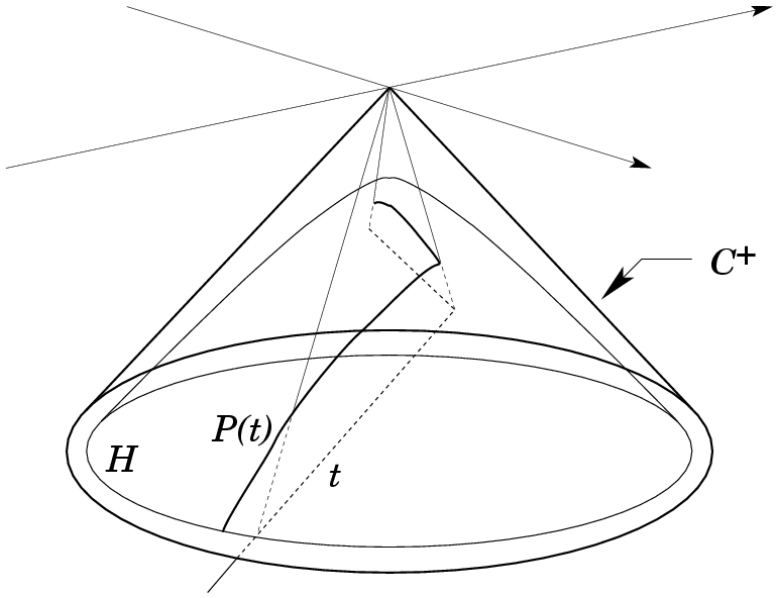

Figure 5.2: If the motion of the universe point is along null lines in γ^j space, then its trajectory t is contained in the light cone $\mathcal{C}^+$ has a projection $P(t)$ onto the hyperboloid H having unit Lorentzian separation from the origin.

as illustrated in Figure 5.2. This is in accord with other results whereby gravitational dynamics are recast as motion on a manifold of negative curvature [34].

If the cone $\mathcal{W}^+$ defined by the simultaneous satisfaction of all of the stability inequalities is completely contained in the forward light cone[1] $\mathcal{C}^+$ in γ^μ space, then the motion of the point on this hyperboloid is confined to a patch of finite volume. (Looking ahead, this is illustrated in Figure 5.4 on page 131) This means that all trajectories for the point will hit a wall after a finite time. This is precisely equivalent to the statement that a Kasner bounce will inevitably occur, or that it is impossible to satisfy all of the stability conditions for the model.

Now the two algebras AE_d (for $d < 10$) and BE_{10} are examples of strictly hyperbolic Kac–Moody algebras. For these algebras, the cone defined by the simple roots lies within the forward light cone. Therefore, we can immediately conclude that these

[1]By our conventions, as the universe approaches the crunch the corresponding point moves in the $-\gamma^0$ direction. Thus, the "forward" light cone points downward in our figures.

theories will be chaotic. This is a special case of a general result that theories whose billiards are root lattices of hyperbolic Kac–Moody algebras are inevitably chaotic. Not all models with p–forms and gravity lead to Kac–Moody root lattices: it is a special feature of string models and pure gravity that they result in wall lattices with such unique properties.

5.2 Avoiding Chaos in Billiards

In the previous section we described the emergence of a particular lattice of walls that determine the dynamics of various models with gravity near a big crunch. Now we will describe how it is possible to use properties of this lattice to determine whether chaos is controlled or not.

In Section 5.2.1 we describe how the elimination of chaos with a $w \geq 1$ fluid appears in this framework. Section 5.2.2 contains the central result of this chapter. We describe how to use the wall lattice to determine the chaotic properties of a theory, and to find non–chaotic solutions.

5.2.1 The $w \geq 1$ Cases

Let us first consider how chaos is avoided by a scalar field in Einstein gravity. With a scalar field, the effective action becomes

$$\mathcal{S} = \int N^{-1} e^{\sum_j \gamma^j} \left(\sum_j \left[\dot{\gamma}^j\right]^2 - \sum_{j,k} \dot{\gamma}^j \dot{\gamma}^k + \left[\dot{\gamma}^\phi\right]^2 \right) - N e^{\sum_j \gamma^j} U(\gamma)\, dt \qquad (5.32)$$

where $\gamma^\phi = \phi$ is our scalar field. The notation reflects the fact that it appears in the kinetic term of this action in the same way as an additional scale factor. The supermetric is precisely the old pure gravity supermetric but with

$$G_{\phi\phi} = +1, \qquad G_{j\phi} = 0. \qquad (5.33)$$

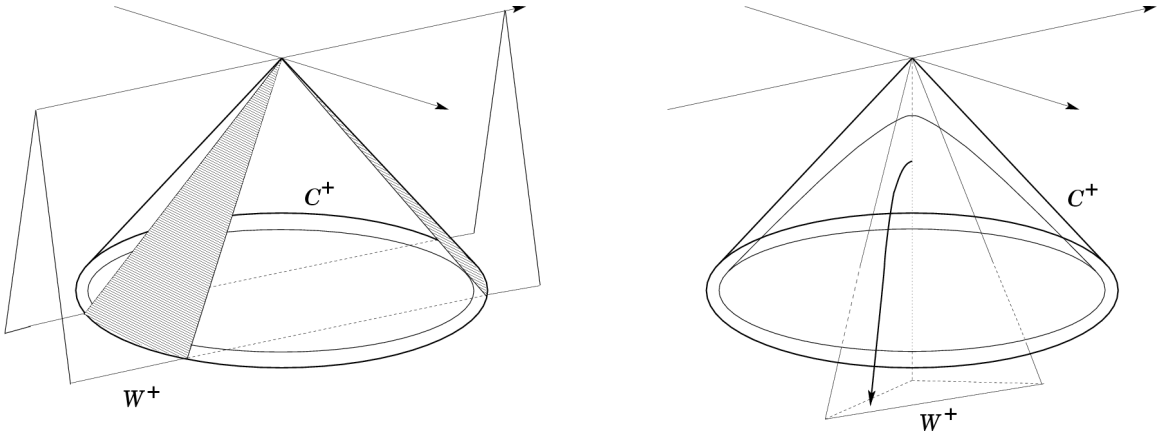

Figure 5.3: Two mechanisms by which chaos is avoided, viewed in the billiard picture. Left panel: with the addition of a free scalar field, the universe point can move in a new direction γ^ϕ along which there are no walls. Right panel: with a $w > 1$ fluid, the mass–shell condition for the point is modified, and its trajectory becomes more and more timelike.

and so in particular it still has the same signature. The potential includes all of the previous gravitational terms, plus a new term arising from the magnetic components (spatial gradients) of ϕ. This new term is subdominant to the gravitational walls in any spacetime dimension.

The essential reason that the scalar field enables the system to avoid chaos is that we have added a new degree of freedom (the scalar field) without adding any new walls. The point can thus "escape" the wall system by moving along the new direction γ^ϕ. As an example, recall that γ^j moves along a null line when far away from the walls. We can now choose the null ray,

$$\gamma^\mu = \begin{cases} -1 & \text{for } \mu = 1 \dots d, \\ \pm\sqrt{d(d-1)} & \text{for } \mu = \phi \end{cases} \tag{5.34}$$

This vector misses the gravitational walls (though it skirts the symmetry walls, which is not important here). This state of affairs is illustrated in Figure 5.3.

Now we turn to the $w > 1$ case. We have the action

$$S = \int N^{-1} e^{\sum_j \gamma^j} \left(\sum_j \left[\dot{\gamma}^j\right]^2 - \sum_{j,k} \dot{\gamma}^j \dot{\gamma}^k \right) - N e^{\sum_j \gamma^j} \left[\rho(\gamma) + U(\gamma)\right] \, dt \tag{5.35}$$

where ρ is our $w > 1$ fluid, and by the conservation equation we have

$$\rho(\gamma) = \rho_0 \exp\left(-(1+w) \sum_j \gamma^j \right) \tag{5.36}$$

Varying with respect to N and setting the usual gauge $N = e^{\sum \gamma}$ gives the Friedmann equation or mass–shell condition

$$\frac{1}{2} G_{jk} \dot{\gamma}^j \dot{\gamma}^j = -\rho = -\rho_0 \exp\left((1-w) \sum_j \gamma^j \right) \tag{5.37}$$

Noting that $\sum_j \gamma^j \to -\infty$ as we approach the big crunch, we see that there are three possibilities,

- ***Case 1***: $w < 1$. As we approach the big crunch, the term above decreases exponentially to zero. The mass–shell condition is unchanged, and the universe point moves along null rays.

- ***Case 2***: $w = 1$. The argument to the exponential vanishes, and the new term is a constant addition to the mass–shell condition. It corresponds to adding a mass to the universe point, and it therefore moves along timelike linear trajectory.

- ***Case 3***: $w > 1$. Now the new term grows as the big crunch is approached. This means that regardless of the initial trajectory, the universe point follows a trajectory that asymptotes to the purely isotropic solution where all γ^j are equal.

These various cases are illustrated in Figure 5.3. By changing the mass–shell condition for the billiard, the $w > 1$ fluid causes its trajectory to become ever more timelike. The billiard point can thereby avoid the cone formed by the gravitational walls. A similar analysis for the case with p–forms yields an analogous interpretation.

5.2.2 The Weight Lattice

Now we will describe how to determine whether chaos is avoided using properties of the wall lattice. We will focus on the situation where no $w > 1$ fluids are present, and as we will see avoiding chaos will occur for reasons more closely akin to the free scalar case described above. The results we describe here will be especially relevant to our analysis of the effect of chaos on compactification in the next section.

Essentially, there are two possibilities. Let us denote, following [25], the forward light cone in the γ space by $\mathcal{C}^+$, and the cone where all of the stability inequalities are satisfied by $\mathcal{W}^+$. Then, as illustrated in Figure 5.4,

1. ***Case 1***, $\mathcal{W}^+ \subset \mathcal{C}^+$. The projection of the billiard motion onto the forward light cone is a finite volume patch. Models of this type are inevitably chaotic: the billiard moves along a null ray which inevitably hits a wall. (See left panel of Figure 5.4) Models of this type are chaotic.

2. ***Case 2***, $\mathcal{W}^+ \not\subset \mathcal{C}^+$. In this case there are points outside the light cone that satisfy the stability inequalities. Since $\mathcal{W}^+$ is convex, this means there exists null rays (and thus solutions of the equations of motion) that never intersect a wall. (See right panel of Figure 5.4) Models of this type are non–chaotic.

Now, the cone $\mathcal{C}^+$ contains all lightlike (and null) vectors. So $\mathcal{W}^+ \not\subset \mathcal{C}^+$ if and only if $\mathcal{W}^+$ contains spacelike vectors. Therefore, the question of whether a model is chaotic or not is reduced to the question of whether $\mathcal{W}^+$ contains spacelike vectors.

There is a simple and systematic way of determining whether this is the case. This works whether or not the wall lattice is of Kac–Moody type. This method does require that the number of wall forms is equal to the dimension of the γ–space, which holds true for all the examples we consider here. Recall each of our wall forms determines

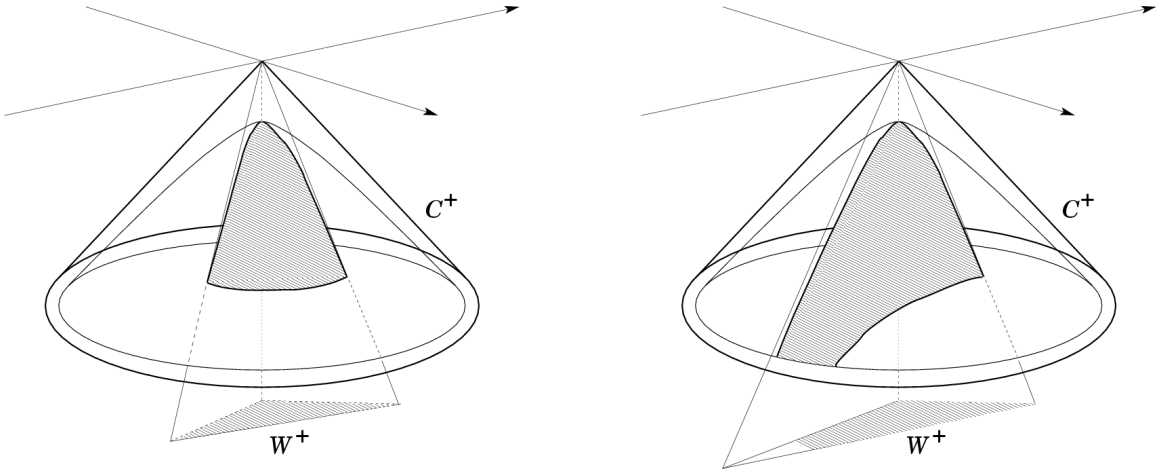

Figure 5.4: Left frame: a case where the cone $\mathcal{W}^+$ in which the stability inequalities are satisfied is contained within the light cone $\mathcal{C}^+$. All vectors in $\mathcal{W}^+$ are timelike and the model is chaotic. Right frame: a case where $\mathcal{W}^+$ is not contained within $\mathcal{C}^+$. Therefore there exist null trajectories (Kasner universes) where the stability inequalities are always satisfied.

a stability inequality by

$$w_{A|m}\gamma^m < 0 \tag{5.38}$$

Next define a set of vectors Λ_B dual to the wall forms, which anticipating the application to Kac–Moody algebras we call the *weights*, by

$$G^{mn}w_{A|m}\Lambda_{B|n} = \delta_{AB} \tag{5.39}$$

and a set of *coweights* $\Lambda^\vee$ by raising the index

$$\Lambda_A^{\vee\,|m} = G^{mn}\Lambda_{A|n} \tag{5.40}$$

If the set of weights is linearly independent and complete (which will be the case for all examples here) the γ^m in terms of the coweights by

$$\gamma^m = -\sum_A c_A \Lambda_A^{\vee\,|m} \tag{5.41}$$

Now the inequalities take the form

$$\sum_B c_B w_{A|m}\Lambda_B^{\vee\,|m} = c_A > 0. \tag{5.42}$$

This means that we have a complete parameterization of $\mathcal{W}^+$ in terms of the c_A. Any tuple of c_A, such that all of the c_A are positive, leads by this construction to a point in $\mathcal{W}^+$.

This parameterization of $\mathcal{W}^+$ is quite useful. It is not quite the same thing as a parameterization of the space of solutions: recall that the solutions to the equations of motion are piecewise linear null trajectories contained in $\mathcal{W}^+$, while this is a parameterization of $\mathcal{W}^+$ itself. Nonetheless, using this parameterization we can make strong statements about what kinds of solutions can exist.

There are three classes of coweight, determined by the norm of the coweight vector in the appropriate supermetric:

- ***Timelike***, or $\Lambda_A^\vee \cdot \Lambda_A^\vee < 0$: This direction inside $\mathcal{W}^+$ remains within the future light cone $\mathcal{C}^+$.

- ***Null***, or $\Lambda_A^\vee \cdot \Lambda_A^\vee = 0$: This direction corresponds to the edge of $\mathcal{W}^+$ touching the forward light cone $\mathcal{C}^+$. This is the only class of coweight for which the coweight vector is the same as a solution to the equations of motion. The corresponding solutions have a wall at infinity, or in other words are marginally chaotic solutions.

- **Spacelike** $\Lambda_A^\vee \cdot \Lambda_A^\vee > 0$: These correspond to rays in $\mathcal{W}^+$ that lie outside the forward light cone. By our arguments above, this implies the existence of non–chaotic solutions.

So, the question of classifying the chaotic properties of the theory comes down to a question of the norms of the coweights. If there are coweights with positive norm, then there exist non–chaotic solutions in a given theory. Otherwise, chaos (or, at best, marginal behavior) is inevitable.

5.3 Controlled Chaos for the Heterotic String

Here we apply the formal results that we have been developing to find the solutions with controlled chaos in the heterotic string. We compactify to $0 + 1$ dimensions, which enables us to scan all possible solutions. Based on our selection rules, we know that setting a Betti number $b_j = 0$ allows us to delete stability conditions (or inequalities) with exactly j indices along the compact space. One can readily see that any compactification with $b_1, b_3 \neq 0$ cannot delete any of the relevant walls for the heterotic string. Furthermore, setting $b_4, \ldots, b_9 = 0$ does not delete any walls, even irrelevant ones. Thus, we will focus on the first three Betti numbers $b_1, \ldots, b_3$.

If we choose a compactification with $b_1 = 0$ or $b_3 = 0$, then some of the relevant walls are deleted. The analysis becomes somewhat nontrivial since deleting a relevant wall "exposes" the irrelevant walls hidden behind it. We will be careful to account for these new walls, and find that it leads to nontrivial transformations of the original Kac–Moody root lattice.

In this manner, each compactification defines a new set of coweights, and thus the BE_{10} root lattice of the uncompactified theory "mutates" into other root lattices. Some (but not all) of these correspond to the root lattices of other Kac–Moody algebras. We consider the following cases:

- The uncompactified case in Section 5.3.1,
- The compactification with $b_3 = 0$, which controls chaos, in Section 5.3.2,
- The compactification with $b_1 = 0$, which fails to control chaos, in Section 5.3.3,
- The $b_1 = b_2 = 0$ compactification, which controls chaos, in Section 5.3.4.

We go on to summarize our findings in Section 5.3.5.

5.3.1 The uncompactified heterotic string

To begin, we consider the uncompactified heterotic string, or what is completely equivalent, one compactified on a space where all de Rham cohomology classes are nontrivial. (For example, the torus $\mathbf{T}^9$). This is in accord with known results that the billiard is invariant under toroidial compactification [25] as well as our considerations in Chapter 4. The set of relevant walls, which determine the root vectors, are

$$-\gamma^0 - \gamma^7 - \gamma^8 - \gamma^9 < 0 \qquad w_0 \qquad \text{magnetic } H_3 \tag{5.43a}$$

$$\gamma^1 < 0 \qquad w_1 \qquad \text{electric } F_2 \tag{5.43b}$$

$$\gamma^j - \gamma^{j-1} < 0 \qquad w_j \qquad \text{symmetry, with } \; j = 2 \ldots 9 \tag{5.43c}$$

These give rise to the following set of coweight vectors and norms

$$\Lambda_A^{\vee|m} = \begin{pmatrix} -1 & 0 & 0 & 0 & 0 & 0 & 0 & 0 & 0 & 0 \\ -3 & 1 & 1 & 1 & 1 & 1 & 1 & 1 & 1 & 1 \\ -3 & 0 & 1 & 1 & 1 & 1 & 1 & 1 & 1 & 1 \\ -3 & 0 & 0 & 1 & 1 & 1 & 1 & 1 & 1 & 1 \\ -3 & 0 & 0 & 0 & 1 & 1 & 1 & 1 & 1 & 1 \\ -3 & 0 & 0 & 0 & 0 & 1 & 1 & 1 & 1 & 1 \\ -3 & 0 & 0 & 0 & 0 & 0 & 1 & 1 & 1 & 1 \\ -3 & 0 & 0 & 0 & 0 & 0 & 0 & 1 & 1 & 1 \\ -2 & 0 & 0 & 0 & 0 & 0 & 0 & 0 & 1 & 1 \\ -1 & 0 & 0 & 0 & 0 & 0 & 0 & 0 & 0 & 1 \end{pmatrix} \qquad \Lambda_A^{\vee} \cdot \Lambda_A^{\vee} = \begin{pmatrix} -1 \\ 0 \\ -1 \\ -2 \\ -3 \\ -4 \\ -5 \\ -6 \\ -2 \\ 0 \end{pmatrix} \tag{5.44}$$

where each coroot is given by a row in the matrix. Since there are no spacelike coweights, we can conclude that the theory is inevitably chaotic. This is in accord with previous results.

5.3.2 The $b_3 = 0$ Case

Here the full set of relevant walls is

$$-\gamma^0 - \gamma^8 - \gamma^9 < 0 \qquad w_0 \qquad \text{magnetic } F_2 \tag{5.45a}$$

$$\gamma^1 < 0 \qquad w_1 \qquad \text{electric } F_2 \tag{5.45b}$$

$$\gamma^j - \gamma^{j-1} < 0 \qquad w_j \qquad \text{symmetry, with } \; j = 2 \ldots 9 \tag{5.45c}$$

We can see that setting $b_3 = 0$ has eliminated the magnetic H_3 wall and exposed the magnetic F_2 wall. The root vectors give rise to the Dynkin diagram shown in Figure 5.5. This Dynkin diagram does not appear to correspond to a named Kac–Moody algebra.

One finds the corresponding coweights and norms

$$\Lambda_A^{\vee|m} = \begin{pmatrix} -1 & 0 & 0 & 0 & 0 & 0 & 0 & 0 & 0 & 0 \\ -2 & 1 & 1 & 1 & 1 & 1 & 1 & 1 & 1 & 1 \\ -2 & 0 & 1 & 1 & 1 & 1 & 1 & 1 & 1 & 1 \\ -2 & 0 & 0 & 1 & 1 & 1 & 1 & 1 & 1 & 1 \\ -2 & 0 & 0 & 0 & 1 & 1 & 1 & 1 & 1 & 1 \\ -2 & 0 & 0 & 0 & 0 & 1 & 1 & 1 & 1 & 1 \\ -2 & 0 & 0 & 0 & 0 & 0 & 1 & 1 & 1 & 1 \\ -2 & 0 & 0 & 0 & 0 & 0 & 0 & 1 & 1 & 1 \\ -2 & 0 & 0 & 0 & 0 & 0 & 0 & 0 & 1 & 1 \\ -1 & 0 & 0 & 0 & 0 & 0 & 0 & 0 & 0 & 1 \end{pmatrix} \qquad \Lambda_A^\vee \cdot \Lambda_A^\vee = \begin{pmatrix} -1 \\ 5 \\ 4 \\ 3 \\ 2 \\ 1 \\ 0 \\ -1 \\ -2 \\ 0 \end{pmatrix} \tag{5.46}$$

It is readily seen that some of the coweights are spacelike. Thus, compactification with $b_3 = 0$ enables chaos to be controlled. This is in accord with our results from Chapter 4, where we found solutions with controlled chaos for the heterotic string and $b_3 = 0$.

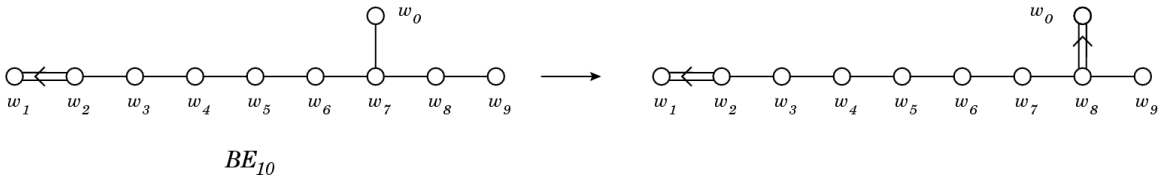

Figure 5.5: Wall forms arising after compactification of the heterotic string with $b_3 = 0$. The original wall lattice BE_{10} mutates into the root lattice of an unnamed Kac–Moody algebra.

5.3.3 The $b_1 = 0$ Case

Setting $b_1 = 0$ results in the set of walls

$$-\gamma^0 - \gamma^7 - \gamma^8 - \gamma^9 < 0 \qquad w_0 \qquad \text{magnetic } H_3 \tag{5.47a}$$

$$\gamma^1 + \gamma^2 < 0 \qquad w_1 \qquad \text{electric } H_3 \tag{5.47b}$$

$$\gamma^j - \gamma^{j-1} < 0 \qquad w_j \qquad \text{symmetry, with } \; j = 2 \ldots 9 \tag{5.47c}$$

This choice has deleted the electric F_2 wall and exposed the electric H_3 one. These root vectors generate a Cartan matrix corresponding to the (strictly) hyperbolic Kac–Moody algebra DE_{10}, shown in Figure 5.6. Because DE_{10} is hyperbolic, we expect that chaos is not controlled. This is confirmed when the coweights and their norms

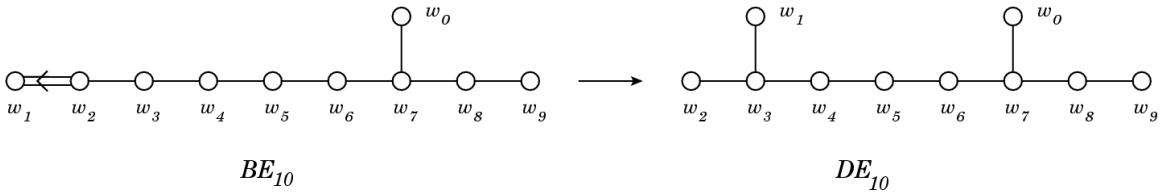

Figure 5.6: Wall forms arising after compactification of the heterotic string with $b_1 = 0$. The original wall lattice BE_{10} mutates into an the strictly hyperbolic Kac–Moody diagram for DE_{10}. Chaos is not controlled.

are computed, giving

$$\Lambda_A^{\vee|m} = \begin{pmatrix} -1 & 0 & 0 & 0 & 0 & 0 & 0 & 0 & 0 & 0 \\ -3 & 1 & 1 & 1 & 1 & 1 & 1 & 1 & 1 & 1 \\ -3 & -1 & 1 & 1 & 1 & 1 & 1 & 1 & 1 & 1 \\ -3 & 0 & 0 & 1 & 1 & 1 & 1 & 1 & 1 & 1 \\ -3 & 0 & 0 & 0 & 1 & 1 & 1 & 1 & 1 & 1 \\ -3 & 0 & 0 & 0 & 0 & 1 & 1 & 1 & 1 & 1 \\ -3 & 0 & 0 & 0 & 0 & 0 & 1 & 1 & 1 & 1 \\ -3 & 0 & 0 & 0 & 0 & 0 & 0 & 1 & 1 & 1 \\ -2 & 0 & 0 & 0 & 0 & 0 & 0 & 0 & 1 & 1 \\ -1 & 0 & 0 & 0 & 0 & 0 & 0 & 0 & 0 & 1 \end{pmatrix} \qquad \Lambda_A^\vee \cdot \Lambda_A^\vee = \begin{pmatrix} -1 \\ 0 \\ 0 \\ -2 \\ -3 \\ -4 \\ -5 \\ -6 \\ -2 \\ 0 \end{pmatrix} \tag{5.48}$$

Above, for simplicity of presentation, we have multiplied $\Lambda_1^\vee$ and $\Lambda_2^\vee$ by 2 to give them integer components. As expected, there are no spacelike coweight vectors. Thus the cone $\mathcal{W}^+$ is completely contained within the forward light cone and the theory is chaotic. We can conclude that setting $b_1 = 0$ is not sufficient to ensure that chaos is controlled.

5.3.4 The $b_1 = b_2 = 0$ Case

As we have found, $b_1 = 0$ is not a sufficient condition to control chaos. We already know that setting $b_1 = b_3 = 0$ will control chaos, since $b_3 = 0$ does. The only case

left is the $b_1 = b_2 = 0$ case. This yields stability inequalities

$$-\gamma^0 - \gamma^7 - \gamma^8 - \gamma^9 < 0 \qquad w_0 \qquad \text{magnetic } H_3 \tag{5.49a}$$

$$-\gamma^0 + \gamma^1 - \gamma^8 - \gamma^9 < 0 \qquad w_1 \qquad \text{gravitational} \tag{5.49b}$$

$$\gamma^j - \gamma^{j-1} < 0 \qquad w_j \qquad \text{symmetry, with } \; j = 2 \ldots 9 \tag{5.49c}$$

where the additional condition $b_2 = 0$ has deleted all of the electric walls, exposing a gravitational wall.

We find the coweights and norms

$$\Lambda_A^{\vee|m} = \begin{pmatrix} 1 & -1 & -1 & -1 & -1 & -1 & -1 & -1 & -1 & -1 \\ -3 & 1 & 1 & 1 & 1 & 1 & 1 & 1 & 1 & 1 \\ -3 & -1 & 1 & 1 & 1 & 1 & 1 & 1 & 1 & 1 \\ -3 & -1 & -1 & 1 & 1 & 1 & 1 & 1 & 1 & 1 \\ -3 & -1 & -1 & -1 & 1 & 1 & 1 & 1 & 1 & 1 \\ -3 & -1 & -1 & -1 & -1 & 1 & 1 & 1 & 1 & 1 \\ -3 & -1 & -1 & -1 & -1 & -1 & 1 & 1 & 1 & 1 \\ -3 & -1 & -1 & -1 & -1 & -1 & -1 & 1 & 1 & 1 \\ -2 & 0 & 0 & 0 & 0 & 0 & 0 & 0 & 1 & 1 \\ -1 & 0 & 0 & 0 & 0 & 0 & 0 & 0 & 0 & 1 \end{pmatrix} \qquad \Lambda_A^\vee \cdot \Lambda_A^\vee = \begin{pmatrix} 8 \\ 0 \\ 0 \\ 0 \\ 0 \\ 0 \\ 0 \\ 0 \\ -2 \\ 0 \end{pmatrix} \tag{5.50}$$

where we have multiplied the first eight coweights by two in order to give them integer coefficients. The presence of a single coweight of positive norm implies that chaos is controlled in this model.

This set of walls does not define a Kac–Moody algebra. The wall forms fail to satisfy the condition $A_{ij} \leq 0$ for $i \neq j$ required of a generalized Cartan matrix A_{ij}. Thus there is no Dynkin diagram for this set of walls. Nevertheless, the p–form and symmetry walls alone correspond to the simple roots of $\mathrm{E}_9^{(1)}$, the untwisted affine extension of the finite Lie algebra E_8. We have drawn its Dynkin diagram

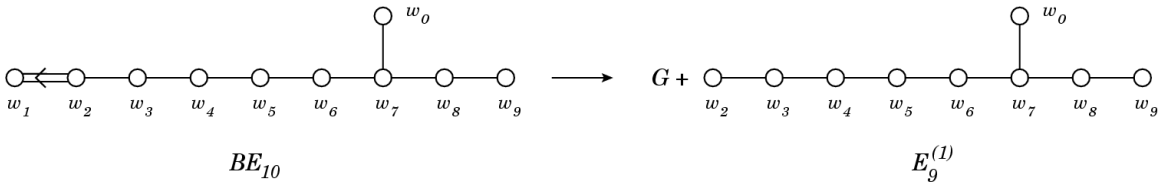

Figure 5.7: Wall forms arising after compactification of the heterotic string with $b_1 = b_2 = 0$. The original wall lattice BE_{10} mutates into a gravitational wall "G," together with a set of walls corresponding to the affine Kac–Moody algebra $\mathrm{E}_9^{(1)}$. Taken together, the full set of p–form and gravitational walls do not form a Kac–Moody lattice.

in Figure 5.7, where we have indicated the node corresponding to the gravitational wall. Because the full set of walls do not correspond to a generalized Cartan matrix, we cannot use any algebraic properties to characterize the chaotic properties of the system. However, our techniques using the coweight vectors still applies.

5.3.5 Summary

The full descent of wall forms in the compactification of the heterotic string is shown in Figure 5.8. We have described explicitly the $b_1 = 0$, $b_1 = b_2 = 0$ and $b_3 = 0$ cases in the preceding text. From this we have found that any compactification with $b_1 = b_2 = 0$ or $b_3 = 0$ will control chaos. (Naturally, setting additional Betti numbers to zero will also control chaos) For completeness, all of the possibilities are shown in the Figure. The Betti numbers $b_4 \ldots b_9$ do not participate at all in the control of chaos through compactification to $0 + 1$ dimensions.

We should note that not all of the possible compactifications preserve the Kac–Moody algebra structure of the uncompactified heterotic string. In particular, when a compactification exposes a gravitational wall (as in the $b_1 = b_2 = 0$, $b_1 = b_3 = 0$ and $b_2 = b_3 = 0$ cases) then it may occur that the full set of walls cannot be expressed as a Dynkin diagram, though the p–form walls alone can be. The only case with an exposed gravitational wall that does have a Dynkin diagram seems to be the

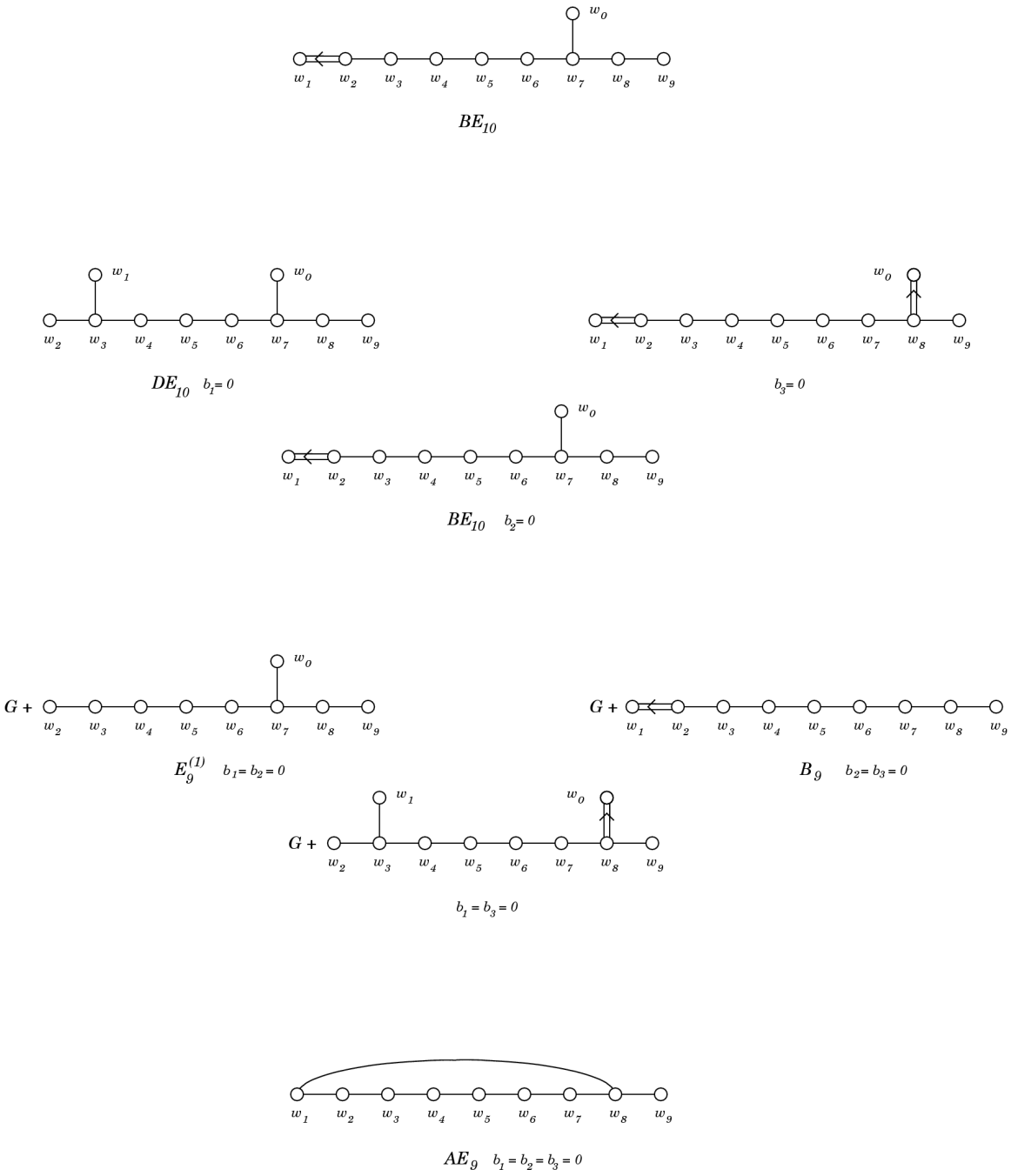

Figure 5.8: Transformation of the wall lattice in compactification of the heterotic string to $0 + 1$ dimensions. In some cases only the p–form walls have an associated Dynkin diagram: for them, we have denoted the gravitational wall by "G" and given the name of the p–form Dynkin diagram. Not all of the Dynkin diagrams are named.

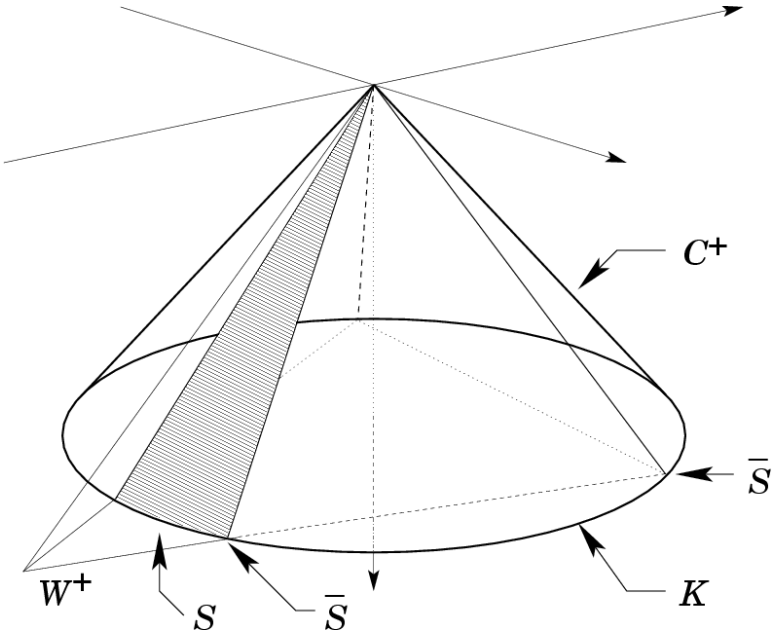

Figure 5.9: Relationship between the billiard picture and the Kasner sphere. The billiard moves along the null cone: null rays on the cone are thus points on the Kasner sphere $\mathcal{K}$. Regions inside $\mathcal{W}^+$ are in $\mathcal{S}$, the boundary of $\mathcal{W}^+$ is $\bar{\mathcal{S}}$. Compare Figure 2.3 on p. 25.

$b_1 = b_2 = b_3 = 0$ compactification, which ends up removing all p–form walls and yielding the relevant wall set of pure gravity with a scalar field in $9 + 1$ dimensions.

5.4 From Coweights to Kasner Exponents

In this section we will complete the connection between the work in the billiard picture and our previous work in terms of Kasner exponents. We have already shown how to test for existence of solutions with controlled chaos by computing the norms of the coweights. In the billiard picture it is then possible to construct explicit trajectories in the γ^j space with controlled chaos. Here we will show how to find the corresponding Kasner exponents.

The relationship between the Kasner sphere $\mathcal{K}$ and the billiard picture is illustrated in Figure 5.9. The billiard moves along null rays contained within the wall cone

$\mathcal{W}^+$. If chaos is controlled, there are rays in the null cone that are contained in $\mathcal{W}^+$, illustrated by the shaded region in the figure. The velocity components of the universe point give the Kasner exponents, and so the null cone can be viewed as a cone over the Kasner circle $\mathcal{K}$. In order to precisely relate the velocity of the universe point to the Kasner exponents, it is necessary to account for differences between the string and Einstein frame, as well as the different time coordinates used with these two pictures. Below we will focus on string models for definiteness.

5.4.1 Between Kasner and Billiard

Here we introduce the general technique to transform trajectories in the billiard space to Kasner exponents, and the inverse process as well.

From Billiard to Kasner

Solutions to the equations of motion (away from the walls) are of the form

$$\gamma^j = \Gamma^j t_{BS} + \Gamma_0^j, \qquad \gamma^0 = \Gamma^0 t_{BS} + \Gamma_0^0 \tag{5.51}$$

where $\Gamma^\mu = (\Gamma^0, \Gamma^j)$ is a null vector in the string action supermetric. The time coordinate t_{BS} is the string frame billiard time coordinate, defined by the choice of gauge $N = \exp(-\gamma^0)$ and the string frame action (5.17). The first step is to convert to string frame proper time t_{PS}. This is accomplished through the relationship

$$N \mathrm{d}t_{BS} = \mathrm{d}t_{PS} \implies \exp\left(-\Gamma^0 t_{BS}\right) \mathrm{d}t_{BS} = \mathrm{d}t_{PS} \tag{5.52}$$

which yields

$$t_{BS} = -\frac{1}{\Gamma^0} \ln\left(-\Gamma^0 t_{PS}\right) \tag{5.53}$$

where we have discarded an irrelevant additive constant. With this choice of signs, as $t_{BS} \to +\infty$, $t_{PS} \to 0^+$ if $\Gamma^0 < 0$. We can immediately use this relationship to find

the string frame Kasner exponents via

$$G^{(S)}_{jk} = \left(\frac{t_{PS}}{t_0}\right)^{p_j^{(S)}} \delta_{jk} \implies p_j^{(S)} = -\frac{\Gamma^j}{\Gamma^0} \tag{5.54}$$

we can also find the string frame dilaton Kasner exponent through the definition of the shifted dilaton γ^0 in (5.16) through

$$\Phi = \frac{1}{2}\left(\gamma^0 + \sum_j \gamma^j\right) \implies \Phi = -\frac{1}{2}\left(1 + \sum_j \frac{\Gamma^j}{\Gamma^0}\right) \ln t_{PS} \tag{5.55}$$

where we have dropped an additive constant. This gives the dilaton Kasner exponent

$$p^{(S)}_\Phi = -\frac{1}{2}\left(1 + \sum_j \frac{\Gamma^j}{\Gamma^0}\right) \tag{5.56}$$

As a check, we can check that the resulting Kasner exponents satisfy the string frame Kasner conditions

$$\sum_j p_j^{(S)} = 1 + 2p^{(S)}_\Phi, \qquad \sum_j \left[p_j^{(S)}\right]^2 = 1 \tag{5.57}$$

The first is satisfied by the definition of $p^{(S)}_\Phi$, while the second is satisfied if

$$\sum_j \left[\Gamma^j\right]^2 = \left[\Gamma^0\right]^2, \tag{5.58}$$

which is precisely our original requirement that Γ^μ is a null vector.

Now that we have the string frame Kasner exponents, we can transform to the Einstein frame with canonically normalized dilaton ϕ. The relevant transformations are

$$p_\phi = \frac{p^{(S)}_\Phi/\sqrt{2}}{1 - p^{(S)}_\Phi/4}, \qquad p_j = \frac{p_j^{(S)} - p^{(S)}_\Phi/4}{1 - p^{(S)}_\Phi/4} \tag{5.59}$$

where the exponents p_ϕ and p_j satisfy the Kasner conditions (2.36), again as a consequence of the fact that Γ^μ is null.

From Kasner to Billiard

Now, let us assume that we have a set of Kasner exponents in the Einstein frame. We wish to determine the trajectory Γ^μ in the billiard space. If we invert the formulae (5.59) we find

$$p_\Phi^{(S)} = \frac{\sqrt{2}p_\phi}{1 + p_\phi/\sqrt{8}}, \qquad p_j^{(S)} = \frac{p_j + p_\phi/\sqrt{8}}{1 + p_\phi/\sqrt{8}} \tag{5.60}$$

Now, note that the transformations between the billiard trajectory Γ^μ and the string frame Kasner exponents depended only on the ratios between Γ^0 and Γ^j. Thus Γ^μ and $\lambda\Gamma^\mu$ define the same trajectory. We can fix this degeneracy by setting, say, Γ^0 to a fixed value and then finding the other components of Γ^μ in terms of this. The formulae from the previous section therefore give

$$\Gamma^j = -\Gamma^0 p_j^{(S)} \tag{5.61}$$

The remaining formulae give no new information, reflecting the fact that Γ^0 is freely specifiable.

5.4.2 Examples

Now we will give some examples of these transformations and their applications in finding solutions with controlled chaos. First, we embed a doubly–isotropic solution found in Chapter 4 into the billiard picture. As a second example, we enumerate all marginal solutions to the $b_1 = 0$ compactification and given the corresponding Kasner exponents.

Embedding of a Known Solution

Here we consider the embedding of a known solution with controlled chaos in the billiard picture. We will use the solution **A** from Table 4.3. In the Einstein frame,

we have

$$p_1 \dots p_3 = 0, \qquad p_4 \dots p_9 = 1/6, \qquad p_\phi = \sqrt{5/6} \tag{5.62}$$

This yields the string frame exponents

$$\begin{aligned} p_\Phi^{(S)} &= \sqrt{\frac{5}{3}} \left(1 + \frac{\sqrt{5/3}}{4}\right)^{-1} && \sim 0.976 \\ p_1^{(S)} \dots p_3^{(S)} &= \frac{1}{4}\sqrt{\frac{5}{3}} \left(1 + \frac{\sqrt{5/3}}{4}\right)^{-1} && \sim 0.244 \\ p_4^{(S)} \dots p_9^{(S)} &= \left(\frac{1}{6} + \frac{1}{4}\sqrt{\frac{5}{3}}\right) \left(1 + \frac{\sqrt{5/3}}{4}\right)^{-1} && \sim 0.370 \end{aligned} \tag{5.63}$$

Now in terms of Γ^0, our billiard trajectory is defined by the velocity

$$\Gamma^m = \Gamma^0(-1, \underbrace{0.244}_{\times 3}, \underbrace{0.370}_{\times 6}) \tag{5.64}$$

Now recall that in Section 5.2.2 we introduced a parameterization of the wall cone $\mathcal{W}^+$ in terms of the coweights $\Lambda_A^{\vee|m}$ and coefficients c_A given by

$$\gamma^m = -\sum_A c_A \Lambda_A^{\vee|m} \tag{5.65}$$

which satisfies all of the stability conditions if all $c_A > 0$. We can determine the c_A by noting that

$$c_A = w_{A|m}\gamma^m, \qquad \gamma^m = \Gamma^m t_{BS} + \Gamma_0^m \tag{5.66}$$

where Γ_0^m is an irrelevant constant that we set to zero. (It determines whether the trajectory begins in $\mathcal{W}^+$ when $t_{BS} = 0$) Using our solution for Γ^m and the wall forms for the $b_3 = 0$ compactification, we have

$$c_0 = -\Gamma^0 \cdot 0.260, \qquad c_1 = -\Gamma^0 \cdot 0.244, \qquad c_4 = -\Gamma^0 \cdot 0.126, \tag{5.67}$$

with all other $c_A = 0$. Clearly the trajectory will be in $\mathcal{W}^+$ if we choose $\Gamma^0 = -1$. Since the walls $c_2 \dots c_9$ are all symmetry walls, then chaos is still avoided despite the

fact that some of these c_A vanish. The important thing is that the p–form stability inequalities are satisfied, thanks to the fact that c_0 and c_1 are positive.

As we expect, from looking at (5.46) we can see that c_1 and c_4 are both spacelike, while c_0 is timelike. The convexity of $\mathcal{W}^+$ ensures that any linear combination of these coweights (with positive coefficients c_A) is in the wall cone $\mathcal{W}^+$, and the timelike weight c_0 is present in this linear combination in order to "pull" the spacelike vectors onto the null cone, and thus satisfy the mass–shell constraint. It is also useful to note that the coweights c_0, c_1 and c_4 are the only coweights compatible with doubly isotropic solutions, since they are the only coweights left invariant by permutations of the coordinates $\{\gamma^1, \gamma^2, \gamma^3\}$ and $\{\gamma^4, \ldots, \gamma^9\}$. Thus an examination of the coweights for a given theory enables one to classify the possible solutions with controlled chaos and specific isotropy properties.

There is an important subtlety to this analysis. Our derivation of the coweights and their use in determining solutions with controlled chaos assumed that the string model was fully compactified down to $0 + 1$ dimensions. Physically interesting solutions are those where three dimensions remain uncompactified. For these directions, the walls corresponding to p–form components in these directions are not deleted by compactification. In the present case, and using the isotropy along $\{\gamma^1, \gamma^2, \gamma^3\}$ the only relevant wall in this subset is

$$-\gamma^0 - \gamma^1 - \gamma^2 - \gamma^3 = -0.268 < 0 \tag{5.68}$$

arising from the magnetic component of H_3. This stability inequality is satisfied in this case. In the general case, when one wishes to interpret some of the dimensions as noncompact, it is necessary to check that additional stability inequalities of this type are satisfied.

Finding Marginal Solutions

Now we show how to go from the billiard picture to the Kasner exponent picture. Along the way, we will illustrate the power of the techniques we have discussed in this chapter by showing how one may classify all marginal solutions to the stability conditions in a given compactification. We will work within the $b_1 = 0$ compactification of the heterotic string. Instead of deriving new solutions with controlled chaos (which in any case we have proved do not exist for this compactification), we will examine the structure of marginal solutions, thus making contact with some of the results found via the computer search in Table 4.4.

The coweights and their norms are given in (5.48). One can readily see that there are three null coweights: c_1, c_2 and c_9. Each of these corresponds to a marginal solution. Up to symmetries, at least in the fully compactified case, these are the only possible marginal solutions. These correspond to the following sets of Einstein frame Kasner exponents

$$c_1 = (-3, \underbrace{1, \ldots, 1}_{\times 9}) \qquad p_\phi = \sqrt{8/9}, \qquad p_j = (\underbrace{1/9, \ldots 1/9}_{\times 9}) \tag{5.69}$$

$$c_2 = (-3, -1, \underbrace{1, \ldots, 1}_{\times 8}) \qquad p_\phi = \frac{2\sqrt{2}}{5} \qquad p_j = (-3/5, \underbrace{1/5, \ldots, 1/5}_{\times 8}) \tag{5.70}$$

$$c_9 = (-1, \underbrace{0, \ldots, 0}_{\times 8}, 1) \qquad p_\phi = 0 \qquad p_j = (\underbrace{0, \ldots, 0}_{\times 8}, 1) \tag{5.71}$$

Of these solutions, it is seen from the coweights of the uncompactified heterotic string (5.44) that c_1 and c_9 are common. They arise from marginally satisfying the magnetic H_3 stability condition. The marginal solution corresponding to c_2 is new to the $b_1 = 0$ compactification. It would violate the electric F_2 stability condition in the uncompactified heterotic string. This inequality is replaced by the electric H_3 stability condition after compactification, which is marginally satisfied by c_2.

As a final calculation, we can check to see which dimensions can be made non-

compact without destroying the marginal nature of these solutions. Since c_1 and c_9 are inherited from the uncompactified heterotic string (5.44) these solutions remain marginal when any dimensions are uncompactified. For the c_2 solution, the direction along which we have the $-3/5$ Kasner exponent must be along a compact direction in order to satisfy the electric F_2 stability condition.

5.5 Conclusions

In this chapter we have developed systematic techniques to study string solutions with controlled chaos. Using these techniques, it is possible to determine the existence of solutions and explicitly construct them for any compactification. In addition, we have shown how to systematically find solutions with any desired degree of isotropy, generalizing the doubly–isotropic solutions discovered through a computer search. While the methods we describe are rooted in the emergence of Kac–Moody root lattices in the dynamics of string models, they do not require that the set of relevant walls possess any special properties. Thus, they can be applied to the dynamics of general gravitating systems.

An unfortunate outcome of the analysis in this chapter is the discovery that is is impossible to control chaos by compactifying the heterotic string on a manifold with $b_1 = 0$. This means that the simplest compactifications of string theory are incompatible with controlled chaos. However it is far from clear that phenomenology requires a "classic" Calabi–Yau compactification. In recent years, string phenomenologists have been focusing on more general set–ups involving fluxes and D–branes. The techniques developed in this chapter are sufficiently general to be applicable to this wider class of compactifications as well.

Chapter 6

Pair Production of Strings and Point Particles

...when they come to model heav'n
And calculate the stars, how they will wield
The mighty frame, how build, unbuild, contrive
To save appearances, how gird the sphere
With centric and eccentric scribbled o'er,
Cycle and epicycle, orb in orb.

Paradise Lost Book VIII, lines 79–84, [90]

In this chapter we turn from the classical realm and explore a quantum phenomenon. In particular, we study the process of *pair production* in time–dependent backgrounds. We will find that the process occurs quite differently, depending on whether the fundamental degrees of freedom are point particles (as in quantum field theory) or strings. The results we describe suggest specific signatures of the string pair creation phenomenon that may survive into the regime of strong gravitational fields.

In a sense, this work is an attempt to go beyond the effective field theory ap-

proximation to string theory. Strings come along with a mass scale, set by the string tension α'. There are many aspects of string physics where they behave differently than any theory of point particles: examples include the behavior of their scattering amplitudes [57, 58, 59] or their propagation on certain singular spaces such as orbifolds [37, 38, 98]. Despite the fact that strings are decidedly not point particles, in the long–wavelength limit $\lambda \gg \sqrt{\alpha'}$ these differences often vanish, and it is possible to describe string physics by an effective theory of point particles [21, 44, 45, 46, 105]. This is the effective field theory approximation. It enables one to study many features of the theory that would be extremely difficult to analyze using worldsheet methods. On the other hand, by casting the theory in a point particle framework, some aspects of "stringy" physics are obscured. The work described in this chapter is an effort to recover some of those stringy effects.

Our calculation reveals two specific differences between the string and point–particle results. We focus on excited string states, and compare their pair production rate and spectrum to those of point particles with the same mass. We can summarize the differences we find as follows:

- ***Rate***: The production rate for excited strings goes like $\sim \exp\left(-A_{str} m^2\right)$ for large m. This is strongly suppressed relative to the point particle rate, which goes like $\sim \exp\left(-A_{pt} m\right)$.

- ***Spectrum (1)***: At tree level in field theory, only identical particles are produced (ie, e^+e^- but not μ^+e^-). In the case of the string, it is possible to produce pairs at different mass levels and states.

- ***Spectrum (2)***: In field theory, the production rate as a function of the wavelength λ of produced particles is independent of λ in the $\lambda \to \infty$ limit. In strings, one sees the production rate vanish as $\lambda \to \infty$ for pairs of strings at the same excitation level.

All of these features can be explained in the context of certain simple features of the string spectrum and scattering amplitudes, as we discuss in more detail later in this chapter.

This chapter is organized as follows: In Section 6.2 we discuss the perturbative approach to calculating pair production, using field theory as a guide to the string calculation. In Section 6.3 we describe a specific background, involving the collision of two plane gravitational waves, for which the perturbative calculation may be applied. In Section 6.4 we perform the explicit string calculation and discuss its properties. Finally, we present our conclusions in Section 6.5. We also include two appendices with additional details on some elements of our work. The four–point amplitude describing pair production is discussed in Appendix E, and a more detailed account of perturbatively computing Bogolubov coefficients is given in Appendix F.

We would like to point out that the material in Sections 6.2.5 and 6.3 is primarily the work of a co–author in a collaborative effort [115]. We include these sections in this work to support the continuity of the argument.

6.1 Introduction

The pair production process is of paramount importance in modern cosmological models. One example is provided by the inflationary universe. This model has provided such a successful paradigm for the early universe thanks to its elegant solution of the horizon, flatness, and monopole problems [61]. One of its most decisive and experimentally testable consequences is its prediction of an (almost) scale–free spectrum of density perturbations and gravitational waves [7]. These fluctuations are produced by what is essentially the pair production of quanta in the early universe. Furthermore, during (p)reheating after inflation, we again have a time–dependent background, and pair production is responsible for transferring the energy density in the inflaton field

to other degrees of freedom. Essentially all known cosmological models depend on pair production to seed the initial spectrum of density perturbations required by observation.

The phenomenon of pair production itself has been studied for many years. An excellent analogy for this process is an atom coupled to an external electromagnetic field. At a time far in the past, we imagine the atom is prepared in its ground state. If the external field evolves with time (perhaps due to a passing electromagnetic wave) the atom may transition into an excited state. Precisely the same physics is at work for quantum fields in time–dependent backgrounds. The quantum field may initially be in its vacuum state, corresponding to an absence of particles. Through its coupling to the background that is changing with time, it may transition to an excited state. This excited state corresponds to the presence of particles.

A recurring theme of this chapter is the interplay between the classical and quantum features of pair production. For the most part, we will focus on the study of quantum fields propagating in classical backgrounds (although in the string case it is sometimes unavoidable to consider the quantum nature of the gravitational field). On the one hand, the pair production process can often (but not always) be studied using only the classical equations of motion, and thus does not necessarily involve truly "quantum" phenomena such as Feynman loops. In this sense it involves many classical aspects. On the other hand, the boundary conditions used to solve the classical equations of motion are those set by the quantum theory, and moreover the pair production becomes physically irrelevant in the $\hbar \to 0$ limit. Thus there are some necessarily quantum features here as well.

We can give a rough guide to the relationship between classical and quantum phenomena in the pair production process. Consider again the case of the electromagnetic field, carrying an energy $E(\omega)\,\mathrm{d}\omega$ in the modes with angular frequencies

between ω and $\omega + \mathrm{d}\omega$. In quantizing, we are accustomed to resolving these modes into quanta, each carrying an energy $\hbar\omega$. Thus the number of quanta $N(\omega)$ in each mode is,

$$N(\omega) = \frac{E(\omega)}{\hbar\omega} \tag{6.1}$$

As $\hbar \to 0$, each quantum carries less and less energy, and each mode of the field corresponds to a larger and larger number of quanta. In the limit that we hold $E(\omega)\,\mathrm{d}\omega$ fixed, and take $\hbar \to 0$, we expect that quantum aspects of the field will scale away, and we should recover the classical physics of the electromagnetic field.

Now let us turn to the somewhat different situation of pair production in a time–dependent background. We take an arbitrary quantum field propagating on a fixed background. It turns out that (for the cases of interest here) the number of "quanta" of the field $N(\omega)$ that are produced in a given mode is independent of $\hbar$, and can be computed using the classical equations of motion. Therefore classical physics determines the left hand side of (6.1). However, physically observable quantities, such as the energy density produced in this way, will vanish in the $\hbar \to 0$ limit, as a consequence of (6.1). As in the case of the electromagnetic field, we recover classical physics in the $\hbar \to 0$ limit, though in a slightly different way.

A second theme in this chapter is the relationship between the string worldsheet theory and the corresponding effective field theory. Recently [47, 60] the pair creation of strings in a cosmological setting was estimated using effective field theory methods. In this work the excited states of the string are treated as massive particles for which the usual field theory calculation applies. One makes contact with string physics by considering the effect of the exponential Hagedorn [5, 62] growth of the density $n(m)$ of string states of mass m, approximated by

$$n(m) \sim \exp\left(m/T_H\right), \qquad T_H = \frac{1}{2\pi\sqrt{\alpha' c_\perp/6}}, \tag{6.2}$$

where $c_\perp$ is the central charge of the transverse modes alone: $c_\perp = 24$ for the bosonic

string considered here. T_H is the *Hagedorn temperature*. Taking this into account, one finds that while the production rate of a single massive state is small, the rapid growth in the number of states (6.2) can give rise to a significant cumulative effect.

Here we test this effective field theory approximation in a weak–field limit, where string pair creation may be computed exactly. Although our real interest is strong gravitational fields, such as those that arise in cosmology, the formalism does not yet exist to calculate pair production of strings here (see [82] for an interesting approach to this and [119] for a calculation in a more specific background). Nevertheless interesting surprises can be seen already for weak fields. Among them, we find that the enhancement of the production of excited string states due to the growing density of states discussed above is greatly suppressed due to the mild hard scattering behavior of the string.

To carry out our calculation of string pair production, we use the familiar idea that a curved geometry can be represented as a coherent state of gravitons [53, 54, 97, 98]. For weak gravitational fields this gives a prescription relating S–matrix amplitudes on a weakly curved spacetime to a sum of those on Minkowski spacetime with multiple graviton vertex operators inserted. To lowest order in the closed string coupling, the pair production of strings is thus the four–point process $gg \to AB$, with two gravitons g interacting to produce two strings in states A and B. This approach has the advantage of leading to a controlled calculation using standard string perturbation theory, but there are many other conceptual and technical obstacles to an understanding of strings in general time–dependent backgrounds. Among them are the subtleties involved in interpreting the S–matrix for strings on curved backgrounds (see, for example, [22, 71]). More generally, in any quantum theory including gravity, the inevitable formation of singularities as predicted by the singularity theorems [64, 65] implies the absence of asymptotically trivial "in" and "out" regions required to

define an S–matrix .

We confront these issues in our analysis in this chapter. We construct a specific geometry describing the collision of two small amplitude plane waves which we embed in an exact nonlinear solution of Einstein's equations. An analysis of the full solution shows the formation of a spacelike singularity in the future of the collision of the plane waves, and also how by making the amplitude of both waves sufficiently small we may push the singularity arbitrarily far into the future of the initial collision region. Consequently perturbation theory is valid for an arbitrarily long period, and we believe the S–matrix formalism can be used to understand the physics in this region. This is as it should be, for the possible formation of a big crunch in our future should not prevent us from understanding physics today!

In this work we primarily focus on the pair production of long–wavelength string states. Since the theory of pair creation in field theory is well developed [13, 35], and since string theory should have an effective field theory description valid for $\lambda \gg \sqrt{\alpha'}$, one might ask why we expect there to be differences between string and point particle pair creation in this regime. When viewed as the four–point process $gg \to AB$, then certainly for massless states A and B, with wavelengths $\lambda \gg \sqrt{\alpha'}$, all momentum scales in the scattering process are well below the string scale. On the other hand, to produce excited string states, with masses $m \sim 1/\sqrt{\alpha'}$, then the typical graviton momenta and momentum exchange will in fact be greater than $1/\sqrt{\alpha'}$. This is beyond the validity of effective field theory, and indeed previous investigations have revealed uniquely "stringy" behavior in this regime [57, 58, 59]. Thus, it is reasonable to expect the pair production of massive *strings* might be fundamentally different from the pair production of massive *particles*.

6.2 Pair Production in Weak Gravitational Fields

In this section we will introduce the techniques we use to analyze the pair production of strings and point particles. We will focus on the regime of weak gravitational fields, since this enables a perturbative calculation on the string worldsheet. In Section 6.2.1 we discuss the calculation of pair production in quantum field theory, focusing on the technique of Bogolubov coefficients. In Section 6.2.2 we discuss examples where pair production is perturbative or non–perturbative. We describe the method by which pair production may be calculated by a perturbation series in quantum field theory in Section 6.2.3. In Section 6.2.4 we generalize this treatment to the string. We also discuss some of the new features that arise in string theory that are not present in the field theory case. We touch on some of these problems in Section 6.2.5. Here, we show that our second order results are unchanged by corrections to the background spacetime required for the consistency of the string theory. Appendix F is also relevant to this section: there, we show that the perturbative treatment we employ is equivalent to the usual calculation using Bogolubov coefficients.

6.2.1 General Technique

The canonical method to study pair production is the use of Bogolubov coefficients. This technique can be used for both strong and weak backgrounds, provided one can solve the equations of motion for the relevant quantum field. Let us begin with the action for some real field ϕ with action

$$\mathcal{S}_\phi = \int \mathcal{L}[\phi]\, \mathrm{d}^D x \tag{6.3}$$

One begins the quantization process by decomposing the field into a complete set of modes $\{u_j, u_j^*\}$ so that

$$\phi(x) = \sum_j a_j u_j(x) + a_j^\dagger u_j^*(x) \tag{6.4}$$

where j some indexing variable (possibly continuous), and so we interpret the summation in the generalized sense of Dirac: summation over the discrete values of j and integration over the continuous ones. The mode functions u_j are usually taken to be *positive frequency* with respect to some time coordinate t in the sense that

$$i\frac{d}{dt}u_j = \lambda u_j, \qquad \lambda > 0. \tag{6.5}$$

The u_j^* are the complex conjugates of the u_j, and are the negative frequency modes. We wish to impose the equal–time commutation relations

$$[\phi(x), \pi(y)] = i\delta^D(x-y), \qquad [\phi(x), \phi(y)] = [\pi(x), \pi(y)] = 0, \tag{6.6}$$

where π is the canonical momentum defined by $\mathcal{S}_\phi$, and also promote the a_j to operators satifsying

$$[a_j, a_k^\dagger] = \delta_{jk}, \qquad [a_j, a_k] = [a_j^\dagger, a_k^\dagger] = 0, \tag{6.7}$$

and wish for the Hamiltoninan corresponding to the action be of the form

$$\mathcal{H} = \sum_j \left(\omega_j a_j a_j^\dagger + \cdots\right) \tag{6.8}$$

These requirements uniquely fix the normalization of the modes u_j. Finally, we can define the *vacuum* as the state annihilated by all the lowering operators

$$a_j|0\rangle = 0, \quad \forall j \tag{6.9}$$

which, again, is uniquely defined by the choice of mode functions $\{u_j, u_j^*\}$. Of special importance is the fact that the vacuum is determined by the choice of mode functions, and different mode functions lead to different vacuum states.

The only arbitrary choice in this construction is the choice of the complete set of modes $\{u_j, u_j^*\}$. We are also free to choose a different complete set $\{\overline{u}_j, \overline{u}_j^*\}$, which will lead to a quantization of the field that is, in general, inequivalent to the first one.

The inequivalence is measured by the *Bogolubov coefficients* α_{jk} and β_{jk}, defined by

$$a_i = \sum_j \alpha_{ij}\overline{a}_j + \beta^*_{ij}\overline{a}^\dagger_j \tag{6.10}$$

When the coefficients $\beta_{jk} = 0$, the quantizations are equivalent since the two vacua are equal, and we can build the u_j as linear combinations of the $\overline{u}_j$. Otherwise, the quantizations are inequivalent. This is sometimes expressed using the *number operator* relative to the different quantizations

$$N_j = a^\dagger_j a_j, \qquad \overline{N}_j = \overline{a}^\dagger_j \overline{a}_j. \tag{6.11}$$

It satisfies the relation

$$\langle\overline{0}|N_j|\overline{0}\rangle = \sum_k |\beta_{kj}|^2 \tag{6.12}$$

which is not zero when $\beta_{jk} \neq 0$. Thus, the vacuum relative to one quantization contains particles relative to the other.

This framework can be used to describe pair production in a time–dependent background. To do this one usually considers a situation in which the spacetime is asymptotically trivial in the far past and future, and constructs a quantum field theory based on a "natural" set of modes. These sets of modes define the "in" and "out" vacua, respectively. The relevant Bogolubov transformation is that between these two quantum field theories. The general idea is that a mode can start out as a positive frequency mode in the "in" quantum field theory, then evolve through the spacetime into a mixture of positive and negative frequency modes in the "out" quantum field theory. When this occurs, we said that pair production has occurred.

6.2.2 Perturbative vs. Non–Perturbative Pair Production

In one sense computing the Bogolubov transformation involves only classical physics. One takes the boundary condition that the field $\phi(x)$ obeys $\phi = u_j$ in the far past,

where u_j is some positive frequency mode in the "in" mode set. This corresponds to taking ϕ to be in its vacuum state in the far past. One then evolves ϕ according to the classical equations of motion. The resulting field ϕ is then decomposed into modes of the "out" mode set. If any negative frequency modes are present in this expansion, the β Bogolubov coefficient will be nonzero. It may be that this "classical" contribution vanishes, at which point one must look at loops and other features of quantum field theory. In the case we are interested in for the current work, the classical contribution will dominate.

In this work we are concerned with the case where the pair production rate is perturbative in some parameter characterizing the geometry. The literature on pair production has examples of both non–perturbative and perturbative pair production rates. Schwinger's classic calculation of e^+e^- production in an electric field [104] is essentially non–perturbative. For a particle of charge e, mass m, and spin J in an electric field $\mathbf{E}$, the production rate Γ per unit time and volume is

$$\Gamma = \frac{2J+1}{8\pi^3} \sum_{n=1}^{\infty} \left[(-1)^{(2J+1)(n+1)} \left(\frac{e\mathbf{E}}{n} \right)^2 \exp\left(-\frac{\pi n m^2}{|e\mathbf{E}|} \right) \right] \tag{6.13}$$

As the electric field $\mathbf{E}$ is taken to zero, the pair production rate vanishes faster than any power of $\mathbf{E}$. The same features are also seen in more recent calculations with open strings [6, 20]. In the open string case there is also an instability at large $\mathbf{E}$ corresponding to a "tearing" of the string.

An example with a different behavior is provided by the pair production of scalars of mass m in a flat FRW spacetime that undergoes a brief period of expansion [11]. In this example we have the metric

$$ds^2 = a(\eta)^2 \left(-d\eta^2 + dx_3^2 \right), \qquad a^2(\eta) = 1 + b \tanh(\rho\eta), \tag{6.14}$$

and the number of particles produced in each mode $k = (\omega, \vec{k})$ is found to be

$$N_{\vec{k}} = \frac{\sinh^2\left[\pi(\omega_{+\infty} - \omega_{-\infty})/2\rho\right]}{\sinh(\pi\omega_{+\infty}/\rho)\sinh(\pi\omega_{-\infty}/\rho)} \tag{6.15}$$

where

$$\omega(\eta) = \left[|\vec{k}|^2 + a(\eta)^2 m^2\right]^{1/2}, \qquad \omega_{\pm\infty} = \omega(\pm\infty). \tag{6.16}$$

For $b \ll 1$ the number of pairs produced goes like $\sim b^2 m^4$ for small b. Thus one might hope that for small values of bm^2 it would be possible to treat this problem in some kind of perturbative expansion. It is backgrounds of this type that we will focus on in this work.

6.2.3 Field Theory

In the case of field theory, the perturbative analysis of pair production can be realized quite straightforwardly through the addition of new vertices in the Feynman diagrams of the theory. This point of view is developed in more detail in Appendix F, where it is shown that this technique yields precisely the same results as the more standard Bogolubov coefficient calculation. The field theory case is useful for our present purposes as it provides a prototype for the string calculation. Note that this technique is not applicable to all pair production scenarios – for example, one cannot use it to compute the Schwinger pair production rate (6.13). One expands the metric about Minkowski space

$$g_{\mu\nu} = \eta_{\mu\nu} + h^{(1)}_{\mu\nu} + h^{(2)}_{\mu\nu} + \cdots, \tag{6.17}$$

where $h^{(1)}_{\mu\nu}$ is the first order metric perturbation, and $h^{(2)}_{\mu\nu}+\ldots$, the corrections required at successively higher order so that the full metric $g_{\mu\nu}$ satisfies the Einstein equations. If we consider a massive minimally coupled scalar field with action

$$\mathcal{S}_\phi = -\frac{1}{2}\int \left(g^{\mu\nu}\partial_\mu\phi\partial_\nu\phi + m^2\phi^2\right)\sqrt{-g}\; d^D x, \tag{6.18}$$

Then the expansion (6.17) of the metric gives a corresponding perturbative expansion of the action,

$$\mathcal{S}_\phi = \mathcal{S}^{(0)}_\phi + \mathcal{S}^{(1)}_\phi + \mathcal{S}^{(2)}_\phi + \cdots \tag{6.19}$$

as well as a series of terms $\mathcal{S}_\phi^{(n)}$ at n^{th} order in the perturbation.

This allows a perturbative evaluation of the n–point functions in the background, denoted by $\langle\cdots\rangle_b$, in terms of the same quantities $\langle\cdots\rangle_0$ in Minkowski space with additional insertions. For any combination of fields $\mathcal{O}$, the expansion of the action (6.19) inserted into the path integral yields,

$$\langle\mathcal{O}\rangle_b = \langle\mathcal{O}\rangle_0 + \int\langle T\mathcal{O}_k\Sigma^{(1)}_{-k}\rangle_0\frac{d^Dk}{(2\pi)^D} + \int\langle T\mathcal{O}_{k'}\Sigma^{(2)}_{-k'}\rangle_0\frac{d^Dk'}{(2\pi)^D} + \cdots \tag{6.20}$$

where $\Sigma^{(1)}$ and $\Sigma^{(2)}$ are the new vertices that appear to first and second order in perturbations. These are determined by the expansion (6.19) of the action

$$\Sigma^{(1)} = i\mathcal{S}_\phi^{(1)}, \tag{6.21a}$$

$$\Sigma^{(2)} = i\mathcal{S}_\phi^{(2)} - \frac{1}{2}\left[\mathcal{S}_\phi^{(1)}\right]^2. \tag{6.21b}$$

The statements that we have made for the n–point functions have analogues for the S–matrix . However, defining an S–matrix involves a choice of asymptotic "in" and "out" states. Therefore this prescription really only makes sense when the spacetime in question is asymptotically Minkowski. In other cases it may be necessary to modify the definition of asymptotic states.

At this point, it is possible to see how even a weak gravitational background can lead to pair production. Pair production is the process with no "in" particles and two "out" particles. While forbidden by momentum conservation in Minkowski space, in the perturbed spacetime each term in the S–matrix carries three momenta; the two momenta of the "out" particles and the momentum carried by the new vertices $\Sigma^{(n)}$. Thus two positive energy particles can appear in the "out" state if one of the terms $\Sigma_k^{(n)}$ supplies the "missing" momentum. So, the amplitude to pair produce two particles with momenta k_1, k_2 will be nonzero provided that we have $\Sigma^{(n)}_{-k_1-k_2} \neq 0$. More physically the missing momentum is coming from the background gravitons.

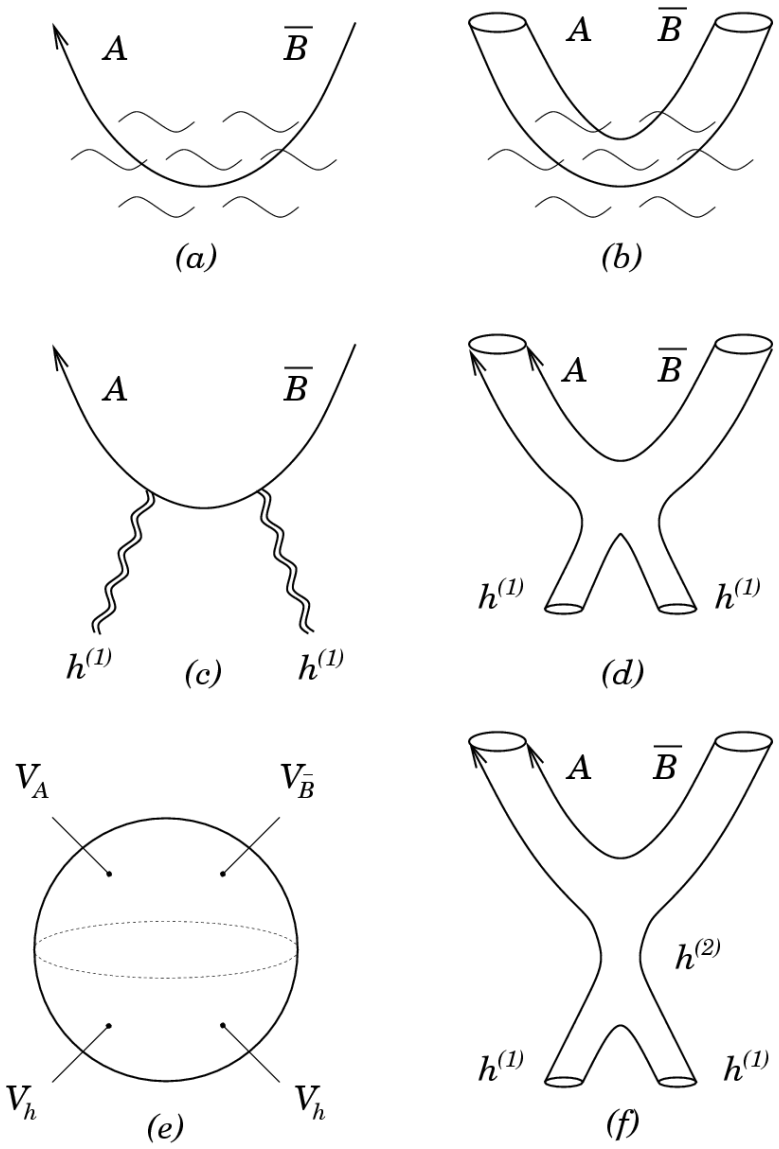

Figure 6.1: Analogies between string and point particle pair production calculations. Time runs in the upward direction in these diagrams. (a) the pair production of point particles can be thought of as reflection from spacetime curvature, shown by wavy lines (b) the analogous picture for the string worldsheet (c) spacetime curvature approximated by gravitons interacting with the point particle, giving a Feynman diagram (d) analogue for the string (e) the graviton absorption corresponds to adding two graviton vertex operators to any correlation function computed on the worldsheet (f) in the worldsheet picture, some off–shell propagating intermediate states (and their corrections to the correlation function) are included automatically in the calculation.

6.2.4 String Theory

Strings in time–dependent spacetimes are currently poorly understood. There are many difficult technical obstacles to formulating a consistent string theory in a nontrivial background. One is that the consistency requirements of the worldsheet theory lead to an infinite number of constraints on physical states, which are difficult to solve simultaneously. Another problem is that string interactions are rooted in the S–matrix approach, and string field theory is a topic still very much under development. Furthermore, even in very simple cases, such as the linear dilaton model [2, 93] the spectrum of physical states can change quite dramatically when the theory is formulated on a nontrivial background. We will encounter some of these problems in the current work, but fortunately we do not need to confront them directly in order to extract sensible results from our technique.

Following the same procedure as the field theory calculation, one may insert the perturbative expansion of the metric $g_{\mu\nu} = \eta_{\mu\nu} + h^{(1)}_{\mu\nu} + h^{(2)}_{\mu\nu} + \cdots$ into the conformal gauge string worldsheet action

$$S = -\frac{1}{2\pi\alpha'} \int g_{\mu\nu}(X) \partial X^\mu \overline{\partial} X^\nu \, d^2z. \tag{6.22}$$

Now, the successive metric perturbations $h^{(n)}_{\mu\nu}$ are chosen to satisfy the string beta function equations.

First order

As is well known [53, 54, 97, 98] the expansion of the metric leads to the insertion of graviton vertex operators in worldsheet correlation functions. For example, if we wish to study the S–matrix element involving two string states A and B then we

must compute the worldsheet correlation function

$$\Big\langle \mathcal{V}_A(k_A)\mathcal{V}_B(k_B)\Big\rangle_b = \Big\langle \mathcal{V}_A(k_A)\mathcal{V}_B(k_B)\Big\rangle_0 + \frac{1}{4\pi g_c}\int h^{(1)}_{\mu\nu}(k')\Big\langle \mathcal{V}_A(k_A)\mathcal{V}_B(k_B)\mathcal{V}_g^{\mu\nu}(k')\Big\rangle_0 \frac{d^Dk'}{(2\pi)^D} + \cdots \quad (6.23)$$

where $\mathcal{V}_{A,B}(k_{A,B})$ are the vertex operators for the created strings in states A and B, $\mathcal{V}_g^{\mu\nu}(k')$ is a graviton vertex operator integrated over the worldsheet representing the metric perturbation, and we have absorbed a factor of g_c in each of the vertex operators. The metric perturbation $h^{(1)}_{\mu\nu}$ appears as the polarization tensor of the background graviton.

The first–order contribution to pair creation (6.23) vanishes when A and B are massive, due to momentum conservation when the graviton is on–shell (as it must be for a consistent string amplitude). Nevertheless, (6.23) is related to the phenomenon of *particle transmutation*, by which a string can change its mass and spin as it passes through a gravitational background [31, 32, 69, 112]. We will not investigate this phenomenon in the current work, but for weakly curved spacetimes it could in principle be studied within the S–matrix framework we apply herein.

Second order

Ideally we would be able to continue this expansion to higher order in the metric perturbation, by analogy to the field theory case. However, at second order issues arise in the string theory that make the situation somewhat more complex. For one, consistency of the of the string amplitude (6.23) requires that each of the vertex operators appearing in be a conformal tensor of weight $(h, \overline{h}) = (1, 1)$, or in other words satisfy the physical state conditions. As is well known, this is equivalent to imposing the linearized Einstein equations on $h^{(1)}_{\mu\nu}$. At second order in the expansion of worldsheet amplitudes, a graviton vertex operator with polarization $h^{(2)}_{\mu\nu}$ appears.

To define a consistent theory, the second–order perturbation $h^{(2)}_{\mu\nu}$ must satisfy the second–order β–function equations for the worldsheet theory [97]. In general, this means that $h^{(2)}_{\mu\nu}$ with *not* in fact satisfy the physical state conditions. Thus, the string amplitude with the corresponding vertex operator will not be consistent.

Another issue that arises is the presence of a nonzero one–point functions or *tadpoles* for some fields. Tadpole cancellation is one of many consistency checks for superstring theories [53, 54, 97, 98]. Typically, tadpoles refer to nonzero one–point functions for massless fields with $k^2 = 0$. In the situation we study here, one–point functions for massless fields automatically vanish, but in a slight abuse of terminology we will use the term "tadpole" to refer to a nonvanishing one–point function for a massive field as well.

Taking our prescription literally, to compute the S–matrix elements on our background to second order involves inserting two graviton vertex operators into the relevant correlation functions. For massive fields A, the tadpole is zero at first order due to momentum conservation. At second order in the metric perturbation, the tadpole for some state A in the background is therefore given by

$$\Big\langle \mathcal{V}_A(k_A) \Big\rangle_b = \Big\langle \mathcal{V}_A(k_A)\mathcal{V}_g(k_1)\mathcal{V}_g(k_2) \Big\rangle + \cdots \tag{6.24}$$

with $\mathcal{V}_g(k) = \frac{1}{4\pi g_c} h^{(1)}_{\mu\nu}\mathcal{V}_g^{\mu\nu}(k)$. This expression does not vanish for the examples we consider. A nonvanishing tadpole is an indication that the classical equations of motion are not exactly obeyed by the background solution. This is to be expected, as here we will use a background solution that solves the leading–order equations of motion for massless string excitations, but we have ignored the massive excitations and higher corrections. The presence of the tadpole is telling us that the equations of motion for these massive fields forbid setting them to zero throughout spacetime. Furthermore, in a curved background the vertex operators and states should change, which we have not taken into account. We expect that the failure of the tadpole to

vanish is due to some combination of all of these effects.

Given these new complexities, it appears that problems are beginning to develop with the technique of inserting new vertex operators at second order. Nevertheless, by considering each of these new problems, we will argue in Sections 6.2.5 that useful results can be obtained from the second order expansion. Therefore, for the purpose of studying pair production we will use the prescription

$$\langle AB|S|vac\rangle = \frac{1}{(4\pi g_c)^2}\int_{\mathbf{S}^2} h^{(1)}_{\mu\nu}(k')h^{(1)}_{\sigma\tau}(k'')\Big\langle \mathcal{V}_A(k_A)\mathcal{V}_B(k_B)\mathcal{V}_g^{\mu\nu}(k')\mathcal{V}_g^{\sigma\tau}(k'')\Big\rangle_0 \frac{d^Dk'}{(2\pi)^D}\frac{d^Dk''}{(2\pi)^D} \quad (6.25)$$

where $\mathcal{V}_{A,B}(k_{A,B})$ are the vertex operators for the pair created string states A and B. In defining this S–matrix element it is understood as usual that the positions of three of the vertex operators are fixed and the remaining one is integrated over the worldsheet. This prescription does not involve a term at first order in the metric perturbation, since the pair production of massive states is forbidden to this order by momentum conservation. Furthermore corrections to the vertex operators and background solution, which should be included in a more complete analysis, only affect this S–matrix element at higher orders in $h^{(1)}_{\mu\nu}$.

6.2.5 Coherent states

The existence of non–zero "tadpoles," or 3–point functions $\langle \mathcal{V}_g\mathcal{V}_g\mathcal{V}_N\rangle$ where $\mathcal{V}_N$ denote the vertex operators for level N string states, implies that turning on a nontrivial gravitational background will, at second order, produce a nontrivial background of excited states. The question we must address is whether we can still trust the pair production results that we will extract at this order. By studying an analogous situation in field theory, we will argue that the corrections to the pair production amplitudes appear at higher order, and thus our second order results may be trusted.

The production of excited string states can be modeled in field theory as the pair production of a massive scalar field χ via interactions with a massless scalar field H, representing the graviton. This can be realized with the action

$$\mathcal{S} = \int \mathrm{d}^d x \left(-\frac{1}{2}(\partial H)^2 - \frac{1}{2}(\partial\chi)^2 - \frac{1}{2}m^2\chi^2 + \lambda H^2\chi - \frac{1}{2}\mu H^2\chi^2 \right). \tag{6.26}$$

The presence of the λ coupling implies that we cannot turn on a background field for H without also exciting a background value for χ, as a consequence of the equations of motion

$$-\Box H = 2\lambda H\chi + \ldots \tag{6.27}$$

$$-\Box\chi + m^2\chi = \lambda H^2 + \ldots.. \tag{6.28}$$

The μ coupling gives rise to pair creation of χ quanta in the presence of a nontrivial 'graviton' background H. Before calculating this effect we must first deal with the background. Assuming $\chi = 0 + O(H^2)$ these equations may be solved perturbatively to second order in H as (here $\int \mathrm{d}\tilde{k} = \int \mathrm{d}^{d-1}k/(2\omega)$, $\omega = |k^0|$ which is valid for massless and massive particles)

$$H(x) = H_0(x) = \int \mathrm{d}\tilde{k} \left(\alpha^*(k) e^{ik.x} + \alpha(k) e^{-ik.x} \right) + O(H_0^3), \tag{6.29}$$

$$\chi(x) = \lambda \int \mathrm{d}^d y \; G_{ret}(x,y) H_0^2(y) + O(H_0^3), \tag{6.30}$$

where $G_{ret}(x,y)$ is the retarded propagator for a scalar of mass m and we have chosen the following boundary conditions

$$\lim_{t\to-\infty} \chi(x) = 0. \tag{6.31}$$

It is well known that in field theory a nontrivial background may be described by a coherent state. The initial state contains only gravitons and may be described by

$$|vac, t \to -\infty\rangle = e^{-\frac{1}{2}\int \mathrm{d}\tilde{k}|\alpha|^2} e^{\int \mathrm{d}\tilde{k}\alpha a^\dagger} |0\rangle. \tag{6.32}$$

Whereas the final state is a coherent state of both 'gravitons' and χ quanta

$$|vac, t \to +\infty\rangle = e^{-\frac{1}{2}\int \mathrm{d}\tilde{k}|\beta|^2} e^{-\int \mathrm{d}\tilde{k}\frac{1}{2}|\alpha|^2} e^{\int \mathrm{d}\tilde{k}\alpha a^\dagger} e^{\int \mathrm{d}\tilde{k}\beta d^\dagger}|0\rangle. \tag{6.33}$$

Here $a^\dagger/a$, $d^\dagger/d$ are the conventionally defined creation/annihilation operators for H and χ respectively, and $\beta(k)$ is the generated background for χ

$$\lim_{t\to+\infty} \chi(x) = \int \mathrm{d}\tilde{k} \ \left(\beta^*(k)e^{ik.x} + \beta(k)e^{-ik.x}\right). \tag{6.34}$$

We now compute the amplitude to create a pair of χ quanta. Because of the nontrivial background for χ as $t \to +\infty$ we must redefine the creation/annihilation operators as $\tilde{d} = d - \beta$. This is the analogue of canceling the tadpole in the string theory. The β are also determined by the condition that the amplitude to create a single particle must vanish (tadpole cancellation)

$$\langle vac, t \to +\infty|\sqrt{2\omega}\tilde{d}S|vac, t \to -\infty\rangle = 0. \tag{6.35}$$

Now the amplitude to create a single pair of χ quanta with momenta (k_3, k_4) is

$$A[vac \to 2] = \langle vac, t \to +\infty|\sqrt{2\omega_3}\tilde{d}(k_3)\sqrt{2\omega_4}\tilde{d}(k_4)S|vac, t \to -\infty\rangle, \tag{6.36}$$

where S is the S–matrix . Utilizing the fact that the amplitude to create a single particle must vanish and expanding $A[vac \to 2]$ to second order we find after making uses of conservation of energy and momentum

$$A[vac \to 2] = \int \mathrm{d}\tilde{k_1} \int \mathrm{d}\tilde{k_2} \ \alpha(k_1)\alpha(k_2)\times$$
$$\langle 0|\sqrt{2\omega_3}d(k_3)\sqrt{2\omega_4}d(k_4)Sa^\dagger(k_1)a^\dagger(k_2)|0\rangle + O(H_0^3). \tag{6.37}$$

This is a very simple result: to second order in perturbations, the amplitude to create a pair of particles is determined by the amplitude for two gravitons to convert to two χ quanta. Furthermore, at second order the result is independent of the modifications to the creation operators required to cancel the tadpole. This suggests that our string results will be reliable, even though we will not carry out the modifications to the vertex operators required to cancel the tadpole in the string case.

6.3 Background

In this section we shall construct a specific example of a perturbative geometry for which our approach may be applied. In doing so we shall also uncover some of the inevitable limitations of the perturbative approach. The issue we must address is whether it makes sense to define a perturbative S–matrix on a time-dependent spacetime, due to the inevitable formation of spacelike singularities or black holes, as predicted by the singularity theorems [64, 65].

We study a background corresponding to two colliding plane gravitational waves. There has been much work in the general relativity community on understanding these spacetimes and their singularities [56]. Many results are known for so–called "shock" gravitational waves, where (in the appropriate coordinates) the wave profile is a δ–function. These wave spacetimes are always singular. The prototypical exact solution for gravitational shock waves is due to Khan and Penrose [76], illustrated in Figure 6.3. One can see that the worldlines of all observers come to an end, either in a curvature singularity to the future of the wave collision region, or in a milder fold singularity in regions that are spacelike separated from the collision. Furthermore, spacetime in the future of the collision region is strongly curved, and so it is not clear whether the S–matrix in this spacetime (even granting that it could be defined) is probing the collision region or the strongly curved region **IV**.

In our case, we also consider colliding gravitational waves, illustrated in Figure 6.2. These are not shock waves. Instead, the gravitational wave packets possess a small amplitude A and are smoothed over some characteristic width L. To study pair production in the collision region of these waves, we require the spacetime to be more akin to the superposition of two linearized waves than the strongly nonlinear Khan–Penrose case. We will find that our setup shares some, but not all of the features of the Khan–Penrose spacetime. On the positive side, spacetime curvature in the

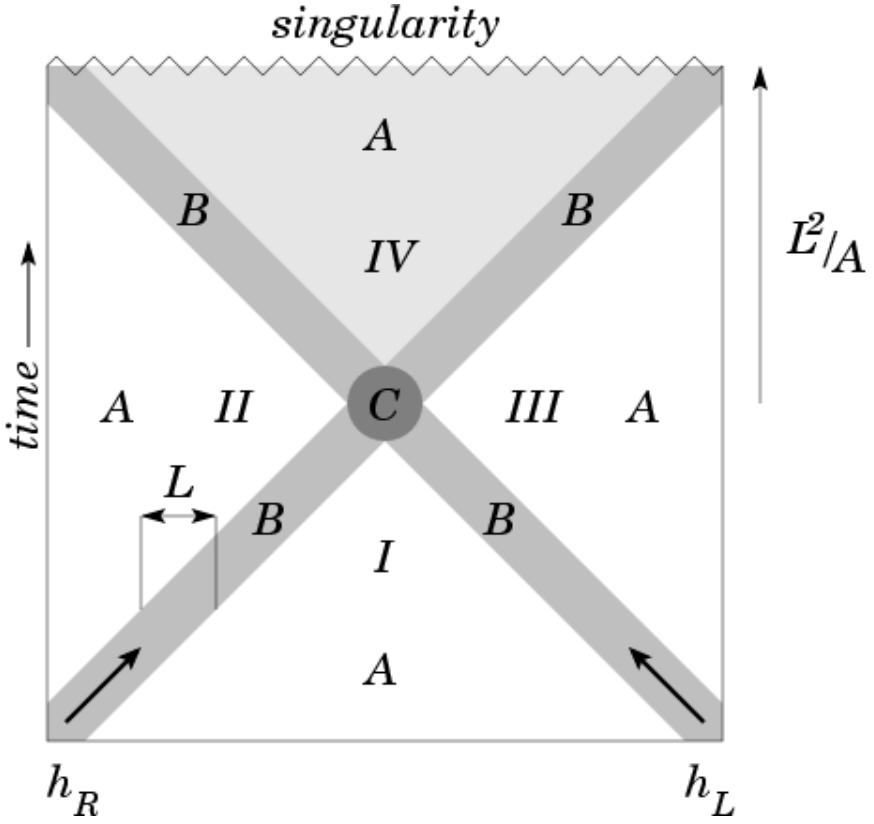

Figure 6.2: The spacetime in which we calculate the pair production of strings and point particles. Two gravitational waves of characteristic width L, amplitude A, and polarizations $h_{L,R}$ collide. In regions of type **A**, far from the waves, spacetime is Minkowski space and no pair production occurs. Spacetime interior to the waves **B** is curved but possesses a null Killing vector, and so no pairs are produced. Pair production is localized to the collision region **C**, which is curved and possesses no Killing vector. Pairs produced in this region propagate into region **IV**, which is where we define the "out" region of our S–matrix . Eventually perturbation theory breaks down at a time $\sim L^2/A$ from the interaction region.

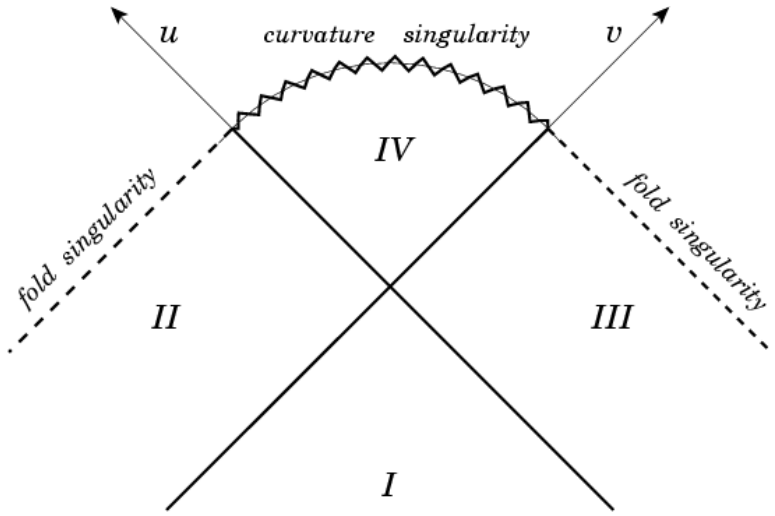

Figure 6.3: The colliding shock gravitational wave spacetime of Khan and Penrose. The gravitational waves themselves are shown with heavy lines. Region **I** is flat Minkowski space. The spacetime in region **IV** (which is timelike separated from the collision) terminates in a curvature singularity. The spacetime in regions **II** and **III** terminates in a fold singularity, beyond which it is impossible to continue the spacetime.

future of the collision event is small, and the curvature of the spacetime is localized there up to fourth order in perturbation theory. On the negative side, perturbation theory eventually breaks down after a time proportional to L^2/A, and we fully expect that this spacetime develops a singularity similar to that in the shock wave case. Nevertheless, we use the fact that perturbation theory is valid for a significant time after the collision to argue that the S–matrix on this spacetime is well–defined, at least to second order.

We introduce our metric in Section 6.3.1, and embed this metric in an exact solution to Einstein's equation, the Einstein–Rosen wave. This enables us to show that a Kasner–type singularity forms in the future, although it can form arbitrarily far in the future by adjusting the parameters of the incoming waves. In Section 6.3.2, we use the Einstein–Rosen solution to perturbatively construct the higher order corrections to our metric. We show that the metric is uncorrected (and thus the

singularity is invisible to perturbation theory) up to fourth order in the perturbations. We use this to argue that our second–order results should therefore be protected from the influence of the singularity.

6.3.1 Colliding plane waves

One of the simplest and best studied time–dependent geometries is the *pp*–wave. This is a solution of Einstein's vacuum equations with metric given by

$$\mathrm{d}s^2 = 2\mathrm{d}u\,\mathrm{d}v + H(u,X)\mathrm{d}u^2 + \mathrm{d}X^i\,\mathrm{d}X_i, \tag{6.38}$$

where $H(u,X)$ is a harmonic function, satisfying

$$\nabla^2 H(u,X) = 0. \tag{6.39}$$

These solutions may easily be extended to include nontrivial dilaton and NS 2-form sources. However, for simplicity of presentation we shall concentrate on pure vacuum solutions. We will focus on the class of "exact" plane waves for which

$$H(u,X) = A_{ij}(u)X^iX^j \qquad \text{with} \qquad \sum_i A_{ii}(u) = 0. \tag{6.40}$$

All *pp*–wave spacetimes admit a null Killing vector $\frac{\partial}{\partial v}$ and this allows a global definition of null time. As a consequence, the natural "in" and "out" field theory vacua are chosen by decomposing modes into positive and negative frequency with respect to this time, and since this is a global definition we find that for a free field $|0\rangle_{in} = |0\rangle_{out}$ implying the absence of particle creation [50]. (This is true provided we make the conventional choice of vacua. If the plane wave geometry is not asymptotically Minkowski at past and future infinity then the reasons for this choice are less clear).

In order to obtain a background with pair creation we will consider a spacetime describing the collision of two plane waves. Treating the amplitude of each wave $A_{ij}^{(\alpha)}$

as small, then at the linearized level this will be described by the metric

$$\mathrm{d}s^2 = 2\mathrm{d}u\mathrm{d}v + A^+_{ij}(u)X^iX^j\mathrm{d}u^2 + A^-_{ij}(v)X^iX^j\mathrm{d}v^2 + \mathrm{d}X^i\mathrm{d}X_i + O(A^2). \tag{6.41}$$

and the two waves pass through each other undisturbed. The $O(A^2)$ terms will include interactions between the waves. If the amplitude of each wave is localized around a given null time, for example if we take

$$A^+_{ij}(u) \approx A\exp\left(-u^2/L^2\right) \tag{6.42}$$

then at leading order the interaction region will be localized near $(|u| < L, |v| < L)$. However, at higher orders we will see that there is a long tail in the future lightcone of the interaction region in which perturbations grow, eventually leading to a singularity.

Fortunately all this can be seen explicitly in a concrete example where A^+_{ij} and A^-_{ij} are both diagonal. In this case it is straightforward to lift the linearized metric (6.41) to an exact nonlinear solution of Einstein's equations. To see this, first perform a linearized gauge transformation to take the metric to the form

$$\mathrm{d}s^2 = 2\mathrm{d}u\mathrm{d}v + (\delta_{ij} + h_{ij}(u,v))\mathrm{d}X^i\mathrm{d}X^j + O(A^2). \tag{6.43}$$

where

$$h_{ij}(u,v) = 2\int\int A^+_{ij}(u)\,\mathrm{d}u\,\mathrm{d}u + 2\int\int A^-_{ij}(v)\,\mathrm{d}v\,\mathrm{d}v. \tag{6.44}$$

This metric is a special case of a more general class of solutions given by

$$\mathrm{d}s^2 = 2e^{\Gamma(u,v)}\mathrm{d}u\mathrm{d}v + \alpha(u,v)\sum_i e^{2\beta_i(u,v)}\mathrm{d}x_i^2, \tag{6.45}$$

where $\sum_i \beta_i = 0$. This is the form of an exact set of solutions to Einstein's equations known as Einstein–Rosen waves. They satisfy

$$\partial_u\partial_v\alpha = 0 \qquad \text{and} \qquad \partial_u(\alpha\partial_v\beta_i) + \partial_u(\alpha\partial_v\beta_i) = 0. \tag{6.46}$$

This form is invariant under transformations

$$u \to f(\overline{u}), \tag{6.47a}$$

$$v \to g(\overline{v}), \tag{6.47b}$$

$$\exp(\Gamma) \to \exp(\overline{\Gamma})/(f_{,\overline{u}} g_{,\overline{v}}). \tag{6.47c}$$

We may use this freedom to set

$$\alpha = (\overline{u} + \overline{v})\sqrt{2} = t, \tag{6.48a}$$

$$z = (\overline{u} - \overline{v})\sqrt{2}, \tag{6.48b}$$

in which case the β_i satisfy

$$\frac{1}{t}\frac{\partial}{\partial t}\left(t\frac{\partial \beta_i}{\partial t}\right) - \frac{\partial^2 \beta_i}{\partial z^2} = 0. \tag{6.49}$$

It is straightforward to see that as $t \to 0$ the solutions to this equation behave as

$$\beta_i \to c_i(z) + d_i(z) \ln t. \tag{6.50}$$

The resulting solution describes a Kasner metric where the Kasner exponents are functions of z. Consequently the generic collision of two plane waves will result in an anisotropic singularity [122].

The existence of a singularity should cause us no surprise, it arises as a simple consequence of the singularity theorems. Although the singularity theorems do not strictly apply here as we have no matter, compactifying the geometry on one direction gives us a theory with gravity and a scalar field which does satisfy the singularity criteria. In the present context it implies that perturbation theory will inevitably breakdown in a finite time period. In the traditional definition of an S–matrix theory, the "out" state is defined at future infinity, thus it would seem at first sight impossible to define an S–matrix on a spacetime with a singularity at future infinity.

6.3.2 Perturbative solution

Our approach to dealing with the fundamental issue of singularities is a pragmatic one,. If there exists a long period of time for which perturbation theory is valid, then the S–matrix should describe physics in that period. Let us now construct the perturbative solution to Einstein's equations. This will enable us to check that nonlinear corrections remain small at low orders in the perturbation expansion, and to explore the breakdown of perturbation theory. To be consistent with the metric (6.43), we take $\beta^i \sim O(A)$, $\alpha \sim 1 + O(A^2)$ and $\Gamma \sim O(A^2)$. The perturbed metric up to and including 3rd order in perturbations is

$$\begin{aligned}
\alpha &= 1 + A^2(\alpha_+(u) + \alpha_-(v)) + O(A^4), && (6.51)\\
\beta^i &= A(\beta^i_+(u) + \beta^i_-(v)) - \frac{1}{2}A^3(\alpha_+(u)\beta^i_-(v) + \alpha_-(v)\beta^i_+(u)) + O(A^4), && (6.52)\\
\Gamma &= -\frac{1}{4}A^2\sum_i \beta^i_+(u)\beta^i_-(v) + O(A^4), && (6.53)
\end{aligned}$$

where

$$\begin{aligned}
\alpha''_+(u) &= -\frac{1}{4}\sum_i \beta^{i\,2}_{+,u},\\
\alpha''_-(v) &= -\frac{1}{4}\sum_i \beta^{i\,2}_{-,v}. && (6.54)
\end{aligned}$$

We are assuming that $\beta_+(u)$ and $\beta_-(v)$ are localized functions, for instance with a Gaussian profile $\beta_+ = \exp(-u^2/L^2)$ and $\beta_- = \exp(-u^2/L^2)$. From this it is clear that up to 3rd order in A, β^i and Γ are both bounded functions localized near the interaction region $u = v = 0$. However, as a consequence of (6.54), α is not bounded. We choose the solution

$$\alpha_+(u) = -\frac{1}{4}\int_{-\infty}^{u} \mathrm{d}u_1 \int_{-\infty}^{u_1}\sum_i \beta^{i\,2}_{+,u_2}(u_2), \qquad (6.55)$$

and similarly for $\alpha_-(v)$. From this it is clear that as $u \to +\infty$, then $\alpha_+(u) \to C_+ + D_+ u$, where,

$$D_+ = -\frac{1}{4}\int_{-\infty}^{\infty} \mathrm{d}u \ \sum_i \beta^{i\,2}_{+,u} \neq 0. \tag{6.56}$$

Trying to remove this divergence by adding the homogeneous solution $-D_+ u$ causes $\alpha_-(u)$ to diverge as $u \to -\infty$. This is the first indication that perturbation theory breaks down at late times. On dimensional grounds, $D_+ \sim O(1)/L$ and so this coordinate system breaks down at $u \approx L/A^2$, $v \approx L/A^2$. Evidently by making A sufficiently small, we can push this region arbitrarily far into the causal future of the interaction region.

Remarkably, to 3rd order in A, the growth of α is a coordinate artifact and does not reflect a genuine breakdown of perturbation theory. One may show this by removing the linear growth in u by means of the following coordinate transformation,

$$x^i \ \to \ x^i(1 + \frac{A^2}{2}(D_+ u + D_- v)) + O(A^3), \tag{6.57}$$

$$u \ \to \ u + \frac{A^2}{4} D_+ \vec{x}^2 + O(A^3), \tag{6.58}$$

$$v \ \to \ v + \frac{A^2}{4} D_- \vec{x}^2 + O(A^3). \tag{6.59}$$

Similarly all components of the Riemann tensor are finite and supported only near $u = v = 0$. In fact we must go to 4th order in perturbations to see the first signal that perturbation theory is breaking down. An explicit calculation shows that certain components of the Riemann tensor diverge linearly for large u and v in any orthonormal frame. However, unsurprisingly this only occurs when $u \approx L/A^2$, $v \approx L/A^2$. So again we may push the inevitable breakdown of perturbation theory off to arbitrarily far in the future of the region of interest.

In what follows we shall only compute the string amplitudes to second order in the background perturbations. As we have seen, at second order the collision of two plane waves results in a localized interaction region and no pathologies occur. Thus

there will be no problem interpreting our amplitudes. If we continue the amplitude calculations to higher order in perturbations, we may expect to see mildly pathological behavior associated with the eventual breakdown in perturbation theory. However, it should always be possible to separate this from the information which describes the interaction region. These above observations show the fundamental limitations of the application of the S–matrix formalism to a time-dependent geometry, these issues would not arise in a more Schrödinger–like prescription where we consider the state at a given time, rather than the transition amplitude to a state at future infinity. This suggests that string field theory or a similar formalism may be a more appropriate way to consider time-dependent spacetimes.

6.4 Pair Production

The first nonvanishing contribution to string pair production arises from the four–point amplitude with two incoming gravitons. In this section we discuss this amplitude for an explicit set of string states, and obtain results in accord with previous investigations on the high–energy behavior of string scattering amplitudes [57, 58, 59]. This suggests that the behavior we observe here may hold for more general excited string states as well. A detailed calculation of the relevant amplitude may be found in Appendix E.

We calculate the pair creation of "representative" string states given in oscillator notation by

$$|\epsilon; k\rangle = (N!)^{-1} \epsilon_{\mu_1 \overline{\mu}_1 \ldots \mu_N \overline{\mu}_N} \left(\prod_{j=1}^{N} \alpha_{-1}^{\mu_j} \tilde{\alpha}_{-1}^{\overline{\mu}_j} \right) |0; k\rangle, \tag{6.60}$$

where we assume that $N > 1$. This set of states includes a unique scalar state at each excitation level N, which provides the most direct comparison with field theory results.

Clearly the polarization ϵ must be symmetric under the interchange of two holomorphic indices. The physical state conditions are satisfied provided that

$$m^2 = \frac{4}{\alpha'}(N-1). \tag{6.61a}$$

$$k^{\mu_j}\epsilon_{\mu_1\overline{\mu}_1\ldots\mu_j\ldots\mu_N\overline{\mu}_N} = 0, \qquad \text{for all } j. \tag{6.61b}$$

$$\eta^{\mu_j\mu_k}\epsilon_{\ldots\mu_j\ldots\mu_k\ldots} = 0, \qquad \text{for all } j,k. \tag{6.61c}$$

along with similar conditions for the barred indices. These states will have unit norm provided that

$$\langle\epsilon;k|\epsilon;k\rangle = 1 \qquad \text{if} \qquad \epsilon^{\mu_1\overline{\mu}_1\ldots\mu_j\ldots\mu_N\overline{\mu}_N}\epsilon_{\mu_1\overline{\mu}_1\ldots\mu_j\ldots\mu_N\overline{\mu}_N} = 1. \tag{6.62}$$

The vertex operators corresponding to these states are given by

$$\mathcal{V}_N(k) = g_c\epsilon_{\mu_1\overline{\mu}_1\ldots\mu_N\overline{\mu}_N}\left(\frac{2}{\alpha'}\right)^N : \left[\prod_{j=1}^{N}\partial X^{\mu_j}\overline{\partial}X^{\overline{\mu}_j}\right] e^{ik\cdot X}(z,\overline{z}) : \tag{6.63}$$

where we have included a factor of the closed string coupling g_c as is conventional.

As we are interested in comparing string results to those in field theory, we focus on the production of "long wavelength" string states, or equivalently those whose spatial momenta are small in comparison with $1/\sqrt{\alpha'}$. Since we are also considering the production of very massive states, the relevant process is therefore one in which the pair of strings are created nearly on threshold. In order to fix notation, we take $k_\pm$ to be the momenta of the created strings, and $-k_{L,R}$ the momenta of the incoming gravitons, so that the equation for conservation of momentum is

$$k_+ + k_- + k_L + k_R = 0. \tag{6.64}$$

We further take the created strings to be scalar representative states of excitation levels $N_\pm$. For simplicity of exposition we take the incoming gravitons to possess momentum in the t,x plane only. Working in the center of mass frame, and focusing

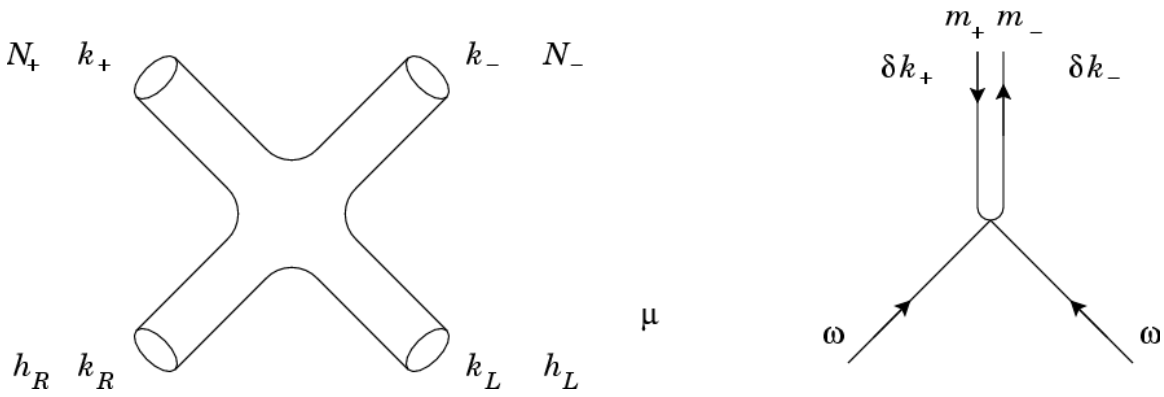

Figure 6.4: Variables used in the string scattering calculation. Left panel: two gravitons with polarizations $h_{L,R}$ and momenta $k_{L,R}$ scatter to produce to strings at excitation levels $N_\pm$ and momenta $k_\pm$. Right panel: we focus on the production of long–wavelength massive strings with masses $m_\pm$ and spatial momenta $\delta k_\pm$ by gravitons of energy ω.

on the case where the outgoing strings are created nearly on threshold, it is convenient to parameterize the momenta as

$$k_+ = (m_+, 0, 0) + (\delta\omega^+, \delta k_x, \delta\vec{k}_T), \tag{6.65a}$$

$$k_- = (m_-, 0, 0) + (\delta\omega^-, -\delta k_x, -\delta\vec{k}_T), \tag{6.65b}$$

$$k_L = (-\omega, -\omega, 0) + (-\delta\omega^L, -\delta k'_x, 0), \tag{6.65c}$$

$$k_R = (-\omega, +\omega, 0) + (-\delta\omega^R, +\delta k'_x, 0), \tag{6.65d}$$

Momentum conservation and the mass–shell conditions imply that that we may choose δk_x and $\delta\vec{k}_T$ to be the independent variables in the problem. The various kinematic variables are illustrated in Figure 6.4.

For our discussion, we will find it useful to define the additional parameters

$$a = N_+ - \frac{\alpha' t}{4}, \tag{6.66a}$$

$$b = N_- - \frac{\alpha' u}{4}, \tag{6.66b}$$

where t and u are the conventional Mandelstam variables. For the problem at hand, when the strings are produced with zero spatial momenta, these variables are given

by

$$s = m_+^2 + m_-^2 + 2m_+m_-, \tag{6.67a}$$

$$t = -m_+m_-, \tag{6.67b}$$

$$u = -m_+m_-. \tag{6.67c}$$

It will be important for our argument below that in the case where an identical pair is produced with zero spatial momentum, these variables are all $4/\alpha'$ multiplied by integers.

With this parameterization of the momenta, standard techniques in string perturbation theory give the following leading–order term in the string S–matrix

$$\epsilon^+_{\mu_1\overline{\mu}_1\cdots\mu_{N_+}\overline{\mu}_{N_+}}\epsilon^-_{\nu_1\overline{\nu}_1\cdots\nu_{N_-}\overline{\nu}_{N_-}}\epsilon^L_{\sigma\overline{\sigma}}\epsilon^R_{\tau\overline{\tau}}(N_+!)^{-1}(N_-!)^{-1}\times \frac{16\pi i}{\alpha'}g_c^2\left(\frac{\alpha'}{2}\right)^{N_++N_-}\prod_{j=1}^{N_+}k_R^{\mu_j}k_R^{\overline{\mu}_j}\prod_{k=1}^{N_-}k_R^{\nu_j}k_R^{\overline{\nu}_j}\eta^{\sigma\tau}\eta^{\overline{\sigma\tau}}\times \left[\frac{\Gamma(a)\Gamma(b)}{\Gamma(a+b)}\right]^2\frac{\sin(\pi a)\sin(\pi b)}{\sin[\pi(a+b)]}. \tag{6.68}$$

This amplitude is then multiplied by the metric perturbations and integrated according to equation (6.25). There are two key features of this amplitude that differ substantially from the field theory case.

The first remarkable feature of this amplitude is that the production of identical string pairs vanishes at zero spatial momentum. This follows directly from the behavior of the sine functions appearing in the amplitude (6.68). When $N_+ = N_- = N$, and when the spatial momentum of the created pair vanishes, then using (6.66) and (6.67) and the string mass shell condition we find

$$a = b = 2N - 1, \tag{6.69}$$

and therefore the trigonometric factors vanish. For field theory, examination of the S–matrix element arising from (6.20) reveals that the pair production amplitude is

independent of $k_{x,T}$ in the long–wavelength limit. For strings, by contrast, it appears that the pair production vanishes as a power law in the long–wavelength limit. Similar behavior obtains whenever the condition $a, b \in \mathbf{Z}$ is satisfied, which occurs for pairs of excitation levels such as

$$(N_+, N_-) = (2, 5), (2, 10), (2, 17), (3, 9), \ldots \tag{6.70}$$

in addition to the $N_+ = N_-$ cases corresponding to the creation of identical pairs. When $N_\pm$ are such that $a \notin \mathbf{Z}$ and $b \notin \mathbf{Z}$, then the production of these string pairs are independent of spatial momentum in the long wavelength limit, similar to the field theory case.

This behavior is a consequence of some fundamental features of string theory. Recall that the open string Veneziano amplitude is essentially uniquely determined by the presence of poles corresponding to excited string states, as well as worldsheet duality [53, 54, 97, 98]. The closed string amplitudes are in a sense products of open string amplitudes, with additional sine factors to ensure that all of poles that occur in the product are simple ones. Again, the closed string amplitudes are essentially uniquely determined by basic features of the theory. Thus different sine factors are zero when the s, t or u Mandelstam variables correspond to a physical string state and compensate for some of the poles arising from the gamma functions in the amplitude. In our case, when the string pairs are produced with zero spatial momentum, the s Mandelstam variable corresponds to an on–shell string state, but the t and u variables are the negative of on–shell values. Thus the sine functions have zeros, but now the gamma functions have no poles, and so the amplitude vanishes. Of course, this argument requires that we establish exactly some additional integers appearing in the arguments to the gamma functions, and this is done in Appendix E. The vanishing of this amplitude holds not only for the leading term in the S–matrix , but for terms of all orders in k appearing in this amplitude.

The second key difference between the string and field theory pair production amplitudes is an exponential suppression of the string pair production rate. To explore this feature we consider the case where excitation level of both strings is approximately N, in which case $a \sim b \sim 2N$ from (50). Applying Stirling's approximation to the gamma function factors in (49) we find

$$\frac{\Gamma(2N)^4}{\Gamma(4N)^2} = \frac{2\pi}{N} 2^{-8N} \left(1 + \frac{1}{8N} + \cdots\right) \qquad N \gg 1. \tag{6.71}$$

Therefore, the string amplitude falls off exponentially with m^2, in contrast to the polynomial dependence of the field theory result. This behavior is characteristic of hard scattering string processes. As we have remarked earlier, typically we expect pair production rates in field theory to fall off exponentially with mass. However, recall that when studied with the S–matrix approach employed herein, there are actually two effects at play. The first is the structure of the field theory amplitude connecting the incoming gravitons to the outgoing particles. The second is the number of gravitons, or Fourier coefficients of the metric perturbations. In field theory, the former behaves polynomially with mass, while the second drops off exponentially. For strings on the same background (that is, with the same Fourier coefficients for metric perturbations) both factors fall off exponentially. Thus fewer pairs are produced.

Again, this may be understood using simple string physics. In studies of string amplitudes, one of the kinematic regions of interest [57, 58, 59] is the so–called "hard scattering" limit

$$s \to \infty, \qquad t/s \quad \text{fixed}. \tag{6.72}$$

This is precisely the limit of interest when we look at particles of the same mass and look at the limit in which $m \to \infty$. In the hard scattering limit, string amplitudes behave as

$$\text{amplitude} \sim e^{-sf(\theta)} \tag{6.73}$$

where $f(\theta) > 0$. This is precisely the behavior observed in our results. It indicates that, just as the scattering of strings is softer than that of point particles at high energy, so too the pair production of strings is reduced.

6.5 Conclusions

In this work we have studied the pair production of excited strings in a time–dependent background. The specific background we consider consists of two colliding plane gravitational waves. Through studying the singularity structure of this background, as well as the nature of corrections needed to cancel "tadpole" diagrams, we have concluded that reliable results may be obtained through standard S–matrix methods at second order in the gravitational wave amplitude. Our calculations revealed two essential differences between the field and string theory results. The pair production of identical string states is suppressed for certain pairs of excitation numbers of the outgoing strings; most significantly, the production of identical string states vanishes in the infinite wavelength limit. In addition, the overall production of strings is suppressed relative to point–particle results, which may be viewed as a consequence of the mild hard scattering behavior of string amplitudes.

Our results are especially relevant to questions regarding the pair production of strings in cosmological spacetimes. In particular, these results may have implications for one motivation for the current work, in which the pair production of strings is studied using an effective field theory approximation [47, 60]. The suppression of production of excited string states suggests that, despite the exponentially growing Hagedorn density of states, effective field theory provides an overestimate of the production of individual string states.

Of course, we have established these results using techniques that are reliable only when spacetime is nearly Minkowski. Nevertheless, our findings suggest phenomena

that may also be present in the strong field regime. It would be quite interesting to know if these effects persist in more highly curved, time–dependent backgrounds. If so, it would be an example of a uniquely "stringy" signature of relevance to cosmology, providing further clues to the role of quantum gravity in the early universe.

Chapter 7

Conclusions

How soon hath thy prediction, seer blest,
Measured this transient world, the race of time
Till time stand fixed: beyond is all abyss,
Eternity, whose end no eye can reach.

Paradise Lost Book XII, lines 552–556, [90]

Returning to the questions posed in the Introduction, it appears that string theory gives cosmological model–builders a host of new tools, as well as new problems. Both the classical and quantum dynamics of these models are quite nontrivial.

In the classical regime, we have seen that embedding a cosmological model in a string theory enables one to construct a viable cyclic universe model, with unique (and observable) predictions. On the other hand, one must confront the problem of chaos near a big crunch. In a sense, this originates from the fact that string models include many degrees of freedom. These new degrees of freedom can be a boon to those searching for an embedding of the Standard Model in string theory. However, this multiplicity of degrees of freedom can present problems cosmologically. Normally one assumes that many of the degrees of freedom are "frozen" to simplify the analysis of string compactifications. We have seen that not only can this assumption be violated

in cosmological settings, but that these neglected degrees of freedom can dominate the universe and lead to chaotic dynamics, destroying the homogeneity and isotropy of the universe.

We have presented two mechanisms by which this chaotic behavior can be avoided. One involves including a matter field with ultra–stiff equation of state $w > 1$. It appears that matter of this type is already required in the cyclic model in order to generate a scale–invariant spectrum of density fluctuations. We also showed that the topology of spacetime can affect the emergence of chaos. This is interesting from a model–building perspective, since the same invariants that relate to the appearance of chaos also relate to some features of the four–dimensional, low–energy effective field theory. In cyclic universes that avoid chaos by this mechanism, these new constraints may help to select preferred string compactifications.

In the quantum regime we have found that there are some important differences between point particle and string pair production, an essential process in all cosmological models. Our results are not directly applicable to cosmological situations as yet: there are a great number of technical obstacles that must be surmounted before this phenomenon can be investigated in the strongly curved backgrounds relevant for cosmology. However, we have shown that in one well–defined spacetime, the spectrum of created strings and point particles differs significantly. If these effects persist into the strong–field regime, it might be possible to find stringy "signatures" in the primordial perturbation spectrum, potentially providing an experimental means to probe quantum gravity through the early universe.

Let us descend now therefore from this top
Of speculation; for the hour precise
Exacts our parting hence...

Paradise Lost Book XII, lines 588–590, [90]

Appendix A

The Bianchi-IX "Mixmaster" Universe

The Mixmaster universe provides a useful example of gravitational chaos. We show how the dynamics of this (exact) solution to general relativity can be reduced to the motion of a point in a potential. This is a great simplification, but as we might expect in a chaotic system, the equations of motion are not integrable. We go on to develop the billiard approach for the Mixmaster model, and derive explicitly the connection between the Mixmaster universe and the overextended affine Lie algebra AE_3.

The Mixmaster universe is based on the Bianchi–IX model. The spatial sections of the universe are therefore homogeneous, though we allow anisotropic evolution. The metric is

$$\mathrm{d}s^2 = -N^2\,\mathrm{d}t^2 + \sum_j \exp\left(2\gamma_j\right)\sigma_j^2 \tag{A.1}$$

where the lapse N and the functions γ_j depend on the coordinate time t only. The

one–forms σ^j are given by

$$\sigma^1 = \cos\psi \, \mathrm{d}\theta + \sin\psi \sin\theta \, \mathrm{d}\phi, \tag{A.2a}$$

$$\sigma^2 = \sin\psi \, \mathrm{d}\theta - \cos\psi \sin\theta \, \mathrm{d}\phi, \tag{A.2b}$$

$$\sigma^3 = \mathrm{d}\psi + \cos\theta \, \mathrm{d}\phi. \tag{A.2c}$$

These enjoy the useful property

$$\mathrm{d}\sigma^j = \frac{1}{2}\epsilon_{jmn} \, \sigma^m \wedge \sigma^n. \tag{A.3}$$

This is reminiscent of the commutation relations for the generators of SU(2). This group manifold is topologically equivalent to the sphere $\mathbf{S}^3$, identical to that of our spatial sections. We are thus modeling each spatial slice as this group manifold. A natural choice for the vierbeins is thus

$$e^t = N \, \mathrm{d}t, \tag{A.4a}$$

$$e^j = \exp(\gamma_j) \, \sigma_j. \tag{A.4b}$$

We will follow the convention that letters $a, b, c \ldots$ are used to denote both timelike and spacelike indices, while $j, k, l \ldots$ are used for spacelike indices only.

A.1 Einstein equations and effective action

The first Mauer–Cartan structure equation

$$\mathrm{d}e^a = \omega^a{}_b \wedge e^b \tag{A.5}$$

is used to find the spin connection $\omega^a{}_b$. To this end one computes

$$\mathrm{d}e^j = \frac{\dot{\gamma}_j}{N} \, e^t \wedge e^j + \frac{1}{2}\epsilon_{jnm} \left[\begin{smallmatrix} +1 & -1 & -1 \\ j & n & m \end{smallmatrix} \right] \, e^n \wedge e^m \tag{A.6}$$

where " $\dot{}$ " indicates derivatives with respect to the coordinate time t, and we have introduced the compact notation

$$\left[\begin{smallmatrix} A & B & C \\ a & b & c \end{smallmatrix}\right] = \exp\left(A\gamma_a + B\gamma_b + C\gamma_c\right) \tag{A.7}$$

since these exponential factors are quite common in the following expressions. The equation (A.5) is solved for the spin connection to yield

$$\omega_{jt} = \frac{\dot{\gamma}_j}{N}\, e^j, \tag{A.8a}$$

$$\omega_{jk} = \frac{1}{2}\left(\left[\begin{smallmatrix} +1 & -1 & -1 \\ j & k & c \end{smallmatrix}\right] + \left[\begin{smallmatrix} -1 & +1 & -1 \\ j & k & c \end{smallmatrix}\right] - \left[\begin{smallmatrix} -1 & -1 & +1 \\ j & k & c \end{smallmatrix}\right]\right) \epsilon_{jkc}\, e^c. \tag{A.8b}$$

These are the only nonvanishing components of the spin connection.

The second of the Mauer–Cartan equations gives the curvature form $\theta^a{}_b$ through

$$\theta^a{}_b = \mathrm{d}\omega^a{}_b + \omega^a{}_c \wedge \omega^c{}_b \tag{A.9}$$

which in turn yields the Riemann tensor through the relation

$$\theta^a{}_b = \frac{1}{2} R^a{}_{bcd}\, e^c \wedge e^d \tag{A.10}$$

Once the Ricci tensor is calculated, we impose the Einstein equations in vacuum by requiring

$$R_{ab} = R_{\mu\nu} = 0 \tag{A.11}$$

This step of the calculation is somewhat more involved, and we will go through the arguments below.

We begin by calculating $\theta^t{}_j$. Applying the second Mauer–Cartan equation one finds

$$\theta^t{}_j = \frac{1}{N^2}\left(\ddot{\gamma}_j + \dot{\gamma}_j^2 - \frac{\dot{N}}{N}\dot{\gamma}_j\right) e^t \wedge e^j + \cdots \tag{A.12}$$

where $\cdots$ represent terms which vanish upon contraction to form the Ricci tensor. This is the only contribution to $R^t{}_t$, and therefore we find

$$R^t{}_t = \frac{1}{N^2}\sum_j \left(\ddot{\gamma}_j + \dot{\gamma}_j^2 - \frac{\dot{N}}{N}\dot{\gamma}_j\right) \tag{A.13}$$

The equations of motion in vacuum (Einstein equations) imply that $R^t{}_t = 0$.

Next we turn to $\theta^j{}_k$. Straightforwardly applying the second Mauer–Cartan equation (A.9) leads to a large number of terms, however many of them will not contribute to the Ricci tensor, and we will drop them here. Equation (A.9) implies

$$\theta^j{}_k = \underbrace{\mathrm{d}\omega_{jk}}_{a} + \underbrace{\omega_{jl} \wedge \omega_{lk}}_{b} + \underbrace{\omega_{jt} \wedge \omega_{kt}}_{c} \tag{A.14}$$

We will go through each term in detail. From term (a) one can neglect the time derivatives since these lead to terms of the form $e^t \wedge e^c$, with $c \neq j, k$, which vanish upon contraction. One does obtain the term

$$(a) = \frac{1}{4}\left(+\left[\begin{smallmatrix}-1\\ j\end{smallmatrix}\begin{smallmatrix}+1\\ k\end{smallmatrix}\begin{smallmatrix}-1\\ c\end{smallmatrix}\right] + \left[\begin{smallmatrix}+1\\ j\end{smallmatrix}\begin{smallmatrix}-1\\ k\end{smallmatrix}\begin{smallmatrix}-1\\ c\end{smallmatrix}\right] - \left[\begin{smallmatrix}-1\\ j\end{smallmatrix}\begin{smallmatrix}-1\\ k\end{smallmatrix}\begin{smallmatrix}+1\\ c\end{smallmatrix}\right]\right)\left[\begin{smallmatrix}-1\\ m\end{smallmatrix}\begin{smallmatrix}-1\\ n\end{smallmatrix}\begin{smallmatrix}+1\\ c\end{smallmatrix}\right]\epsilon_{jkc}\epsilon_{cmn}\, e^m \wedge e^n \tag{A.15}$$

Using the properties of the ϵ tensor, one can replace

$$\epsilon_{jkc}\epsilon_{cmn} \to 2\delta_{jm}\delta_{kn} \tag{A.16}$$

and therefore

$$(a) = \frac{1}{4}\left(2\left[\begin{smallmatrix}-2\\ j\end{smallmatrix}\begin{smallmatrix}0\\ k\end{smallmatrix}\begin{smallmatrix}0\\ c\end{smallmatrix}\right] + 2\left[\begin{smallmatrix}0\\ j\end{smallmatrix}\begin{smallmatrix}-2\\ k\end{smallmatrix}\begin{smallmatrix}0\\ c\end{smallmatrix}\right] - 2\left[\begin{smallmatrix}-2\\ j\end{smallmatrix}\begin{smallmatrix}-2\\ k\end{smallmatrix}\begin{smallmatrix}2\\ c\end{smallmatrix}\right]\right)\, e^j \wedge e^k \tag{A.17}$$

The next term of interest is (b). One finds an expression similar to that of (a), and upon applying the identity

$$\epsilon_{jrc}\epsilon_{rkd}\, e^c \wedge e^d = \delta_{ck}\delta_{dj} \tag{A.18}$$

one finds

$$(b) = \frac{1}{4}\left(-2\left[\begin{smallmatrix}0\\ j\end{smallmatrix}\begin{smallmatrix}-2\\ k\end{smallmatrix}\begin{smallmatrix}0\\ c\end{smallmatrix}\right] + \left[\begin{smallmatrix}2\\ j\end{smallmatrix}\begin{smallmatrix}-2\\ k\end{smallmatrix}\begin{smallmatrix}-2\\ c\end{smallmatrix}\right] - \left[\begin{smallmatrix}-2\\ j\end{smallmatrix}\begin{smallmatrix}2\\ k\end{smallmatrix}\begin{smallmatrix}-2\\ c\end{smallmatrix}\right] + \left[\begin{smallmatrix}-2\\ j\end{smallmatrix}\begin{smallmatrix}-2\\ k\end{smallmatrix}\begin{smallmatrix}2\\ c\end{smallmatrix}\right]\right)\, e^j \wedge e^k \tag{A.19}$$

Combining (a) and (b) we find

$$(a) + (b) = \frac{1}{4}\left(2\left[\begin{smallmatrix}-2\\ j\end{smallmatrix}\begin{smallmatrix}0\\ k\end{smallmatrix}\begin{smallmatrix}0\\ c\end{smallmatrix}\right] + \left[\begin{smallmatrix}2\\ j\end{smallmatrix}\begin{smallmatrix}-2\\ k\end{smallmatrix}\begin{smallmatrix}-2\\ c\end{smallmatrix}\right] - \left[\begin{smallmatrix}-2\\ j\end{smallmatrix}\begin{smallmatrix}2\\ k\end{smallmatrix}\begin{smallmatrix}-2\\ c\end{smallmatrix}\right] - \left[\begin{smallmatrix}-2\\ j\end{smallmatrix}\begin{smallmatrix}-2\\ k\end{smallmatrix}\begin{smallmatrix}2\\ c\end{smallmatrix}\right]\right)\, e^j \wedge e^k \tag{A.20}$$

The final term (c) is simply

$$(c) = \frac{\dot\gamma_j \dot\gamma_k}{N^2}\, e^j \wedge e^k \tag{A.21}$$

These three terms are the only ones that contribute to the Ricci tensor. Upon contracting one finds

$$R^j{}_j = \frac{1}{N^2}\left(\ddot\gamma_j + \dot\gamma_j\left[-\frac{\dot N}{N} + \sum_k \dot\gamma_k\right]\right) \tag{A.22}$$

$$+ \left[\begin{smallmatrix} -2 & 0 & 0 \\ j & k & c \end{smallmatrix}\right] + \frac{1}{2}\left(\left[\begin{smallmatrix} 2 & -2 & -2 \\ j & k & c \end{smallmatrix}\right] - \left[\begin{smallmatrix} -2 & 2 & -2 \\ j & k & c \end{smallmatrix}\right] - \left[\begin{smallmatrix} -2 & -2 & 2 \\ j & k & c \end{smallmatrix}\right]\right) \tag{A.23}$$

where the triplet $\{jkc\}$ is understood to be some permutation of (123), and no sum is implied by repeated j indices. Again, the equations of motion imply that $R^j{}_j = 0$.

The equations of motion for the γ_j, (A.13) and (A.22), are precisely those found by variations of the action

$$S_{eff}[\gamma] = \int e^{\sum_m \gamma_m}\left(\frac{1}{2N^2} G_{jk}\dot\gamma^j\dot\gamma^k - U(\gamma)\right) N\, dt \tag{A.24}$$

where we have written the γ^j with raised indices for later convenience, and also defined the potential

$$U(\gamma) = \frac{1}{2}\left(\left[\begin{smallmatrix} 2 & -2 & -2 \\ j & k & c \end{smallmatrix}\right]\left[\begin{smallmatrix} -2 & 2 & -2 \\ j & k & c \end{smallmatrix}\right]\left[\begin{smallmatrix} -2 & -2 & 2 \\ j & k & c \end{smallmatrix}\right]\right) - \left[\begin{smallmatrix} -2 & 0 & 0 \\ j & k & c \end{smallmatrix}\right] - \left[\begin{smallmatrix} 0 & -2 & 0 \\ j & k & c \end{smallmatrix}\right] - \left[\begin{smallmatrix} 0 & 0 & -2 \\ j & k & c \end{smallmatrix}\right] \tag{A.25}$$

as well as the metric (or, properly speaking, the supermetric)

$$G_{jk} = 2\begin{pmatrix} 0 & -1 & -1 \\ -1 & 0 & -1 \\ -1 & -1 & 0 \end{pmatrix}, \qquad \text{and} \qquad G^{jk} = \frac{1}{4}\begin{pmatrix} +1 & -1 & -1 \\ -1 & +1 & -1 \\ -1 & -1 & +1 \end{pmatrix} \tag{A.26}$$

This metric has eigenvalues $(-4, 2, 2)$ and is therefore of Lorentzian signature. Consequently, the action (A.24) encodes the dynamics of a $(3+1)$–dimensional universe in the motion of a point particle, under forces, in a $(2+1)$–dimensional auxiliary Lorentzian spacetime. The mass–shell condition for the particle is found by variation of (A.24) with respect to N, yielding

$$\frac{1}{2N^2} G_{jk}\dot\gamma^j\dot\gamma^k + U(\gamma) = 0, \tag{A.27}$$

J	A_J	$(\gamma_1, \gamma_2, \gamma_3)$	$(\beta_1, \beta_2, \beta_3)$	(β_+, β_-)
-1	-1	$(-2, 0, 0)$	(-2/3)(+2,-1,-1)	$+\sqrt{2/3}(+\sqrt{3}, +1)$
-2	-1	$(0, -2, 0)$	(-2/3)(-1,+2,-1)	$+\sqrt{2/3}(-\sqrt{3}, +1)$
-3	-1	$(0, 0, -2)$	(-2/3)(-1,-1,+2)	$+\sqrt{2/3}(0, -2)$
$+1$	$1/2$	$(+2, -2, -2)$	(+4/3)(+2,-1,-1)	$-\sqrt{8/3}(+\sqrt{3}, +1)$
$+2$	$1/2$	$(-2, +2, -2)$	(+4/3)(-1,+2,-1)	$-\sqrt{8/3}(-\sqrt{3}, +1)$
$+3$	$1/2$	$(-2, -2, +2)$	(+4/3)(-1,-1,+2)	$-\sqrt{8/3}(0, -2)$

Table A.1: Table of exponential walls and their amplitudes appearing in the Mixmaster universe. These quantities are defined in (A.28).

which is roughly the analogue of the Friedmann equation, an idea we develop in the next section. The potential is a sum of exponential "walls," for

$$U(\gamma) = \sum_J A_J \exp\left([w_J]_j \gamma^j\right) \tag{A.28}$$

where the various amplitudes A_J and wall vectors w_J are summarized in A.1.

A.2 The β–parameterization

Here we discuss a parameterization of the degrees of freedom in (A.24) that reveals a useful connection to the FRW universe. It is also more closely related to the parameterization used by Misner [91]. Instead of the three γ^j, define a variable a and three β_j, defined by

$$\gamma^j = \log(a) + \beta_j \tag{A.29}$$

where we relax the superscript on the β_j. To ensure a unique definition of a, we enforce the constraint

$$\sum_j \beta_j = 0. \tag{A.30}$$

With this constraint, the volume of the spatial sections is a^3, and therefore a is the effective FRW scale factor for the Mixmaster universe.

Since only two of the β_j are independent, we will parameterize them in terms of two variables, β_+ and β_-. These are defined by

$$\beta_+ = \frac{1}{\sqrt{2}}\left(-\beta_1 + \beta_2\right) \tag{A.31a}$$

$$\beta_- = \frac{1}{\sqrt{6}}\left(-\beta_1 - \beta_2 + 2\beta_3\right) \tag{A.31b}$$

with inverse transformations

$$\beta_1 = -\frac{\beta_+}{\sqrt{2}} - \frac{\beta_-}{\sqrt{6}} \tag{A.32a}$$

$$\beta_2 = +\frac{\beta_+}{\sqrt{2}} - \frac{\beta_-}{\sqrt{6}} \tag{A.32b}$$

$$\beta_3 = \frac{2\beta_-}{\sqrt{6}} \tag{A.32c}$$

When one chooses to examine the system in physical time ($N = 1$) the energy condition (A.27) reads

$$3\left(\frac{\dot{a}}{a}\right)^2 = \frac{1}{2}\left(\dot{\beta}_+^2 + \dot{\beta}_-^2\right) + \frac{\tilde{U}(\beta)}{2a^2} \tag{A.33}$$

where $\tilde{U}(\beta)/a^2 = U(\gamma)$, all that has been done is to factor out the dependence on a. This potential is illustrated in Figure A.1. The associated wall forms after this factoring are given in Table A.1. Note that, when the $\dot{\beta} = 0$, corresponding to the isotropic case, then we recover precisely the Friedmann equation (2.2). Since $\tilde{U}(\beta = 0) < 0$, we also recover the correct sign for the curvature term. The equations of motion for the $\beta_\pm$ variables are

$$\ddot{\beta}_\pm + 3\frac{\dot{a}}{a}\dot{\beta}_\pm + \frac{1}{2a^2}\frac{\partial \tilde{U}}{\partial \beta_\pm} = 0 \tag{A.34}$$

and therefore the $\beta_\pm$ move in a potential well with blueshifting. This potential also grows stronger as the big crunch is approached, and the scale factor $a \to 0$.

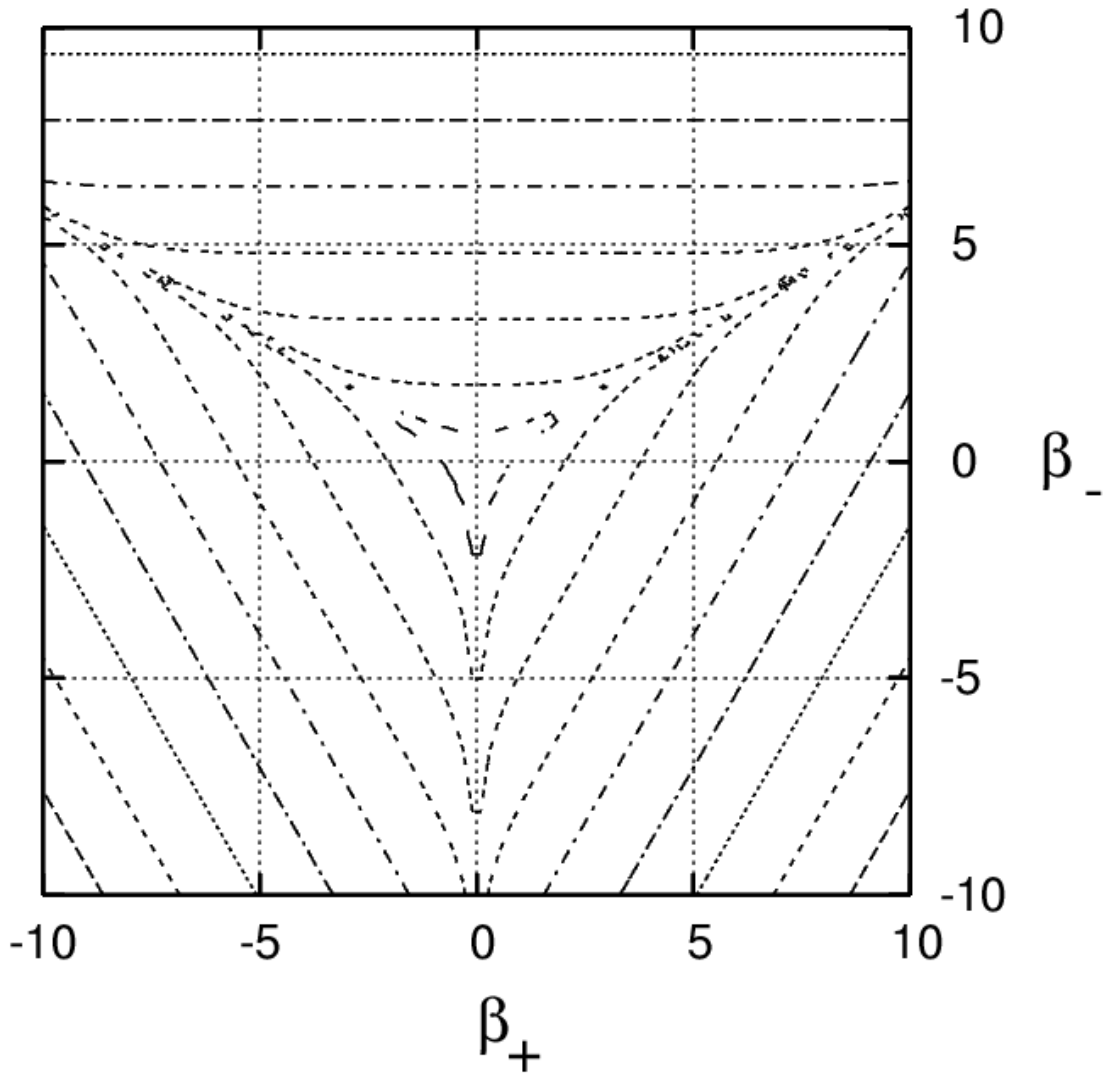

Figure A.1: The potential $\tilde{U}$. on the (β_+, β_-) plane. Contours are plotted logarithmically: thus each contour is at a level higher than the last by a factor of e. Near the origin, $\tilde{U} < 0$, which forbids isotropic contraction. All of the contours shown are positive, and the potential asymptotes to zero along the three "troughs" radiating from the origin. When the point moves along these troughs, the Mixmaster universe is near the Milne solution of the Kasner conditions.

A.3 The γ–parameterization

We now use another parameterization of the degrees of freedom. This parameterization is most useful very near the big crunch, where the dynamics of the universe reduces to a "billiard" moving on a hyperboloid, undergoing specular reflections from a set of sharp walls. The remarkable feature of this wall system is that is is defined by the root lattice of a Kac–Moody algebra, a connection which exists in pure gravity in all dimensions and is common to other models including gravity.

In this parameterization, we keep the γ_j as defined in the action (A.24) and perform some additional reparameterizations. First we define new coordinates $\{r, y^j\}$ as follows

$$r^2 = -G_{jk}\gamma^j\gamma^k, \qquad y^j = \frac{\gamma^j}{r} \tag{A.35}$$

and then note that

$$G_{jk}y^j y^k = -1 \tag{A.36}$$

Thus, the coordinates $\{y^j\}$ run over the future unit hyperboloid. Next we fix the gauge and choose a new time coordinate T by

$$N = \exp\left(\sum_j \gamma_j\right), \qquad dT = \frac{dt}{r^2} \tag{A.37}$$

With these redefinitions, the action (A.24) becomes

$$S_{eff}[r, y^j] = \int \left(-\frac{1}{2}\left[\frac{d\ln r}{dT}\right]^2 + \frac{1}{2}G_{jk}\frac{dy^j}{dT}\frac{dy^k}{dT} - V_T(r, y^j)\right) dT \tag{A.38}$$

where the new potential V_T is defined by

$$V_T(r, y^j) = r^2 \exp\left(2\sum_j \gamma^j\right) U(\gamma) \tag{A.39}$$

A remarkable feature of this potential comes from the fact that $U(\gamma)$ is a sum of exponentials whose arguments are linear in the γ^j. This means that

$$V_T = \sum_A r^2 C_A \exp\left[2r w_A(y)\right] \tag{A.40}$$

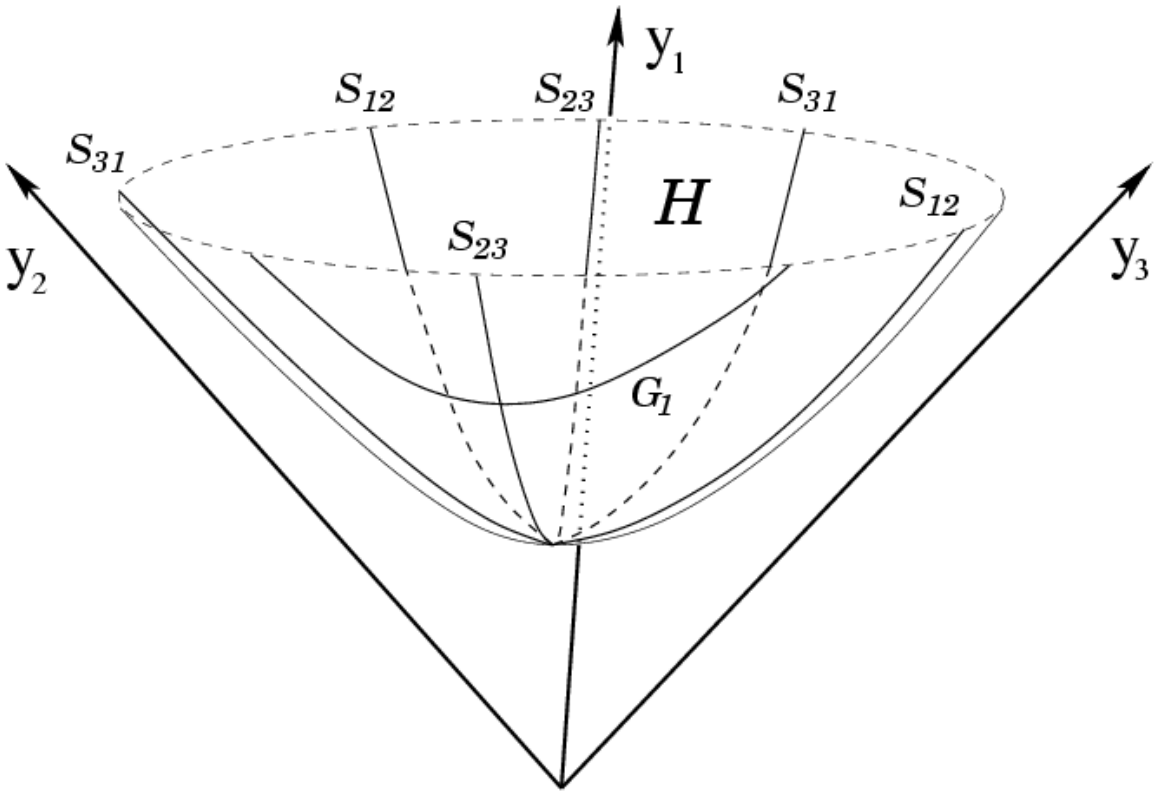

Figure A.2: The structure of the sharp walls appearing near the big crunch. The billiard moves on the unit hyperboloid H and reflects from the sharp walls denoted by the heavy lines. The symmetry walls S_{jk} result from the interchange of $y_j \leftrightarrow y_k$. They serve to "mod out" the discrete symmetries of the problem. A single gravitational wall G_1 is shown, corresponding to the stability condition mentioned in the text. The additional walls G_2 and G_3 are suppressed for clarity.

where the sum is over all wall forms, indexed by A. But one can see that

$$\lim_{x\to\infty}\left[x^2\exp\left(xy\right)\right] = \Theta(y) = \begin{cases}\infty, & \text{when} \quad y > 0,\\ 0, & \text{when} \quad y < 0.\end{cases} \tag{A.41}$$

and therefore as we approach the big crunch the walls become perfectly sharp. Therefore, the dynamics on the system is that of a billiard ball moving on a hyperboloid with sharp walls. The geometry of this system is illustrated in Figure A.2.

Because of the symmetry of the system, we can make it somewhat less degenerate. We can fix the symmetry by imposing the condition $y_3 > y_2 > y_1$, which corresponds

to adding two walls to the system:

$$[w_{32}]_j = (0, -1, 1,), \qquad [w_{21}]_j = (-1, 1, 0) \tag{A.42}$$

Finally, some walls are hidden behind other walls and can be removed without loss of generality from the wall system. The only relevant wall in this case is

$$[w_1]_j = (2, 0, 0) \tag{A.43}$$

Define the inner product matrix A_{IJ} of these forms as follows

$$A_{IJ} = G^{jk}[w_I]_j[w_J]_k \tag{A.44}$$

Taking the inner product of these walls using the metric (A.26), we find

$$A_{IJ} = 2\begin{pmatrix} 2 & -1 & 0 \\ -1 & 2 & -2 \\ 0 & -1 & 2 \end{pmatrix} \tag{A.45}$$

Remarkably, this is the Cartan matrix of the strictly hyperbolic Kac–Moody algebra AE_3. Thus these walls are precisely the simple roots of AE_3. The connection between Kac–Moody algebras and Mixmaster dynamics is explored in more depth in Chapter 5.

Appendix B

Virial Theorem for p–forms

Below, we treat the case of a general p–form field with coupling to the dilaton ϕ, in a collapsing universe. We concern ourselves with the case where spacetime is isotropic, as this is the cosmologically relevant situation after compactification. We show that far from the big crunch, the energy density in massive fields evolves like that of a pressureless fluid, $\rho \sim 1/(\text{comoving volume})$. We will first recast the p–form dynamics in Hamiltonian form. This allows us to apply the virial theorem and stress energy conservation to obtain the scaling in energy density far from the crunch. The p–form action with mass term and dilaton coupling is

$$S = -\frac{1}{(p+1)!}\int \left(\mathrm{d}A\cdot\mathrm{d}A + m^2 A\cdot A\right) e^{\lambda\phi}\sqrt{-G}\, d^D x, \tag{B.1}$$

where we have fixed the coordinate gauge so that

$$\mathrm{d}s^2 = -n^2\mathrm{d}t^2 + h_{jk}\mathrm{d}x^j\mathrm{d}x^k. \tag{B.2}$$

We choose the canonical coordinates to be the gauge potential $A_{\alpha_1\ldots\alpha_p}$. The corresponding canonical momenta are

$$\Pi^{j_1\ldots j_p} = -F^{tj_1\ldots j_p} n e^{\lambda\phi}\sqrt{h} \tag{B.3}$$

where $h = \det h_{ij}$. Passing to the Hamiltonian, we find

$$H = \frac{1}{2}\int \tilde{n}\big(\Pi\cdot\Pi + he^{2\lambda\phi}F^{(B)}\cdot F^{(B)} + he^{2\lambda\phi}m^2 A\cdot A - he^{2\lambda\phi}A_{t\alpha_2\ldots\alpha_p}\partial_a\Pi^{a\alpha_2\ldots\alpha_p}\big)\, d^{D-1}x \quad \text{(B.4)}$$

where we use a rescaled lapse function $\tilde{n} = ne^{-\lambda\phi}/\sqrt{h}$, and denote the magnetic components of F_p by $F^{(B)}$. Dot products are taken with respect to the metric h_{ij}. The last term in the integral shows that the "electric" gauge field modes $A_{tj_2\ldots j_{p-1}}$ appear as Lagrange multipliers necessary to enforce the Gauss's law constraint, but are otherwise nondynamical [36]. We will choose the Coloumb gauge, in which $A_{tj_2\ldots j_p} = 0$, and drop this constraint term from now on.

The Hamiltonian is in fact exactly that of a set of simple harmonic oscillators. After decomposing the functions A_p in an appropriate orthonormal set of Fourier components, different Fourier modes decouple and the Hamiltonian is quadratic in Π and A. The electric field modes appear as the kinetic terms, and the magnetic field and mass terms correspond to the potential of the oscillators. The oscillator potential is time dependent, both due to the appearance of $e^{2\lambda\phi}h$ and individual metric components in the magnetic and mass terms.

We are primarily interested in the dynamics of the p–form far from the big crunch. In this regime, we may view the changing scale factors as slowly varying parameters in our Hamiltonian. They will change the spring constants on a timescale given by t, the proper time to the big crunch. The dynamical timescale (typical period) for the oscillator Hamiltonian is given by the mass term. Thus, we expect that the fractional change in the fundamental angular frequency ω of the oscillator system over a typical cycle will be

$$\frac{\delta\omega}{\omega} \sim \frac{1}{\omega t} \quad \text{(B.5)}$$

Provided we are at a time $t \gg \omega^{-1}$, we will be in the adiabatic regime, and we may

take the oscillation frequencies to be constants. This corresponds to the $m/H \gg 1$ regime that concerns us.

To find how the energy density scales with time, we apply the virial theorem and stress energy conservation. The adiabatic condition (B.5) implies that we may neglect the time variation of the metric and dilaton over a single cycle. For our Hamiltonian, the virial theorem then implies that the time average $\langle\cdot\rangle$ of the potential energy is equal to that of the kinetic energy, or

$$\langle \Pi \cdot \Pi \rangle = e^{2\lambda\phi}\gamma\langle F^{(B)} \cdot F^{(B)} + m^2 A \cdot A\rangle. \tag{B.6}$$

In the virialized system, there are two possible regimes, corresponding to either the $F^{(B)} \cdot F^{(B)}$ term or the $m^2 A \cdot A$ term dominating. We will consider both of these cases in turn.

The stress energy for the p–form field is

$$T_\mu{}^\nu = \frac{e^{\lambda\phi}}{(p+1)!}\Bigg[(p+1)F_{\mu\alpha_2\ldots\alpha_p}F^{\nu\alpha_2\ldots\alpha_p} - \frac{1}{2}\delta_\mu{}^\nu F^2 + pm^2 A_{\mu\alpha_2\ldots\alpha_{p-1}}A^{\nu\alpha_2\ldots\alpha_{p-1}} - \frac{m^2}{2}\delta_\mu{}^\nu A^2\Bigg] \tag{B.7}$$

We will find it convenient to break the stress energy into three parts

$$T_\mu{}^\nu = T^{(E)}{}_\mu{}^\nu + T^{(B)}{}_\mu{}^\nu + T^{(m)}{}_\mu{}^\nu \tag{B.8}$$

corresponding to the energy in electric modes, magnetic modes, and the mass term. It is sufficient to consider a single component of F_p, since different components will be uncorrelated and therefore will have vanishing time average. The electric modes give rise to a contribution

$$T^{(E)}{}_\mu{}^\nu = \delta_\mu{}^\nu \frac{e^{\lambda\phi}}{2(p+1)!}|F^2_{(E)}| \times \begin{cases} -1 & \text{if } F^{(E)} \text{ has index } \mu, \\ +1 & \text{otherwise.} \end{cases} \tag{B.9}$$

while the magnetic modes give

$$T^{(B)}{}_{\mu}{}^{\nu} = \delta_{\mu}{}^{\nu}\frac{e^{\lambda\phi}}{2(p+1)!}F^2_{(B)} \times \begin{cases} +1 & \text{if } F^{(B)} \text{ has index } \mu, \\ -1 & \text{otherwise.} \end{cases} \tag{B.10}$$

and the mass term yields

$$T^{(m)}{}_{\mu}{}^{\nu} = \delta_{\mu}{}^{\nu}\frac{e^{\lambda\phi}}{2(p+1)!}m^2A^2 \times \begin{cases} +1 & \text{if } A \text{ has index } \mu, \\ -1 & \text{otherwise.} \end{cases} \tag{B.11}$$

Note that $F^{(B)}$ cannot have any timelike indices, nor can A thanks to our gauge choice. Thus the contributions to the energy density $\rho = -T_0{}^0$ are all positive.

First, we consider the case where the mass term dominates in the virial relationship (B.6). This corresponds to inhomogeneities in the p–form field being negligible. The virial result implies that $\langle|F^2_{(E)}|\rangle = m^2\langle A^2\rangle$. Due to our gauge choice, A and $F^{(E)}$ have the same combination of p spatial indices, and therefore contributions to the pressure components $T_j{}^j$ coming from $T^{(E)}{}_j{}^j$ and $T^{(m)}{}_j{}^j$ exactly cancel. The vanishing pressure reveals that the effective equation of state is that of dust, $w = 0$.

When the magnetic terms dominate the virial result (B.6), we obtain a slightly different effective equation of state. Here it is necessary to average over polarizations of F_p, since unlike $F^{(E)}$ and A, $F^{(E)}$ and $F^{(B)}$ do not enjoy any relationships between their indices. Regardless of polarization, the sum of stress energy tensors $T^{(E)}$ and $T^{(B)}$ has vanishing trace. This, combined with isotropy, implies the pressure components are given by

$$T_j{}^j = -\frac{T_0{}^0}{d}. \tag{B.12}$$

This corresponds to the equation of state of radiation, which in four dimensional spacetime is $w = 1/3$.

Physically, this result may be understood in simple terms. Far from the big crunch, the contraction of space is very slow in comparison to the mass of the p–form field.

Thus, the corresponding particles are far from being relativistic, and behave as a dust of approximately comoving mass points. Their energy density therefore scales in inverse proportion to the comoving volume. The case where magnetic components dominate the virial relationship corresponds to a relativistic gas of particles. This yields the equation of state of radiation, as we expect.

Appendix C

Kaluza–Klein Reduction with Vectors

In this appendix we consider the general Kaluza–Klein reduction of Einstein gravity with an arbitrary number of extra dimensions. We focus on the gravitational degrees of freedom, and are primarily concerned with computing the effective masses of all Kaluza–Klein vector fields We will find that these masses are zero only when $\mathcal{M}$ possesses Killing vectors. This calculation parallels standard treatments of Kaluza–Klein reduction [40], but in these treatments the fact that $\mathcal{M}$ may not possess isometries is often not emphasized. For $n > 1$ extra dimensions, we will generalize the decomposition given in (4.37) using the vielbein formalism. We begin by defining one form fields $e^A = e_M{}^A \mathrm{d}x^M$ so that,

$$ds^2 = e^A e^B \eta_{AB}, \tag{C.1}$$

with η_{AB} the $(4+n)$–dimensional Minkowski metric. The ${e_M}^A$ are chosen so that

$$h_{\mu\nu} = {e_\mu}^\alpha {e_\nu}^\beta \eta_{\alpha\beta}, \tag{C.2a}$$

$$f_{mn} = {e_m}^a {e_n}^b \delta_{ab}, \tag{C.2b}$$

$${e_\mu}^a = K^{aj}(x^m) A^j_\mu(x^\mu), \tag{C.2c}$$

$${e_m}^\alpha = 0, \tag{C.2d}$$

where δ_{ab} the Euclidean flat space metric. The K^{aj} are a basis for vector fields on $\mathcal{M}$, indexed by j, that depend only on the compact coordinates x^m. The coefficients in this expansion are the A^j_μ, which depend only the noncompact coordinates x^μ. The A^j_μ, known as Kaluza–Klein vectors, will emerge after compactification as vector fields on the noncompact space Σ. The commutators of the K^{aj} define a set of structure constants ${f^{jk}}_l$

$$[K^j, K^k] = {f^{jk}}_l K^l. \tag{C.3}$$

The calculation is most conveniently carried out using an orthonormal basis $\{\hat{e}^a, \hat{e}^\alpha\}$ given by

$$\hat{e}^\alpha = e^\alpha \qquad \hat{e}^a = e^a - K^{aj} A^j_\mu \mathrm{d}x^\mu, \tag{C.4}$$

in which the line element assumes the simple form $ds^2 = \hat{e}^\alpha \hat{e}^\beta \eta_{\alpha\beta} + \hat{e}^a \hat{e}^b \delta_{ab}$. In the event that some of the K^{aj} are Killing fields on $\mathcal{M}$, then the lower dimensional theory will possess a gauge symmetry. The Killing fields are generators of the isometry group of $\mathcal{M}$, and this isometry group reemerges as the gauge group in the lower dimensional theory. This motivates the definition of a "field strength" $F^i_{\mu\nu}$ as

$$F^i = \mathrm{d}A^i + \frac{1}{2} f^{ijk} A^j \wedge A^k. \tag{C.5}$$

In the general case, the Killing fields alone do not provide a full basis for vector fields on $\mathcal{M}$. Thus, in addition to the massless modes (if any) of the gauge theory, there will also be an infinite set of massive gauge fields in the lower dimensional theory.

In order to derive the mass spectrum in the lower dimension explicitly, we may use the vielbeins to decompose the gravitational action in $4+n$ dimensions. The spin connections are

$$\hat{\omega}_{ab} = \omega_{ab} - \frac{1}{2}(\nabla_b K^j_a - \nabla_a K^j_b) A^j_\beta e^\beta, \tag{C.6a}$$

$$\hat{\omega}_{a\beta} = \frac{1}{2} K^j_a F^j_{\alpha\beta} e^\alpha + \nabla_{(b} K^j_{a)} A^j_\beta \hat{e}^\beta, \tag{C.6b}$$

$$\hat{\omega}_{\alpha\beta} = \omega_{\alpha\beta} + \frac{1}{2} K^j_b F^j_{\alpha\beta} \hat{e}^b, \tag{C.6c}$$

where ω_{ab} and $\omega_{\alpha\beta}$ are the spin connections defined by the metrics f_{mn} on $\mathcal{M}$, and $h_{\mu\nu}$ on Σ, respectively. Using these spin connections to compute the Ricci scalar, one obtains

$$R(G) = R(h) + R(f) - \frac{1}{4} K^j_a K^{ka} F^j_{\mu\nu} F^{k\mu\nu} - 2\nabla_{(c} K^j_{d)} \nabla^{(c} K^{kd)} A^{j\mu} A^k_\mu. \tag{C.7}$$

We see that a mass term for the A^j has appeared. Upon integrating over the compact coordinates, one arrives at the Jordan frame action

$$S = \int \left(W(f) R(h) - S(f) - \frac{1}{4} \alpha_{jk} F^j_{\mu\nu} F^{k\mu\nu} - \beta_{jk} A^{j\mu} A^k_\mu \right) \sqrt{h}\, d^4x. \tag{C.8}$$

where

$$W(f) = \int_{\mathcal{M}} \sqrt{f}\, d^n x \tag{C.9a}$$

$$S(f) = -\int_{\mathcal{M}} R(f)\, \sqrt{f}\, d^n x \tag{C.9b}$$

$$\alpha_{jk} = \int_{\mathcal{M}} K_{ja} K^a_k\, \sqrt{f}\, d^n x \tag{C.9c}$$

$$\beta_{jk} = 2 \int_{\mathcal{M}} \nabla_{(c} K_{jd)} \nabla^{(c} K^{d)}_k\, \sqrt{f}\, d^n x. \tag{C.9d}$$

The $W(f)$ factor may be removed by a rescaling of the metric $h_{\mu\nu}$, putting the action in the Einstein frame form. The $S(f)$ term will yield a system of scalar fields, of which ϕ in our five dimensional reduction (4.37) is an example. Applying the Gram–Schmidt orthonormalization process to the K^j, one can reduce $\alpha_{jk} = \delta_{jk}$, giving the vectors a

canonical kinetic term. Thus, we see Kaluza–Klein reduction of pure gravity results in a theory with scalars and vector fields, generalizing the $n = 1$ result discussed above.

Of crucial importance to the present work is that massless Kaluza–Klein vectors are in one–to–one correspondence with Killing fields on $\mathcal{M}$, or equivalently the zero eigenvalues of β_{jk}. This follows from the fact that β_{jk} functions as a mass matrix for the Kaluza–Klein vector fields. Since β_{jk} is symmetric, we are guaranteed that m^2 will be real for all modes. In our discussion of p–form fields, we were able to apply powerful results regarding the Hodge–de Rham operator Δ that guaranteed that $m^2 \geq 0$, regardless of the topology and metric structure of $\mathcal{M}$. In the present situation, we have no guarantee that the masses of Kaluza–Klein vectors will satisfy $m^2 \geq 0$, or equivalently that the eigenvalues of the mass matrix are nonnegative.

In this work we will assume that all eigenvalues of the mass matrix are nonnegative, so that $m^2 \geq 0$ for all Kaluza–Klein vectors. In the general case, it is necessary to compute α_{jk} and β_{jk} for each manifold of interest, and then check that this assumption holds on a case–by–case basis. A simple example is provided by the n–torus $\mathbf{T}^n$. Realizing the torus as $\mathbf{R}^n/\mathbb{Z}^n$, with coordinates $(\theta_1 \ldots \theta_n)$ ranging on $(0, 2\pi)$, a convenient basis for vector fields on $\mathbf{T}^n$ is provided by

$$K^{(a,n)} = \frac{\sqrt{2}}{(2\pi)^{n/2}}\, \hat{\theta^a} \times \begin{cases} \cos n\theta, & \text{for } n \geq 0, \\ \sin n\theta, & \text{for } n < 0 \end{cases} \tag{C.10}$$

where $n \in \mathbb{Z}$, the $\hat{\theta}^a$ are unit vectors associated to each coordinate, and (a, n) label each basis field, replacing the abstract indices used above. Substituting this into (C.9) we find

$$\alpha_{(a,n)(b,m)} = \delta_{ab}\delta_{nm}, \tag{C.11a}$$

$$\beta_{(a,n)(b,m)} = 2n^2\delta_{ab}\delta_{nm}. \tag{C.11b}$$

The Kaluza–Klein vector fields are therefore canonically normalized, with masses $\sqrt{2}n$ for $n = 0, 1, 2 \ldots$, showing our assumption is valid in this case. More sophisticated examples may be found in the literature. As explained in Chapter 4, the $m^2 \geq 0$ assumption will enable us to treat p–forms and Kaluza–Klein vectors on the same footing.

Appendix D

Kasner Universes in Various Dimensions and Frames

In this appendix we collect various useful formulae related to Kasner universes in a variety of dimensions and conformal frames. The formulae in this section are used throughout this text and are collected here for convenience. We give the relation between string and Einstein frame actions, and the transformation of p–form couplings in Section D.1.1. The formulae relating Kasner exponents before and after compactification are given in D.1.2. Expressions for the Kasner exponents in doubly isotropic Kasner universes are given in D.1.3. Various useful formulae for transforming between different conformal frames are given in D.2. String dualities map Kasner universes into different Kasner universes: we give the expressions relating the two sets of exponents in D.3. Additional useful facts about Kasner universes and string models can be found in [83].

theory	$p=0$	1	2	3	4	notes
I		$1/\sqrt{2}$	$\sqrt{2}$			
het		$-1/\sqrt{2}$	$-\sqrt{2}$			
IIA		$3/\sqrt{2}$	$-\sqrt{2}$	$1/\sqrt{2}$		
IIB	$2\sqrt{2}$		$\pm\sqrt{2}$		0	$-\sqrt{2}$ for NS–NS two–form
M				0		no dilaton, $D=11$

Table D.1: Einstein frame couplings for the p–form menu of various string and M–theory models.

D.1 Key Results

D.1.1 String and Einstein frame couplings

One of the key results we use is the relation between the string frame actions and the Einstein frame one. The string frame action is of the form

$$\mathcal{S}_{\text{string}} = \int \left(e^{-2\Phi} \left[R(G^{(S)}) + 4(\partial\Phi)^2 \right] - \sum_j e^{\lambda_j^{(S)}\Phi} F^2_{p_j+1} \right) \sqrt{-G^{(S)}}\, d^{10}x \qquad \text{(D.1)}$$

where the $\lambda_j^{(S)}$ are the string frame couplings to the dilaton field, and $G^{(S)}$ the string frame metric. The defining feature of the string frame action, for any string model, is the $e^{2\Phi}$ in front of the Ricci scalar, together with the normalization (and wrong sign!) of the kinetic term for the dilaton. One arrives at the Einstein frame action by the transformation

$$G^{(E)}_{MN} = e^{-\Phi/2} G^{(S)}_{MN} \qquad \text{(D.2)}$$

resulting in

$$\mathcal{S}_{\text{Einstein}} = \int \left(R(G^{(E)}) - (\partial\phi)^2 - \sum_j e^{\lambda_j^{(E)}\phi} F^2_{p_j+1} \right) \sqrt{-G^{(E)}}\, d^{10}x \qquad \text{(D.3)}$$

where we have defined

$$\phi = \Phi/\sqrt{2}, \tag{D.4a}$$

$$\lambda_j^{(E)} = \sqrt{2}\left(\lambda^{(S)} + \frac{8-2p_j}{4}\right), \tag{D.4b}$$

The field ϕ, which we shall refer to as the "dilaton" below, is canonically normalized, and the couplings between the dilaton and p–forms have transformed. In the following, we will always use the Einstein frame couplings, and so will drop the superscript (E) for clarity in notation.

D.1.2 Compactified Kasner Universes

We begin with a $(1+d+n)$–dimensional Kasner universe with exponents

$$(r_i, s_j) \qquad i = 1\ldots d,\ j = 1\ldots n. \tag{D.5}$$

Compactifying the last n dimensions results in a $(d+1)$–dimensional Kasner universe with matter. Define

$$\hat{s} = \frac{1}{d-1}\sum_{j=1}^{n} s_j. \tag{D.6}$$

Then, in the $(d+1)$–dimensional Einstein frame, the resulting universe has Kasner exponents

$$p_i = \frac{r_i + \hat{s}}{1+\hat{s}}. \tag{D.7}$$

There will also be n^2 scalars and n vector fields in the 4D theory. One of these is the usual Kaluza–Klein scalar ϕ representing the volume of the compact dimensions. It will behave as $\phi = q\ln t$, where

$$q = \frac{(d-1)\hat{s}}{1+\hat{s}}\sqrt{\frac{1}{n} + \frac{1}{d-1}}. \tag{D.8}$$

It is possible to show that the compactification of a Kasner universe always results in a $w = 1$ universe in the lower dimension.

D.1.3 Doubly Isotropic Solutions

Doubly–isotropic Kasner universes are those for which in which d Kasner exponents take the value p_d, and n take the value p_d, with $d + n = D - 1$. These are primarily useful in the context of Kasner universes in higher dimensions, where they correspond to an isotropically evolving $(d+1)$–dimensional noncompact space and an isotropically evolving n–dimensional compact space.

In the absence of a dilaton, the Kasner conditions (2.5) result in a quadratic equation for p_d and p_n, and therefore two solutions for each choice of d and n. First define the discriminant

$$\Delta = [dn(d + n - 1)]^{1/2} . \tag{D.9}$$

Then the two branches are given by

$$p_d^{(\pm)} = \frac{d \pm \Delta}{d(n + d)}, \tag{D.10a}$$

$$p_n^{(\pm)} = \frac{n \mp \Delta}{n(n + d)}. \tag{D.10b}$$

These two branches are the only doubly–isotropic solutions without a dilaton. When a dilaton is present, then there are two one–parameter families of p_d and p_n, which depend on the value of the dilaton "Kasner exponent" p_ϕ, and satisfy the Kasner conditions (2.36). In the string case (which is the only one we consider) we set $d = 3$ and $n = 6$ and obtain

$$p_6^{(\pm)} = \frac{2 \pm \sqrt{16 - 18p_\phi^2}}{17}, \tag{D.11a}$$

$$p_3^{(\pm)} = \frac{1 - 6p_6}{3}. \tag{D.11b}$$

These expressions are consistent with the fact that the maximum possible value of p_ϕ in ten spacetime dimensions is $p_\phi = 8/9$.

D.2 Different Conformal Frames

Throughout this section, we use the convention in use for the rest of this work, that d denotes the number of spatial dimensions in a $(d+1)$–dimensional spacetime. The key to transforming between conformal frames is the transformation of the Ricci scalar. Under the substitution

$$h_{ij} = e^{2\omega} g_{ij} \tag{D.12}$$

one finds

$$R(h) = e^{-2\omega} \left(R(g) - d(d-1)(\partial\omega)^2 + \cdots \right) \tag{D.13}$$

we go on to enumerate some important special cases.

A general Einstein–scalar system has the action

$$\mathcal{S}_{Einstein-scalar} = \int e^{A\psi} \left(R(h) - B(\partial\psi)^2 \right) \sqrt{h}\, \mathrm{d}^{d+1}x, \tag{D.14}$$

under the transformation

$$h_{ij} = e^{2C\psi} g_{ij} \tag{D.15}$$

the action is mapped into another of the same form (D.14) with,

$$\tilde{A} = A + (d-1)C, \tag{D.16a}$$

$$\tilde{B} = B + d(d-1)C^2. \tag{D.16b}$$

Note that generally ψ is not canonically normalized in either frame. The p–form action is defined by

$$\mathcal{S}_{p-form} = \int e^{\lambda\psi} F_{p+1}^2 \sqrt{h}\, \mathrm{d}^{d+1}x. \tag{D.17}$$

under the transformation

$$h_{ij} = e^{2C\psi} g_{ij} \tag{D.18}$$

it is mapped into a similar form with

$$\tilde{\lambda} = \lambda + C(d-1-2p). \tag{D.19}$$

Now we have the tools required to analyze the specific case of the string frame action. The string frame is defined by the NS–NS action

$$\mathcal{S}_{str} = \int e^{-2\Phi} \left(R(h) + 4(\partial\Phi)^2 + \cdots \right) \sqrt{h}\, \mathrm{d}^{d+1}x, \tag{D.20}$$

which can be transformed into Einstein frame with a canonically normalized dilaton field ϕ. The usual transformation with

$$\omega = \frac{2}{d-1}\Phi \tag{D.21}$$

puts the action in Einstein frame

$$\int R(g) - \frac{4}{d-1}(\partial\Phi)^2 \sqrt{g}\, \mathrm{d}^{d+1}x. \tag{D.22}$$

the further definition of

$$\phi = \Phi \cdot \sqrt{\frac{4}{d-1}} \tag{D.23}$$

canonically normalizes the dilaton to yield

$$\int R(g) - (\partial\phi)^2 \sqrt{g}\, \mathrm{d}^{d+1}x. \tag{D.24}$$

Returning to the p–form transformation rule and specializing to $d = 9$, we find that the combined conformal transformation and rescaling of ϕ yield

$$\phi = \Phi/\sqrt{2}, \tag{D.25a}$$

$$\tilde{\lambda} = \sqrt{2}\left(\lambda + 2\frac{10 - 2(p+1)}{8} \right). \tag{D.25b}$$

D.3 String Dualities

Various string actions are connected by duality transformations. These dualities also map Kasner universes to other Kasner universes. Here we give the formulae relating the Kasner exponents in these dual universes.

D.3.1 T–duality

T–duality is a symmetry of the string frame action in string theories. Dualizing a single dimension involves the transformation

$$\rho_j \to \frac{\alpha'}{\rho_j}, \tag{D.26a}$$

$$\Phi \to \Phi - \ln\left(\frac{\rho_j}{\sqrt{\alpha'}}\right). \tag{D.26b}$$

we will use units where $\alpha' = 1$ for convenience. We wish to find how the Einstein frame Kasner exponents change under the T–duality transformation. We begin with the Einstein frame, proper time metric and dilaton

$$ds^2 = -dt_1^2 + \sum_j t^{2p_j} dx_j, \qquad \phi = q \ln t_1. \tag{D.27}$$

This results in the string frame metric

$$ds^2 = t_1^{q/\sqrt{2}} \left(-dt_1^2 + \sum_j t^{2p_j} dx_j^2\right), \qquad \Phi = \sqrt{2} \ln t_1. \tag{D.28}$$

Denoting the string frame proper time before dualization as t_2, we find that

$$t_2 = t_1^{1+\frac{q}{2\sqrt{2}}}, \tag{D.29a}$$

$$ds^2 = -dt_2^2 + \sum_j t^{2q_j} dx_j^2, \tag{D.29b}$$

$$q_j = \frac{p_j + \frac{q}{2\sqrt{2}}}{1 + \frac{q}{2\sqrt{2}}}, \tag{D.29c}$$

$$\Phi = \frac{\sqrt{2}q}{1 + + \frac{q}{2\sqrt{2}}} \ln t_2. \tag{D.29d}$$

where the string frame Kasner exponents q_j have been defined. Now we may apply the T–duality. This defines a new set of exponents, r_j, by

$$r_j = \begin{cases} -q_j & \text{if we dualize along } x^j, \\ +q_j & \text{otherwise.} \end{cases} \tag{D.30}$$

further define

$$\sigma = \text{sum of } q_j \text{ along dualized directions.} \tag{D.31}$$

Now, apply the duality. This keeps the metric in the proper time gauge, but changes the Kasner exponents as above, and shifts the dilaton to

$$\tilde{\Phi} = \left(\frac{\sqrt{2}q}{1 + + \frac{q}{2\sqrt{2}}} - \sigma \right) \ln t_2 \tag{D.32}$$

Now we can descend back down to the Einstein frame again. This defines the Einstein frame proper time after dualization t_3, given by

$$t_3 = t_2^{\frac{\sigma}{4} + \frac{1}{1 + \frac{q}{2\sqrt{2}}}} \tag{D.33}$$

and gives the expressions for the (canonically normalized) dilaton and Einstein frame Kasner exponents s_j, which are

$$\tilde{\phi} = \frac{\frac{q}{1+\frac{q}{2\sqrt{2}}} - \frac{\sigma}{\sqrt{2}}}{\frac{\sigma}{4} + \frac{1}{1+\frac{q}{2\sqrt{2}}}}, \tag{D.34a}$$

$$s_j = \frac{\frac{\sigma}{4} - \frac{\frac{q}{2\sqrt{2}}}{1+\frac{q}{2\sqrt{2}}} + r_j}{\frac{\sigma}{4} + \frac{1}{1+\frac{q}{2\sqrt{2}}}} \tag{D.34b}$$

Clearly these are rather complicated formulae. As a simple example, consider the Milne solution

$$p_1 \cdots p_8 = 0, \tag{D.35a}$$

$$p_9 = 1, \tag{D.35b}$$

$$\phi = \text{const.} \tag{D.35c}$$

T–dualizing on x^9 results in

$$s_1 \cdots s_8 = 1/5, \tag{D.36a}$$

$$s_9 = -3/5, \tag{D.36b}$$

$$\tilde{\phi} = -\frac{2\sqrt{2}}{5} \ln t. \tag{D.36c}$$

Another example is the isotropic solution

$$p_1 \cdots p_9 = 1/9, \tag{D.37a}$$

$$\phi = \sqrt{8/9}. \tag{D.37b}$$

dualizing on x^9 gives

$$s_1 \cdots s_8 = 1/5, \tag{D.38a}$$

$$s_9 = -3/5, \tag{D.38b}$$

$$\tilde{\phi} = +\frac{2\sqrt{2}}{5} \ln t. \tag{D.38c}$$

D.3.2 S–duality of SO(32) heterotic/ Type I

The heterotic SO(32) and Type I SO(32) string actions possess the S–duality given by

$$h_I = e^{-\Phi_{het}} h_{het}, \qquad \Phi_I = -\Phi_{het} \tag{D.39}$$

we can follow a similar (though somewhat simpler) path to the one used for T–duality to find how the Einstein frame actions change under this transformation. Let us assume that we begin in the heterotic theory. Then, the string frame metric and dilaton are

$$\Phi_{het} = \sqrt{2} q \ln t_1, \tag{D.40a}$$

$$ds^2_{het} = t^{q/\sqrt{2}} \left(-dt_1^2 + \sum_j t^{2p_j} dx_j^2 \right). \tag{D.40b}$$

applying the S–duality results in

$$\Phi_I = -\sqrt{2} q \ln t_1, \tag{D.41a}$$

$$ds^2_I = t^{-q/\sqrt{2}} \left(-dt_1^2 + \sum_j t^{2p_j} dx_j^2 \right). \tag{D.41b}$$

but, this is exactly the string frame action for the original solution, with $q \to -q$! Thus, the behavior under S–duality is much simpler than that under T–duality.

Appendix E

The $1+1 \to N+M$ String Amplitude

Standard techniques in string perturbation theory give the form of the four–point string S–matrix amplitude as

$$\mathcal{M} = \frac{8\pi i}{\alpha' g_c^2} \langle : c(z_+)\tilde{c}(z_+)\mathcal{V}^+_{k_+}(z_+) :: c(z_-)\tilde{c}(z_-)\mathcal{V}^-_{k_-}(z_-) : \times \\ : c(z_L)\tilde{c}(z_L)\mathcal{V}^L_{k_L}(z_L) :: \mathcal{V}^R_{k_L}(z_R) : \rangle \quad \text{(E.1)}$$

where the fact that this expression is to be integrated over the unfixed vertex operator position is understood. We have also suppressed the momentum conservation factor, so that the full S–matrix element is

$$S_4(k_+, k_-, k_L, k_R) = (2\pi)^{26}\delta^{26}(k_+ + k_- + k_L + k_R)\mathcal{M} \quad \text{(E.2)}$$

In this work, we take $\mathcal{V}^+_{k_+}(z_+)$ and $\mathcal{V}^-_{k_-}(z_-)$ to be representative states at level N_+ and N_-, respectively, and $\mathcal{V}^L_{k_L}(z_L)$ and $\mathcal{V}^R_{k_L}(z_R)$ to be the massless graviton states. We fix the three vertex operator positions $z_+ = 0$, $z_- = 1$ and $z_L = \infty$. Next, using momentum conservation and the transverse property of the polarization tensors of

each state, it is possible to put the matrix element in the form

$$\left\langle : \prod_{j=1}^{N_+} \left(\partial X^{\mu_j} + \frac{i\alpha'}{2} \left[\kappa^{\mu_j} + \frac{k_R^{\mu_j}}{z} \right] \right) :: \prod_{k=1}^{N_-} \left(\partial X^{\nu_k} - \frac{i\alpha'}{2} \left[\kappa^{\nu_k} + \frac{k_R^{\nu_k}}{1-z} \right] \right) : \times \right.$$
$$\left. : \left(\partial X^{\sigma} + \frac{i\alpha'}{2} \left[z\kappa^{\sigma} - k_-^{\sigma} \right] \right) :: \left(\partial X^{\tau} - \frac{i\alpha'}{2} \left[\frac{\kappa^{\tau}}{z} - \frac{k_-^{\tau}}{z(1-z)} \right] \right) : \right\rangle \times$$
$$z^{\alpha' k_+ \cdot k_R/2} (1-z)^{\alpha' k_- \cdot k_R/2}. \quad \text{(E.3)}$$

multiplied by its complex conjugate from the antiholomorphic sector, multiplied by an overall factor

$$\frac{8\pi i g_c^2}{\alpha'} \left(\frac{2}{\alpha'} \right)^{N+M+2} \quad \text{(E.4)}$$

and of course the appropriate polarization tensor for each state. In this expression we have defined, $\kappa^{\sigma} = k_+^{\sigma} + k_-^{\sigma}$. This expression for the amplitude results from evaluating the ghost path integral and contractions between the ∂X and e^{ikX} terms, as well as between two e^{ikX} terms. The remaining contractions are those between two ∂X terms.

Given this pattern of contractions, each possible contraction of operators results in an integral of the form

$$\int_{\mathbf{C}} z^{a-1+m_1} \bar{z}^{a-1+n_1} (1-z)^{b-1+m_2} (1-\bar{z})^{b-1+n_2} \, d^2z$$
$$= 2\pi \frac{\Gamma(a+m_1)\Gamma(b+m_2)\Gamma(1-a-b-n_1-n_2)}{\Gamma(a+b+m_1+m_2)\Gamma(1-a-n_1)\Gamma(1-b-n_2)} \quad \text{(E.5)}$$

For $m_1, m_2, n_1, n_2 \in \mathbf{Z}$. We can simplify our discussion by focusing on the leading terms in this expression. Our concern in the present work is on the production of long–wavelength, highly excited string states. Thus, we parameterize the momenta

in the problem as

$$k_+ = (m_+, 0, 0) + (\delta\omega^+, \delta k_x^+, \delta\vec{k}_T^+), \tag{E.6a}$$

$$k_- = (m_-, 0, 0) + (\delta\omega^-, \delta k_x^-, \delta\vec{k}_T^-), \tag{E.6b}$$

$$k_L = (-\omega, -\omega, 0) + (-\delta\omega^L, -\delta k_x^L, -\delta\vec{k}_T^L), \tag{E.6c}$$

$$k_R = (-\omega, +\omega, 0) + (-\delta\omega^R, -\delta k_x^R, -\delta\vec{k}_T^R), \tag{E.6d}$$

where we assume that $\delta k, \delta\omega \ll m_\pm$. We focus on the case where

$$0 = \delta\vec{k}_T^L = \delta\vec{k}_T^R, \tag{E.7a}$$

$$\delta k_x = \delta k_x^+ = -\delta k_x^-, \tag{E.7b}$$

Now applying the mass–shell conditions and momentum conservation, we find, $\omega = \frac{m_+ + m_-}{2}$ and furthermore, $\delta\vec{k}_T = \delta\vec{k}_T^+ = -\delta\vec{k}_T^-$, and $\delta k_x' = \delta k_x^L = -\delta k_x^R$. We can take the two remaining free variables to be δk_x and $\delta\vec{k}_T$. The mass–shell conditions further imply,

$$\delta\omega^\pm = \frac{(\delta k_x)^2 + (\delta\vec{k}_T)^2}{2m_\pm} + \mathcal{O}(k_{x,T}^4), \tag{E.8}$$

and $\delta\omega^L = \delta k_x'$, $\delta\omega^R = \delta k_x'$. So now we can reexpress all variables in terms of δk_x and $\delta\vec{k}_T$, by noting, $\delta k_x' = \frac{\delta\omega^+ + \delta\omega^-}{2}$. Now returning to the expression (E.5), we can see that

$$a - 1 = (\alpha'/2)k_+ \cdot k_R = N_+ - 1 + \Delta + \delta_{+R}, \tag{E.9a}$$

$$b - 1 = (\alpha'/2)k_- \cdot k_R = N_- - 1 + \Delta + \delta_{-R}, \tag{E.9b}$$

with $\Delta = [(N_+ - 1)(N_- - 1)]^{1/2}$ and,

$$\delta_{-R} = \frac{\alpha'}{2}\left(\frac{m_-}{2}\delta\omega^+ + \left[\frac{m_+ + 2m_-}{2}\right]\delta\omega^- - \omega\delta k_x\right), \tag{E.10a}$$

$$\delta_{+R} = \frac{\alpha'}{2}\left(\frac{m_+}{2}\delta\omega^- + \left[\frac{m_- + 2m_+}{2}\right]\delta\omega^+ + \omega\delta k_x\right), \tag{E.10b}$$

At this point we have all of the information we need to compute each term in the amplitude. In order to find the dominant term, it suffices to examine each of the possible contractions between momentum vectors and polarization tensors. These are given by, $(k_R \cdot e^+, k_R \cdot e^-) = \mathcal{O}(\sqrt{\alpha'}m)$ and $(\kappa \cdot e^+, \kappa \cdot e^-, \kappa \cdot e^L, k_- \cdot e^L, \kappa \cdot e^R, k_- \cdot e^R) = \mathcal{O}(\sqrt{\alpha'}\delta k)$. Thus it is seen that the term with the greatest number of k_R contracted with polarization tensors will be dominant. It will be convenient to rewrite the integral (E.5) as

$$\pi \frac{\Gamma(a+m_1)\Gamma(b+m_2)\Gamma(1-a-b-n_1-n_2)}{\Gamma(a+b+m_1+m_2)\Gamma(1-a-n_1)\Gamma(1-b-n_2)} = \frac{\sin[\pi(a+n_1)]\sin[\pi(b+n_2)]}{\sin[\pi(a+b+n_1+n_2)]} \frac{\Gamma(a+m_1)\Gamma(b+m_2)}{\Gamma(a+b+m_1+m_2)} \frac{\Gamma(a+n_1)\Gamma(b+n_2)}{\Gamma(a+b+n_1+n_2)} \quad \text{(E.11)}$$

From our discussion above, the leading term with have the largest possible number of k_R contractions, implying $m_1 = n_1 = -N_+$ and $m_2 = n_2 = -N_-$. (This depends somewhat on the pattern of contractions involving the graviton polarization tensors, but this turns out to be unimportant in the final result) Thus we find the value of the integral to be

$$\frac{\sin[\pi(\Delta+\delta_{+R})]\sin[\pi(\Delta+\delta_{-R})]}{\sin[\pi(2\Delta+\delta_{+R}+\delta_{-R})]} \left[\frac{\Gamma(\Delta+\delta_{+R})\Gamma(\Delta+\delta_{-R})}{\Gamma(2\Delta+\delta_{+R}+\delta_{-R})}\right]^2 \quad \text{(E.12)}$$

From this it is possible to work backwards and obtain the full S–matrix expression, although we will not require the full amplitude.

A key feature of this amplitude is its behavior when $\Delta \in \mathbf{Z}$. The leading term derived above clearly vanishes as $\delta_{\pm R} \to 0$ in this case, due to the structure of the zeros of the sine functions. While we have only displayed the leading order term above, this behavior in fact holds for all of the terms contributing to this amplitude. This can be seen from the structure of the integral over the complex plane used to derive (E.12). Regardless of the pattern of contractions corresponding to a given term, the arguments to all of the gamma functions appearing in (E.12) are positive.

Since the gamma function has no zeros, and only has poles for negative values of the argument, the amplitude must vanish when $\Delta \in \mathbf{Z}$ and $\delta_{\pm R} \to 0$.

Appendix F

Pair Production via the S–matrix

In this appendix we carry out explicit calculations of the pair production rate using both S–matrix and Bogolubov coefficient techniques. This provides a check that, while the two methods differ, the end result is precisely the same (for a related analysis, see also [63]). We study a minimally coupled scalar field in $D \neq 2$ spacetime dimensions, with action

$$\mathcal{S}_\phi = -\frac{1}{2}\int \left(g^{\mu\nu}\partial_\mu\phi\partial_\nu\phi + m^2\phi^2\right)\sqrt{-g}\; d^D x, \tag{F.1}$$

Our gravitational background is defined by

$$g_{\mu\nu} = a(t)^2\eta_{\mu\nu} \tag{F.2}$$

where the "scale factor" $a(t)$ is an arbitrary function of time. In order to better make contact with the examples considered in this work, we will assume that $a(t)$ is unity, except for a localized "bump" of small amplitude near $t = 0$. Thus, there will be well–defined "in" and "out" regions where the geometry is Minkowski space.

For future convenience we define a field variable ψ, given by

$$\phi(t, x_j) = a(t)^{1-D/2}\psi(t, x_j). \tag{F.3}$$

We Fourier expand ψ along the spatial coordinates, so $\psi(t, x_j) = \psi_k(t)e^{ik_j x^j}$, and define $g(t) = a^{1/n}$, $n = \frac{1}{D/2-1}$, and

$$\Delta(t) = \left(g(t)^{2n} - 1\right) m^2 - \frac{\ddot{g}}{g}, \tag{F.4}$$

With these replacements, the action for ψ becomes

$$\mathcal{S}_\psi = -\frac{1}{2}\int \left(-\dot{\psi}_k^2 + \omega_k^2\psi_k^2 + \Delta(t)\psi_k^2\right) \frac{d^{D-1}k}{(2\pi)^{D-1}}dt, \tag{F.5}$$

where $\omega_k^2 = m^2 + k^2$ as usual. The equation of motion for ψ_k is

$$\ddot{\psi} + \left[\omega_k^2 + \Delta(t)\right]\psi = 0. \tag{F.6}$$

F.1 Bogolubov Coefficient Calculation

Now, we will calculate precisely what the β Bogolubov coefficient is in the theory described in the previous section. Because the perturbation to the action is localized in time, the canonical Minkowski vacuum is a natural choice for the "in" and "out" regions, and so

$$u_j(t, x) = \bar{u}_j(t, x) = e^{-i\omega t + ik_j x^j}, \qquad u_j^*(t, x) = \bar{u}_j^*(t, x) = e^{+i\omega t - ik_j x^j}, \tag{F.7}$$

We now consider the following (approximate) solution to the equation of motion for ψ

$$\psi_k(t) = \frac{1}{\sqrt{2\omega(k)}}\left(e^{-i\omega_k t} + \beta_{k,-k'}(t)e^{i\omega_k t}\right) \tag{F.8}$$

along with the boundary condition that $\beta_{k,-k}(t) \to 0$ as $t \to -\infty$. This boundary condition ensures that $\psi_k(t)$ is a pure positive–frequency mode in the "in" region. Using the definitions above, it is clear that $\beta_{k,-k}(t)$ at $t = +\infty$ is the Bogolubov $\beta_{k,-k}$ coefficient.

Substituting our solution (F.8) into the wave equation, and making the assumption that $\beta \ll 1$, we find

$$\ddot{\beta}_{k,-k} + 2i\omega_k\dot{\beta}_{k,-k} = -\Delta(t)e^{-2i\omega_k t} \tag{F.9}$$

This equation has the solution

$$\beta_{k,-k}(t) = -\int_{t'=-\infty}^{t} e^{-2i\omega_k t'} \int_{t''=-\infty}^{t'} \Delta(t'')\, dt'\, dt'' \to \frac{i}{2\omega_k}\Delta(2\omega_k), \tag{F.10}$$

where in the last step we have taken $t \to +\infty$. Note that our derivation is self–consistent even in $\Delta(t)$ is large; we have only assumed that $\beta_k(t) \ll 1$ and thus we only need require that $\Delta(\omega)/\omega$ is small.

To compare with the S–matrix calculation, we must switch to the Lorentz–invariant particle states, defined by

$$|k\rangle = \sqrt{2\omega_k} a_k^+ |0\rangle. \tag{F.11}$$

When this is done, one arrives at the invariant matrix element describing the particle production process,

$$\mathcal{M}\left(|0\rangle \to |k,-k\rangle\right) = -\Delta(2\omega_k) \tag{F.12}$$

We will see in the next section how precisely the same result is obtained using conventional field theory techniques.

F.2 S–matrix Calculation

The S–matrix element may be calculated using the rules of standard flat–space quantum field theory. The calculation is much simpler than using the Bogolubov coefficient method. In quantum field theory, if we have a perturbation to the action $\delta S[\psi]$, then

$$S = \int_{vol} \langle 0|i\delta S[\psi]|k_1 k_2\rangle \tag{F.13}$$

where we "contract" any ψ appearing in the perturbation according to the rule,

$$\psi(x)|k_1\rangle = e^{-ik_1\cdot x}|0\rangle \tag{F.14}$$

In our situation, we have $\delta S = -\Delta(t)\psi^2/2$. Again, after including the factor of two from summing over the two possible contractions with the final state momenta, we

find that,

$$S = -i \int e^{-i(k_1+k_2)\cdot x} \Delta(t)\, d^D x, \tag{F.15}$$

which is precisely the Fourier transform of $\Delta(t)$. Imposing momentum conservation, we find the invariant matrix element,

$$\mathcal{M}\left(|0\rangle \to |k, -k\rangle\right) = -\Delta(2\omega_k) \tag{F.16}$$

which is precisely the one found by other means in the previous section.

Appendix G

Conventions

Throughout this work we use a spacetime with a "mostly plus" signature. Our conventions for spacetime and general relativity are those of Misner, Thorne and Wheeler [92]. We also use natural units throughout this work, and set $8\pi G = 1$. Where relevant, we use d to denote the number of spatial (noncompact) dimensions, and D for the total dimensionality of spacetime; thus $D = d + 1$.

When discussing compactification, we assume that spacetime has the form $\Sigma \times \mathcal{M}$, with $\mathcal{M}$ a compact manifold. Indices $M, N, P \ldots$ denote directions in the total spacetime $\Sigma \times \mathcal{M}$, while $\mu, \nu \ldots$ denotes directions along Σ and $m, n, p \ldots$ along $\mathcal{M}$. G_{MN} denotes the total metric, with $h_{\mu\nu}$ the metric on Σ and f_{mn} the metric on $\mathcal{M}$. In later sections we will need to distinguish between coordinate indices and tangent space indices on $\Sigma \times \mathcal{M}$. We use $A, B, C...$ for tangent space indices along the full space, $\alpha, \beta...$ for those along Σ, and $a, b...$ for those along $\mathcal{M}$.

List of Figures

List of Tables

Index

References

[1] L. Andersson and A. D. Rendall. Quiescent cosmological singularities. *Commun. Math. Phys.*, 218:479–511, 2001.

[2] I. Antoniadis, C. Bachas, J. R. Ellis, and D. V. Nanopoulos. An expanding universe in string theory. *Nucl. Phys.*, B328:117–139, 1989.

[3] T. Appelquist and A. Chodos. The quantum dynamics of Kaluza-Klein theories. *Phys. Rev.*, D28:772, 1983.

[4] P. S. Aspinwall, B. R. Greene, and D. R. Morrison. Calabi-Yau moduli space, mirror manifolds and spacetime topology change in string theory. *Nucl. Phys.*, B416:414–480, 1994.

[5] J. J. Atick and E. Witten. The Hagedorn transition and the number of degrees of freedom of string theory. *Nucl. Phys.*, B310:291–334, 1988.

[6] C. Bachas and M. Porrati. Pair creation of open strings in an electric field. *Phys. Lett.*, B296:77–84, 1992.

[7] J. M. Bardeen, P. J. Steinhardt, and M. S. Turner. Spontaneous creation of almost scale–free density perturbations in an inflationary universe. *Phys. Rev.*, D28:679, 1983.

[8] J. D. Barrow. Quiescent cosmology. *Nature*, 272:211–215, 1978.

[9] V. A. Belinsky and I. M. Khalatnikov. Effect of scalar and vector fields on the nature of the cosmological singularity. *Soviet Physics JETP*, 36:591–597, 1973.

[10] V. A. Belinsky, I. M. Khalatnikov, and E. M. Lifshitz. Oscillatory approach to a singular point in the relativistic cosmology. *Adv. Phys.*, 19:525–573, 1970.

[11] C. W. Bernard and A. Duncan. Regularization and renormalization of quantum field theory in curved space-time. *Ann. Phys.*, 107:201, 1977.

[12] A. L. Besse. *Einstein Manifolds*. Springer–Verlag, 1987.

[13] N. D. Birrell and P. C. W. Davies. *Quantum Field Theory in Curved Space*. Cambridge University Press, 1984.

[14] W. Boucher. Positive energy without supersymmetry. *Nucl. Phys.*, B242:282, 1984.

[15] R. Bousso and J. Polchinski. Quantization of four-form fluxes and dynamical neutralization of the cosmological constant. *JHEP*, 06:006, 2000.

[16] L. A. Boyle, P. J. Steinhardt, and N. Turok. The cosmic gravitational wave background in a cyclic universe. *Phys. Rev.*, D69:127302, 2004.

[17] L. A. Boyle, P. J. Steinhardt, and N. Turok. A new duality relating density perturbations in expanding and contracting Friedmann cosmologies. *Phys. Rev.*, D70:023504, 2004.

[18] R. H. Brandenberger and C. Vafa. Superstrings in the early universe. *Nucl. Phys.*, B316:391, 1989.

[19] C. Brans and R. H. Dicke. Mach's principle and a relativistic theory of gravitation. *Phys. Rev.*, 124:925–935, 1961.

[20] C. P. Burgess. Open string instability in background electric fields. *Nucl. Phys.*, B294:427, 1987.

[21] J. Callan, Curtis G., I. R. Klebanov, and M. J. Perry. String theory effective actions. *Nucl. Phys.*, B278:78, 1986.

[22] M. Campbell, P. C. Nelson, and E. Wong. Stress tensor perturbations in conformal field theory. *Int. J. Mod. Phys.*, A6:4909–4924, 1991.

[23] P. Candelas and X. C. de la Ossa. Comments on conifolds. *Nucl. Phys.*, B342:246–268, 1990.

[24] N. J. Cornish and J. J. Levin. The Mixmaster universe is chaotic. *Phys. Rev. Lett.*, 78:998–1001, 1997.

[25] T. Damour, S. de Buyl, M. Henneaux, and C. Schomblond. Einstein billiards and overextensions of finite-dimensional simple Lie algebras. *JHEP*, 08:030, 2002.

[26] T. Damour and M. Henneaux. Chaos in superstring cosmology. *Gen. Rel. Grav.*, 32:2339–2343, 2000.

[27] T. Damour and M. Henneaux. Chaos in superstring cosmology. *Phys. Rev. Lett.*, 85:920–923, 2000.

[28] T. Damour and M. Henneaux. $E(10)$, $BE(10)$ and arithmetical chaos in superstring cosmology. *Phys. Rev. Lett.*, 86:4749–4752, 2001.

[29] T. Damour, M. Henneaux, B. Julia, and H. Nicolai. Hyperbolic Kac-Moody algebras and chaos in Kaluza-Klein models. *Phys. Lett.*, B509:323–330, 2001.

[30] T. Damour, M. Henneaux, A. D. Rendall, and M. Weaver. Kasner-like behaviour for subcritical Einstein-matter systems. *Annales Henri Poincare*, 3:1049–1111, 2002.

[31] H. J. de Vega, M. Ramon-Medrano, and N. Sanchez. Particle transmutation from the scattering of strings and superstrings in curved space-time. *Nucl. Phys.*, B351:277–297, 1991.

[32] H. J. De Vega, M. Ramon Medrano, and N. Sanchez. Boson - fermion and fermion - boson transmutations induced by supergravity backgrounds in superstring theory. *Phys. Lett.*, B285:206–211, 1992.

[33] J. Demaret, M. Henneaux, and P. Spindel. Nonoscillatory behavior in vacuum Kaluza-Klein cosmologies. *Phys. Lett.*, B164:27–30, 1985.

[34] B. S. DeWitt. Quantum theory of gravity. 1. the canonical theory. *Phys. Rev.*, 160:1113–1148, 1967.

[35] B. S. DeWitt. Quantum field theory in curved space-time. *Phys. Rept.*, 19:295–357, 1975.

[36] P. A. M. Dirac. *Lectures on Quantum Mechanics*. Belfer Graduate School of Science, 1964.

[37] L. J. Dixon, J. A. Harvey, C. Vafa, and E. Witten. Strings on orbifolds. *Nucl. Phys.*, B261:678–686, 1985.

[38] L. J. Dixon, J. A. Harvey, C. Vafa, and E. Witten. Strings on orbifolds. 2. *Nucl. Phys.*, B274:285–314, 1986.

[39] M. R. Douglas. The statistics of string / M theory vacua. *JHEP*, 05:046, 2003.

[40] M. J. Duff, B. E. W. Nilsson, and C. N. Pope. Kaluza-Klein supergravity. *Phys. Rept.*, 130:1–142, 1986.

[41] T. Eguchi, P. B. Gilkey, and A. J. Hanson. Gravitation, gauge theories and differential geometry. *Phys. Rept.*, 66:213, 1980.

[42] G. F. R. Ellis and M. A. H. MacCallum. A class of homogeneous cosmological models. *Commun. Math. Phys.*, 12:108–141, 1969.

[43] J. K. Erickson, D. H. Wesley, P. J. Steinhardt, and N. Turok. Kasner and Mixmaster behavior in universes with equation of state w $\geq$ 1. *Phys. Rev.*, D69:063514, 2004.

[44] E. S. Fradkin and A. A. Tseytlin. Effective action approach to superstring theory. *Phys. Lett.*, B160:69–76, 1985.

[45] E. S. Fradkin and A. A. Tseytlin. Effective field theory from quantized strings. *Phys. Lett.*, B158:316, 1985.

[46] E. S. Fradkin and A. A. Tseytlin. Quantum string theory effective action. *Nucl. Phys.*, B261:1–27, 1985.

[47] J. J. Friess, S. S. Gubser, and I. Mitra. String creation in cosmologies with a varying dilaton. *Nucl. Phys.*, B689:243–256, 2004.

[48] M. Gasperini and V. G. The pre–big bang scenario in string cosmology. *Phys. Rept.*, 373:1–212, 2003.

[49] H. Georgi. *Lie Algebras in Particle Physics*. Frontiers in Physics. Perseus, 1999.

[50] G. W. Gibbons. Quantized fields propagating in plane wave space-times. *Commun. Math. Phys.*, 45:191–202, 1975.

[51] P. Goddard and D. I. Olive. Kac-Moody and Virasoro algebras in relation to quantum physics. *Int. J. Mod. Phys.*, A1:303, 1986.

[52] S. Gratton, J. Khoury, P. J. Steinhardt, and N. Turok. Conditions for generating scale-invariant density perturbations. *Phys. Rev.*, D69:103505, 2004.

[53] M. B. Green, J. H. Schwarz, and E. Witten. *Superstring Theory, Volume I: Introduction*. Cambridge University Press, 1987.

[54] M. B. Green, J. H. Schwarz, and E. Witten. *Superstring Theory, Volume II: Loop Amplitudes, Anomalies, and Phenomenology*. Cambridge University Press, 1987.

[55] B. R. Greene, D. R. Morrison, and A. Strominger. Black hole condensation and the unification of string vacua. *Nucl. Phys.*, B451:109–120, 1995.

[56] J. B. Griffiths. *Colliding plane waves in general relativity*. Oxford Mathematical Mongraphs. Oxford Clarendon Press, 1991.

[57] D. J. Gross. High-energy symmetries of string theory. *Phys. Rev. Lett.*, 60:1229, 1988.

[58] D. J. Gross and P. F. Mende. The high-energy behavior of string scattering amplitudes. *Phys. Lett.*, B197:129, 1987.

[59] D. J. Gross and P. F. Mende. String theory beyond the Planck scale. *Nucl. Phys.*, B303:407, 1988.

[60] S. S. Gubser. String production at the level of effective field theory. *Phys. Rev.*, D69:123507, 2004.

[61] A. H. Guth. The inflationary universe: A possible solution to the horizon and flatness problems. *Phys. Rev.*, D23:347–356, 1981.

[62] R. Hagedorn. Statistical thermodynamics of strong interactions at high- energies. *Nuovo Cim. Suppl.*, 3:147–186, 1965.

[63] A. J. Hamilton, D. Kabat, and M. K. Parikh. Cosmological particle production without Bogolubov coefficients. *JHEP*, 07:024, 2004.

[64] S. W. Hawking. Breakdown of predictability in gravitational collapse. *Phys. Rev.*, D14:2460–2473, 1976.

[65] S. W. Hawking and G. F. R. Ellis. *The Large–Scale Structure of Space–Time*. Cambridge University Press, 1973.

[66] T. Hertog, G. T. Horowitz, and K. Maeda. Negative energy density in Calabi-Yau compactifications. *JHEP*, 05:060, 2003.

[67] P. Horava and E. Witten. Eleven-dimensional supergravity on a manifold with boundary. *Nucl. Phys.*, B475:94–114, 1996.

[68] P. Horava and E. Witten. Heterotic and Type I string dynamics from eleven dimensions. *Nucl. Phys.*, B460:506–524, 1996.

[69] G. T. Horowitz and A. R. Steif. Strings in strong gravitational fields. *Phys. Rev.*, D42:1950–1959, 1990.

[70] W. Hu and S. Dodelson. Cosmic microwave background anisotropies. *Ann. Rev. Astron. Astrophys.*, 40:171–216, 2002.

[71] J. Hughes, J. Liu, and J. Polchinski. Virasoro-Shapiro from Wilson. *Nucl. Phys.*, B316:15, 1989.

[72] J. E. Humphreys. *Introduction to Lie Algebras and Representation Theory*. Graduate Texts in Mathematics. Springer–Verlag, 1972.

[73] V. G. Kac. *Infinite Dimensional Lie Algebras*. Cambridge University Press, 1990.

[74] S. Kachru, R. Kallosh, A. Linde, and S. P. Trivedi. De Sitter vacua in string theory. *Phys. Rev.*, D68:046005, 2003.

[75] E. Kasner. Geometrical theorems on Einstein's cosmological equations. *Amer. J. Math.*, 43:217–221, 1921.

[76] K. A. Khan and R. Penrose. Scattering of two impulsive plane gravitational waves. *Nature*, 229:185–186, 1971.

[77] J. Khoury, B. A. Ovrut, N. Seiberg, P. J. Steinhardt, and N. Turok. From big crunch to big bang. *Phys. Rev.*, D65:086007, 2002.

[78] J. Khoury, B. A. Ovrut, P. J. Steinhardt, and N. Turok. The ekpyrotic universe: Colliding branes and the origin of the hot big bang. *Phys. Rev.*, D64:123522, 2001.

[79] J. Khoury, P. J. Steinhardt, and N. Turok. Great expectations: Inflation versus cyclic predictions for spectral tilt. *Phys. Rev. Lett.*, 91:161301, 2003.

[80] J. Khoury, P. J. Steinhardt, and N. Turok. Designing cyclic universe models. *Phys. Rev. Lett.*, 92:031302, 2004.

[81] E. W. Kolb and M. S. Turner. *The Early Universe*. Frontiers in Physics. Addison–Wesley, 1994.

[82] A. E. Lawrence and E. J. Martinec. String field theory in curved spacetime and the resolution of spacelike singularities. *Class. Quant. Grav.*, 13:63–96, 1996.

[83] J. E. Lidsey, D. Wands, and E. J. Copeland. Superstring cosmology. *Phys. Rept.*, 337:343–492, 2000.

[84] E. M. Lifshitz and I. M. Khalatnikov. Investigations in relativistic cosmology. *Adv. Phys.*, 12:185–249, 1963.

[85] H. Liu, G. W. Moore, and N. Seiberg. Strings in a time-dependent orbifold. *JHEP*, 06:045, 2002.

[86] H. Liu, G. W. Moore, and N. Seiberg. Strings in time-dependent orbifolds. *JHEP*, 10:031, 2002.

[87] A. Lukas, B. A. Ovrut, and D. Waldram. On the four-dimensional effective action of strongly coupled heterotic string theory. *Nucl. Phys.*, B532:43–82, 1998.

[88] I. Madsen and J. Tornehave. *From Calculus to Cohomology.* Cambridge University Press, 1997.

[89] W. S. Massey. *A Basic Course in Algebraic Topology.* Springer–Verlag, 1991.

[90] J. Milton. *Paradise Lost.* Norton Critical Editions. Norton, 1993. edited by Scott Elledge.

[91] C. W. Misner. Mixmaster universe. *Phys. Rev. Lett.*, 22:1071–1074, 1969.

[92] C. W. Misner, K. S. Thorne, and J. A. Wheeler. *Gravitation.* W. H. Freeman, 1973.

[93] R. C. Myers. New dimensions for old strings. *Phys. Lett.*, B199:371, 1987.

[94] M. Nakahara. *Geometry, Topology and Physics.* Graduate Student Series in Phyics. Institute of Physics Publishing, 1990.

[95] J. P. Peebles. Light out of darkness vs. order out of chaos. *Comments on Astrophys. Space Phys.*, 4:53, 1972.

[96] J. P. Peebles. *Principles of Physical Cosmology*. Princeton University Press, 1993.

[97] J. Polchinski. *String Theory, Volume I: An Introduction to the Bosonic String*. Cambridge University Press, 1999.

[98] J. Polchinski. *String Theory, Volume II: Superstring Theory and Beyond*. Cambridge University Press, 1999.

[99] J. Polchinski and E. Witten. Evidence for Heterotic - Type I string duality. *Nucl. Phys.*, B460:525–540, 1996.

[100] L. Randall and R. Sundrum. An alternative to compactification. *Phys. Rev. Lett.*, 83:4690–4693, 1999.

[101] L. Randall and R. Sundrum. A large mass hierarchy from a small extra dimension. *Phys. Rev. Lett.*, 83:3370–3373, 1999.

[102] L. Randall and R. Sundrum. Out of this world supersymmetry breaking. *Nucl. Phys.*, B557:79–118, 1999.

[103] M. P. J. Ryan and L. C. Shepley. *Homogeneous Relativistic Cosmologies*. Princeton Series in Physics. Princeton University Press, 1975.

[104] J. S. Schwinger. On gauge invariance and vacuum polarization. *Phys. Rev.*, 82:664–679, 1951.

[105] A. Sen. Equations of motion for the heterotic string theory from the conformal invariance of the sigma model. *Phys. Rev. Lett.*, 55:1846, 1985.

[106] D. N. Spergel et al. First year Wilkinson Microwave Anisotropy Probe (WMAP) observations: Determination of cosmological parameters. *Astrophys. J. Suppl.*, 148:175, 2003.

[107] G. Steigman. Primordial nucleosynthesis: Successes and challenges. *Int. J. Mod. Phys.*, E15:1–36, 2006.

[108] P. J. Steinhardt and N. Turok. Cosmic evolution in a cyclic universe. *Phys. Rev.*, D65:126003, 2002.

[109] P. J. Steinhardt and N. Turok. A cyclic model of the universe. *Science*, 296:1436–1439, 2002.

[110] A. Strominger. Massless black holes and conifolds in string theory. *Nucl. Phys.*, B451:96–108, 1995.

[111] A. H. Taub. Empty space-times admitting a three parameter group of motions. *Annals Math.*, 53:472–490, 1951.

[112] A. J. Tolley. String propagation through a big crunch / big bang transition. 2005.

[113] A. J. Tolley and N. Turok. Quantum fields in a big crunch / big bang spacetime. *Phys. Rev.*, D66:106005, 2002.

[114] A. J. Tolley, N. Turok, and P. J. Steinhardt. Cosmological perturbations in a big crunch / big bang space-time. *Phys. Rev.*, D69:106005, 2004.

[115] A. J. Tolley and D. H. Wesley. String pair production in a time-dependent gravitational field. *Phys. Rev.*, D72:124009, 2005.

[116] R. C. Tolman. On the theoretical requirements for a periodic behaviour of the universe. *Phys. Rev.*, 38:1758–1771, 1931.

[117] R. C. Tolman. *Relativity, Thermodynamics, and Cosmology.* International Series of Monographs on Physics. Oxford Clarendon Press, 1934.

[118] M. S. Turner. Coherent scalar field oscillations in an expanding universe. *Phys. Rev.*, D28:1243, 1983.

[119] N. Turok, M. Perry, and P. J. Steinhardt. M theory model of a big crunch / big bang transition. *Phys. Rev.*, D70:106004, 2004.

[120] D. H. Wesley, P. J. Steinhardt, and N. Turok. Controlling chaos through compactification in cosmological models with a collapsing phase. *Phys. Rev.*, D72:063513, 2005.

[121] J.-M. Yang, M. S. Turner, G. Steigman, D. N. Schramm, and K. A. Olive. Primordial nucleosynthesis - a critical comparison of theory and observation. *Astrophys J.*, 281:493–511, 1984.

[122] U. Yurtsever. Structure of the singularities produced by colliding plane waves. *Phys. Rev.*, D38:1706–1730, 1988.